PATENT

IN THE UNITED STATES PATENT AND TRADEMARK OFFICE

Applicant:	Rajagopalan, et al.
Serial No.:	09/898,809
Filed:	July 3, 2001
Group Art Unit:	1624
Confirmation No:	5120
Examiner:	McKenzie
Title:	**DYE-SULFENATES FOR DUAL PHOTOTHERAPY**
Our Ref. No.:	MRD-63

Cincinnati, Ohio 45202 January 24, 2005

Mail Stop AFTER FINAL
Commissioner for Patents
P.O. Box 1450
Alexandria, VA 22311450

DECLARATION OF RAGHAVAN RAJAGOPALAN PURSUANT TO 37 C.F.R. §1.132

Sir:

I, RAGHAVAN RAJAGOPALAN, declare as follows:

1. I am a named inventor in the above-identified patent application.

2. I hold a Ph.D. in Organic Chemistry from Columbia University. I have 22 years of experience in the synthesis and use of compounds for medical diagnosis and therapy, which is the subject of the application. I have read the May 21, 2004 Office Action and understand the position of the Examiner.

3. I participated in the December 13, 2004 personal interview with Examiner McKenzie. As I understood the Examiner, and as noted in the Interview Summary, the Examiner indicated that documents showing that each of the claimed structures of receptor binding molecules was art-recognized would overcome each of the following points in the May 21, 2004 Final Rejection:

- the 35 U.S.C. §112 ¶2 indefiniteness rejection made in point 5,
- the 35 U.S.C. §112 ¶1 enablement rejection made in point 7, and
- the 35 U.S.C. §112 ¶1 written description rejection made in point 8

4. Although I respectfully disagree with the Examiner's position that such documents are required, and reaffirm my opinion that the application sufficiently enables and describes the claimed methods and that the claimed methods are sufficiently definite to one skilled in the art, solely to advance prosecution I submit an exemplary reference for each of (1) somatostatin receptor binding molecules, (2) heat sensitive bacterioendotoxin receptor binding molecules, (3) neurotensin receptor binding molecules, (4) bombesin receptor binding molecules, (5) cholecystekinin receptor binding molecules, (6) steroid receptor binding molecules, and (7) carbohydrate receptor binding molecules demonstrating each of these are known to one skilled in the art, and hence the specification sufficiently enables and describes the claimed methods, and that the claims are sufficiently definite.

5. I have attached the following references to this Declaration, noting these are exemplary only and respectfully requesting permission to supplement this list should the Examiner request more references from each group:

SOMATOSTATIN RECEPTOR

1. C. Nunn. European Journal of Pharmacology 2003, 465(3), 211-218.
2. R.T. Bass. Molecular Pharmacology 1996, 50(4), 709-715.

ST (HEAT-SENSITIVE BACTERIOENTEROTOXIN) RECEPTOR

1. S.A. Waldman. U.S. Patent No. 5,518,888 1996.
2. T. Okumura. Peptide Chemistry 1993, 31st, 217-220.

NEUROTENSIN RECEPTOR

1. D.A. Nugiel. Bioorganic and Medicinal Chemistry Letters 1995, 5(11), 1203-1206.
2. A. Sefler. Journal of Medicinal Chemistry 1995, 38(2), 249-257.

BOMBESIN RECEPTOR

1. D.H. Coy. Journal of Biological Chemistry 1991, 266(25), 16441-16448.
2. D.H. Coy. Journal of Biological Chemistry 1988, 263(11), 5056-5060.

CHOLECYSTOKININ RECEPTOR

1. E. Sugg. Journal of Medicinal Chemistry 1995, 38(1), 207-211.
2. A.R. Batt. Bioorganic and Medicinal Chemistry Letters 1994, 4(7), 867-872.

STEROID RECEPTOR

1. S.C. Conzen. Progress in Oncology 2003, 211-230.
2. G. Teutsch. Biochemical Society Transactions 1991, 19(4), 901-908.

CARBOHYDRATE RECEPTOR

1. M. Mazik. Tetrahedron Letters 2004, 45(15), 3117-3121.
2. N. Kaila. Medicinal Research Reviews 2002, 22(6), 566-601.

I hereby declare that all statements made herein of my own knowledge are true and that all statements made on information and belief are believed to be true; and further that these statements were made with the knowledge that willful false statements and the like so made are punishable by fine or imprisonment or both, under Section 1001 of Title 18 of the United States Code and that such willful false statements may jeopardize the validity of the subject application or any patent issued thereon.

January 24, 2005
Date

Raghavan Rajagopalan
Raghavan Rajagopalan, Ph.D.

Available online at www.sciencedirect.com
SCIENCE @ DIRECT®
ELSEVIER
European Journal of Pharmacology 465 (2003) 211–218
ejp
www.elsevier.com/locate/ejphar

Agonist properties of putative small-molecule somatostatin sst_2 receptor-selective antagonists

Caroline Nunn, Daniel Langenegger, Konstanze Hurth, Kerstin Schmidt, Dominique Fehlmann, Daniel Hoyer*

Nervous System Research, Novartis Pharma AG, CH-4002, Basel, Switzerland

Received 24 October 2002; received in revised form 6 February 2003; accepted 14 February 2003

Abstract

The availability of antagonist ligands for somatostatin receptors is very limited, with those that are available often displaying agonist properties or limited receptor subtype selectivity. Hay et al. [Bioorg. Med. Chem. Lett. 11 (2001) 2731] recently described the development of small-molecule somatostatin receptor subtype 2 (sst_2) selective compounds. This study investigates the binding affinity and functional characteristics of two of those antagonists (2 and 3) and the agonist compound, from which they were derived (1). In radioligand binding studies using the agonist radioligands [^{125}I][Tyr^{11}]SRIF-14 (Ala-Gly-c[Cys-Lys-Asn-Phe-Phe-Trp-Lys-Thr-(^{125}I-Tyr)-Thr-Ser-Cys]-OH), [^{125}I]LTT-SRIF-28 ([Leu^{8},DTrp^{22},^{125}I-Tyr^{25}]SRIF-28; Ser-Ala-Asn-Ser-Asn-Pro-Ala-Leu-Ala-Pro-Arg-Glu-Arg-Lys-Ala-Gly-c[Cys-Lys-Asn-Phe-Phe-DTrp-Lys-Thr-(^{125}I-Tyr)-Thr-Ser-Cys]-OH), [^{125}I]CGP 23996 (c[Lys-Asu-Phe-Phe-Trp-Lys-Thr-(^{125}I-Tyr)-Thr-Ser]), [^{125}I][Tyr^{3}]octreotide (DPhe-c[Cys-(^{125}I-Tyr)-DTrp-Lys-Thr-Cys]-Thr-OH) and [^{125}I][Tyr^{10}]cortistatin-14 (Pro-c[Cys-Lys-Asn-Phe-Phe-Trp-Lys-Thr-(^{125}I-Tyr)-Ser-Ser-Cys]-Lys) at human recombinant somatostatin receptors expressed in Chinese hamster lung fibroblast (CCL39) cells and native rat cortex, the compounds bound with high affinity (pK_d 6.8–9.7) and selectivity to human sst_2 receptors. Some affinity was also observed for sst_5 labelled by [^{125}I][Tyr^{3}]octreotide and [^{125}I]CGP 23996. In functional studies at human sst_2 receptors expressed in Chinese hamster ovary (CHO) cells, both the agonist 1 and the two putative antagonists 2 and 3 concentration dependently inhibited forskolin-stimulated adenylate cyclase and stimulated luciferase reporter gene expression, with similar efficacy to the natural ligand somatotropin release inhibiting factor (SRIF)-14. Compound 1 had similar potency to SRIF-14, which was in the nanomolar range, whereas 2 and 3 were 10–100-fold less potent. The intrinsic activity of 2 and 3 was too high to allow antagonist studies to be carried out. In conclusion, in contrast to previous findings, all three compounds are potent agonists at recombinant human sst_2 receptors.

Keywords: Somatostatin; Somatostatin sst_2 receptor 2; Non-peptide antagonist; Luciferase; SRE (serum response element); cAMP

1. Introduction

Somatostatin (SRIF, somatotropin release inhibiting factor) is expressed by neuroendocrine, inflammatory, immune and tumour cells, neurones and osteoblasts (for review, see Epelbaum et al., 1994). Its first discovered role was as an inhibitor of growth hormone secretion from the anterior pituitary (Krulich et al., 1968; Brazeau et al., 1973), but it has since been shown to have many physiological inhibitory effects including modulation of neurotransmitter release in the brain, inhibition of endocrine and exocrine secretions (such as thyroid-stimulating hormone and prolactin from the anterior pituitary, and insulin and glucagon from pancreas), and inhibition of cell proliferation in normal and tumour cells (for review, see Patel, 1999).

Somatostatin produces its effects via interaction with specific cell-surface G protein-coupled receptors of which five subtypes have so far been cloned (somatostatin receptor subtype 1–5 [sst_{1-5}]; Hoyer et al., 1995). In rodents, the sst_2 receptor exists in two splice variant forms—sst_{2a} and sst_{2b} (Vanetti et al., 1992; Schindler et al., 1998). From original operational studies, the receptors were classified into two groups—$SRIF_1$, with high affinity for the short chain synthetic somatostatin analogues such as SMS 201 995 (octreotide) and MK 678 (seglitide), and $SRIF_2$, which has high affinity for the analogue CGP 23996 (Reubi, 1984; Tran et al., 1985; Raynor and Reisine, 1989; Martin et al.,

* Corresponding author. Tel.: +41-61-324-4209; fax: +41-61-324-4866.

E-mail address: daniel1.hoyer@pharma.novartis.com (D. Hoyer).

0014-2999/03/$ - see front matter © 2003 Elsevier Science B.V. All rights reserved.
doi:10.1016/S0014-2999(03)01482-1

1991; Raynor et al., 1992). Subsequent molecular cloning and further pharmacological characterisation showed that $SRIF_1$ consists of $sst_{2,\ 3\ and\ 5}$ and $SRIF_2$ of $sst_{1\ and\ 4}$ (Hoyer et al., 1994). Somatostatin receptors modulate multiple cellular effectors via activation of heterotrimeric G-proteins. These include adenylate cyclase, phospholipase C, K^+ channels, Ca^{2+} channels, Ser/Thr phosphatases and mitogen-activated protein kinase cascades (Patel, 1999).

In any system where a single ligand can modulate numerous receptors and effectors, selective synthetic ligands are essential; both as tools to elucidate physiological and biochemical effects mediated by individual receptor subtypes, and as potential therapeutic compounds. This is especially true for the somatostatin system where it is common for more than one receptor subtype to be expressed in the same cell (Patel, 1997). While somatostatin receptor subtypes have been characterised by molecular cloning and pharmacology, the availability of "selective" ligands for individual subtypes is still relatively limited. Early synthetic peptide analogues of somatostatin, such as octreotide, BIM 23014, RC 160 and MK 678, bind to two or more receptor subtypes with similar high affinity (Raynor et al., 1993; Hoyer et al., 1994; Siehler et al., 1999).

Merck scientists recently developed a series of non-peptide agonists with high affinity and selectivity for the individual somatostatin receptor subtypes (Rohrer et al., 1998; Rohrer and Berk, 1999; Yang et al., 1998a,b). Of these, the sst_2-selective L-054,522 has been shown to mediate inhibition of growth hormone release from rat anterior pituitary and glucagon release from rat pancreas at nanomolar concentrations (Yang et al., 1998a). The advantage of non-peptidic compounds is that they have potential for greater oral bioavailability than peptides that must be administered by subcutaneous or intravenous injection (Yang et al., 1998b) and, in most cases, have short duration of action and little, if any, brain penetration.

However, receptor-selective antagonists are also needed, to conclusively prove that a particular receptor subtype mediates a particular physiological function of somatostatin. Unfortunately, at the present time, very few somatostatin receptor-subtype selective antagonists have been identified. With regards to sst_2-selective compounds specifically, a number of antagonist ligands have been have been reported (Bass et al., 1996; Baumbach et al., 1998; Hocart et al., 1998, 1999) and have been used to distinguish effects of SRIF which are mediated by sst_2, including inhibition of gastric acid release (Rossowski et al., 1998) and growth hormone release from pituitary cells (Hocart et al., 1999). However, these are all modifications of peptides, making them poor candidates for therapeutic or diagnostic use.

Scientists at Pfizer have recently described a series of small sst_2-selective non-peptide ligands, presented as antagonists (Hay et al., 2001a). These compounds are based on the structure of the Merck sst_2-selective non-peptide agonists such as L-054,522 (Yang et al., 1998a), but have been modified to produce compounds that bind with nanomolar affinity to sst_2 and to behave as antagonists of SRIF-14-mediated inhibition of vasoactive intestinal peptide (VIP)-stimulated cAMP accumulation. Their rationale for this study was that sst_2-selective antagonists might be useful to upregulate growth hormone levels in livestock.

Thus, the present study examines radioligand binding and functional properties of three compounds: **1**, **2** and **3** that correspond to compounds **6**, **7e** and **7a** reported by Hay et al. (2001a). Compound **1** is the agonist from which the two putative antagonists **2** and **3** were derived.

2. Methods

2.1. Cell culture

Chinese hamster ovary (CHO) and Chinese hamster lung fibroblast cells, which have been engineered to express the luciferase reporter gene under the control of the serum responsive element (CHO-SRE-Luci and CCL39-SRE-Luci cells), expressing recombinant human somatostatin receptors, were cultured in Dulbecco's Modified Eagle's Medium/Ham's F-12 Nutrient Mix (1:1, glutamax I and pyridoxine, Gibco BRL), supplemented with 10% (v/v) foetal bovine serum (Gibco BRL), 100 μg ml^{-1} Hygromycin B (Calbiochem, La Jolla, CA, USA) and 100 μg ml^{-1} geneticin sulphate (Gibco BRL) at 37°C, 5% CO_2, 95% relative humidity. The cells were passaged every 2 days by washing with phosphate-buffered saline (Gibco BRL) and brief incubation with trypsin (0.5 mg ml^{-1})/EDTA (0.2 mg ml^{-1}) (Gibco BRL). For storage, the cells were resuspended in medium containing 10% (v/v) dimethyl sulfoxide and 20% (v/v) foetal bovine serum, and frozen in liquid nitrogen.

2.2. Radioligand binding assay

For rat cerebral cortex preparations, rat brains were purchased from ANAWA Trading (Wangen, Switzerland), and cortex was dissected on ice and homogenised in 10 mM HEPES, pH 7.5, using a Polytron homogeniser at full speed for 45 s. The homogenate was centrifuged at 4°C for 20 min at 22,000 rpm (Kontron ultra-centrifuge, rotor TFT 50.38). The resulting supernatant was discarded and the pellet was resuspended in 10 mM HEPES, pH 7.5, and homogenisation and centrifugation steps were repeated. The resulting pellet was resuspended in 10 mM HEPES, pH 7.5 (0.1 g original tissue ml^{-1}), homogenised as before and frozen at −80 °C.

For crude cell membrane preparations, cells were washed with 10 mM HEPES, pH 7.5, scraped off the culture plates with the same buffer and centrifuged at 4°C for 5 min at 2500 × g. The cell pellet was either stored at −80 °C or used directly.

Cell/tissue membranes were resuspended in binding assay buffer (10 mM HEPES, 0.5% (w/v) bovine serum albumin, pH 7.5) by homogenisation with a Polytron

homogeniser at 50 Hz for 20 s. Final quantities used were as follows: rat cortex: 0.01 mg ml^{-1}, CCL39 cells expressing recombinant human somatostatin receptors: 50,000 cells well^{-1}, except sst$_2$ 100,000 cells well^{-1}. A total of 150 μl of cell or tissue homogenate was incubated with 50 μl of [^{125}I]LTT-SRIF-28 ([Leu^8,DTrp^{22},^{125}I-Tyr^{25}]SRIF-28; Ser-Ala-Asn-Ser-Asn-Pro-Ala-Leu-Ala-Pro-Arg-Glu-Arg-Lys-Ala-Gly-c[Cys-Lys-Asn-Phe-Phe-DTrp-Lys-Thr-(^{125}I-Tyr)-Thr-Ser-Cys]-OH), [^{125}I][Tyr^3]octreotide (DPhe-c [Cys-(^{125}I-Tyr)-DTrp-Lys-Thr-Cys]-Thr-OH), [^{125}I]CGP 23996 (c[Lys-Asu-Phe-Phe-Trp-Lys-Thr-(^{125}I-Tyr)-Thr-Ser]), [^{125}I][Tyr^{11}]SRIF-14 (Ala-Gly-c[Cys-Lys-Asn-Phe-Phe-Trp-Lys-Thr-(^{125}I-Tyr)-Thr-Ser-Cys]-OH) or [^{125}I][Tyr^{10}]CST-14 (2175 Ci mmol^{-1}, 25–35 pM final concentration), in binding assay buffer containing $MgCl_2$ (5 mM) (for rat cortex experiments using [^{125}I][Tyr^{11}]SRIF-14, NaCl (120 mM) was used instead of $MgCl_2$), and the protease inhibitor bacitracin (5 μg ml^{-1}) and either 50 μl assay buffer (total binding); SRIF-14 at a concentration of 10 μM (non-specific binding) or various test compound concentrations. Experiments were conducted in triplicate. Incubation was terminated after 1 h at room temperature by vacuum filtration through glass fibre filters pre-soaked in 0.3% polyethyleneimine. The filters were washed three times with ice-cold 10 mM Tris–HCl buffer containing 154 mM NaCl, pH 7.4, and dried. Bound radioactivity was measured in a β-scintillation counter (Packard TopCount) using scintillation liquid (80% counting efficiency). Where not specified, chemicals were purchased from Sigma.

2.3. Measurement of forskolin-stimulated cAMP accumulation

CHO cells stably expressing human sst$_2$ receptors and the luciferase reporter gene under the control of the serum responsive element (CHO-SRE-Luci-hsst$_2$) were grown to confluence in 24-well plates. The cells were incubated with 6 μCi ml^{-1} of [^{3}H]adenine (23 Ci mmol^{-1}, Anawa Trading) in 500 μl assay buffer (130 mM NaCl, 5.4 mM KCl, 1.8 mM $CaCl_2$, 0.8 mM $MgSO_4$, 0.9 mM NaH_2PO_4, 25 mM glucose, 20 mM HEPES, pH 7.4) for 2 h at 37 °C. Cells were washed twice with assay buffer containing 1 mM isobutylmethylxanthine and incubated at 37 °C in 1 ml assay buffer containing isobutylmethylxanthine in the absence (basal stimulation) and presence of forskolin (10 μM) with various SRIF-14 or test compound concentrations. Experiments were conducted in duplicate. After 15 min, medium was removed and replaced with 5% (v/v) trichloroacetic acid containing 100 μM ATP and 100 μM cAMP.

After 30 min at 4 °C, [^{3}H]ATP and [^{3}H]cAMP were separated from the trichloroacetic acid extracts by sequential chromatography on Dowex AG 50W-X4 and Alumina columns. Dowex columns were washed with 10 ml H_2O and then loaded with cell extract and 3 ml H_2O. The eluate ([^{3}H]ATP) was measured in a β-scintillation counter. The 8-ml H_2O was loaded onto the Dowex columns; the eluate was loaded on Alumina columns, which had been washed with 0.1 M imidazole (10 ml) and the flow-through discarded. The [^{3}H]cAMP was eluted from the columns with 0.1 M imidazole (6 ml) and measured in a β-scintillation counter. Dowex columns were regenerated with 2 N HCl (10 ml), the alumina columns with 1 M imidazole (5 ml). cAMP formation was calculated as the ratio cAMP/(cAMP + ATP) and data points were calculated as a percentage of the forskolin response (= 100%). Where not specified, chemicals were purchased from Sigma.

2.4. Luciferase assay

CHO-SRE-Luci-hsst$_2$ cells were seeded at 60,000 cells well^{-1} in 96-well plates. After 24 h, the medium was removed and the cells were washed once with phosphate-buffered saline and serum-deprived for 24 h in assay buffer (130 mM NaCl, 5.4 mM KCl, 1.8 mM $CaCl_2$, 0.8 mM $MgSO_4$, 0.9 mM NaH_2PO_4, 25 mM glucose, 20 mM HEPES, 1% (w/v) bovine serum albumin, pH 7.4). The cells were treated for 5 h at 37 °C, 5% CO_2, 95% relative humidity with assay buffer alone (background) or containing various concentrations of SRIF-14 or test compounds in triplicate. Ten percent (v/v) foetal bovine serum was used as a positive control to show that the SRE-Luci construct was functioning in the cells. Cells were lysed in 25 μl lysis buffer (25 mM Tris–phosphate, 2 mM DL-dithiothreitol, 2 mM 1,2-diaminocyclohexane-*N,N,N′,N′*-tetraacetic acid, 10% (v/v) glycerol, 1% (v/v) triton-X, pH 7.8) and, after 15 min, luciferase activity was measured using a Luminoskan luminometer by injection of 50 μl luciferase reaction buffer (20 mM Tris, 1.07 mM $Mg(CO_3)_4$, 2.67 mM $MgSO_4$, 0.1 mM EDTA, 33.3 mM DL-dithiothreitol, 0.27 mM coenzyme A, 0.47 mM D-luciferin, 0.53 mM ATP, pH 7.8). Measuring parameters: lag time 0 s, total integration time 5 s. Activation (% increase over basal) was calculated as: activation (%) = 100 × [(experimenxperimental – background)/background]. Where not specified, chemicals were purchased from Sigma.

2.5. Analysis of data

Radioligand binding data were analysed by non-linear regression curve fitting with the computer program SCTFIT (De Lean, 1979) and pK_d was derived from this fit. Concentration response curves were analysed by non-linear regression curve fitting using the programme Graph Pad Prism. Values of maximal effect and pEC$_{50}$ ($-\log_{10}$ of the concentration producing half the maximal effect) were derived from this fit. Maximal responses of compounds were normalised to the maximal response induced by SRIF-14 alone (= 100%) and this was used as the E_{max} value (relative maximal effect). Results are given as means ± S.E.M. Statistical analysis was also carried out using Graph Pad Prism and unless otherwise indicated. Student's *t*-tests were used to analyse the data.

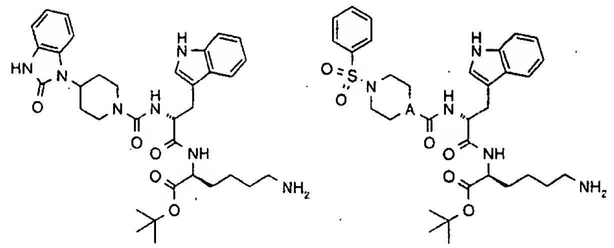

1

2 (A = CH)
3 (A = N)

Fig. 1. Structures of compounds 1 to 3.

Table 2
Agonist effects of compounds

Compound	Forskolin-stimulated cAMP accumulation				Luciferase expression			
	pEC_{50}	S.E.M.	E_{max}	S.E.M.	pEC_{50}	S.E.M.	E_{max}	S.E.M.
SRIF-14	9.79	0.08	100		9.20	0.11	100	
1	9.81	0.13	117.9	3.9	8.99	0.06	124.5	9.9
2	7.89	0.06	119.1	4.2	6.90	0.06	122.5	11.0
3	8.20	0.18	117.5	4.4	7.26	0.07	108.1	8.3

Inhibition of forskolin-stimulated cAMP accumulation and stimulation of luciferase expression in CHO cells expressing human sst_2 receptors. The data are expressed as pEC_{50} values ($-\log_{10}$ of the molar concentration required for a half-maximal effect) and E_{max} (% stimulation of the maximal effect produced by SRIF-14). Data are listed as means ± S.E.M. of at least four determinations.

2.6. Ligands

[^{125}I][Tyr^{11}]SRIF-14, [^{125}I]LTT-SRIF-28, [^{125}I][Tyr^3]octreotide, [^{125}I][Tyr^{10}]cortistatin-14 (Pro-c[Cys-Lys-Asn-Phe-Phe-Trp-Lys-Thr-(^{125}I-Tyr)-Ser-Ser-Cys]-Lys) and [^{125}I]CGP 23996 were custom-synthesised by ANAWA Trading. SRIF-14 (Ala-Gly-c[Cys-Lys-Asn-Phe-Phe-Trp-Lys-Thr-Phe-Thr-Ser-Cys]-OH) was purchased from Bachem (Bubendorf, Switzerland). Compounds **1** to **3** were synthesised at Novartis according to published procedures (Hay et al., 2001a,b) (Fig. 1).

3. Results

3.1. Radioligand binding

The binding potential of the compounds at human recombinant (expressed in CCL39 cells) and native rat (cortex) somatostatin receptors was measured using the agonist radioligands [^{125}I][Tyr^{11}]SRIF-14, [^{125}I]LTT-SRIF-28, [^{125}I]CGP 23996, [^{125}I][Tyr^{10}]CST-14 and [^{125}I][Tyr^3]octreotide (Table 1). Compounds **2** and **3** displayed some selectivity for sst_2 over sst_1, sst_3 and sst_4 with affinities (pK_d) for sst_2 of 6.82–8.92 (**2**) and 6.99–8.23 (**3**), depending on radioligand and tissue used. These values are 10–100-fold lower than those reached by the natural tetradecapeptide SRIF-14. Compound **1** was more sst_2-selective than **2** and **3** with pK_d values (8.4–9.7) 100–10,000-fold greater than for sst_1, sst_3 or sst_4 sites, which were similar to those of SRIF-14. The three compounds showed radioligand-dependent affinities for sst_5, which were relatively high for [^{125}I]CGP 23996- and [^{125}I][Tyr^3]octreotide-labelled sites (7.17–7.97 and 7.34–8.24, respectively), but considerably lower for [^{125}I]LTT-SRIF-28- and [^{125}I][Tyr^{10}]CST-14-labelled sites (5.95–6.90 and 5.58–6.46, respectively). We therefore decided to examine

Table 1
Affinity of compounds 1, 2 and 3 for somatostatin receptors, either native in rat cortex or human recombinant expressed in CCL39 cells

Receptor	Ligand	Receptor, tissue/cells	1		2		3	
			pK_d	S.E.M.	pK_d	S.E.M.	pK_d	S.E.M.
sst_1	[^{125}I][Tyr^{11}]SRIF-14	rat, cortex	5.33	0.13	5.01	0.20	5.02	0.07
	[^{125}I]LTT-SRIF-28	human, CCL39	5.55	0.02	5.26	0.04	5.24	0.02
	[^{125}I]CGP 23996	human, CCL39	5.73	0.04	5.51	0.06	5.44	0.02
	[^{125}I][Tyr^{10}]CST-14	human, CCL39	5.35	0.04	5.23	0.01	5.24	0.02
sst_2	[^{125}I][Tyr^3]octreotide	rat, cortex	8.40	0.03	6.82	0.06	6.99	0.10
	[^{125}I][Tyr^3]octreotide	human, CCL39	8.98	0.14	7.74	0.10	7.82	0.10
	[^{125}I]LTT-SRIF-28	human, CCL39	9.25	0.01	7.73	0.02	7.72	0.03
	[^{125}I]CGP 23996	human, CCL39	9.66	0.10	7.94	0.04	8.03	0.09
	[^{125}I][Tyr^{10}]CST-14	human, CCL39	9.47	0.19	8.92	0.13	8.23	0.06
sst_3	[^{125}I]LTT-SRIF-28	human, CCL39	6.61	0.03	5.57	0.04	6.13	0.02
	[^{125}I]CGP 23996	human, CCL39	7.08	0.12	6.08	0.11	6.85	0.06
	[^{125}I][Tyr^{10}]CST-14	human, CCL39	6.62	0.10	5.51	0.08	6.06	0.14
sst_4	[^{125}I]LTT-SRIF-28	human, CCL39	6.88	0.04	6.62	0.10	6.62	0.04
	[^{125}I]CGP 23996	human, CCL39	6.41	0.02	6.29	0.02	6.05	0.02
	[^{125}I][Tyr^{10}]CST-14	human, CCL39	5.58	0.20	5.66	0.21	5.29	0.2
sst_5	[^{125}I][Tyr^3]octreotide	human, CCL39	8.24	0.06	7.34	0.05	8.17	0.03
	[^{125}I]LTT-SRIF-28	human, CCL39	6.90	0.10	5.95	0.09	6.84	0.01
	[^{125}I]CGP 23996	human, CCL39	7.93	0.07	7.17	0.09	7.97	0.09
	[^{125}I][Tyr^{10}]CST-14	human, CCL39	6.43	0.01	5.58	0.04	6.46	0.02

The data are listed as pK_d values ± S.E.M. of n = at least three independent values.

the functional effects of the compounds on sst_2 receptors to test for possible agonism and/or antagonism.

3.2. *Forskolin-stimulated adenylate cyclase*

SRIF-14 inhibited forskolin-stimulated adenylate cyclase in CHO cells expressing human sst_2 receptors in a concentration-dependent manner with maximal inhibition of 55.7 ± 3.2% and high potency (pEC_{50}: 9.79 ± 0.08) (Table 2, Fig. 2). All three compounds inhibited forskolin-stimulated adenylate cyclase with greater relative efficacy than SRIF-14 (E_{max}: 117.9 ± 3.9%, 119.1 ± 4.2% and 117.5 ± 4.4% relative intrinsic activity; **1**, **2** and **3**, respectively). Compound **1** was as potent as SRIF-14 (pEC_{50}: 9.81 ± 0.13), while **2** and **3** were 10- to 40-fold less potent than SRIF-14 (pEC_{50}: 8.89 ± 0.06 and 8.20 ± 0.18, respectively). The relative efficacy of the compounds was too high to enable antagonist properties of the compounds against SRIF-14 mediated inhibition of forskolin-stimulated adenylate cyclase to be measured.

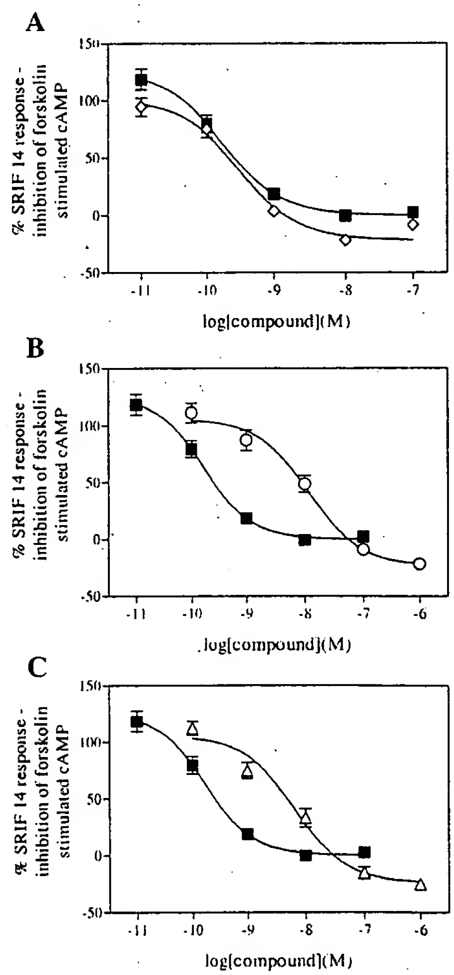

Fig. 2. Inhibition of forskolin-stimulated adenylate cyclase activity in CHO cells stably expressing human sst_2 receptors. [^{3}H]Adenine-loaded cells were incubated at 37 °C in the absence (basal) and presence of forskolin and the indicated concentrations of SRIF-14 (■) and (A) **1** (◇), (B) **2** (O) and (C) **3** (Δ). After 15 min, cells were lysed, and [^{3}H]ATP and [^{3}H]cAMP fraction were separated by sequential chromatography. Data is expressed as percentage of the forskolin response (= 100%). All plots represent one example of at least three experiments.

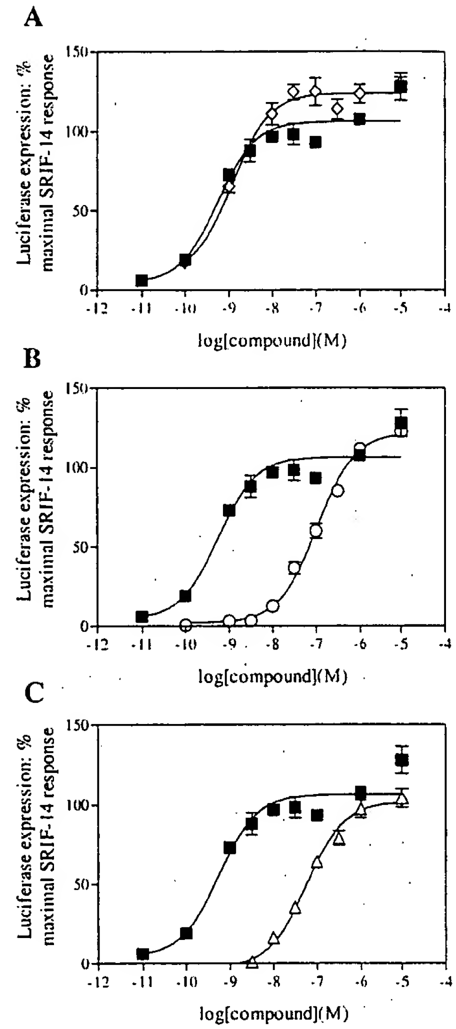

Fig. 3. Stimulation of luciferase reporter gene activity in CHO cells stably expressing human sst_2 receptors. Cells were incubated at 37 °C, 5% CO_2, 95% relative humidity with triplicates of the indicated concentrations of SRIF-14 (■) and (A) **1** (◇), (B) **2** (O) and (C) **3** (Δ). Cells were lysed after 5 h and luciferase activity was measured using a luminometer. Data is expressed as percent stimulation of maximal SRIF-14 effect. All plots represent one example of at least three experiments.

3.3. *Luciferase expression*

SRIF-14 produced a concentration-dependent increase in luciferase expression in CHO cells expressing human sst_2 and the luciferase reporter gene under the control of the serum responsive element (pEC_{50}: 9.20 ± 0.11), with maximal stimulation of five- to six-fold over basal levels (Table 2, Fig. 3). As in forskolin-stimulated adenylate cyclase, all three compounds had similar/greater relative efficacy to

SRIF-14. Compound **1** was as potent as SRIF-14 (pEC_{50}: 8.99 ± 0.06), while **2** and **3** were 100- to 200-fold less potent (pEC_{50}: 6.90 ± 0.11 and 7.26 ± 0.07, respectively). Potency was significantly lower than that measured in forskolin-stimulated adenylate cyclase for all three compounds ($P<0.0001$, $n \geq 12$). The intrinsic efficacy of the compounds was too high to enable antagonist properties of the compounds against SRIF-14-mediated stimulation of luciferase expression to be measured.

4. Discussion

The neuropeptide/neurohormone somatostatin exerts its effects via binding to specific G-protein coupled receptors, of which five subtypes have been shown to exist by molecular cloning. The five subtypes may be expressed in the same tissue and even cell, and therefore the availability of receptor-subtype-selective agonist and antagonist ligands would be extremely useful, as tools to elucidate the physiological contribution of individual receptor subtypes. Unfortunately, very few receptor subtype-selective ligands have been developed thus far (for review, see Hannon et al., 2002).

A recent publication reported the structures of a number of compounds which were reported to be sst_2 antagonists (Hay et al., 2001a). These compounds are non-peptides and are based on the structure of the non-peptide somatostatin receptor subtype selective agonists recently developed at Merck (Rohrer et al., 1998; Rohrer and Berk, 1999; Yang et al., 1998a), which have been shown to mediate inhibition of growth hormone release from rat anterior pituitary, and glucagon release from rat pancreas at nanomolar concentrations (Yang et al., 1998a).

Thus, the aim of the present study was to further characterise the properties of three compounds from the study by Hay et al. (2001a)—the initial agonist compound, **1**, which was the lead compound for antagonist development, and two of the antagonists, **2** and **3** (corresponding to compounds **6**, **7e** and **7a**, respectively, in the paper by Hay et al., 2001a).

In radioligand binding studies in native rat cortex, and in CCL39 cells expressing recombinant human somatostatin receptors, all three compounds bound with high (nanomolar) affinity to sst_2 receptors, with **1** having 10–100-fold higher affinity than **2** and **3**. This is in agreement with Hay et al. (2001a), who report IC_{50} values of 0.26, 2.9 and 3.2 nM for **1**, **2** and **3**, respectively, and this was similar to affinity values for the natural peptide ligand SRIF-14. While all three compounds were selective for sst_2 over $sst_{1,\ 3\ \text{and}\ 4}$, they also bound with high affinity to $[^{125}I][Tyr^3]$octreotide- and $[^{125}I]$CGP 23996-labelled sst_5 sites, suggesting that they may not be entirely selective for sst_2. The compounds displayed somewhat lower affinity for sst_5 labelled by $[^{125}I]$LTT-SRIF-28 and $[^{125}I][Tyr^{10}]$CST-14; however, we have previously shown this to be the case for a number of ligands including octreotide, L362,855 and cortistatin, and we suggested that this may be caused by some ligands having higher affinity for receptors, which are in a G-protein-coupled state ($[^{125}I][Tyr^3]$octreotide- and $[^{125}I]$CGP 23996-labelled sites), than for receptors which may be less well coupled to G-proteins ($[^{125}I]$LTT-SRIF-28- or $[^{125}I][Tyr^{10}]$CST-14-labelled sites; Siehler et al., 1999).

In functional studies, namely measurement of inhibition of forskolin-stimulated adenylate cyclase and agonist-driven expression of the luciferase reporter gene, both the agonist and, surprisingly, the two 'antagonists' displayed full agonist properties. Thus, **1** was a full agonist with potency and efficacy similar to that of SRIF-14, as shown previously. Compounds **2** and **3** were also full agonists, but had lower potency than SRIF-14. All three compounds were more potent at inhibiting forskolin-stimulated adenylate cyclase than stimulating luciferase expression, which may be less well coupled.

Due to the high intrinsic efficacy of the compounds, we could not measure antagonist potential and would therefore conclude from these data that in our system these compounds are in fact agonists rather, than antagonists. This is in contrast to what has previously been reported for these compounds.

It is possible that the differences observed are due to differences in the systems used in this study: we are using recombinant human sst_2 receptors expressed in CHO cells, whereas previous cAMP experiments were carried out in rat pituitary GH_4C_1 cells which may have different complements of G-proteins and enzyme isoforms. Interestingly, we have found that in mouse pituitary AtT-20 cells, **2** has only very low potency in forskolin-stimulated adenylate cyclase (6.61), although still with high relative efficacy (88% of SRIF-14 response; Cervia et al., in press). Therefore, the compound may have lower affinity and agonist potential at rodent receptors than at human receptors. Alternatively, the recombinant system used in this study may be "overexpressed", causing an agonist response to be observed, when in natural systems (AtT-20 and GH_4C_1) where receptor density and coupling efficiency may be lower, the compounds are antagonists, although this is more normal for compounds which have a tendency to be partial agonists, even in recombinant systems, unlike the full agonism demonstrated by these compounds.

Alternatively, it is possible that the compounds are producing antagonism through a mechanism, which is not mediated by sst_2 receptors. Previously, the binding affinity at other receptors was not established as the compounds were tested in mouse neuroblastoma Neuro 2A cells which naturally express mainly sst_2 receptors, but may also express very low amounts (10% of total binding sites) of sst_3 and sst_5 (Koenig et al., 1997). The Neuro 2A cells used in that study had also been transfected with porcine sst_2 (Hay et al., 2001a). In our binding studies, the compounds bind to both sst_2 and sst_5 receptors with high affinity, suggesting a possible antagonist action at sst_5. However, this does not

account for the antagonism shown previously in GH_4C_1 cells where sst_1 and sst_2 are the predominant receptors (Florio et al., 1994; Gu et al., 1995).

Finally, it is possible that the antagonism displayed previously by these compounds is not mediated via somatostatin receptors, but a receptor for another neuropeptide or other neurotransmitter. The antagonism of somatostatin-mediated effects shown previously was assumed, from a reversal of somatostatin-mediated inhibition of VIP-stimulated cAMP accumulation. However, this effect could equally be caused by a VIP agonist as a somatostatin antagonist or by an effect (either antagonistic or agonistic) at another receptor, which causes an increase in cAMP. As the GH_4C_1 cells used in that study are cells derived from pituitary tumours (Tashjian, 1979; Dorflinger and Schonbrunn, 1983), they are likely to endogenously express receptors for any number of neuropeptides and neurotransmitters. It is perfectly possible for a compound to have agonist/antagonist properties at different receptors-as shown recently by Liu et al. (2000), who synthesised a compound which bound with high affinity to both somatostatin and tachykinin NK_1 receptors, acting as an agonist at somatostatin receptors, but as an antagonist at tachykinin NK_1 receptors.

In summary, putative sst_2-selective agonist and antagonist compounds were characterised in in vitro systems. While the agonist compound is indeed a highly sst_2-selective compound with potency similar to that of SRIF-14, the two antagonists that were tested both exhibited agonist properties in forskolin-stimulated adenylate cyclase and stimulation of luciferase expression, and may also show significant activity at sst_5 receptors.

Acknowledgements

This work was supported by EC contract QLG3-CT-1999-00908 and Swiss grant BBW 00-0427.

References

Bass, R.T., Buckwalter, B.L., Patel, B.P., Pausch, M.H., Price, L.A., Strnad, J., Hadcock, J.R., 1996. Identification and characterization of novel somatostatin antagonists [Erratum appears in Mol. Pharmacol. Jan. 1997;51(1):170]. Mol. Pharmacol. 50, 709–715.

Baumbach, W.R., Carrick, T.A., Pausch, M.H., Bingham, B., Carmignac, D., Robinson, I.C., Houghten, R., Eppler, C.M., Price, L.A., Zysk, J.R., 1998. A linear hexapeptide somatostatin antagonist blocks somatostatin activity in vitro and influences growth hormone release in rats. Mol. Pharmacol. 54, 864–873.

Brazeau, P., Vale, W., Burgus, R., Ling, N., Butcher, M., Rivier, J., Guillemin, R., 1973. Hypothalamic polypeptide that inhibits the secretion of immunoreactive pituitary growth hormone. Science 179, 77–79.

Cervia, D., Nunn, C., Fehlmann, D., Langenegger, D., Schuepbach, E., Hoyer, D., 2003. Pharmacological characterisation of native somatostatin receptors in AtT-20 mouse tumour corticotrophs. Br. J. Pharmacol. (in press).

De Lean, 1979. SCTFIT: a computer program for simultaneous analysis of saturation and competition curves. Howard Hughes Medical Institute, Duke University Medical Center, Durham, NC.

Dorflinger, L.J., Schonbrunn, A., 1983. Somatostatin inhibits vasoactive intestinal peptide-stimulated cyclic adenosine monophosphate accumulation in GH pituitary cells. Endocrinology 113, 1541–1550.

Epelbaum, J., Dournaud, P., Fodor, M., Viollet, C., 1994. The neurobiology of somatostatin. Crit. Rev. Neurobiol. 8, 25–44.

Florio, T., Rim, C., Hershberger, R.E., Loda, M., Stork, P.J., 1994. The somatostatin receptor SSTR1 is coupled to phosphotyrosine phosphatase activity in CHO-K1 cells. Mol. Endocrinol. 8, 1289–1297.

Gu, Y.Z., Brown, P.J., Loose-Mitchell, D.S., Stork, P.J.S., Schonbrunn, A., 1995. Development and use of a receptor antibody to characterize the interaction between somatostatin receptor subtype 1 and G proteins. Mol. Pharmacol. 48, 1004–1014.

Hannon, J.P., Nunn, C., Stolz, B., Bruns, C., Weckbecker, G., Lewis, I., Troxler, T., Hurth, K., Hoyer, D., 2002. Drug design at peptide receptors: somatostatin receptor ligands. J. Mol. Neurosci. 18, 15–27.

Hay, B.A., Cole, B.M., DiCapua, F.M., Kirk, G.W., Murray, M.C., Nardone, R.A., Pelletier, D.J., Ricketts, A.P., Robertson, A.S., Siegel, T.W., 2001a. Small molecule somatostatin receptor subtype-2 antagonists. Bioorg. Med. Chem. Lett. 11, 2731–2734.

Hay, B.A., Cole, B.M., Ricketts, A.P., 2001b. Somatostatin antagonists and agonists that act at the SST subtype 2 receptor. European Patent Application EP 1 086 947 A1.

Hocart, S.J., Jain, R., Murphy, W.A., Taylor, J.E., Morgan, B., Coy, D.H., 1998. Potent antagonists of somatostatin: synthesis and biology. J. Med. Chem. 41, 1146–1154.

Hocart, S.J., Jain, R., Murphy, W.A., Taylor, J.E., Coy, D.H., 1999. Highly potent cyclic disulfide antagonists of somatostatin. J. Med. Chem. 42, 1863–1871.

Hoyer, D., Luebbert, H., Bruns, C., 1994. Molecular pharmacology of somatostatin receptors. Naunyn-Schmiedeberg's Arch. Pharmacol. 350, 441–453.

Hoyer, D., Bell, G.I., Berelowitz, M., Epelbaum, J., Feniuk, W., Humphrey, P.P., O'Carroll, A.M., Patel, Y.C., Schonbrunn, A., Taylor, J.E., Reisine, T., 1995. Classification and nomenclature of somatostatin receptors. Trends Pharmacol. Sci. 16, 86–88.

Koenig, J.A., Edwardson, J.M., Humphrey, P.P., 1997. Somatostatin receptors in Neuro2A neuroblastoma cells: ligand internalization. Br. J. Pharmacol. 120, 52–59.

Krulich, L., Dhariwal, A.P., McCann, S.M., 1968. Stimulatory and inhibitory effects of purified hypothalamic extracts on growth hormone release from rat pituitary in vitro. Endocrinology 83, 783–790.

Liu, J., Underwood, D.J., Cascieri, M.A., Rohrer, S.P., Cantin, L.D., Chicchi, G., Smith, A.B., Hirschmann, R., 2000. Synthesis of a substance P antagonist with a somatostatin scaffold: factors affecting agonism/antagonism at GPCRs and the role of pseudosymmetry. J. Med. Chem. 43, 3827–3831.

Martin, J.L., Chesselet, M.F., Raynor, K., Gonzales, C., Reisine, T., 1991. Differential distribution of somatostatin receptor subtypes in rat brain revealed by newly developed somatostatin analogs. Neuroscience 41, 581–593.

Patel, Y.C., 1997. Molecular pharmacology of somatostatin receptor subtypes. J. Endocrinol. Invest. 20, 348–367.

Patel, Y.C., 1999. Somatostatin and its receptor family. Front. Neuroendocrinol. 20, 157–198.

Raynor, K., Reisine, T., 1989. Analogs of somatostatin selectively label distinct subtypes of somatostatin receptors in rat brain. J. Pharmacol. Exp. Ther. 251, 510–517.

Raynor, K., Coy, D.C., Reisine, T., 1992. Analogs of somatostatin bind selectively to brain somatostatin receptor subtypes. J. Neurochem. 59, 1241–1250.

Raynor, K., O'Carroll, A.M., Kong, H., Yasuda, K., Mahana, L.C., Bell, G.I., Reisine, T., 1993. Characterization of cloned somatostatin receptors SSTR4 and SSTR5. Mol. Pharmacol. 44, 385–392.

Reubi, J.C., 1984. Evidence for two somatostatin-14 receptor types in rat brain cortex. Neurosci. Lett. 49, 259–263.

Rohrer, S.P., Berk, S.C., 1999. Development of somatostatin receptor subtype selective agonists through combinatorial chemistry. Curr. Opin. Drug Discov. Dev. 2, 293–303.

Rohrer, S.P., Birzin, E.T., Mosley, R.T., Berk, S.C., Hutchins, S.M., Shen, D.M., Xiong, Y., Hayes, E.C., Parmar, R.M., Foor, F., Mitra, S.W., Degrado, S.J., Shu, M., Klopp, J.M., Cai, S.J., Blake, A., Chan, W.W.S., Pasternak, A., Yang, L., Patchett, A.A., Smith, R.G., Chapman, K.T., Schaeffer, J.M., 1998. Rapid identification of subtype-selective agonists of the somatostatin receptor through combinatorial chemistry. Science 282, 737–740.

Rossowski, W.J., Cheng, B.L., Jiang, N.Y., Coy, D.H., 1998. Examination of somatostatin involvement in the inhibitory action of GIP, GLP-1, amylin and adrenomedullin on gastric acid release using a new SRIF antagonist analogue. Br. J. Pharmacol. 125, 1081–1087.

Schindler, M., Kidd, E.J., Carruthers, A.M., Wyatt, M.A., Jarvie, E.M., Sellers, L.A., Feniuk, W., Humphrey, P.P.A., 1998. Molecular cloning and functional characterization of a rat somatostatin sst_{2b} receptor splice variant. Br. J. Pharmacol. 125, 209–217.

Siehler, S., Seuwen, K., Hoyer, D., 1999. Characterization of human recombinant somatostatin receptors: 1. Radioligand binding studies. Naunyn-Schmiedeberg's Arch. Pharmacol. 360, 488–499.

Tashjian Jr., A.H., 1979. Clonal strains of hormone-producing pituitary cells. Methods Enzymol. 58, 527–535.

Tran, V.T., Beal, M.F., Martin, J.B., 1985. Two types of somatostatin receptors differentiated by cyclic somatostatin analogs. Science 228, 492–495.

Vanetti, M., Kouba, M., Wang, X., Vogt, G., Hollt, V., 1992. Cloning and expression of a novel mouse somatostatin receptor (SSTR2B). FEBS Lett. 311, 290–294.

Yang, L., Berk, S.C., Rohrer, S.P., Mosley, R.T., Guo, L., Underwood, D.J., Arison, B.H., Birzin, E.T., Hayes, E.C., Mitra, S.W., Parmar, R.M., Cheng, K., Wu, T.-J., Butler, B.S., Foor, F., Pasternak, A., Pan, Y., Silva, M., Freidinger, R.M., Smith, R.G., Chapman, K., Schaeffer, J.M., Patchett, A.A., 1998a. Synthesis and biological activities of potent peptidomimetics selective for somatostatin receptor subtype 2. Proc. Natl. Acad. Sci. U. S. A. 95, 10836–10841.

Yang, L., Guo, L., Pasternak, A., Mosley, R., Rohrer, S., Birzin, E., Foor, F., Cheng, K., Schaeffer, J., Patchett, A.A., 1998b. Spiro[1*H*-indene-1,4′-piperidine] derivatives as potent and selective non-peptide human somatostatin receptor subtype 2 (sst_2) agonists. J. Med. Chem. 41, 2175–2179.

0026-895X/96/040709-07$3.00/0

MOLECULAR PHARMACOLOGY, 50:709–715 (1996).

ACCELERATED COMMUNICATIONS

Identification and Characterization of Novel Somatostatin Antagonists

ROY T. BASS, BRIAN L. BUCKWALTER, BOMI P. PATEL, MARK H. PAUSCH, LAURA A. PRICE, JOANN STRNAD,[1] and JOHN R. HADCOCK[1]

Cyanamid Agricultural Research Center, Princeton, NJ 08543-0400

Received June 3, 1996; Accepted July 17, 1996

SUMMARY

The study of the five somatostatin receptor subtypes (SST_x, where *x* is the subtype number) has been hampered by the lack of high affinity antagonists. Potent and selective antagonists would increase our understanding of SST structure, function, and regulation. In this study, the identification of novel disulfide-linked cyclic octapeptide antagonists of somatostatin is described. The antagonists contain a core structure of a DL-cysteine pair at positions 2 and 7 of the peptides. Substitution of a D-cysteine at position 2 with an L-cysteine converts the full antagonist into a full agonist. All somatostatin receptor subtypes are coupled to inhibition of adenylate cyclase. The functional properties of these peptides have been determined in radioligand binding assays, in functional coupling of the SST_2 subtype to yeast pheromone response pathway, and in cAMP accumulations. One peptide antagonist [Ac-4-NO_2-Phe-c(D-Cys-Tyr-D-Trp-Lys-Thr-Cys)-D-Tyr-NH_2] displays a binding affinity to SST_2 comparable with that observed for the native hormone (K_i = 0.2 nM) and reverses somatostatin-mediated inhibition of cAMP accumulation in rat somatomammotroph GH_4C_1 cells, cells transfected with the SST_2 and SST_5 subtypes, as well as somatostatin-stimulated growth of yeast cells expressing the SST_2 subtype. This class of somatostatin antagonists, which are the first to be described, should be useful for determination of somatostatin's diverse functions *in vivo* and *in vitro*.

The cyclic tetradecapeptide somatostatin is a potent regulator of endocrine function by inhibiting the secretion of growth hormone from the pituitary, glucagon and insulin from the pancreas, and gastrin from the gut. Somatostatin also functions as a neurotransmitter and a neuromodulator in the central nervous system and peripheral tissues (1). The effects of somatostatin are transduced through binding of the hormone to high affinity, G protein-coupled somatostatin receptors (SST_x, where *x* is the subtype number) encoded in five distinct subtypes (2). These five different subtypes account for the majority of tissue-specific differences in response to somatostatin (3–9). SSTs modulate the activity of several different classes of effector molecules, including activation of potassium channels, serine/threonine and tyrosine phosphatases, Na^+/H^+ antiporters, and inhibition of calcium channels and adenylyl cyclases by transducing the signal from receptor to the effector through G proteins (10–18).

Somatostatin's central role in regulating endocrine function has made it an important research target. Many highly active analogs have been described; the comparative simplicity of many of these molecules, along with the availability of the receptor subtypes, has made somatostatin an excellent model for probing peptide-receptor interactions. Veber and his co-workers demonstrated that only four of the amino acid residues in somatostatin were required for full activity. Their general strategy has been to retain the crucial Phe^7-D-Trp^8-Lys^9-Thr^{10} segment (somatostatin numbering) and incorporate a variety of cyclic and bicyclic restraints to stabilize the β-type II turn about the conserved residues (19). The cyclic SST_2/SST_5-selective hexapeptide, MK-678 (Table 1), is a superagonist with 50% greater potency than somatostatin. A disulfide bond can also stabilize a β-turn. This ultimately led to the discovery and development of the potent, long-lasting somatostatin agonist SMS 201–995 (octreotide) by Bauer *et al.* (20). This octapeptide skeleton has become an excellent template for analog synthesis and a variety of potent somatostatin analogs have been prepared. Cai *et al.*, Murphy *et al.*, and Weinants *et al.* studied extensively the related disulfides and described the biological activity and conformation of numerous potent agonists (21–23). Among their most active

[1] Current affiliation: Wyeth-Ayerst Research, Princeton, NJ 08543-8000

ABBREVIATIONS: SST, somatostatin receptor; S-14, somatostatin-14; SRIF, somatostatin response inhibitory factor; FMOC, 9-fluorenylmethoxycarbonyl; DMSO, dimethylsulfoxide; TFA, trifluoroacetic acid; EDT, ethanedithiol; EGTA, ethylene glycol bis(β-aminoethyl ether)-*N,N,N′,N′*-tetraacetic acid; SC, synthetic complete; HEK, human embryonic kidney; HEPES, 4-(2-hydroxyethyl)-1-piperazineethanesulfonic acid.

TABLE 1
Structures of somatostatin peptide analogs

S-14	Ala-Gly-c[Cys-Lys-Asn-Phe^6-Phe-Trp^8-Lys-Thr-Phe-Thr-Ser-Cys]-OH
MK-678	c[N-Me-Ala-Tyr-D-Trp-Lys-Val-Thr]
SMS 201-995	H_2N-D-Phe-c[Cys-Phe-D-Trp-Lys-Thr-Cys]-Thr-ol
NC4-28-B	H_2N-D-Phe-c[Cys-Tyr-D-Trp-Lys-Ser-Cys]-Nal-NH_2
RC-160	H_2N-D-Phe-c[Cys-Tyr-D-Trp-Lys-Val-Cys]-Thr-NH_2
BIM-23066	H_2N-D-Phe-p-NO_2-Phe-Tyr-D-Trp-Lys-Val-Phe-Thr-NH_2
1	H_2N-4-NO_2-Phe-c[Cys-Tyr-D-Trp-Lys-Val-Cys]-Tyr-NH_2
2	H_2N-4-NO_2-Phe-c[D-Cys-Tyr-D-Trp-Lys-Val-Cys]-Tyr-NH_2
3	AcNH-4-NO_2-Phe-c[Cys-Tyr-D-Trp-Lys-Thr-Cys]-Tyr-NH_2
4	AcNH-4-NO_2-Phe-c[D-Cys-Tyr-D-Trp-Lys-Thr-Cys]-Tyr-NH_2
5	H_2N-4-NO_2-D-Phe-c[D-Cys-Tyr-D-Trp-Lys-Val-Cys]-Tyr-NH_2

agonists were RC-160 (21) and NC4-28-B (23) (Table 1), which are closely related to octreotide. More recently, Raynor *et al.* have shown that linear peptides (e.g., BIM-23066) also can bind to the somatostatin receptor, and these compounds exhibit subtype selectivity (24). Throughout the development of these highly potent somatostatin ligands, however, none has yet been described that is an effective antagonist of somatostatin. Potent antagonists would be a useful pharmacological tool for studying somatostatin actions and potentially enhancing the secretion of growth hormone, insulin, and other hormones.

Experimental Procedures

Materials. Protected amino acids and 1-hydroxy-benzotriazole were purchased from SNPE, Inc. (Princeton, NJ); FMOC-*p*-nitrophenylalanine and FMOC-D-tyrosine were purchased from Bachem Bioscience (King of Prussia, PA); FMOC-D-cysteine was purchased from Advanced Chemtech (Louisville, KY); dimethylformamide was purchased from Baxter (Edison, NJ); piperidine, TFA, EDT, and diisopropylethylamine were purchased from Aldrich Chemical (Milwaukee WI); BOP was purchased from Richealieu Biotechnologies (Montreal, Quebec, Canada); anhydrous ether and DMSO were purchased from J. T. Baker (Phillipsburg, NJ); leupeptin was purchased from Bachem (Philadelphia, PA); aprotinin, bacitracin, and benzamidine were purchased from Sigma (St. Louis, MO) and ^{125}I-Tyr^{11}S-14 was purchased from Amersham (Arlington Heights, IL).

Peptide synthesis. The automated, continuous-flow, solid-phase synthesis of peptides was carried out on FMOC-PAL-PEG resin (Millipore, Burlington, MA) in a Millipore 9050 Peptide Synthesizer by standard protocols. Free peptides (0.3 mmol) were cleaved from the resin by stirring in 30 ml of 5% EDT in TFA for 4 hr at 25°. The resin was removed by filtration, the TFA evaporated and the crude peptide was precipitated with anhydrous ether.

The cyclic disulfide was formed by stirring the crude peptide in 250 ml of DMSO (25) (20–50%) in water for 24–48 hr at 25° until the solution was negative to Ellman's reagent (26). DMSO and water were evaporated and the crude cyclic peptides were purified by high performance liquid chromatography on a C18 column (300 Å, 12 mm, 21.4- × 250-mm column (Rainin Instruments, Woburn, MA) with a linear gradient of acetonitrile in 0.1% TFA in water. The fraction containing the peptide was evaporated and the residue was lyophilized. Homogeneity was confirmed by reversed-phase analytical high performance liquid chromatography (>98%) and electrospray mass spectrometry. Yields ranged from 9% to 27%.

Cloning and expression of somatostatin receptor subtypes. The cloning and expression of rat SST$_1$, SST$_2$, and SST$_5$ have been described previously (15, 27, 28). Rat SST$_3$ cDNA was cloned using a polymerase chain reaction-based strategy.[2] SST$_1$, SST$_2$, and SST$_3$ were expressed in Chinese hamster ovary cells. SST$_5$ was expressed in HEK 293 cells.

Membrane preparation. Crude plasma membranes were prepared according to Hadcock *et al.* (29). Cells were detached from plates with phosphate-buffered saline, pH 7.4, and 2 mM EDTA and centrifuged at 1500 × *g* for 10 min at 4°. Cells were then resuspended in 10 ml of homogenization buffer (1 mM sodium bicarbonate, pH 7.4, 1 mM EDTA, 1 mM EGTA, 5 μg/ml leupeptin, 5 μg/ml aprotinin, 100 μg/ml bacitracin, 100 μg/ml benzamidine) for 10 min on ice. The cells were lysed in a glass/glass dounce homogenizer (20 strokes). The lysates were centrifuged at 1500 × *g* for 10 min at 4°. The supernatant was centrifuged at 40,000 × *g* for 20 min at 4°. This step was repeated twice. The pellet was then resuspended at 1–5 mg/ml in binding buffer (50 mM HEPES, pH 7.4, 5 mM $MgCl_2$, 0.25% bovine serum albumin) and stored at -80°.

Radioligand binding. All radioligand binding assays were performed in 96-well microtiter plates using binding buffer that contained protease inhibitors (5 μg/ml leupeptin, 5 μg/ml aprotinin, 100 μg/ml bacitracin, and 100 μg/ml benzamidine). ^{125}I-Tyr^{11}S-14 (150,000 cpm at 2,000 Ci/mmole, 250 pM final concentration). The final volume was 200 μl/well. All incubations were carried out at 25° for 2 hr. Free radioligand was separated from bound ligand by rapid filtration through a glass fiber filter (IH-201-HA) using an Inotech cell harvester. The filter was then washed several times with cold (4°) binding buffer without bovine serum albumin and protease inhibitors before counting in an LKB γ master counter (Wallac, Gaithersburg, MD) (78% efficiency).

cAMP accumulations. cAMP accumulation was measured in intact GH$_4$C$_1$ cells and cells that express SST$_2$ and SST$_5$ subtypes as described previously (27). Inhibition of cAMP accumulation was measured in the presence of 10 μM forskolin. Cells were detached from plates and suspended in Krebs-Ringer phosphate buffer containing 2 mM $CaCl_2$ and 100 μM isobutylmethylxanthine. Reactions (50,000 cells per assay tube) were allowed to proceed for 15 min at 37° and were terminated by the addition of 1 N HCl. The samples were then heated for 3 min at 100° and neutralized with 1 N NaOH. Amounts of cAMP in each sample were determined as described by Hadcock *et al.* (30).

Yeast expression. Assay of stimulation and inhibition of growth of yeast in response to somatostatin receptor agonists and antagonists was performed as described (31) except that 0.2% sucrose was added to improve growth conditions. LY268 cells were plated in agar medium in the absence (agonist plate) or presence (antagonist plate) of 100 nM S-14. Somatostatin analogs (in 5 μl of DMSO) were applied to the plates directly or on sterile filter disks. The plates were then incubated at 30° for 48 hr.

Data analysis. All data were analyzed using GraphPAD Prism (San Diego, CA) and are presented as the mean ± standard deviation unless otherwise noted. K_i values were determined using the equation of Cheng and Prusoff (32).

Results and Discussion

Raynor *et al.* reported recently a series of linear peptides that exhibited subtype selectivity (24). One of these analogs, BIM-23066 (Table 1), contained a 4-NO_2-Phe residue. BIM-

[2] R. T. Bass, B. L. Buckwalter, B. P. Patel, M. H. Pausch, L. A. Price, J. Strnad, and J. R. Hadcock, manuscript in preparation.

23066 has an affinity for the SST_2 that is comparable with related peptides in described in Table 1 but had a very weak effect on growth hormone levels. We believe this suggests an analog with potential antagonist properties. In earlier work in our laboratories with related D-Cys[1],Cys[8] cyclic octapeptides, compounds that ultimately proved to be agonists, we noted that substitution of the aromatic side-chain residues of position 2 or 3 of these related analogs frequently led to substantial increases in affinity for the SST_2.

We decided to investigate the effect of substitution of the corresponding aromatic side chains in the related Cys[2], Cys[7] octapeptide series (1-5). Bauer *et al.*, Cai *et al.*, Murphy *et al.*, and Weinants *et al.* have shown that this backbone is an effective ligand for the SST_2. In addition to a clearly demonstrated utility in the somatostatin series, we were intrigued by the apparent utility of this scaffold for preparing agonists and antagonists of a variety of other G protein-coupled peptide receptors. Hruby *et al.* developed oxytocin antagonists that use a cyclic disulfide scaffold (33). Pelton *et al.* (34) and Walker *et al.* (35) have independently demonstrated that molecular modification can convert a potent cyclic disulfide somatostatin agonist with weak binding to opioid receptors into potent μ-selective opioid antagonists with little residual somatostatin activity. More recently, Orbuch *et al.* followed a similar strategy to convert a somatostatin agonist into a neuromedin B antagonist (36). The last two receptors were particularly interesting because their endogenous ligands are linear peptides, not cyclic disulfides. Thus, there seems to be sufficient structural homology among these seven membrane-spanning G-protein-linked peptide receptors to accommodate the 20-membered cyclic peptides at the binding site; receptor selective agonist/antagonist properties can be conferred by optimizing the side-chain structure and the stereochemistry of the amino acids. The role of the side chains in relation to the peptide backbone has been explored and emphasized by several groups (37, 38).

We report herein the preparation of two pairs of cyclic disulfide somatostatin analogs, 1-2 and 3-4, which differ primarily at position 6 (octapeptide numbering). The former pair have a valine residue at position 6, whereas the latter have a threonine residue and the amino terminus is acetylated. Both valine and threonine are known to produce somatostatin agonists; valine generally exhibits higher affinity binding (39). *N*-acetylation did not qualitatively alter their properties.

Three different assays were used to characterize the pharmacological properties of these peptide analogs *in vitro*: competition binding assays with individual somatostatin receptor subtypes (Table 2), cAMP accumulation assays in rat GH_4C_1 somatomammotroph cells and cells that express the SST_2 and SST_5 subtypes (Table 3), and a novel yeast-based expression system for SST_2 subtype (31).

TABLE 2

Binding affinities to SST subtypes for peptide analogs in the current study

Membranes from CHO or HEK 293 cells expressing the SST_2 (CHO), SST_3 (CHO), and SST_5 (HEK 293) subtypes were prepared. The ability of increasing concentrations of each compound (10^{-12} M to 10^{-6} M) to displace ^{125}I-Tyr[11]-S-14 (50 fmol, 250 pM) was examined in membranes prepared from the cell expressing each subtype. For each value, 3 μg of protein/tube was used for SST_2 and SST_3, and 10 μg of protein/tube for SST_1 and SST_5. Displayed are the means of two or three determinations, each performed in duplicate. The standard deviations for each determination are <10% of the mean.

Compound	Radioligand binding			
	SST_1	SST_2	SST_3	SST_5
	K_i (nM)			
S-14	0.2	0.2	0.1	5
1	>10^3	0.2	300	0.1
2	>10^3	12.9	>10^3	18.1
3	>10^3	0.1	>10^3	2.2
4	>10^3	0.3	10^2	2.5
5	n.d.	17.3	n.d.	0.42

n.d., not determined.

TABLE 3

Inhibition of cAMP accumulation in intact GH_4C_1, CHO, and HEK cells and yeast data for peptide analogs

The values for inhibition of cAMP accumulation for the peptides at 1 μM concentration in GH_4C_1 cells, CHO cells transfected with the SST_2 receptor, and HEK cells transfected with SST_5 receptors are presented relative to that observed for 1 μM S-14, where the activity of 1 μM S-14 is 1. Relative activity = $[cAMP]_{forskolin} - [cAMP]_{peptide}/[cAMP]_{forskolin} - [cAMP]_{S\text{-}14}$. Yeast activity was scored on a qualitative 1–5 scale based on the radius of the zone of growth (agonist screen) or lack of growth (antagonist screen). Positive numbers were active in the agonist screen and negative numbers were active in the antagonist screen. All determinations are the means of at least three independent experiments. The standard deviations for each determination are <10% of the mean.

Compound	cAMP accumulation			Yeast
	GH_4C_1	SST_2 (CHO)	SST_5 (HEK)	
S-14	1.00	1.00	1.00	+5
1	0.73	0.81	0.94	+3
2	0.11	0.12	0.29	−5
3	0.95	1.02	1.00	+4
4	0.03	0.08	0.20	−5
5	0.42	n.d.	n.d.	−2
2 + SRIF[a]	n.d.	0.16	0.51	
4 + SRIF[a]	n.d.	0.10	0.36	
Basal[b]	6 ± 3	10	6	
Forskolin[c]	110 ± 15	147	185	
SRIF + forskolin[d]	44 ± 9	88	115	

n.d., not determined.

[a] 1 μM peptide + 10 nM S-14.

[b] Control cAMP levels (pmol/10^6 cells ± standard deviation) for three experiments.

[c] Forskolin (10 μM) stimulated cAMP levels (pmol/10^6 cells ± standard deviation).

[d] Reversal of forskolin (10 μM) stimulated cAMP levels by 1 μM S-14 (GH_4C_1) or 10 nM S-14 (SST_2 or SST_5) (pmol/10^6 cells ± standard deviation).

Competitive binding with ^{125}I-Tyr[11]S-14 to cloned SST subtypes. Both pairs (1-2 and 3-4) of disulfide-linked somatostatin ligands (Table 1) bound SST_2 and SST_5 subtypes. Three of the peptides, 1, 3, and 4 (Table 2) all bind to the SST_2 with affinity comparable with that of S-14. Only 2, which contained the D-Cys[2], L-Cys[7], and Val[6] exhibited weaker binding affinity than did S-14. Likewise 2, 3, and 4 all bind to the SST_5 with affinity better than that of S-14. The K_i values for all the compounds at both subtypes ranged from 0.1 to 18 nM. In the Val[6] series, the L-Cys,L-Cys analog 1 had much higher affinity for both subtypes than the D-Cys,L-Cys peptide 2. There was essentially no selectivity for either subtype. In the Thr[6] series, however, the stereochemistry of Cys[2] had little effect on receptor affinity for both subtypes. For 3 and 4, there was a distinct preference for the SST_2. Inversion of the configuration at the first residue (2 versus 5) caused a marked increase in the affinity for the SST_5 compared with the SST_2. In contrast, the binding affinities of the analogs was poor against SST_1 and SST_3 subtypes. In general, the K_i values were in the high nanomolar to low micromolar range for SST_1 and SST_3.

Somatostatin receptor subtypes have been subdivided into

two groups: SRIF subgroups 1 (SST_2, SST_3, SST_5) and 2 (SST_1, SST_4). The work of Raynor *et al.* (24) has shown that the SST_3 subtype has an intermediate affinity for short peptide analogs compared with SST_1 (poor affinity) and SST_2 (high affinity). Our findings are in agreement with these observations: we have found that these peptides exhibit high affinity for the SST_2 and SST_5 and much lower affinity for the SST_1 and SST_3 subtypes.

cAMP data. To determine the functional properties of these somatostatin ligands, cAMP accumulations were performed in rat GH_4C_1 somatomammotroph cells (Table 3; Fig. 1). Based upon purification of somatostatin receptors from rat GH_4C_1 cells, SST_2 is the predominant subtype expressed by these cells (40). The peptides that contained a L-Cys^2,L-Cys^7 pair, **1** and **3**, inhibited forskolin-stimulated cAMP accumulation (Table 3) with efficacy similar to that observed for S-14, which suggests that both **1** and **3** were full agonists. To further characterize the functional properties of **1** and **3**, dose-dependent inhibition of cAMP accumulation was performed in GH_4C_1 cells and both analogs inhibited forskolin-stimulated cAMP accumulation in a dose-dependent manner. Maximal activity was comparable with that of somatostatin (Fig. 1, B and D).

In contrast, the compounds that contained a D-Cys^2,L-Cys^7 pair, **2** and **4**, caused little inhibition of cAMP accumulation (11% and 3% of S-14 activity, respectively) despite exhibiting high affinity binding to the SST_2. Dose titrations (Fig. 1, A and C; *dark bars*) indicated that **2** and **4** exhibit little, if any, agonist activity. However, when the dose titrations were carried out in the presence of somatostatin (Fig. 1, B and D; *light bars*) both readily reversed S-14 mediated inhibition of cAMP accumulation in a dose-dependent manner, which suggests that these two analogs are, in fact, somatostatin antagonists. Similar results were obtained in GH_4C_1 cells that express the rat A_{2a} adenosine receptor and with use of adenosine agonists rather than forskolin to stimulate cAMP accumulation (data not shown).

The effect of the two antagonists on somatostatin-mediated inhibition of cAMP accumulation was examined in S-14 dose-response curves. In the absence of antagonist, ED_{50} values

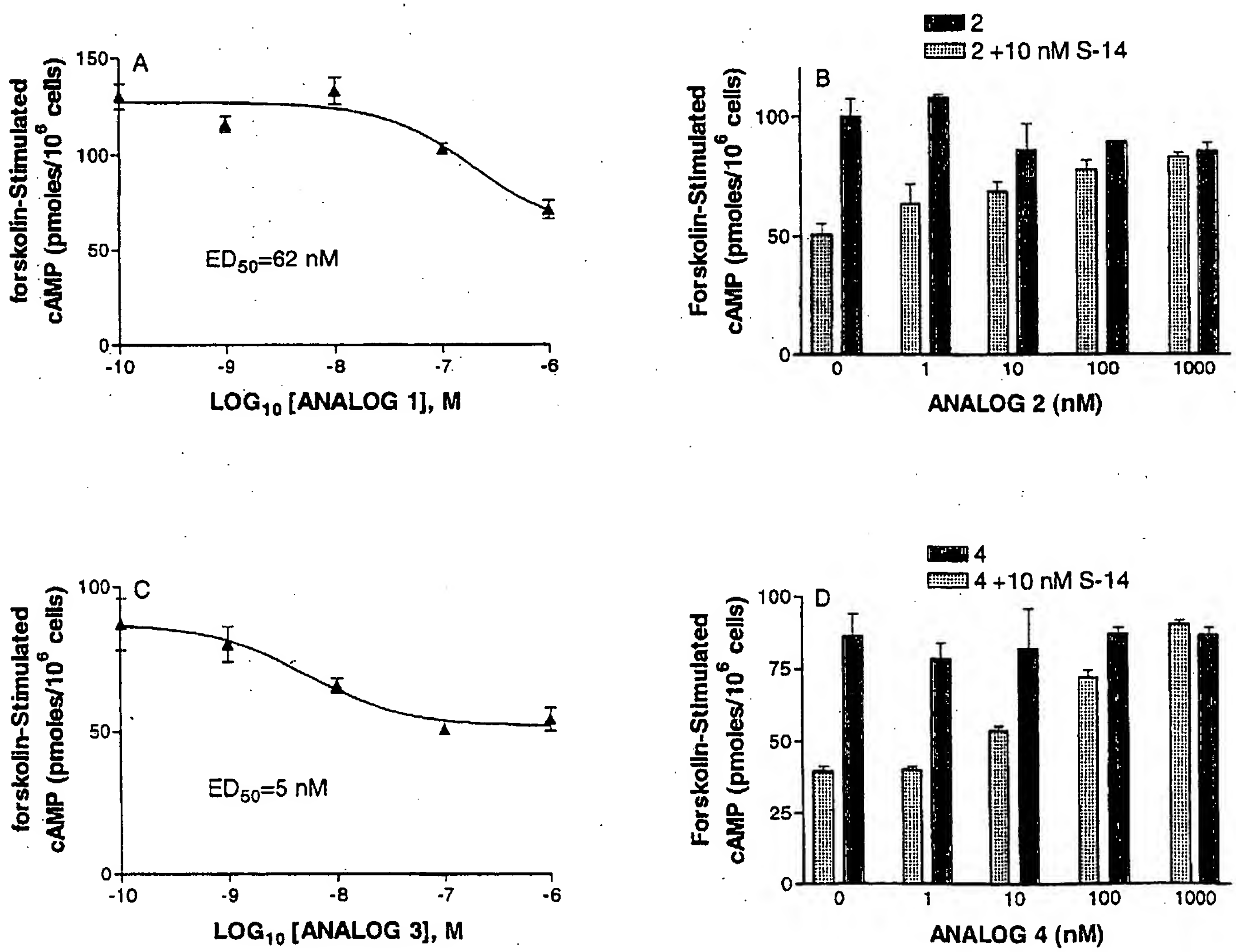

Fig. 1. Comparison of the functional properties of somatostatin analogs in GH_4C_1 somatomammotroph cells. The ability of somatostatin analogs **1–4** to inhibit forskolin-stimulated cAMP accumulation in intact cells was examined. Rat GH_4C_1 somatomammotroph cells were challenged with 5 μM forskolin and increasing doses of analogs **1** (A), **2** (B), **3** (C), and **4** (D). Analogs **2** and **4** were also tested in the presence of 10 nM S-14 (B and D). cAMP accumulations were performed as described in Experimental Procedures. Displayed is a representative experiment performed either two times (analogs **1** and **3**) or three times (analogs **2** and **4**) with equivalent results.

(half-maximal inhibition of the S-14 response) of somatostatin-mediated inhibition of cAMP accumulation was calculated to be 10 nM (Fig. 2, A and B). The presence of 2 (1 μM) shifted the S-14 dose response curve to the right by 40-fold, to 0.4 μM, whereas the presence of 4 (1 μM) shifted the S-14 dose response curve to the right by 500-fold, to 6 μM. From these curves, ED_{50} values were calculated to be 90 nM for 2 and 15 nM for 4. Neither analog decreased the maximal inhibition of cAMP accumulation mediated by S-14, which suggests that both 2 and 4 are acting as competitive antagonists.

Analogs 1-4 were also tested for their ability to inhibit forskolin-induced elevation of cAMP in CHO cells transfected with SST_2 and in HEK 293 cells transfected with SST_5 (Table 3). In general, the results parallel those observed in the GH_4C_1 cells. Both 2 and 4 reversed S-14 antagonism of forskolin-induced elevation of cAMP. The reversal was more

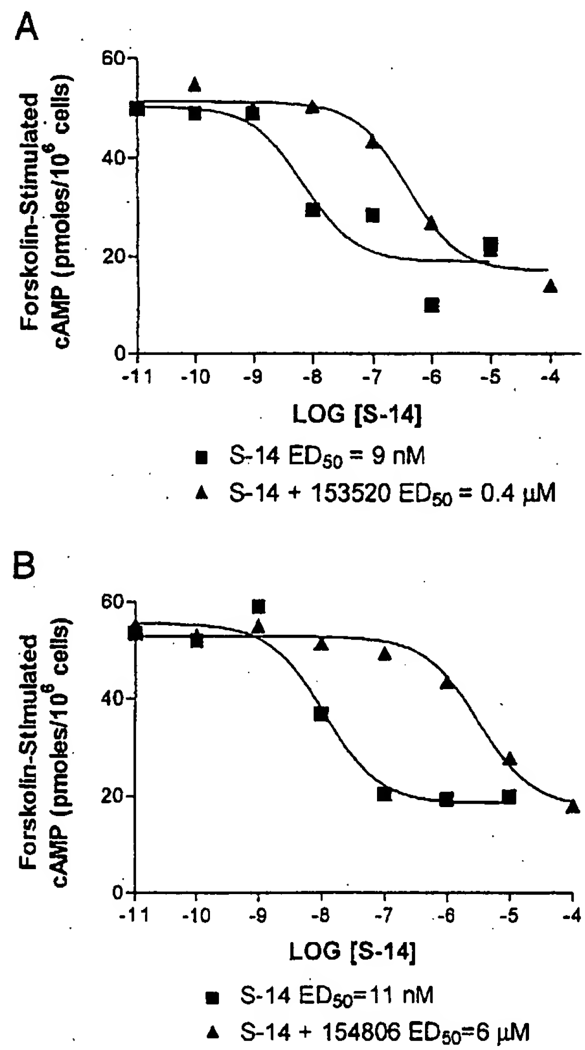

Fig. 2. Somatostatin analogs **2** and **4** reverse the dose-dependent inhibition of cAMP accumulation by S-14 in rat GH_4C_1 somatomammotroph cells. The ability of analogs **2** and **4** to antagonize S-14 mediated inhibition of cAMP accumulation was examined in rat GH_4C_1 somatomammotroph cells. Cells were challenged with 5 μM forskolin and increasing concentrations of S-14 (10^{-10} to 10^{-4} M) in the absence or presence of 1 μM analog 2 (A) or analog 4 (B). cAMP accumulations were performed as described in Experimental Procedures. Displayed is a representative experiment performed three times with equivalent results.

complete with the SST_2 subtype. These peptides may be showing some partial agonist activity at the SST_5.

The key difference in both pairs of compounds is the stereochemistry of Cys^2: D-Cys^2 analogs are antagonists at the SST_2, whereas L-Cys^2 analogs are agonists. A second important element required for antagonist activity is the stereochemistry, but not the substitution, on Phe^1. Replacement of 4-NO_2-Phe^1 with 4-NO_2-D-Phe^1 produced peptide **5**, which had properties similar to **2** in the cAMP accumulation assay but was unable to reach the same efficacy exhibited by S-14. This activity is consistent with substantial partial agonist activity.

Yeast Data. A novel yeast-based expression system for the characterization of individual peptides played an important role in this study. A distinct advantage of the yeast expression over mammalian systems is the expression of only one receptor and one heterotrimeric G protein. Thus, the properties of the receptor-ligand interaction may be assessed without complication from contaminating receptor subtypes. The rat SST_2, when expressed in yeast, exhibited radioligand binding properties that are similar to those it expressed in mammalian cells and functionally coupled to the yeast pheromone response pathway (31). The yeast expression system provides a functional readout in response to agonist (growth) or antagonist (inhibition of growth) properties of a particular somatostatin analog. This response is manifested by an observable zone of growing yeast cell around the site of the agonist administration. In this manner, agonists of varying affinity and potency may be assayed. Because concentration varies with the square of the radius as it diffuses radially from the site of the application, small changes in the radius of the growth zone correspond to large differences in the affinity of a particular compound for the SST_2. Similarly, the extent to which cells grow within the zone is related to the potency of a particular compound. To assay the effects of compounds with potential antagonist activity, it was necessary to add S-14 (100 nM) to the agar, which stimulated the growth of all cells within the plate. Application of an antagonist blocked the growth-promoting effect of S-14, which yielded a clear zone in an otherwise uniform lawn of growing yeast cells. Because compounds that are toxic would be expected to produce a similar response, all compounds reported herein were tested for growth inhibitory activity that was not receptor-dependent. None of the compounds exhibited toxic effects.

Based on the yeast bioassay, analogs with the L-Cys^2,L-Cys^7 pair (**1** and **3**) were potent agonists (Fig. 3). Analogs with a D-Cys^2,L-Cys^7 pair (**2** and **4**) display potent antagonist properties. The compound with a D-Phe^1 residue (**5**), which seemed to be a partial agonist in the cAMP accumulation assay, seemed to be a weak antagonist in the yeast screen. The data agree well with results obtained from cAMP accumulation studies in mammalian cells.

cAMP versus yeast. The combination of three assays (radioligand binding, cAMP, and yeast bioassay) allows for both quantitative characterization of molecular properties as well as qualitative high-throughput evaluations of the functional properties of large numbers of novel somatostatin ligands. We have used all three assays for the discovery of novel somatostatin antagonists. The radioligand binding assays and cAMP accumulations are well-established quantitative assays. Unfortunately, functional assays, like the

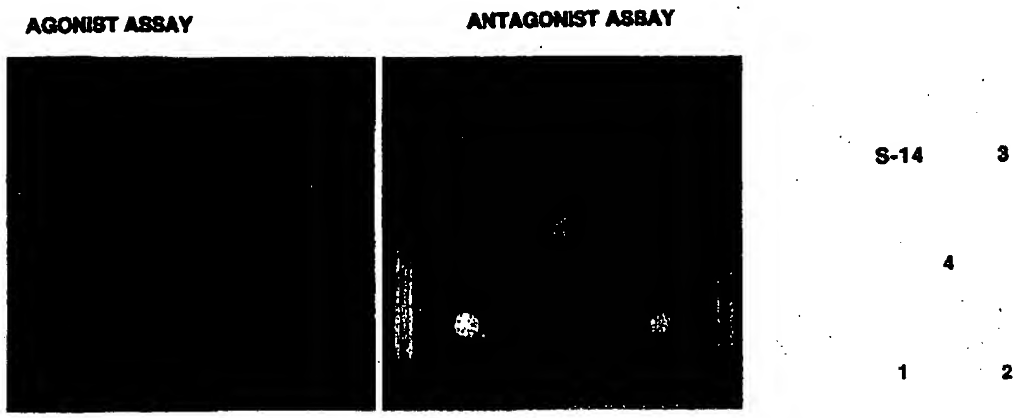

Fig. 3. Yeast-based bioassay of SST ligands. The activity of compounds described herein were assayed in an agar plate bioassay modified from that reported in Price *et al.* (31). Overnight liquid cultures of LY268 [containing the SST_2 (29)] cells in 2 ml of SC medium containing glucose (2%) and lacking tryptophan and uracil were centrifuged, resuspended in 5 ml of SC liquid medium containing galactose (2%), sucrose (0.2%), and lacking tryptophan and uracil, and was incubated overnight at 30°. Cells (2×10^5) were dispersed in 30 ml of SC-galactose (2%), sucrose (0.2%) agar medium lacking tryptophan, uracil, and histidine (adjusted to pH 6.8 with concentrated KOH before autoclaving and equilibrated to 50°) and poured in a 10- × 10-cm sterile Petri plate. For the antagonist assay, S-14 was added to a final concentration of 100 nM before plating. After allowing the agar to harden, 5-μl samples of the designated compounds (1 mM in DMSO) were pipetted onto the surface (agonist assay) or onto sterile filter disks placed on the surface of the agar (antagonist assay). The plates were incubated at 30° for 48 hr. *Right*, identities of the applied compounds.

cAMP accumulation assay, are relatively time consuming and not generally suited for large-scale, rapid screening. The yeast assay complements these traditional assays because it is rapid and provides functional data. A large number of analogs can be screened to identify candidates for further screening in more laborious quantitative assays.

These data are all consistent with the hypothesis that 2 and 4 are selective antagonists of the SST_2 subtype. The key difference between these antagonists and the numerous agonists previously described are the D stereochemistry of Cys^2 and the L stereochemistry of residue 1. In our studies, 4 was the most potent antagonist; the binding affinities were equal to somatostatin but exhibited virtually no residual agonist behavior. The affinity for the receptor is equivalent to somatostatin, and both functional assays, cAMP accumulation and yeast-growth, are consistent with full antagonism of SST_2 subtype. To our knowledge, this is the first full antagonist of somatostatin to be identified. This should provide a valuable tool for studying this receptor *in vitro* and *in vivo*.

References

1. Brazeau, P., W. Vale, R. Burgus, N. Ling, M. Butcher, J. Rivier, and R. Guillemin. R. Hypothalamic polypeptide that inhibits the secretion of immunoreactive pituitary growth hormone. *Science (Washington, D. C.)* **129:**77–79 (1973).
2. Reisine, T., and G. I. Bell. Molecular biology of somatostatin receptors. *Trends Neurosci.* **16:**34–38 (1993).
3. Bruno, J. F., Y. Xu, J. Song, and M. Berelowitz. Molecular cloning and functional expression of a brain-specific somatostatin receptor. *Proc. Natl. Acad. Sci. USA* **89:**11151–11155 (1992).
4. Kluxen, F.-W., C. Bruns, and H. Lubbert. Expression cloning of a rat brain somatostatin receptor. *Proc. Natl. Acad. Sci. USA* **89:**4618–4622 (1992).
5. Li, X.-J., M. Forte, R. A. North, C. A. Ross, and S. H. Snyder. Cloning and expression of a rat somatostatin receptor enriched in the brain. *J. Biol. Chem.* **267:**21307–21312 (1992).
6. Meyerhof, W., H.-J. Paust, C. Schonrock, and D. Richter. Cloning of a cDNA encoding putative G protein-coupled receptor expressed in specific rat brain regions. *DNA Cell Biol.* **10:**689–694 (1991).
7. O'Carrol, O. M., S. J. Lolait, M. Konig, and L. Mahan. Molecular cloning and expression of a pituitary somatostatin receptor with preferential affinity for somatostatin-28. *Mol. Pharmacol.* **42:**939–946 (1992).
8. Yamada, Y., S. Post, K. Wang, H. S. Tager, G. I. Bell, and S. Seino. Cloning and functional characterization of a family of human and mouse somatostatin receptors expressed in brain, gastrointestinal tract, and kidney. *Proc. Natl. Acad. Sci. USA* **89:**251–255 (1992).
9. Yasuda, K., S. Rens-Domiano, C. D. Breder, S. F. Law, C. B. Saper, T. Reisine, and G. I. Bell. Cloning of a novel somatostatin receptor, SSTR3, coupled to adenylate cyclase. *J. Biol. Chem.* **28:**20422–20428 (1992).
10. Heisler, S., T. D. Reisine, V. Y. H. Hook, and J. Axelrod. Somatostatin inhibits multireceptor stimulation of cyclic AMP formation and corticotropin secretion in mouse pituitary tumor cells. *Proc. Natl. Acad. Sci. USA* **79:**6502–6506 (1982).
11. Hou, C., R. L. Gilbert, and D. L. Barber. Subtype-specific signaling mechanisms of somatostatin receptors SSTR1 and SSTR2. *J. Biol. Chem.* **269:** 10357–10362 (1994).
12. Lewis, D. L., F. F. Weight, and A. Luini. A guanine nucleotide-binding protein mediates the inhibition of voltage-dependent calcium channel current by somatostatin in pituitary cell line. *Proc. Natl. Acad. Sci. USA* **83:**9035–9039 (1986).
13. Liebow, C., C. Reilly, M. Serrano, and A. V. Schally. Somatostatin analogs inhibit growth of pancreatic cancer by stimulating tyrosine phosphatase. *Proc. Natl. Acad. Sci. USA* **86:**2003–2007 (1989).
14. Schlegel, W. F., C. B. Waurin, C. B. Wollheim, and G. R. Zahnd. Somatostatin lowers the cytosolic free Ca^{2+} concentration in clonal pituitary cells (GH_3). *Cell Calcium* **5:**223–226 (1984).
15. Strnad, J., C. Eppler, M. Corbett, and J. R. Hadcock. The rat SSTR2 receptor subtype is coupled to inhibition of cyclic AMP accumulation. *Biochem. Biophys. Res. Commun.* **191:**968–976 (1993).
16. Tatsumi, H., M. Costa, M. Schimerlik, and R. A. North. Potassium conductance increased by noradrenaline, opioids, somatostatin, and G-protein: whole-cell recording from guinea pig submucous neurons. *J. Neurosci.* **10:**1675–1682 (1990).
17. White, R. E., A. Schonbrunn, and D. L. Armstrong. Somatostatin stimulates Ca^{2+}-activated K^+ channels through protein dephosphorylation. *Nature (Lond.)* **351:**570–573 (1991).
18. Yamashita, N., N. Shibuya, and E. Ogata. Hyperpolarization of the membrane potential caused by somatostatin in dissociated human pituitary adenoma cells that secrete growth hormone. *Proc. Natl. Acad. Sci. USA* **83:**6198–6202 (1986).
19. Veber, D. E. Design and discovery in the development of peptide analogs, in *Proceedings of the Twelfth American Peptide Symposium* (J. A. Smith and J. E. Rivier, eds.). ESCOM, Leiden, the Netherlands, 3–14 (1992).
20. Bauer, W., U. Briner, W. Doepfner, R. Haller, R. Huguenin, P. Marbach, T. J. Petcher, and J. Pless. SMS 201–995: A very potent and selective octapeptide analogue of somatostatin with prolonged action. *Life Sci.* **31:** 1133–1140 (1982).
21. Cai, R.-Z., B. Szoke, R. Lu, D. Fu, T. W. Redding, and A. V. Schally. Synthesis and biological activity of highly potent octapeptide analogs of somatostatin. *Proc. Natl. Acad. Sci. USA*, **83:**1896–1900 (1986).
22. Murphy, W. A., M. L. Heiman, V. Lance, I. Mezo, and D. H. Coy, D. Octapeptide analogs of somatostatin exhibiting greatly enhance in vivo amd in vitro inhibition of growth hormone secretion in the rat. *Biochem. Biophys. Res. Commun.* **132:**922–928 (1985).
23. Wynants, C., D. H. Coy, and G. Van Binst. Conformational study of superactive analogues of somatostatin with reduced ring size by. 1H NMR. *Tetrahedron* **44:**941–973 (1988).
24. Raynor, K., W. A. Murphy, D. H. Coy, J. H. Taylor, J.-P. Moreau, K. Yasuda, G. I. Bell, and T. Reisine. Cloned somatostatin receptors: identi-

fication of subtype selective peptides and demonstration of high affinity binding of linear peptides. *Mol. Pharmacol.* **43**:838–844 (1993).
25. Tam, J. P., C.-R. Wu, W. Liu, and J.-W. Zhang. A highly selective and effective reagent for disulfide bond formation in peptide synthesis and protein folding, in *Proceedings of the Twelfth American Peptide Symposium* (J. A. Smith and J. E. Rivier, eds.). ESCOM, Leiden, the Netherlands, 499–500 (1992).
26. Ellman, G. L. A Colorometric method for determining low concentration of mercaptans. *Arch. Biochem. Biophys.* **74**:443–450 (1958).
27. Hadcock, J. R., J. Strnad, and C. Eppler. The rat SSTR1 somatostatin receptor couples to G-proteins and inhibition of cyclic AMP accumulation. *Mol. Pharmacol.* **45**:410–416 (1994).
28. Ozenberger, B. A., and J. R. Hadcock. A single amino acid substitution in the somatostatin receptor subtype five increases affinity for somatostatin-14. *Mol. Pharmacol.* **47**:82–87 (1995)
29. Hadcock, J. R., and J. Strnad. Somatostatin receptor coupling to G proteins. *Methods Neurosci.* **29**:120–132 (1996).
30. Hadcock, J. R., M. Ros, and C. C. Malbon. Agonist regulation of β-adrenergic receptor mRNA: analysis in S49 mouse lymphoma mutants. *J. Biol. Chem.* **264**:13956–13961 (1989).
31. Price, L. A., E. M. Kajkowski, J. R. Hadcock, B. A. Ozenberger, and M. H. Pausch. Functional coupling of a mammalian somatostatin receptor to the yeast pheromone response pathway. *Mol. Cell. Biol.* **15**:6188–6195 (1995).
32. Cheng, Y., and W. H. Prusoff. Relationship between the inhibition constant (K_i) and the concentration of inhibitor which causes 50 per cent inhibition (I_{50}) of an enzymatic reaction. *Biochem. Pharmacol.* **22**:3099–3108 (1973).
33. Hruby, V. J. Implications of the X-ray structure of deamino-oxytocin to agonist/antagonist-receptor interactions. *Trends Pharmacol. Sci.* **8**:336–339 (1987).
34. Pelton, J. T., W. Kazmierski, K. Gulya, H. I. Yamamura, and V. J. Hruby. Design and synthesis of conformationally constrained somatostatin analogues with high potency and specificity for μ opioid receptors. *J. Med. Chem.* **29**:2370–2375 (1986).
35. Walker, J. M., W. D. Bowen, S. T. Atkins, M. K. Hemstreet, and D. H. Coy. μ-Opiate binding and morphine antagonism by octapeptide analogs of somatostatin. *Peptide Res.* **8**:869–875 (1987).
36. Orbuch, M., J. E. Taylor, D. H. Coy, J. E. Mrozinski, Jr., S. A. Mantey, J. F. Battey, J.-P. Moreau, and R. T. Jensen. Discovery of a novel class of neuromedin B receptor antagonists, substituted somatostatin analogues. *Mol. Pharmacol.* **44**:841–850 (1993).
37. Nicolaou, K. C., J. M. Salvine, K. Raynor, S. Pietranico, T. Reisine, R. M. Freidinger, and R. Hirschmann. Design and synthesis of peptidomimetic employing a β-D-glucose for scaffolding, in *Proceedings of the Eleventh American Peptide Symposium* (J. E. Rivier and G. R. Marshall, eds.). ESCOM, Leiden, the Netherlands, 881–884 (1990).
38. He, Y.-B., Z. Huang, K. Raynor, T. Reisine, and M. Goodman. Synthesis and conformations of somatostatin-related cyclic hexapeptides incorporating specific α- and β-methylated residues. *J. Am. Chem. Soc.* **115**:8066–8072 (1993).
39. Veber, D. A., R. Saperstein, R. F. Nutt, R. M. Freidinger. S. F. Brady, P. Curley, D. S. Perlow, W. J. Paleveda, C. D. Colton, A. G. Zacchei, D. J. Tocco, D. R. Hoff, R. L. Vandlen, J. E. Gerich, L. Hall, L. Mandarino, E. H. Cordes, P. S. Anderson, and R. Hirschmann, R. A super active cyclic hexapeptide analog of somatostatin. *Life Sci.* **34**:1372–1378 (1984).
40. Eppler, C. M., J. R. Zysk, M. Corbett, and H. M. Shieh. Purification of a pituitary receptor for somatostatin. The utility of biotinylated somatostatin analogs. *J. Biol. Chem.* **267**:15603–15612 (1992).

Send reprint requests to: John R. Hadcock, Wyeth-Ayerst Research, CN 8000, Princeton, NJ 08543-8000. E-mail: hadcocj@war.wyeth.com

Pergamon

Bioorganic & Medicinal Chemistry Letters, Vol. 5, No. 11, pp. 1203-1206, 1995

0960-894X/95 $9.50+0.00

0960-894X(95)00195-6

PREPARATION OF NEUROTENSIN ANALOGS WITH A NOVEL PRO-TYR REPLACEMENT

David A. Nugiel*, Regina M. Wagner and William K. Schmidt
The DuPont Merck Pharmaceutical Co., Box 80353, Wilmington, DE, 19880-0353.

Abstract. Synthesis of novel Neurotensin (NT) 9-13 analogs is described. The Pro-Tyr sequence of NT (9-13) was replaced with a 1-*m*-aminophenyl-1-benzyl urea template, substituting two amino acids with a simple substituted urea linkage.

Introduction. Neurotensin (NT)[1] is a 13 amino acid peptide (pGlu-Leu-Tyr-Glu-Asn-Lys-Pro-Arg-Arg-Pro-Tyr-Ile-Leu) found distributed throughout the central and peripheral nervous system. Several biological properties are attributed to NT including analgesic,[2] psychotropic,[3] and hypothermic[4] actions. NT is more potent than morphine when administered by i.c.v. route.[5] In addition, NT has been linked with the biology of schizophrenia where depressed levels of NT in the cerebrospinal fluid are found.[6] As a result, a selective NT agonist may have therapeutic benefits in treating schizophrenia and pain.

Several groups have reported smaller fragments of NT (1-13) with similar activity. The minimal native sequence needed for full biological activity is the C-terminal hexapeptide (Arg-Arg-Pro-Tyr-Ile-Leu), NT (8-13). Several studies show similar activity with the NT (8-13) fragment when compared to the complete sequence NT (1-13).[7] In addition, it is possible to replace the Arg-Arg N-terminal fragment in NT (8-13) with Lys without a significant loss of binding affinity.[8] Other studies have explored the replacement of amino acids from the NT (8-13) fragment with simple heterocycles to increase metabolic stability and bioavailability.[9]

This report describes the preparation of novel NT analogs using the NT (9-13) Lys-Pro-Tyr-Ile-Leu sequence as a starting point. Our efforts centered on the Pro-Tyr section of NT (9-13). By replacing the Pro-Tyr fragment with a simpler entity, we could increase the compound's metabolic stability, improve bioavailability, and possibly modulate its agonist or antagonist properties.

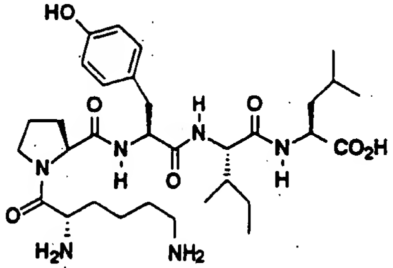

NT (9-13)

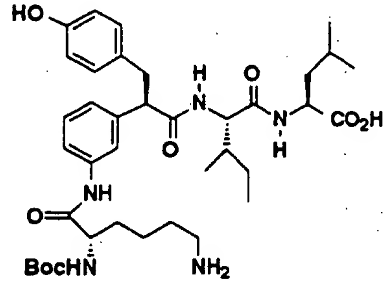

1

Modeling studies performed on NT (9-13) showed the Pro-Tyr fragment would be a good replacement target.[10] A simple *m*-disubstituted benzene induces a similar type of bend as seen in the native peptide while aligning the other residues in a desirable orientation relative to NT (9-13). Introduction of a *p*-hydroxybenyl substituent would mimic the Tyr side chain. A recent report [11] showed compound 1 had good biological activity in the NT binding assay, and was shown to have agonistic properties in a functional assay. We hoped to improve the activity of 1 and further simplify the molecule by replacing the carbon linker of the aniline ring with a nitrogen atom. Additional modeling studies indicated the urea linkage would slightly alter the desired bend angle, but would retain the necessary binding elements in a similar orientation compared to 1. Forming a urea linkage would also remove a chiral center and simplify the synthesis.

Scheme 1[a]

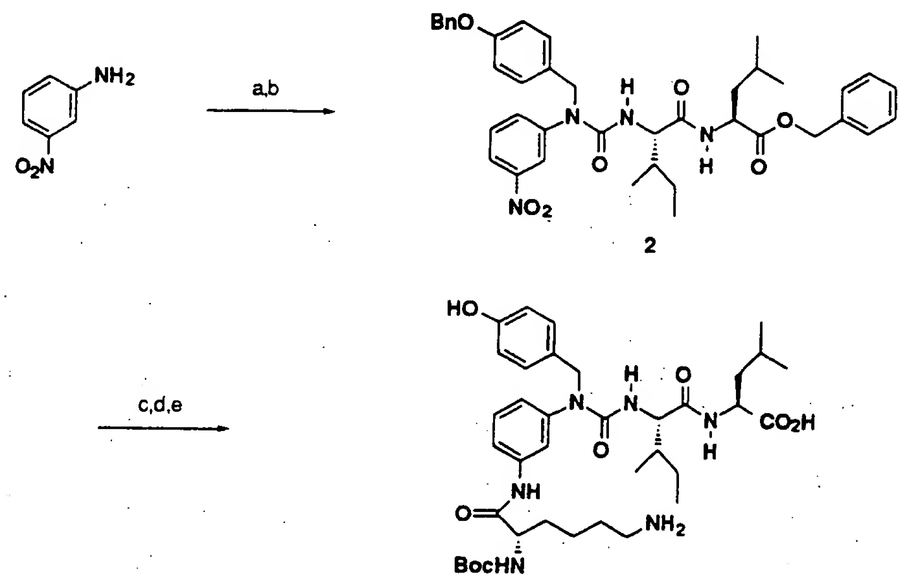

[a]**Reagents and conditions**: a) *p*-Benzyloxybenzaldehyde, $Na(CN)BH_3$, MeOH, 0 °C (90%); b) diphosgene, THF, 0 °C, then H_2NIleLeuOBn, reflux (85%); c) $SnCl_2$, EtOH, reflux (90%); d) Boc(Z)Lys, DCC, CH_2Cl_2, 25 °C (90%); e) H_2, 10% Pd/C (95%).

Chemistry. A representative approach to these analogs is shown in Scheme 1. Reductive amination of *p*-benzyloxybenzaldehyde with *m*-nitroaniline introduced the Tyr-like fragment in good yield. Activation of this secondary amine with diphosgene and coupling with the dipeptide fragment H-Ile-LeuOBn gave compound 2 in 77% overall yield. The nitro group was reduced using $SnCl_2$. The resulting amine was coupled to the Lys portion of NT (9-13) using a standard dicyclohexylcarbodiimide (DCC) promoted coupling reaction. At this point it was also possible to introduce reduced amide bond surrogates. Substituting the DCC coupling reaction with a reductive amination, using Boc(Z)Lys aldehyde, led to the reduced amide bond surrogate 5. Finally, catalytic hydrogenation

removed the three protecting groups (benzyl ether, benzyl ester, and Cbz) in one pot to give the desired compound 3. The Boc protecting group was left intact on these compounds. Previous studies showed increased hydrolytic stability and blood-brain-barrier penetration with NT (9-13) analogs carrying a large lipophilic N-terminal protecting group.[12]

Table 1

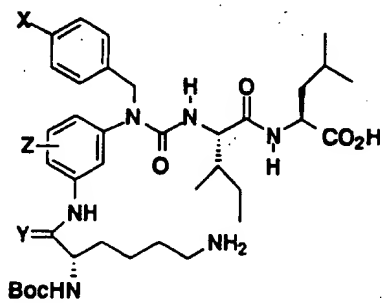

compound	X	Y	Z	K_i (μM)
1				0.029
3	OH	O	H	1.25
4	OH	O	2-fluoro	2.20
5	OH	H, H	H	0.73
6	F	O	H	0.89
7	OH	O	4-fluoro	>10

Results and Discussion. Compounds were evaluated in a NT binding assay[13] and the results are shown in Table 1. Although the compounds do not bind with similar affinity to the NT receptor as our model compound 1, they still show submicromolar activity. Replacing a sp^3 carbon with a sp^2 hybridized nitrogen effects the angle of the bend we originally tried to mimic. The bend angle, induced by the urea linkage, mostly effected the Lys residue's orientation when compared to compound 1. The reduced amide bond surrogate 5 shows a slight increase in affinity. The resulting increased mobility of the Lys moiety, allows it to adopt a more favorable conformation and increase binding afinity. Attempts at gaining additional hydrogen bond interactions, using fluorine substitution on the aromatic ring, reduced the binding affinity. It is also possible to replace the Tyr phenolic hydroxyl group with a fluorine atom with positive results. Compound 6 shows a slight increase in binding relative to compound 3. This may ultimately improve the pharmacokinetic profile of these compounds. By replacing an undesirable metabolic handle (substituting F for OH), we may decrease the clearance rate of subsequent analogs and increase bioavailability.

Conclusion. We presented a series of nuerotensin analogs with a novel Pro-Tyr replacement having submicromolar binding affinities. This study shows the ability to replace two amino acids in the NT (9-13) sequence with a simple 1-*m*-aminophenyl-1-benzyl urea template and retain binding affinity. The synthetic scheme is straightforward and high yielding starting from simple commercially available materials. It also allows for generating a wide variety of compounds by varying the amino acids in the subsequent coupling reactions. Additional analogs need to be made to fully exploit this finding. The preparation and evaluation of such compounds is in progress and will be reported in due course.

Acknowledgments. We would like to thank the CNS pharmacologists at DuPont Merck Pharmaceuticals for providing the binding assay data. In addition, we thank Tom Maduskie for helpful discussions.

References and notes.

1. Carraway, R.; Leeman, S.E. *J. Biol. Chem.* **1973**, *248*, 6854.

2. Clineschmidt, B.V.; McGuffin, J.C. *Eur. J. Pharmacol.* **1979**, *54*, 129.

3. Nemeroff, C.B. *Psychoneuroendocrinology* **1986**, *11*, 15.

4. Rivier, J.E.; Lazarus, L.H.; Perrin, M.H.; Brown, M.R. *J. Med. Chem.* **1977**, *20*, 1409.

5. Goedert, M. *Trends in Neurosciences* **1984**, *7*, 3.

6. Garver, D.L.; Bissette, G.; Widerlov, E.; Nemeroff, C.B. *Am. J. Psychiat.* **1991**, *148*, 484.

7. Nicolaides, E.D.; Lunney, E.A.; Kaltenbronn, J.S.; Wiley, J.N.; Downs, D.A. *J. Peptide Protien Res.* **1985**, *25*, 435; Carraway, R.; Leeman, S.E. in *Peptides: Chemistry, Structure, and Biology*; Walter, R., Meienhofer, J., Eds.; Ann Arbor Sciences: Ann Arbor, MI, 1975; p 679; Furuta, S.; Kisara, K.; Sakurada, S.; Sakurada, T.; Sasaki, Y.; Suzuki, K. *Br. J. Pharmacol.* **1984**, *83*, 43.

8. Christos, T.E.; Arvanitis, A.; Cain, G.A.; Johnson, A.L.; Pottorf, R.S.; Tam, S.W.; Schmidt, W.K. *BioMed. Chem. Lett.* **1993**, *3(6)*, 1035.

9. Dodd, D.S.; Kozikowski, A.P.; Cusak, B.; Richelson, E. *BioMed. Chem. Lett.* **1994**, *4(10)*, 1241.

10. A proposed active conformation of NT (9-13) was obtained using Ensemble Dynamics (D. Spellmeyer, unpublished results). This conformation was then used as a template for compound modeling. The Pro-Tyr replacements were designed and fitted to this template using a superimpose routine in PSSHOW. MOGLI/PSSHOW, Evans & Sutherland Computer Corporation, Salt Lake City, Utah.

11. Maduskie, T.P.; Schmidt, W.K.; Bliecher, L.S.; Cacciola, J.; Cheatam, W.; Fevig, J.M.; Johnson, A.L.; Mccomb, S.A.; Nugiel, D.A.; Spellmeyer, D.A.; Tam, S.W.; Voss, M.E.; Wagner, R.M. *J. Cell. Biochem.* **1993**, Supp. 17C, 232.

12. Cain, G.A. *et al BioMed. Chem. Lett.* **1993**, *3(10)*, 2055.

13. Receptor binding performed according to the method of Goedert *et al* in *Brain Research* **1984**, *304*, 71.

(*Received in USA* 20 *December* 1994; *accepted* 29 *April* 1995)

Design and Structure–Activity Relationships of C-Terminal Cyclic Neurotensin Fragment Analogues

Andrea M. Sefler,[†,‡] John X. He,[†] Tomi K. Sawyer,[†] Katherine E. Holub,[†] Diana O. Omecinsky,[†] Michael D. Reily,[†] Venkataraman Thanabal,[†] Hyacinth C. Akunne,[§] and Wayne L. Cody*,[†]

Departments of Chemistry and Pharmacology, Parke-Davis Pharmaceutical Research, Division of the Warner-Lambert Company, 2800 Plymouth Road, Ann Arbor, Michigan 48106

Received March 28, 1994[®]

Neurotensin (NT) is a linear tridecapeptide with a broad range of central and peripheral pharmacological effects. The C-terminal hexapeptide of NT (NT_{8-13}) has been shown to possess similar properties to NT itself, and in fact, an analogue of NT_{8-13} ($N^{\alpha}MeArg^{8}$-Lys-Pro-Trp-Tle-Leu^{13}, Tle = *tert*-leucine) has been reported to possess central activity after peripheral administration. Cyclic derivatives of this hexapeptide were synthesized by a combination of solution and solid-phase peptide synthetic methodologies, and several analogues had low nanomolar binding affinity for the NT receptor. In particular, cyclo[Arg-Lys-Pro-Trp-Glu]-Leu (cyclized between the α amine of Arg and the γ carboxylate of Glu) possessed 16 nM NT receptor affinity and was determined to be an agonist *in vitro*. ^{1}H-NMR and ^{13}C-edited ^{1}H-NMR spectroscopy were performed on this and related cyclic analogues to help identify structural properties which may be important for receptor recognition. These cyclic peptides represent novel molecular probes to further investigate NT receptor pharmacology, as well as to advance our understanding of the structure–conformation relationships of NT and to help establish a working basis for additional pharmacophore mapping studies.

Introduction[1]

Neurotensin (NT, $pGlu^{1}$-Leu^{2}-Tyr^{3}-Glu^{4}-Asn^{5}-Lys^{6}-Pro^{7}-Arg^{8}-Arg^{9}-Pro^{10}-Tyr^{11}-Ile^{12}-Leu^{13}) is a linear tridecapeptide that was originally isolated from the bovine hypothalamus.[2] NT is found in high concentrations in the ileum and the hypothalamus and has a broad range of biological effects including hypotension, analgesia, gut contraction, and increase of vascular permeability.[3–5] In addition, NT has been shown to possess pharmacological properties similar to dopamine antagonists that are effective antipsychotics.[6]

NT is one member of a family of biologically active peptides that includes xenopsin (pGlu-Gly-Lys-Arg-Pro-Trp-Ile-Leu, isolated from the skin of *Xenopus laevis*)[7] and neuromedin N (Lys-Ile-Pro-Tyr-Ile-Leu, isolated from the porcine spinal cord).[8] Both of these peptides interact with the NT receptor[9,10] and are homologous with the C-terminal hexapeptide of NT (NT_{8-13}, Arg^{8}-Arg-Pro-Tyr-Ile-Leu^{13}).

Historically, the design and syntheses of NT analogues, including fragment derivatives and prototypic cyclic congeners, dates to the very important work of a number of research groups, as exemplified by Carraway and Leeman,[11] Folkers *et al.*,[12] Rivier *et al.*,[13,14] St-Pierre *et al.*,[15] Bayer *et al.*,[16] Quirion *et al.*,[17] Kitabgi *et al.*,[18] Jolicoeur *et al.*,[19] and Clineschmidt *et al.*[20] In particular, these pioneering studies provided the first systematic analysis of NT in terms of the structure–activity relationships (SAR) of the critical NT_{9-13} message sequence and provided insight to the structure–conformation properties of both the native peptide and a NT_{6-13} analogue. More recently, NT research has focused primarily on the C-terminal pentapeptide or hexapeptide sequence to further advance structure–activity studies and NT-based drug discovery, *vide infra*.

Both NT and NT_{8-13} fail to cross the blood–brain barrier when administered intravenously (iv) or orally,[5] and their relatively short *in vivo* half-lives have prompted a search for metabolically stable analogues for further evaluation. Reduced peptide bond analogues (Ψ[CH_2-NH]) of NT_{8-13} have shown increased stability, especially when the Arg^{8}–Arg^{9} bond was modified.[21–24] In addition, it has been reported that a modified NT_{8-13} hexapeptide (**1**, $N^{\alpha}MeArg^{8}$-Lys-Pro-Trp-Tle-Leu^{13}, Tle = *tert*-leucine)[25] binds to the NT receptor with low nanomolar affinity. Interestingly, this compound possessed central nervous system (CNS) activity after peripheral administration, suggesting that it may cross the blood–brain barrier and be metabolically stable.[25–27]

NT has been suggested to have a role in the effects of antipsychotic drug action. Enhanced NT levels have been found in the cerebrospinal fluid of a subpopulation of schizophrenic patients undergoing antipsychotic drug therapy versus a control group.[28] Antipsychotic drugs have also been shown to increase NT immunoreactivity in the brain and levels of NT messenger RNA in the rat.[29] Thus, NT agonists could potentially be a novel class of antipsychotics. Such compounds could replace current anti-dopamine therapies, since they may not possess the extrapyramidal side effects and tardive dyskinesia.[30] Also, the antinociceptive effects of NT are of interest, since they are not associated with the respiratory depression and addictive properties of the opiates.[31]

The three-dimensional solution conformation of NT has been studied by two-dimensional proton NMR spectroscopy in water and methanol, but due to its inherent flexibility little structural information was obtained.[32] In NT_{8-13}, the replacement of the Pro^{10}-

* Author to whom correspondence should be addressed. Phone: (313) 996-7729. Fax: (313) 996-3107. E-mail: codyw@aa.wl.com.
† Department of Chemistry.
§ Department of Pharmacology.
‡ Current address: University of California, Department of Chemistry, Berkeley, CA 94720.
® Abstract published in *Advance ACS Abstracts*, December 15, 1994.

Table 1. N-Terminal to Side Chain Cyclized Neurotensin and Related Analogues

no.	compound	constraint	NT binding (± SEM)[a] (nM, K_i)
1[b]	N$^\alpha$MeArg^8-Lys-Pro-Trp-Tle-Leu^{13}	none	0.67 ± 0.03
2	cyclo[Arg^8-Lys-Pro-Trp-Glu]-Leu^{13}	α-NH$_2$(Arg)→γ-CO$_2$H(Glu)	16 ± 4
3	cyclo[Arg^8-Lys-Pro-Trp-Asp]-Leu^{13}	α-NH$_2$(Arg)→β-CO$_2$H(Asp)	910 ± 25
4	cyclo[Arg^8-Lys-Pro-Trp-Glu]-Gly^{13}	α-NH$_2$(Arg)→γ-CO$_2$H(Glu)	250 ± 13
5	cyclo[Arg^8-Ala-Pro-Trp-Glu]-Leu^{13}	α-NH$_2$(Arg)→γ-CO$_2$H(Glu)	>10000
6	cyclo[Arg^8-Lys-Pro-Trp-Glu^{12}]	α-NH$_2$(Arg)→γ-CO$_2$H(Glu)	>10000
7	cyclo[Arg^8-Pro-Trp-Glu]-Leu^{12}	α-NH$_2$(Arg)→γ-CO$_2$H(Glu)	340 ± 8
8	N$^\alpha$MeArg^8-cyclo[Lys-Pro-Trp-Tle-Asp^{13}]	ε-NH$_2$(Lys)→β-CO$_2$H(Asp)	>10000
9	cyclo[Gly-N$^\alpha$MeArg^8-Lys-Pro-Trp-Asp]-Leu^{13}	α-NH$_2$(Gly)→β-CO$_2$H(Asp)	560 ± 44
10	cyclo[Gly-N$^\alpha$MeArg^8-Lys-Pro-Trp-Glu]-Leu^{13}	α-NH$_2$(Gly)→γ-CO$_2$H(Glu)	28 ± 11
11	cyclo[N$^\alpha$MeArg^8-Lys-Pro-Trp-Glu]-Leu^{13}	α-NH(MeArg)→γ-CO$_2$H(Glu)	700 ± 20
12	cyclo[D-Arg^8-Lys-Pro-Trp-D-Glu]-Leu^{13}	α-NH$_2$(D-Arg)→γ-CO$_2$H(D-Glu)	>10000[c]
13	cyclo[Arg^8-Lys-Pro-Trp-Hgl[d]]-Leu^{13}	α-NH$_2$(Arg)→δ-CO$_2$H(Hgl[d])	830[c] ± 175

[a] $n = 6$ (number of replicate determinations) unless otherwise noted. [b] See refs 25, 26, 27, and 39. [c] $n = 3$. [d] Hgl = homoglutamic acid.

Table 2. N-Terminal to Side Chain Cyclized Neurotensin Analogues and Corresponding Linear Analogues

no.	compound	constraint	NT binding (± SEM)[a] (nM, K_i)
2	cyclo[Arg^8-Lys-Pro-Trp-Glu]-Leu^{13}	α-NH$_2$(Arg)→γ-CO$_2$H(Glu)	16 ± 4
14	N$^\alpha$AcArg^8-Lys-Pro-Trp-Gln-Leu^{13}	none	260 ± 80
11	cyclo[N$^\alpha$MeArg^8-Lys-Pro-Trp-Glu]-Leu^{13}	α-NH(MeArg)→γ-CO$_2$H(Glu)	700[b] ± 20
15	N$^\alpha$MeArg^8-Lys-Pro-Trp-Glu-Leu^{13}	none	>10000[b]

[a] $n = 6$ (number of replicate determinations) unless otherwise noted. [b] $n = 3$.

Tyr^{11} dipeptide with β-turn mimetics has suggested the presence of a β-turn-like structure, but overall there is a paucity of information about the biologically active conformation of NT or its C-terminal hexapeptide.[33-35] Recently, we have systematically investigated the Pro^{10}-Tyr^{11} sites of the NT$_{8-13}$ analogue 1 by incorporating a series of backbone and/or side chain modified amino acids which induced striking biological effects *in vitro* and *in vivo*.[27] In order to prepare conformationally rigid analogues of NT$_{8-13}$ and further understand the three-dimensional pharmacophore, we have synthesized a series of cyclic derivatives of the linear hexapeptide 1.

Several approaches were undertaken to obtain a cyclic NT$_{8-13}$ analogue that possessed high binding affinity for the NT receptor. Previous NT$_{8-13}$ structure–activity relationships have indicated residues that are critical for receptor recognition. For example, an alanine scan of NT$_{8-13}$ suggested[36] the relative importance of the individual amino acid side chains to be as follows: Leu^{13} > Tyr^{11} ≫ Ile^{12} > Arg^9 > Pro^{10} > Arg^8. Fragment studies also suggested[13-16] the requirement of at least one basic residue, since NT$_{8-13}$ and NT$_{9-13}$ have similar binding affinities, while the NT$_{10-13}$ fragment has much lower affinity. Finally, a free C-terminal carboxylate also appears to be essential for high receptor affinity since the NT$_{8-13}$ C-terminal amide has 2 orders of magnitude less binding.[36]

Given this information, we replaced the Tle^{12} of compound 1 with either a glutamic acid or aspartic acid residue. These substitutions provided a free carboxylate for cyclization via a lactam bridge, to either the Lys^9 side chain or the N-terminal amine, without removal of the important C-terminal carboxylic acid moiety. The preferred stereochemistry of the side chains forming the lactam bridge was also explored. Furthermore, alanine and glycine substitutions were incorporated to probe the importance of individual side chains. In several peptides glycine was added to the N-terminal Arg^9 and cyclized through the side chain carboxylate of position 12 to increase the flexibility of the lactam bridge. The Leu^{13} residue was replaced with aspartic acid such that the cyclic head-to-tail compound could be prepared to probe the relative importance of the Leu^{13} side chain and/or the free C-terminal carboxylate. Finally, cyclic disulfide-containing peptides were prepared for comparison with the corresponding cyclic lactams.

Results and Discussion

The side chain to N-terminus and side chain to side chain cyclics were prepared and cyclized on a solid support. Utilizing an N^α-*t*-Boc (*tert*-butyloxycarbonyl) protection strategy for the solid phase synthesis, the side chain carboxylates of Asp^{12} or Glu^{12} were protected as Fmo (9-fluorenylmethyl) esters. For the side chain to side chain cyclic analogues, the Lys^9 side chain was also Fmoc protected and was simultaneously deprotected along with the Asp^{12} or Glu^{12} side chain using piperidine. Cyclization on the resin takes advantage of the self-diluting effects of the resin.[37,38] Each peptide chain is isolated by the polymeric matrix such that the cyclization can occur rapidly and with less oligomeric byproducts. In general, for the cyclic neurotensin analogues prepared in this study on resin cyclization led to crude products that were relatively pure and easily isolated by subsequent RP-HPLC.

Neurotensin Receptor Binding Studies. Table 1 illustrates the NT binding affinity for compounds cyclized from the N-terminus to a side chain carboxylate. Compound 2 is the most potent analogue with 16 nM binding for the NT receptor. This is only 20-fold less potent than the linear NT$_{8-13}$ analogue (compound 1), from which these compounds were designed. In the preparation of compound 2, the α amine of Arg^8 of compound 1 was incorporated in the lactam reducing the overall basicity of the molecule. Previously, it has been reported that Ac-Arg^8-Lys-Pro-Trp-Tle-Leu^{13} exhibited similar affinity for the NT receptor (1.4 nM) as compound 1, suggesting that the loss of the N-terminal backbone basic group does not alone account for the differences in NT binding affinity of compounds 1 and 2.[39] In addition, compound 14, was prepared as an acyclic control of compound 2 (Table 2) is 20-fold less potent than compound 2. This suggests that cyclization provides peptide 2 with an entropic advantage for binding. The linear analogue of compound 11, compound 15 also possesses less binding affinity (see Table

Table 3. N-Terminal to C-Terminal Cyclized Neurotensin Analogues

no.	compound	constraint	NT binding (± SEM)[a] (nM, K_i)
16	cyclo[Arg^8-Lys-Pro-Trp-Tle-Leu^{13}]	α-NH_2(Arg)→α-CO_2H(Leu)	410 ± 106
17	cyclo[Arg^8-Lys-Pro-Tyr-Tle-Leu^{13}]	α-NH_2(Arg)→α-CO_2H(Leu)	440[b] ± 18
18	cyclo[Lys^9-Pro-Trp-Tle-Leu^{13}]	α-NH(Lys)→α-CO_2H(Leu)	350 ± 158

[a] $n = 6$ (number of replicate determinations) unless otherwise noted. [b] $n = 9$.

Table 4. Side Chain to Side Chain Cyclized Neurotensin Analogues

no.	compound	constraint	NT binding (± SEM)[a] (nM, K_i)
19	$N^\alpha MeArg^8$-cyclo[Lys-Pro-Trp-Glu-Leu^{13}]	ε-NH_2(Lys)→γ-CO_2H(Glu)	770 ± 26
20	$N^\alpha MeArg^8$-cyclo[D-Lys-Pro-Trp-Glu-Leu^{13}]	ε-NH_2(Lys)→γ-CO_2H(Glu)	8500 ± 500
21	$N^\alpha MeArg^8$-cyclo[Lys-Pro-Trp-D-Glu-Leu^{13}]	ε-NH_2(Lys)→γ-CO_2H(Glu)	1600 ± 152
22	$N^\alpha MeArg^8$-cyclo[D-Lys-Pro-Trp-D-Glu-Leu^{13}]	ε-NH_2(Lys)→γ-CO_2H(Glu)	2500[b] ± 200

[a] $n = 6$ (number of replicate determinations) unless otherwise noted. [b] $n = 9$.

Table 5. Disulfide Side Chain to Side Chain Cyclized Neurotensin Analogues

no.	compound	constraint	NT binding (± SEM)[a] (nM, K_i)
23	$N^\alpha MeArg^8$-cyclo[Cys-Pro-Trp-Pen[b]]-Leu^{13}	Cys→Pen[b]	83 ± 19
24	$N^\alpha MeArg^8$-cyclo[Cys-Pro-Trp-Cys]-Leu^{13}	Cys→Cys	810[c] ± 200
25	$N^\alpha MeArg^8$-cyclo[Pen-Pro-Trp-Pen]-Leu^{13}	Pen[b]→Pen[b]	4400[c] ± 19
26	cyclo[Cys-Arg^8-Lys-Pro-Trp-Pen]-Leu^{13}	Cys→Pen[b]	640[c] ± 10

[a] $n = 6$ (number of replicate determinations) unless otherwise noted. [b] Pen = penicillamine (β,β-dimethylcysteine). [c] $n = 3$.

2), providing further evidence that cyclization can be beneficial to ligand-receptor recognition. Here, the differences in binding affinities between cyclic and acyclic compounds is greater than that for compounds **2** and **14**, but it should be noted that compound **15** has an extra charge on the free Glu^{12} side chain and the amine terminus that are not present in acyclic compound **11**. Compound **11**, however, has nearly 50-fold less binding affinity than compound **2**. It is possible that N-methylation of the Arg^8 residue may remove an essential hydrogen bonding interaction, or, perhaps, the N-Me amide bond leads to a conformational change of the ring via *cis/trans* amide isomerization.

Compounds **9** and **13**, which have larger ring sizes than compound **2**, have lower binding affinities, perhaps due to their flexibility. (Compound **10**, which also has a larger ring size, exhibits a similar trend in binding affinity, although it is not statistically significant.) Interestingly, replacement of the Glu^{12} in compound **2** with Asp (compound **3**), which should constrain the molecule further, decreased the binding affinity by more than 50-fold. This suggests that the smaller ring may have changed the orientation of key side chains such that the molecule can no longer adopt a favorable conformation for NT binding.

Table 3 summarizes the NT binding results for compounds cyclized from the N- to C-terminus (head-to-tail). All compounds possessed less binding affinity than compound **2**, underlining the importance of the free C-terminal carboxylate. The reduced binding affinities of compounds **4**, **6**, and **8** (Table 1), however, may indicate that the side chain of the C-terminal Leu^{13} is important, as well. Compound **5** did not bind to the NT receptor, suggesting an important role for the Lys^9 side chain in this series of compounds. In contrast, compound **7**, in which one of the two basic residues is deleted, displayed only 20-fold lower binding affinity with respect to compound **2**. Also, compound **18**, which has only one basic side chain, had virtually the same if not better binding when compared to the cyclic hexapeptides **16** and **17**, which contain both the Arg^8 and the Lys^9 side chains. This suggests that the position next to the Pro is more important than the Arg^8 position in this series, which is consistent with the previous data from the Ala scan performed on the C-terminal hexapeptide.[36]

Table 4 provides binding data for the side chain to side chain cyclic analogues, all of which have weak affinity for the NT receptor (compounds **19** to **22**). This may be due to the fact that two key side chains are involved in the cyclization and not available for receptor interaction, or that the peptide is constrained in a conformation that is unfavorable for receptor recognition. In any case, the orientation of the amino acids in position 9 (Lys) or 12 (Glu) seemed to have little effect on NT binding affinity.

Comparison of these data to the data in Table 5 for the disulfide cyclized peptides shows that the Lys^9 side chain can be removed while retaining moderate affinity for the NT receptor (83 nM) (compound **23**). Therefore, the disulfide bridge may constrain the molecule differently than a lactam (Table 4) and orient the peptide in a favorable conformation for binding. These data contradict the data for the N-terminus to side chain cyclics, which suggests that the Lys^9 side chain is critical for binding, but it is possible that the smaller ring of the disulfide has moved the Arg^8 side chain to a position where it is able to mimic the Lys^9 side chain. Nevertheless, the binding affinity of compound **23** is still 5-fold less than that of compound **2**, so both basic side chains may be contributing to the binding.

Table 5 also illustrates the effect of structural modifications proximate to the disulfide (i.e., cysteine versus penicillamine). Specifically, removal of the β,β-dimethyls from Pen^{12} in compound **23** by replacement with a cysteine residue, as in compound **24**, resulted in a 10-fold loss in binding affinity. It could be postulated that the penicillamine β,β-dimethyl groups may be binding in the same pocket as the methyl groups of Tle^{12} (compound **1**). Interestingly, compound **25** exhibited a 50-fold decrease in NT binding affinity relative to compound **23** and suggested the possibility that the β,β-dimethyls of Pen^9 effected steric hinderance to ligand-receptor recognition and/or intramolecular effects to the conformation of the cyclic NT_{8-13} analogue which compromised binding to the NT receptor, *vide infra*. Also,

compound **26** exhibited approximately an 8-fold loss of affinity with respect to compound **23**. This may simply be an effect of the excess entropy resulting from the larger ring size.

Intracellular Calcium Mobilization Studies. The relatively low binding affinity of the cyclic analogues versus neurotensin, itself or compound **1**, precluded the evaluation of functional activity in an *in vivo* system. In lieu of this, several compounds were evaluated for their ability to stimulate calcium mobilization in HT-29 cells. NT and compound **1** were shown to be agonists with EC_{50}'s of 12 and 120 nM, respectively. Likewise, preliminary studies for compounds **2**, **18**, and **23** revealed that these were able to stimulate intracellular calcium mobilization with low micromolar EC_{50}'s. In fact, compounds **1** and **2** were full agonists, using NT as a control for a full agonist, while compounds **18** and **23** were only partial agonists. Clearly, the receptor binding affinities observed with 10-day-old postnatal mouse brain do not correlate directly to the functional activity observed in HT-29 cells making a concise evaluation of weaker binding compounds very difficult. Additional studies with these and other cyclic analogues, including an evaluation of their ability to stimulate intracellular calcium mobilization, are in progress and will be published elsewhere.

^{1}H-NMR Studies. While NOE measurements provide a rich source of structural constraints for small proteins, their utility for the structural analysis of peptides is limited, due to the inherent flexibility and relatively large surface area of these compounds. Therefore, in order to assess the structural characteristics of some of these cyclic/constrained NT analogues, coupling constants and amide proton temperature coefficients were measured for compounds **2**, **3**, **23**, and **25** (Table 6). Typically, limited conformational averaging can be inferred if the $^3J_{NH,H\alpha}$ value is less than 6 Hz or greater than 8 Hz. However, even when this condition is met $^3J_{NH,H\alpha}$ values may be consistent with more than one distinct dihedral angle, but such ambiguity can be resolved by determining heteronuclear coupling constants. For compounds **2** and **3**, a ^{13}C-edited TOCSY experiment[40,41] was used to determine $^3J_{NH,C\beta}$ values. Also, reduced temperature coefficients for exchangeable protons can be employed to suggest reduced contact with the solvent. In water, a fully exposed backbone amide proton is expected to possess a temperature coefficient of about −10 ppb/K. A smaller temperature coefficient (closer to zero) indicates reduced exchange with the bulk solvent and possible involvement in hydrogen bonding especially when it ($\Delta\delta/\Delta T$) is less than or equal to ~3 ppb/K. Unfortunately, for these compounds the $^3J_{NH,H\alpha}$ values are in the motionally averaged range. Also, the distinct lack of long-range crosspeaks in the NOESY and ROESY spectra suggest that all of these compounds are somewhat flexible. These factors have precluded the determination of highly refined structures, although some interesting trends do exist and deserve comment.

Table 6. Proton NMR Data for Compounds **2**, **3**, **23** and **25**

residue	$^3J_{NH,H\alpha}$ (Hz)	$^3J_{NH,C\beta}$ (Hz)	$\Delta\delta/\Delta T$ (ppb/K)	288 K	δNH (ppm) 293 K	298 K	308 K
			Compound 2				
Arg^8	8.0	1.0	−8.0	8.20		8.12	
Lys^9	5.9		−8.0	8.27		8.19	
Trp^{11}	7.0	1.5	−4.0	7.88		7.84	
Glu^{12}	8.7	0.6	−6.0	7.92		7.86	
Leu^{13}	8.3	1.5	−9.0	8.03		7.94	
			Compound 3				
Arg^8	6.4		−8.3	7.52		7.43	
Lys^9	2.6		−7.7	8.66		8.58	
Trp^{11}	8.1	1.8	−1.2	7.44		7.43	
Asp^{12}	9.4	1.6	−5.2	8.38		8.33	
Leu^{13}	7.7	2.9	−3.8	7.31		7.27	
			Compound 23				
Cys^9	major: 6.3		−7.0	9.18		9.05	8.98
	minor: 8.2		−8.0	8.98		8.90	
Trp^{11}	major: 6.7		−12.0	8.01		7.88	7.77
	minor: 6.5		−8.0	8.77		8.69	
Pen^{12}	major: 9.1		−4.0	7.77		7.73	7.69
	minor: 8.1		−3.0	7.65		7.68	
Leu^{13}	major: 6.7		−6.5	8.41		8.35	8.28
	minor: 7.5		−9.5	8.68		8.58	
			Compound 25				
Pen^9	major: 7.4		−7.0	8.68	8.71		
	minor: 10.0		−8.0	8.62	8.66		
Trp^{11}	major: 8.3		−8.0	6.80	6.84		
	minor: 11.0		−7.8	7.68	7.72		
Pen^{12}	major: 7.0		−4.4	7.65	7.68		
	minor: 10.3		−2.0	8.72	8.73		
Leu^{13}	major: 7.6		−9.2	8.58	8.62		
	minor: 6.2		−5.8	8.37	8.40		

Compounds **2** and **3** have 17 and 16 membered rings, respectively, and as expected for such large cyclic systems both are somewhat flexible. As might be anticipated from a comparison of the two peptides, the smaller of the two, compound **3**, has some spectral features that are consistent with a greater degree of conformational rigidity. The $^3J_{NH,H\alpha}$ values for Lys^9 (2.6 Hz) and Asp^{12} (9.4 Hz) lie outside the range expected for motional averaging. Furthermore, for compound **3**, the Trp^{11} and Leu^{13} residues have relatively small amide proton temperature coefficients of −1.2 and −3.8 ppb/K, respectively. In compound **2**, all of the ^{1}H-NMR parameters are indicative of a more flexible peptide. However, it should be noted that, with the exception of the Leu^{13} amide proton temperature coefficient, the same trend is observed for compounds **2** and **3** (e.g., for both compounds the residues Lys^9 and Glu/Asp^{12} possesses the smallest and largest $^3J_{NH,H\alpha}$ values, respectively, and Trp^{11} possesses the smallest amide temperature coefficient). This suggests that while compound **2** is more flexible than compound **3**, they may both share one or more common three-dimensional conformation(s). Interestingly, both peptides show strong Lys$^9{}_{H\alpha}$ to Pro$^{10}{}_{H\alpha}$ NOE's indicating a *cis* amide bond between Lys^9 and Pro^{10}. Linear proline-containing peptides commonly exhibit *cis* and *trans* isomers that are in slow exchange (relative to the chemical shift time scale), but for compounds **2** and **3**, these peptides exist exclusively in the *cis*-proline conformation.

Compounds **23** and **25** represent two extremes in terms of NT receptor binding affinity (Table 5) for the 14-membered ring disulfide-cyclized NT analogues, yet they only differ by two methyl groups. A critical examination of the ^{1}H-NMR data in Table 6 reveals that several interesting features exist. First, both compounds **23** and **25** exist as a major (~80%) and minor (~20%) isomer on the ^{1}H-NMR time scale. In the case of compound **25**, the major isomer has a *trans*-proline and the minor has a *cis*-proline amide bond. This is based upon the strong NOE's observed between Pen$^9{}_{H\alpha}$−Pro$^{10}{}_{H\delta}$ and Pen$^9{}_{H\alpha}$−Pro$^{10}{}_{H\alpha}$, respectively. (The equivalent NOEs could not be identified for compound **23** due to poor signal-to-noise and spectral overlap.) For both

of the peptides the major isomer has medium sized $^3J_{NH,H\alpha}$ values (except for Pen[12] in **23** and Trp[11] in **25**) and large amide proton temperature coefficients. Both of these observations are consistent with motional averaging. Two features distinguish the major isomers of compounds **23** and **25** and suggest that their preferred conformations are not identical. First, the only residues that display $^3J_{NH,H\alpha}$ values greater than 8 Hz are Pen[12] in compound **23** and Trp[11] in compound **25**, *vide supra*. Secondly, a 1 ppm chemical shift difference exists between the NH resonances of Trp[11] in the major isomers of compounds **23** and **25**.

In contrast to the major isomers, several differences in chemical shifts and coupling constants are even more obvious in the minor isomers. For example, the minor (*cis*) isomer of compound **25** has large $^3J_{NH,H\alpha}$ values for all of the amino acids in the cyclic portion of the molecule (Table 6). This limits the allowed conformational space for the ϕ angle from approximately $-170°$ to $-80°$. This further suggests that the backbone conformation of the minor isomer of compound **25** is well defined, at least with respect to the other cyclic NT peptides discussed here. Also, the Pen[12] amide proton in the minor isomer has the smallest temperature coefficient (-2.0 ppb/K) of any of the these analogues. For all of the peptides presently investigated, the minor conformer of compound **25** is clearly the most conformationally constrained. Due to the relatively low abundance (15–20%) of this conformer, we could not determine meaningful NOE's for structural analysis. Currently, we are optimizing conditions for the structural analysis of these peptides.

Conclusions

We report the synthesis of several conformationally constrained cyclic neurotensin fragment (NT_{8-13}) analogues, several of which possess nanomolar binding affinities at the NT receptor. Specifically, compounds **2**, **10**, and **23** are the only cyclic peptides of the C-terminal hexapeptide that have been shown to possess low nanomolar affinity for the NT receptor. These analogues provide further evidence that a reverse-turn in the C-terminal hexapeptide in NT may be important for NT binding.[27] It is interesting that compounds **2** and **23**, which are structurally very different, have similar binding affinities. These compounds may provide novel molecular probes to further investigate NT receptor pharmacology, as well as further advance our understanding of the structure–conformation relationships of NT and establish a working basis for future pharmacophore mapping studies. To this extent, future molecular modeling and ^{1}H-NMR studies of these compounds may provide some insight toward the identification of the three-dimensional structural requirements for NT binding. Such work will extend previous studies[27] which implicated reverse-turn type conformational preferences within a series of linear NT_{8-13} analogues as a result of modifications of the Pro[10]-Tyr[11] dipeptide. Future studies will be directed at the design of NT_{8-13} pseudopeptides and peptidomimetics that may exploit such structure–conformation relationships in the discovery of yet more effective NT agonists.

Experimental Section

General. All reagents and solvents were purchased from commercial sources unless otherwise specified. Solvents were of reagent or HPLC grade as indicated. All amino acids and substituted peptide resins were purchased from commercial sources, used without further purification, and amino acids were of the L configuration unless indicated. Routine ^{1}H-NMR spectra were obtained on a Bruker AM-250 spectrometer, and all samples were dissolved in D_2O or DMSO-d_6, as indicated. Mass spectra were recorded on a VG Analytical 7070E/HF, a VG Masslab Trio-2A, or a Fisons VG Trio200 mass spectrometer. Amino acid analyses were performed on an Applied Biosystems International (ABI) 420H derivatizer with a 130A separation system.

Peptide Synthesis Method A (PAM Resin). The peptides were prepared by standard solid phase peptide methodology[42] on an ABI 430A peptide synthesizer using the N^α-*t*-Boc *N*-hydroxybenzotriazole (HOBt), *N*-methylpyrrolidone (NMP) strategy (Version 1.40). Single couplings were performed with 4 equiv of the suitably protected amino acid activated ester formed by reaction with *N,N'*-dicyclohexylcarbodiimide (DCC) and HOBt. A typical cycle for the coupling of an individual amino acid was as follows: (1) activation of the next amino acid to be coupled with DCC and HOBt; (2) deprotection of the amino acid on the resin with 50% trifluoroacetic acid (TFA)/dichloromethane (DCM) + indole (1 mg/mL, used as a scavenger); (3) washes with DCM and neutralization with 10% diisopropylethylamine (DIEA)/DCM; (4) coupling of the HOBt activated ester in NMP; (5) five washes with NMP and capping with 10% acetic anhydride (Ac_2O)/DCM. The N-terminal Boc group was removed with 50% TFA/DCM, and the resin was neutralized with 10% DIEA/DCM (except for peptides to be cyclized by cyclization method A). The resin was then washed with DCM and dried under reduced pressure.

Peptide Synthesis Method B (Sasrin Resin[43]). Sasrin resin (1 g, 1 mmol) was placed in a shaker vessel and washed with 3 × 25 mL of DCM. The first coupling was performed using 3 equiv of the Fmoc-protected amino acid, 3 equiv of *N,N'*-diisopropylcarbodiimide (DIC), and 0.3 equiv of 4-(dimethylamino)pyridine (DMAP), in 25 mL of DCM overnight. The resin was then rinsed with *N,N*-dimethylformamide (DMF) (3 × 25 mL). The Fmoc group was removed by treatment with 20% piperidine/DMF for 1 and 10 min (2 × 25 mL). Amino acids were successively coupled using 3 equiv of 2-(1*H*-benzotriazol-1-yl)-1,1,3,3-tetramethyluronium hexafluorophosphate (HBTU),[44] 3 equiv of DIEA, and 3 equiv of the amino acid (N^α-Fmoc-protected, Arg and Lys side chains protected as the tosyl and *t*-Boc derivatives, respectively) in DMF for 60 min, followed by Fmoc deprotection. After the final Fmoc deprotection, the resin was washed with DMF (3 × 25 mL) and DCM (3 × 25 mL) and was dried under reduced pressure.

Resin Cyclization, Method A (Side Chain to Side Chain, PAM Resin). To deprotect the Fmo-ester-protected side chains of Glu and Lys, 25 mL of 20% piperidine/DCM was added to a shaker vessel containing the resin, and the mixture was shaken for 15 min and drained. Another 25 mL of 20% piperidine/DCM was added to the shaker vessel, and the mixture was shaken for 30 min. The vessel was drained and washed with DCM (3 × 25 mL) and DMF (3 × 25 mL). For side chain to side chain cyclizations, the resin was suspended in 25 mL of DMF, and 400 μL of DIEA was added followed by 270 mg of HOBt and 300 μL of DIC. The mixture was shaken continuously, and the solvent/reagents were changed every 24 h until the resin yielded a negative Kaiser test.[45] The vessel was then drained, and the resin was washed with DMF (3 × 25 mL) and DCM (3 × 25 mL). To deprotect the N-terminal *t*-Boc group, 25 mL of 50% TFA/DCM was added, and the mixture was shaken for 15 min. The vessel was drained, another 25 mL of 50% TFA/DCM was added, and the mixture was shaken for an additional 30 min. The vessel was drained, and the resin was washed with DCM (3 × 25 mL), 10% DIEA/DCM (3 x 25 mL), and DCM (3 × 25 mL), and the resin was dried under reduced pressure.

Resin Cyclization, Method B (Side Chain to N-Terminus, PAM Resin). To deprotect the Fmo-ester-protected side chains of Glu or Asp, 25 mL of 20% piperidine/DCM was added to a shaker vessel containing the resin, and the mixture was shaken for 15 min and drained. Another 25 mL of 20% piperidine/DCM was added to the shaker vessel, and the

mixture was shaken for 30 min. The vessel was drained and washed with DCM (3 × 25 mL) and DMF (3 × 25 mL). The resin was suspended in 25 mL of DMF, and 400 μL of DIEA was added followed by 270 mg of HOBt and 300 μL of DIC. The mixture was shaken continuously, and the solvent/reagents were changed every 24 h until the resin yielded a negative Kaiser test.[45] The vessel was then drained, and the resin was washed with DMF (3 × 25 mL) and DCM (3 × 25 mL) and dried under reduced pressure.

Peptide Cleavage Method A (PAM Resin). The peptides were removed from the resin and the side chains deprotected by treatment with 90% anhydrous hydrogen fluoride (HF) and 10% scavengers (3-methylindole and anisole) at 0 °C for 1 h. Nitrogen was bubbled through the mixture to evaporate the HF, and the residue was triturated with 75 mL of Et_2O and filtered. The crude precipitate was dissolved in 70% CH_3CN/H_2O + 0.1% TFA and filtered, and the solvent was removed under reduced pressure. The residue was resuspended in ~100 mL of H_2O and lyophilized.

Peptide Cleavage Method B (Sasrin Resin[43]). A solution of 1% TFA/DCM (20 mL) was added to the resin in a shaker vessel, and the mixture was agitated for 10 min and drained. This procedure was repeated three times, and the combined eluants were evaporated under reduced pressure. The residue was resuspended in ~100 mL of H_2O and lyophilized.

Solution Cyclization, Method C (Disulfides). The crude lyophilized peptide after HF cleavage (peptide cleavage method A) (~300 mg) was dissolved in 2.5 L of H_2O, and the pH was adjusted to 8.5 with 1 N potassium hydroxide (KOH). Dithiothreitol (DTT, ~200 mg) was added, and the mixture was stirred for 1 h. Potassium ferricyanide ($K_3Fe(CN)_6$, 500 mg in 100 mL of H_2O) was then added dropwise to the solution while the pH was maintained at ~8–9 with 1 N KOH until a pale yellow color was maintained for 60 min. At this point, the pH was then adjusted to 4.5 with glacial acetic acid, and the solution was stirred for 10 min with an excess of BioRad AG4-X4 anion exchange resin (~10-fold). The solution was filtered and passed through a C18 cartridge preequilibrated with H_2O. The absorbed cyclic peptide was eluted with 70% CH_3CN/H_2O + 0.1% TFA, concentrated under reduced pressure, resuspended in H_2O (~100 mL), and lyophilized.

Solution Cyclization, Method D (C-Terminus to N-Terminus). A solution of the linear peptide (240 mg) in 30 mL of DMF was added dropwise with stirring over 60 min to a solution of (benzotriazol-1-yloxy)tris(dimethylamino)phosphonium hexafluorophosphate (BOP)[38,46] or HBTU[44] (0.6 mmol, 3 equiv) and DIEA (0.6 mmol, 3 equiv) in 200 mL of DMF at 0 °C. The reaction was followed by analytical HPLC, which showed the disappearance of starting material after 60 min. The reaction mixture was allowed to slowly warm to room temperature, the solvent was removed under reduced pressure, and the peptide was lyophilized from H_2O (~100 mL). The side chain protecting groups were then removed with HF as described above (peptide cleavage method A).

Peptide Purification. The crude peptide was dissolved in approximately 3–5 mL of H_2O + 20% CH_3CN (with increasing amounts of CH_3CN as needed for dissolution) and chromatographed on a Vydac 218TP1022 (2.2 × 25.0 cm) preparative HPLC column. A linear gradient of 0.1% TFA/water to 0.1% TFA/CH_3CN was used to elute the peptide from the column. A flow rate of 15 mL/min was maintained on a Waters 600E System Controller, and the absorbance of the eluant at 214 and 280 nm was recorded on a Waters 490E programmable multiwavelength detector. Individual fractions were collected and analyzed by analytical HPLC. Appropriate fractions were combined and concentrated under reduced pressure, diluted with H_2O, and lyophilized to give the purified peptide.

Peptide Characterization. The peptides were assayed for purity by analytical HPLC on a Vydac 218TP54 (0.46 × 25.0 cm) analytical HPLC column connected to a Waters 600E system controller with a Waters 490E programmable multiwavelength detector. A gradient of 20–86% B over 22 min (A = 0.1% TFA/H_2O, B = 0.1% TFA/CH_3CN) was used with a flow rate of 1.5 mL/min. The purity of the peptides was confirmed by capillary zone electrophoresis (CZE) using an ABI 270A capillary electrophoresis system with a 72 cm capillary at +20 kV and a buffer of 20 mM sodium citrate, pH 2.5. The peptides were also analyzed by fast-atom bombardment (FAB) or electrospray (ES) mass spectrometry, amino acid analysis (AAA), and ^{1}H-NMR. Values found were in good agreement with the predicted values.

Compound 2 was synthesized using peptide synthesis method A, cyclization method B, followed by peptide cleavage method A. Analytical; RP-HPLC, t_R 8.07 min; purity, 91% at 214 nm. CZE: t_R 17.54 min; purity, >99% at 214 nm. MS (ES, m/z): 809.8 $[MH]^+$. AAA and ^{1}H-NMR (D_2O) were consistent with the proposed structure.

Compound 3 was synthesized using peptide synthesis method A, cyclization method B, followed by peptide cleavage method A. Analytical; RP-HPLC, t_R 9.16 min; purity, 90% at 214 nm. CZE: t_R 9.44 min; purity, 89% at 214 nm. MS (FAB, m/z): 796.4 $[MH]^+$. AAA and ^{1}H-NMR (D_2O) were consistent with the proposed structure.

Compound 4 was synthesized using peptide synthesis method A, cyclization method B, followed by peptide cleavage method A. Analytical; RP-HPLC, t_R 5.18 min; purity, 97% at 214 nm. CZE: t_R 9.18 min; purity, 95% at 214 nm. MS (FAB, m/z): 754.3 $[MH]^+$. AAA and ^{1}H-NMR (DMSO-d_6) were consistent with the proposed structure.

Compound 5 was synthesized using peptide synthesis method A, cyclization method B, followed by peptide cleavage method A. Analytical; RP-HPLC, t_R 10.18 min; purity, 95% at 214 nm. CZE: t_R 12.68 min; purity, >99% at 214 nm. MS (FAB, m/z): 753.8 $[MH]^+$. AAA and ^{1}H-NMR (DMSO-d_6) were consistent with the proposed structure.

Compound 6 was synthesized using peptide synthesis method A, cyclization method B, followed by peptide cleavage method A. Analytical; RP-HPLC, t_R 13.33 min; purity, 90% at 214 nm. CZE: t_R 6.06 min; purity, 95% at 214 nm. MS (FAB, m/z): 697.6 $[MH]^+$. AAA and ^{1}H-NMR (DMSO-d_6) were consistent with the proposed structure.

Compound 7 was synthesized using peptide synthesis method A, cyclization method B, followed by peptide cleavage method A. Analytical; RP-HPLC, t_R 10.63 min; purity, >99% at 214 nm. CZE: t_R 17.32 min; purity, >99% at 214 nm. MS (ES, m/z): 682.6 $[MH]^+$. AAA and ^{1}H-NMR (DMSO-d_6) were consistent with the proposed structure.

Compound 8 was synthesized using peptide synthesis method A, cyclization method B, followed by peptide cleavage method A. Analytical; RP-HPLC, t_R 6.77 min; purity, >99% at 214 nm. CZE: t_R 10.10 min; purity, >99% at 214 nm. MS (FAB, m/z): 810.7 $[MH]^+$. AAA and ^{1}H-NMR (DMSO-d_6) were consistent with the proposed structure.

Compound 9 was synthesized using peptide synthesis method A, cyclization method B, followed by peptide cleavage method A. Analytical; RP-HPLC, t_R 7.38 min; purity, 91% at 214 nm. CZE: t_R 13.83 min; purity, >99% at 214 nm. MS (ES, m/z): 867.4 $[MH]^+$. AAA and ^{1}H-NMR (DMSO-d_6) were consistent with the proposed structure.

Compound 10 was synthesized using peptide synthesis method A, cyclization method B, followed by peptide cleavage method A. Analytical; RP-HPLC, t_R 9.07 min; purity, 95% at 214 nm. CZE: t_R 10.58 min; purity, 93% at 214 nm. MS (FAB, m/z): 881.4 $[MH]^+$. AAA and ^{1}H-NMR (DMSO-d_6) were consistent with the proposed structure.

Compound 11 was synthesized using peptide synthesis method A, cyclization method B, followed by peptide cleavage method A. Analytical; RP-HPLC, t_R 7.88 min; purity, 90% at 214 nm. CZE: t_R 14.78 min; purity, 93% at 214 nm. MS (FAB, m/z): 824.8 $[MH]^+$. AAA and ^{1}H-NMR (DMSO-d_6) were consistent with the proposed structure.

Compound 12 was synthesized using peptide synthesis method A, cyclization method B, followed by peptide cleavage method A. Analytical; RP-HPLC, t_R 9.42 min; purity, 94% at 214 nm. CZE: t_R 9.41 min; purity, 90% at 214 nm. MS (ES, m/z): 405.7 $[M + 2H]^{2+}$. AAA and ^{1}H-NMR (DMSO-d_6) were consistent with the proposed structure.

Compound 13. N^α-Boc-homoglutamic acid γ-Fmo ester (homoglutamic acid (Hgl) = 2-aminoadipic acid) was prepared according to the procedure of Al-Obeidi *et al.*[47] Compound 13

was synthesized using peptide synthesis method A, cyclization method B, followed by peptide cleavage method A. Analytical; RP-HPLC, t_R 10.47 min; purity, 93% at 214 nm. CZE: t_R 6.04 min; purity, >99% at 214 nm. MS (ES, m/z): 823.8 $[MH]^+$. AAA and ^{1}H-NMR (DMSO-d_6) were consistent with the proposed structure.

Compound 14 was synthesized using peptide synthesis method A, followed by peptide cleavage method A. Analytical; RP-HPLC, t_R 6.78 min; purity, 95% at 214 nm. CZE: t_R 10.03 min; purity, 96% at 214 nm. MS (FAB, m/z): 869.5 $[MH]^+$. AAA and ^{1}H-NMR (DMSO-d_6) were consistent with the proposed structure.

Compound 15 was synthesized using peptide synthesis method A, followed by peptide cleavage method A. Analytical; RP-HPLC, t_R 6.13 min; purity, >99% at 214 nm. CZE: t_R 12.27 min; purity, >99% at 214 nm. MS (FAB, m/z): 842.9 $[MH]^+$. AAA and ^{1}H-NMR (DMSO-d_6) were consistent with the proposed structure.

Compound 16 was synthesized using peptide synthesis method B, peptide cleavage method B, followed by cyclization method D. Analytical; RP-HPLC, t_R 9.73 min; purity, 98% at 214 nm. CZE: t_R 9.46 min; purity, 98% at 214 nm. MS (FAB, m/z): 794.7 $[MH]^+$. AAA and ^{1}H-NMR (DMSO-d_6) were consistent with the proposed structure.

Compound 17 was synthesized using peptide synthesis method B, peptide cleavage method B, followed by cyclization method D. Analytical; RP-HPLC, t_R 9.95 min; purity, 96% at 214 nm. CZE: t_R 13.06 min; purity, 97% at 214 nm. MS (FAB, m/z): 799.7 $[MH]^+$. AAA and ^{1}H-NMR (DMSO-d_6) were consistent with the proposed structure.

Compound 18 was synthesized using peptide synthesis method B, peptide cleavage method B, followed by cyclization method D. Analytical; RP-HPLC, t_R 13.04 min; purity, >95% at 214 nm. CZE: t_R 13.96 min; purity, 95% at 214 nm. MS (ES, m/z): 638.4 $[MH]^+$. AAA was consistent with the proposed structure.

Compound 19 was synthesized using peptide synthesis method A, cyclization method A, followed by peptide cleavage method A. Analytical; RP-HPLC, t_R 9.38 min; purity, 98% at 214 nm. CZE: t_R 7.34 min; purity, 93% at 214 nm. MS (ES, m/z): 823.5 $[MH]^+$. AAA and ^{1}H-NMR (DMSO-d_6) were consistent with the proposed structure.

Compound 20 was synthesized using peptide synthesis method A, cyclization method A, followed by peptide cleavage method A. Analytical; RP-HPLC, t_R 9.43 min; purity, 92% at 214 nm. CZE: t_R 10.30 min; purity, 95% at 214 nm. MS (FAB, m/z): 824.5 $[MH]^+$. AAA and ^{1}H-NMR (DMSO-d_6) were consistent with the proposed structure.

Compound 21 was synthesized using peptide synthesis method A, cyclization method A, followed by peptide cleavage method A. Analytical; RP-HPLC, t_R 9.28 min; purity, >99% at 214 nm. CZE: t_R 9.99 min; purity, 99% at 214 nm. MS (FAB, m/z): 824.5 $[MH]^+$. AAA and ^{1}H-NMR (DMSO-d_6) were consistent with the proposed structure.

Compound 22 was synthesized using peptide synthesis method A, cyclization method A, followed by peptide cleavage method A. Analytical; RP-HPLC, t_R 9.26 min; purity, 95% at 214 nm. CZE: t_R 10.71 min; purity, 93% at 214 nm. MS (FAB, m/z): 824.6 $[MH]^+$. AAA and ^{1}H-NMR (DMSO-d_6) were consistent with the proposed structure.

Compound 23 was synthesized using peptide synthesis method A, peptide cleavage method A, followed by cyclization method C. Analytical; RP-HPLC, t_R 10.69 min; purity, 99% at 214 nm. CZE: t_R 7.10 min; purity, 98% at 214 nm. MS (FAB, m/z): 818.5 $[MH]^+$. AAA and ^{1}H-NMR (D_2O) were consistent with the proposed structure.

Compound 24 was synthesized using peptide synthesis method A, peptide cleavage method A, followed by cyclization method C. Analytical; RP-HPLC, t_R 9.28 min; purity, 99% at 214 nm. CZE: t_R 14.95 min; purity, 98% at 214 nm. MS (ES, m/z): 789.3 $[MH]^+$. AAA and ^{1}H-NMR (DMSO-d_6) were consistent with the proposed structure.

Compound 25 was synthesized using peptide synthesis method A, peptide cleavage method A, followed by cyclization method C. Analytical; RP-HPLC, t_R 9.33 min; purity, 98% at 214 nm. CZE: t_R 6.03 min; purity, 98% at 214 nm. MS (FAB, m/z): 845.6 $[MH]^+$. AAA and ^{1}H-NMR (DMSO-d_6) were consistent with the proposed structure.

Compound 26 was synthesized using peptide synthesis method A, peptide cleavage method A, followed by cyclization method C. Analytical; RP-HPLC, t_R 11.95 min; purity, 98% at 214 nm. CZE: t_R 6.70 min; purity, 99% at 214 nm. MS (FAB, m/z): 931.4 $[MH]^+$. AAA and ^{1}H-NMR (DMSO-d_6) were consistent with the proposed structure.

NMR Measurements for Structural Studies. The NMR spectra were acquired on a Bruker AMX500 spectrometer using 2 mg of peptide dissolved in 0.5 mL of H_2O/5% D_2O. The proton chemical shifts were referenced to tetramethylsilane (TMS) at 0.00 ppm, and the water signal was presaturated during acquisition. Proton assignments were based on the TOCSY[40] experiment acquired into 512 t1 blocks of 2048 t2 data points using a 7 kHz MLEV-17[48] spin lock field applied at the transmitter frequency (ca. 4.76 ppm) for 65 ms. Sequential assignments were based on the rotating frame nuclear Overhauser spectroscopy (ROESY)[49] experiment (512 t1 blocks of 2048 t2 data points). A 4 kHz continuous wave spin-lock field was applied during the 250 ms mixing time at the transmitter frequency. The temperature dependence of the amide protons was determined by acquiring proton spectra at 5° increments between 288 and 308 K. Homonuclear coupling constants were measured directly from the resolution-enhanced proton spectra (Gaussian broadening (GB) = 0.6, line broadening (LB) = −6). Heteronuclear coupling constants were measured from the ^{13}C-edited TOCSY[41] spectra at natural abundance of the ^{13}C nuclei. The pulse sequence includes BIRD type heteronuclear editing to select protons attached to ^{13}C nuclei followed by a conventional TOCSY pulse sequence.

Neurotensin Binding Assay. [^{3}H]NT (107.2 Ci/mmol) or [^{125}I-Tyr^3]NT (2200 Ci/mmol) was obtained from Dupont-New England Nuclear, Boston, MA. Membranes were prepared according to the methods of Mazella *et al.*[50] with minor modifications. Briefly, seven frozen 10-day-old postnatal mouse brains were thawed and the cerebellum removed. The membranes were homogenized in 20 volumes of ice cold 5 mM tris(hydroxymethyl)aminomethane (TRIZMA) buffer, pH 7.5 (buffer A). The homogenates were centrifuged at 100000g for 15 min at 4 °C. Resulting pellets were resuspended in the same volume of buffer and recentrifuged as above, twice repeated. Final pellets were resuspended in 1 g wet weight in each milliliter of buffer B (50 mM TRIZMA, pH 7.4, 0.1% bovine serum albumin (BSA), 0.2 mM bacitracin, 1 mM ethylenediaminetetraacetic acid (EDTA), 1 mM phenanthroline, 0.3 mM toluenesulfonyl fluoride (PMSF)) and used for the assay.

To label the NT receptor, [^{3}H]NT or [^{125}I-Tyr^3]NT (0.20 nM or 0.21 nM final concentration, respectively) was used. (In general, [^{3}H]NT was used for all the analyses, with the exception of compounds **2**, **20**, and **21** for which [^{125}I-Tyr^3]NT was the radioligand.) The binding assay was slightly modified from that of Kitabgi *et al.*[51] Briefly, 25 μL of [^{3}H]ligand, 25 μL of either drug or buffer, and 200 μL of brain membranes (all diluted with ice cold buffer B) were added to polypropylene microtubes (96-well microplate format; total volume 250 μL). Incubation proceeded for 30 min at 25 °C and was terminated by rapid filtration through Whatman GF/B glass fiber filters which had been presoaked for 1 h in 0.5% polyethylenimine. Radioactivity on the filters was determined on a γ or β counter following the addition of liquid scintillation cocktail. Under these conditions 96% specific binding was observed for [^{125}I-Tyr^3]NT and 90% specific binding for [^{3}H]NT. Nonspecific binding was determined using 1 μM NT. Binding affinities for NT standards were determined from competition curves.

Cellular Calcium Measurements. Changes in $[Ca^{2+}]_i$ were determined with the Ca^{2+}-sensitive dye fura-2/AM and a Proton Technology International Photoscan-2 dual excitation spectrofluorometer. The protocol followed was essentially that of Turner *et al.*[52] Briefly, a suspension of HT-29 cells pelleted by centrifugation at 1000g was washed in a balanced salt solution consisting of 130 mM NaCl, 5 mM KCl, 1 mM Na_2HPO_4, 15 mM glucose, 10 mM HEPES, 0.1% BSA, 1.0 mM $MgCl_2$, and 0.2 mM $CaCl_2$ at pH 7.4 (solution 1). The pellet obtained was suspended in a different balanced salt solution

containing 1.0 mM $MgCl_2$ 0.2 mM $CaCl_2$, and 0.1% BSA (solution 2). To load cells, cell suspensions (3×10^6 cells/mL) were incubated with 2 μM fura-2/AM for 40 min at 37 °C in a shaking incubator. After washing and resuspension in solution 2 at the original density, the cell suspensions were further incubated for 40 min to appropriately allow for the maximal de-esterification process. Measurement of autofluorescence was conducted in an equal aliquot of cell suspension taken through the same steps as in the fura-2/AM-treated suspension, but without the dye added. After centrifugation, cells were washed twice in solution 2. The final pellet was resuspended in a balanced salt solution containing 1.0 mM $MgCl_2$ 1.0 mM $CaCl_2$, and 0.1% BSA. Samples were temporarily stored in a water bath maintained at 37 °C which was placed on top of a stir plate. For $[Ca^{2+}]$ measurements, 1 mL aliquots of fura-2/AM-loaded cells were transferred to quartz cuvettes and the latter placed in the spectrophotometer to establish a stable baseline. Compounds were then added to the cell suspension. A magnetic stir bar was always placed in each cuvette to allow proper mixing of compounds and to prevent cells form settling to the bottom.

The $[Ca^{2+}]_i$ concentration was determined using the Proton Technology International Deltascan II spectrofluorometer by measuring the ratio of fluorescence excited by 340 nm to that excited by 380 nm (emission was at 505–510 nm). This was calibrated using the equation developed by Grynkiewicz *et al.*[53]: $[Ca^{2+}]_i = K_D Sf_2/Sb_2(R - R_{min}/R_{max} - R)$, where K_D = 224 nM, Sf_2 is the signal of the free fura-2/AM at 380 nm, Sb_2 is the signal of the bound fura-2/AM at 380 nm, and R is the ratio of the fluorescence. Values for R_{min} were obtained from measurements with a final concentration of 500 nM EGTA (pH balanced to 7.4 with TRIZMA base) added to the cuvette containing a 2 mL sample of cells; while R_{max} was determined in a different sample of cells after addition of 0.1% Triton-X. The 340 and 380 nm values for a sample of unloaded cells were determined to correct for tissue or background autofluorescence. Percent of maximal calcium mobilized for each compound was measured and the EC_{50} values determined.

Acknowledgment. We would like to thank S. Buckel, A. Giordani, B. Tobias, and S. Werness for analytical and spectral data. Also, we would like to thank M. D. Davis, D. Wustrow, and E. Lunney for helpful discussions.

Supplementary Material Available: A table of the amino acid analyses and ^{1}H-NMR spectra (except for compound **18**) and mass spectra for compounds **2–26** (50 pages). Ordering information is given on any current masthead page.

References

(1) Symbols and abbreviations are in accordance with the recommendation of the IUPAC–IUB Commission on Biochemical Nomenclature (*Eur. J. Biochem.* **1984**, *138*, 9–37). The optically active amino acids are of the L-stereochemistry unless otherwise noted. Other abbreviations included: AAA, amino acid analysis; ABI, Applied Biosystems Incorporated; Ac_2O, acetic anhydride; *t*-Boc, *tert*-butyloxycarbonyl; BOP, (benzotriazol-1-yloxy)tris(dimethylamino)phosphonium hexafluorophosphate; BSA, bovine serum albumin; CZE, capillary zone electrophoresis; DCC, *N,N'*-dicyclohexylcarbodiimide; DCM, dichloromethane; DIC, *N,N'*-diisopropylcarbodiimide; DIEA, diisopropylethylamine; DMAP, 4-(dimethylamino)pyridine; DMF, *N,N*-dimethylformamide; DMSO, dimethyl sulfoxide; D_2O, deuterium oxide; DTT, dithiothreitol; EDTA, ethylenediaminetetraacetic acid; EGTA, ethylene glycol bis(β-aminoethyl ether); ES, electrospray; FAB, fast atom bombardment; Fmo, 9-fluorenylmethyl; Fmoc, 9-fluorenylmethoxycarbonyl; HBTU, 2-(1*H*-benzotriazol-1-yl)-1,1,3,3-tetramethyluronium hexafluorophosphate; HEPES, *N*-(2-hydroxyethyl)piperazine-*N'*-(2-ethanesulfonic acid); HF, hydrogen fluoride; Hgl, homoglutamic acid or 2-aminoadipic acid; ^{1}H-NMR, proton nuclear magnetic resonance; HOBt, *N*-hydroxybenzotriazole; N^αMeArg, N^α-methylarginine; MS, mass spectrometry; NMP, *N*-methylpyrrolidone; NOE, nuclear Overhauser effect, NT, neurotensin (pGlu^1-Leu-Tyr-Glu^4-Asn-Lys-Pro-Arg^8-Arg-Pro-Tyr-Ile-Leu^{13}); NT_{8-13}, Arg^8-Arg-Pro-Tyr-Ile-Leu^{13}; PAM, [(phenylacetyl)amino]methyl; Pen, penicillamine or β,β-dimethylcysteine; pGlu, pyroglutamic acid or 2-pyrrolidone-5-carboxylic acid; PMSF, phenylmethylsulfonyl fluoride; Sasrin resin, super acid sensitive resin or 2-methoxy-4-alkoxybenzyl alcohol resin; ROESY, rotating frame nuclear Overhauser spectroscopy; RP-HPLC, reversed-phase high-performance liquid chromatography; SAR, structure–activity relationships; TFA, trifluoroacetic acid; Tle, *tert*-leucine; TMS, tetramethylsilane; TOCSY, total correlation spectroscopy; TRIZMA, tris(hydroxymethyl)aminomethane.

(2) Carraway, R.; Leeman, S. E. The isolation of a new hypotensive peptide, neurotensin, from bovine hypothalami. *J. Biol. Chem.* **1973**, *248*, 6854–6861.

(3) Clineschmidt, B. V.; McGuffin, J. C.; Bunting, P. B. Neurotensin: Antinociceptive action in rodents. *Eur. J. Pharmacol.* **1979**, *54*, 129–139.

(4) St-Pierre, S. A.; Kérouac, R.; Quirion, R.; Jolicouer, F. B.; Rioux, F. Neurotensin. In *Peptide Protein Review*; Hearn, M. T. W., Ed.; Marcel Dekker Inc.: New York, 1984; Vol. 2, pp 83–171.

(5) Nemeroff, C. B.; Cain, S. T. Neurotensin-dopamine interactions in the CNS. *Trends Pharmacol. Sci.* **1985**, *6*, 201–205.

(6) Davis, M. D.; Nemeroff, C. B. Neurotensin, dopamine and schizophrenia. In *Receptors and Ligands in Psychiatry*; Sen, A. K., Lee, T., Eds.; Cambridge University Press: Cambridge, 1988; pp 167–186.

(7) Araki, K.; Tachibana, S.; Uchiyama, M.; Nakajima, T.; Yasuhara, T. Isolation and structure of a new active peptide "xenopsin" on the smooth muscle, especially on a strip of fundus from a rat stomach, from the skin of *Xenopus Laevis*. *Chem. Pharm. Bull.* **1973**, *21*, 2801–2804.

(8) Minamino, N.; Kangawa, K.; Matsuo, H. Neuromedin N: A novel neurotensin-like peptide identified in porcine spinal cord. *Biochem. Biophys. Res. Commun.* **1984**, *122*, 542–549.

(9) Checler, F.; Vincent, J. P.; Kitabgi, P. Neuromedin N: High affinity interaction with brain neurotensin receptors and rapid inactivation by brain synaptic peptidases. *Eur. J. Pharmacol.* **1986**, *126*, 239–244.

(10) Checler, F.; Labbé, C.; Granier, C.; van Rietschoten, J.; Kitabgi, P.; Vincent, J. P. [Trp^{11}]-Neurotensin and xenopsin discriminate between rat and guinea-pig neurotensin receptors. *Life Sci.* **1982**, *31*, 1145–1150.

(11) Carraway, R. E.; Leeman, S. E. The synthesis of neurotensin. *J. Biol. Chem.* **1975**, *250*, 1912–1918.

(12) Folkers, K.; Chang, D.; Humphries, J.; Carraway, R. E.; Leeman, S. E.; Bowers, C. Y. Synthesis and activities of neurotensin and its acid and amide analogues: Possible natural occurrence of [Gln^4]-neurotensin. *Proc. Natl. Acad. Sci. U.S.A.* **1976**, *73*, 3833–3837.

(13) Rivier, J. E.; Lazarus, L. H.; Perrin, M. H.; Brown, M. R. Neurotensin analogues. stucture-activity relationships. *J. Med. Chem.* **1977**, *20*, 1409–1413.

(14) Lazarus, L. H.; Perrin, M. H.; Brown, M. R.; Rivier, J. E. Verification of both the sequence and conformational specificity of neurotensin in binding to mast cells. *Biochem. Biophys. Res. Commun.* **1977**, *76*, 1079–1085. (b) Lazarus, L. H.; Perrin, M. H.; Brown, M. R.; Rivier, J. E. Mast cell binding of neurotensin. II. Molecular conformation of neurotensin involved in the stereospecific binding to mast cell receptor sites. *J. Biol. Chem.* **1977**, *252*, 7180–7183.

(15) St-Pierre, S.; Lalonde, J. M.; Gendreau, M.; Quirion, R.; Regoli, D.; Rioux, F. Synthesis of peptides by the solid-phase method. 6. Neurotensin, fragments, and analogues. *J. Med. Chem.* **1981**, *24*, 370–376.

(16) Bayer, V. V.; Miroshnikov, A. I.; Klusa, V. I. Misina, I. P. Synthesis and biological activity of neurotensin and its analogues. *Bioorg. Khim.* **1980**, *6*, 379–385.

(17) Quirion, R.; Rioux, F.; Regoli, D.; St-Pierre, S. Pharmacological studies of neurotensin, several fragments and analogues in the isolated perfused rat heart. *Eur. J. Pharmacol.* **1980**, *66*, 257–266.

(18) Kitabgi, P.; Poustis, C.; Granier, C.; van Rietschoten, J.; Rivier, J.; Morgat, J. L.; Freychet, P. Neurotensin binding to extraneural and neural receptors: Comparison with biological activity and structure–actvity relationships. *Mol. Pharmacol.* **1980**, *18*, 11–19.

(19) (a) Jolicoeur, F. B.; Rioux, F.; St-Pierre, S.; Barbeau, A. Structure–activity studies of neurotensin's neurobehavioral effects. *Neuroendocrinol. Lett.* **1981**, *3*, 77–84. (b) Jolicoeur, F. B.; St-Pierre, S.: Aubé, Rivest, R.; Gagné, M. A. Relationships between structure and duration of neurotensin's central action: Emergence of long acting analogues. *Neuropeptides* **1984**, *4*, 467–476.

(20) Clineschmidt, B. V.; Martin, E. E.; Veber, D. F. Antinocisponsive effects of neurotensin and neurotensin-related peptides. *Ann. N. Y. Acad. Sci.* **1982**, *400*, 283–306.

(21) Lugrin, D.; Vecchini, F.; Doulut, S.; Rodriguez, M.; Martinez, J.; Kitabgi, P. Reduced peptide bond pseudopeptide analogues of neurotensin: binding and biological activities, and in vitro metabolic stability. *Eur. J. Pharmacol.* **1991**, *205*, 191–198.

(22) Dubuc, I.; Costentin, J.; Doulut, S.; Rodriguez, M.; Martinez, J.; Kitabgi, P. JMV 449: A pseudopeptide analogue of neurotensin-(8–13) with highly potent and long-lasting hypothermic and analgesic effects in the mouse. *Eur. J. Pharmacol.* **1992**, *219*, 327–329.

(23) Doulut, S.; Rodriguez, M.; Lugrin, D.; Vecchini, F.; Kitabgi, P.; Aumelas, A.; Martinez, J. Reduced peptide bond pseudopeptide analogues of neurotensin. *Pept. Res.* **1992**, *5*, 30–38.
(24) Couder, J.; Tourwé D.; van Binst, G.; Schuurkens, J.; Leysen, J. E. Synthesis and biological activities of $\Psi(CH_2NH)$ pseudopeptide analogues of the *C*-terminal hexapeptide of neurotensin. *Int. J. Peptide Res.* **1993**, *41*, 181–184.
(25) (a) Tsuchiya, Y.; Sasaki, A.; Yoshino, H.; Karibe, N.; Sugimoto, H.; Kubota, A.; Kosasa, M.; Araki, S.; Ikeda, M.; Yamanishi, Y.; Machida, R.; Yamatsu, K. New hexapeptide neurotensin analogues useful as cerebral medicaments, antipsychotic agents, analgesics, and methamphetamine antagonists. European Patent Application 89104302.8, 1989. (b) Machida, R.; Tokumura, T.; Sasaki, A.; Tsuchiya, Y.; Abe, K. High-performance liquid chromatographic determination of (Me)Arg-Lys-Pro-Trp-*tert*.-Leu-Leu in plasma. *J. Chromatogr.* **1990**, *534*, 190–195. (c) Tokumura, T.; Tanaka, T.; Sasaki, A.; Tsuchiya, Y.; Abe, K.; Machida, R. Stability of a novel hexapeptide, (Me)Arg-Lys-Pro-Trp-*tert*-Leu-Leu-OEt, with neurotensin activity, in aqueous solution and in the solid state. *Chem. Pharm. Bull.* **1990**, *38*, 3094–3098.
(26) Cooke, L. W.; Wustrow, D. J.; Pugsley, T. A.; Akunne, H. C.; Heffner, T. G.; Cody, W. L.; Davis, M. D. Effect of systemic and central administration of natural and novel neurotensin analogues on behavior and neurotransmitter turnover in the rodent brain. *Soc. Neurosci. Abstr.* **1992**, *18*, 273.
(27) Heyl, D. L.; Sefler, A. M.; He, J. X.; Sawyer, T. K.; Wustrow, D. J.; Akunne, H. C.; Davis, M. D.; Pugsley, T. A.; Heffner, T. G.; Corbin, A. E.; Cody, W. L. Structure–activity and conformational studies of a series of modified C-terminal hexapeptide neurotensin analogues. *Int. J. Pept. Protein Res.* **1994**, *44*, 233–238.
(28) Widerlöv, E.; Lindström, L. H.; Besev, G.; Manberg, P. J.; Nemeroff, C. B. Breese, G. R.; Kizer, J. S.; Prange, A. J., Jr. Subnormal CSF levels of neurotensin in a subgroup of schizophrenic patients: Normalization after neuroleptic treatment. *Am. J. Psychiatry* **1982**, *139*, 1122–1126.
(29) Nemeroff, C. B.; Luttinger, D.; Hernandez, D. E.; Mailman, R. B.; Mason, G. A.; Davis, S. D.; Widerlöv, E.; Frye, G. D.; Kilts, C. A.; Beaumont, K.; Breese, G. R.; Prange, A. J. Jr. Interactions of neurotensin with brain dopamine systems: Biochemical and behavioral studies. *J. Pharmacol. Exp. Ther.* **1983**, *225*, 337–345.
(30) Garver, D. L.; Bissette, G.; Yao, J. K.; Nemeroff, C. B. Relation of CSF neurotensin concentrations to symptoms and drug response of psychotic patients. *Am. J. Psychiatry* **1991**, *148*, 484–488.
(31) al-Rodhan, N. R.; Richelson, E.; Gilbert, J. A.; McCormick, D. J.; Kanba, K. S.; Pfenning, M. A.; Nelson, A.; Larson, E. W.; Yaksh, T. L. Structure-antinociceptive activity of neurotensin and some novel analogues in the periaqueductal gray region of the brainstem. *Brain Res.* **1991**, *557*, 227–235.
(32) Xu, G. Y.; Deber, C. M. Conformations of neurotensin in solution and in membrane environments studied by 2-D NMR spectroscopy. *Int. J. Pept. Protein Res.* **1991**, *37*, 528–535.
(33) (a) García-López, M. T.; Domínguez, M. J.; González-Muñiz, R.; Herranz, R.; Johansen, N. L.; Madsen, K.; Suzdak, P.; Thøgersen, H. β-Turn constrained analogues of neurotensin(8–13) containing a 3-oxoindolizidine skeleton. In *Peptides 1992: Proceedings of the Twenty-Second European Peptide Symposium*; Schneider, C. H., Eberle, A. N., Eds.; ESCOM Science Publishers B.V.: Leiden, The Netherlands, 1993; pp 623–624. (b) García-López, M. T.; Domínguez, M. J.; González-Muñiz, R.; Herranz, R.; Johansen, N. L.; Madsen, K.; Suzdak, P.; Thøgersen, H. Novel 3-oxoindolizidine containing neurotensin (8–13) analogues. In *Program and Abstracts: The Thirteenth American Peptide Symposium*, Edmonton, Canada, 1993; p 212.
(34) Maduskuie, T. P., Jr.; Bleicher, L. S.; Cacciola, J.; Cheatham, W.; Fevig, J. M.; Johnson, A. L.; McComb, S. A.; Nugiel, D. A.; Schimdt, W. K.; Spellmeyer, D. A.; Voss, M. E.; Wagner, R. M. The design and synthesis of a peptidomimetic for neurotensin. *J. Cell. Biochem.* **1993**, *51* (Suppl. 17C), 232.
(35) Johansen, N. L.; Thøgersen H.; Madsen, K.; Suzdak, P.; Hansen, K. T.; Weis, J. U.; García-López; M. T.; Gomez-Monterrey, I.; González-Muniz, R.; Herranz, R. Receptor specific neurotensin peptide mimics. In *Program and Abstracts: The Thirteenth American Peptide Symposium*, Edmonton, Canada, 1993; p 216.
(36) Henry, J. A.; Horwell, D. C.; Meecham, K. G.; Rees, D. C. A structure-affinity study of the amino acid side-chains in neurotensin: N and C terminal deletions and Ala-scan. *Bioorg. Med. Chem. Lett.* **1993**, *3*, 949–952.
(37) (a) Schiller, P. W.; Nguyen, T. M.; Miller, J. Synthesis of side-chain to side-chain cyclized peptide analogues on solid supports. *Int. J. Pept. Protein Res.* **1985**, *25*, 171–177. (b) Al-Obeidi, F.; Castrucci, A. M. de L.; Hadley, M. E.; Hruby, V. J. Potent and prolonged acting cyclic lactam analogues of α-melanotropin: Design based upon molecular dynamics. *J. Med. Chem.* **1989**, *32*, 2555–2561.
(38) Felix, A. M.; Wang, C. T.; Heimer, E. P.; Fournier, A. Applications of BOP reagent in solid phase synthesis. II. Solid phase side-chain to side-chain cyclizations using BOP reagent. *Int. J. Pept. Protein Res.* **1988**, *31*, 231–238.
(39) Cody, W. L.; He, J. X.; Heyl, D. L.; Thieme-Sefler, A. M.; Wustrow, D. J.; Sawyer, T. K.; Akunne, H.; Pugsley T. A.; Corbin, A. E.; Davis, M. D. Neurotensin: Structure–activity relationships of the C-terminal hexapeptide (Arg-Arg-Pro-Tyr-Ile-Leu). In *Peptides 1992: Proceedings of the Twenty-Second European Peptide Symposium*; Schneider, C. H., Eberle, A. N., Eds.; ESCOM Science Publishers B.V.: Leiden, The Netherlands, 1993; pp 677–678.
(40) Braunschweiler, L.; Ernst, R. R. Coherence transfer by isotropic mixing: Application to proton correlation spectroscopy. *J. Magn. Reson.* **1983**, *53*, 521–528.
(41) (a) Wagner, G. NMR investigations of protein structures. *Prog. Nucl. Magn. Reson. Spectrosc.* **1991**, *22*, 101–140. (b) Reily, M. D.; Thanabal, V.; Lunney, E. A.; Repine, J. T.; Humblet, C. C.; Wagner, G. Design, synthesis and solution structure of a renin inhibitor. *FEBS Lett.* **1992**, *302*, 97–103.
(42) (a) Stewart, J. M.; Young, J. D. *Solid Phase Peptide Synthesis, 2nd ed.*; Pierce Chemical Co.: Rockford, IL, 1984. (b) Fields, G. B.; Noble, R. L. Solid phase peptide synthesis utilizing 9-fluorenylmethoxycarbonyl amino acids. *Int. J. Pept. Protein Res.* **1990**, *35*, 161–214.
(43) (a) Mergler, M.; Tanner, R.; Gosteli, J. Grogg, P. Peptide synthesis by a combination of solid-phase and solution methods I: A new very acid-labile anchor group for the solid phase synthesis of fully protected fragments. *Tetrahedron Lett.* **1988**, *29*, 4005–4008. (b) Mergler, M.; Nyfeler, R.; Tanner, R.; Gosteli, J. Grogg, P. Peptide synthesis by a combination of solid-phase and solution methods II: Synthesis of fully protected peptide fragments of 2-methoxy-4-alkoxy-benzyl alcohol resin. *Tetrahedron Lett.* **1988**, *29*, 4009–4012.
(44) (a) Knorr, R.; Trzeciak, A.; Bannwarth, W.; Gillessen, D. New coupling reagents in peptide chemistry. *Tetrahedron Lett.* **1989**, *30*, 1927–1930. (b) Beck-Sickinger, A. G.; Dürr, H.; Jung, G. Semiautomated T-bag peptide synthesis using 9-fluorenylmethoxycarbonyl strategy and benzotriazol-1-yl-tetramethyluronium tetrafluoroborate activation. *Pept. Res.* **1991**, *4*, 88–94. (c) Fields, C. G.; Lloyd, D. H.; Macdonald, R. L.; Otteson, K. M.; Noble, R. L. HBTU activation for automated Fmoc solid-phase peptide synthesis. *Pept. Res.* **1991**, *4*, 95–101. (d) Reid, G. E.; Simpson, R. J. Automated solid-phase peptide synthesis: Use of 2-(1*H*-benzotriazol-1-yl)-1,1,3,3-tetramethyluronium tetrafluoroborate for coupling of *tert*-butyloxycarbonyl amino acids. *Anal. Biochem.* **1992**, *200*, 301–309.
(45) Kaiser, E.; Colescott, R. L.; Bossinger, C. D.; Cook, P. I. Color test for detection of free terminal amino groups in the solid-phase synthesis of peptides. *Anal. Biochem.* **1970**, *34*, 595–598.
(46) (a) Castro, B.; Dormoy, J. R.; Evin, G.; Selve, C. Reactifs de couplage peptidique IV. (1)-L' hexafluorophosphate de benzotriazolyl N-oxytrisdimethylamino phosphonium (B. O. P.). (Peptide coupling reagents. IV. N-[Oxytris(dimethylamino)phosphonium]benzotriazole hexafluorophosate.) *Tetrahedron Lett.* **1975**, *14*, 1219–1222. (b) Hudson, D. Methodological implications of simultaneous solid-phase peptide synthesis. 1. Comparison of different coupling procedures. *J. Org. Chem.* **1988**, 617–624. (c) Fournier, A.; Wang, C. T.; Felix, A. M. Applications of BOP reagent in solid phase synthesis. Advantages of BOP reagent for difficult couplings exemplified by a synthesis of [Ala^{15}]-GRF-(1–29)-NH_2. *Int. J. Pept. Protein Res.* **1988**, *31*, 86–97.
(47) Al-Obeidi, F.; Sanderson, D. G.; Hruby, V. J. Synthesis of β- and γ-fluorenylmethyl esters of respectively N^{α}-Boc-L-aspartic acid and N^{α}-Boc-L-glutamic acid. *Int. J. Pept. Protein Res.* **1990**, *35*, 215–218.
(48) Bax, A.; Davis, D. G. MLEV-17-based two-dimensional homonuclear magnetization transfer spectroscopy. *J. Magn. Reson.* **1985**, *65*, 355–360.
(49) Bothner-By, A. A.; Stephens, R. L.; Lee, J.; Warren, C. D.; Jeanloz, R. W. Structure determination of a tetrasaccharide: Transient nuclear Overhauser effects in the rotating frame. *J. Am. Chem. Soc.* **1984**, *106*, 811–813.
(50) Mazella, J.; Chabry, J.; Kitabgi, P.; Vincent, J. Solubilization and characterization of active neurotensin receptors from mouse brain. *J. Biol. Chem.* **1988**, *263*, 144–149.
(51) Kitabgi, P.; Rostene, W.; Dussaillant, M.; Schotte, A.; Laduron, P.; Vincent, J. Two populations of neurotensin binding sites in murine brain: Discrimination by the antihistamine levocabastine reveals markedly different radioautographic distribution. *Eur. J. Pharmacol.* **1987**, *140*, 285–293.
(52) Turner, J. T.; James-Krcake, M. R.; Camden, J. M. Regulation of the neurotensin receptor and intracellular calcium mobilization in HT29 cells. *J. Pharmacol. Exp. Ther.* **1989**, *253*, 1049–1056.
(53) Grynkiewicz, G.; Poenie, M.; Tsien, R. Y. A new generation of Ca^{2+} indicators with greatly improved fluorescence properties. *J. Biol. Chem.* **1985**, *260*, 3440–3450.

JM9401974

THE JOURNAL OF BIOLOGICAL CHEMISTRY

Vol. 266, No. 25, Issue of September 5, pp. 16441-16447, 1991
Printed in U.S.A.

Covalently Cyclized Agonist and Antagonist Analogues of Bombesin and Related Peptides*

(Received for publication, April 15, 1991)

David H. Coy‡, Ning-Yi Jiang‡, Sun Hyuk Kim§, Jacques-Pierre Moreau§, Jaw-Town Lin¶, Harold Frucht¶, Jia-Ming Qian¶, Lu-Wa Wang¶, and Robert T. Jensen¶

From the ‡Peptide Research Laboratories, Department of Medicine, Tulane University Medical Center, New Orleans, Louisiana 70112, §Biomeasure, Inc., Hopkinton, Massachusetts 01748, and the ¶Digestive Diseases Branch, National Institutes of Health, Bethesda, Maryland 20892

During a search for possible cyclization points in shortened, potent bombesin agonists and antagonists, it was found that the joining of amino acid residues in positions 6 and 14 by various means resulted in retention of significant binding affinity for rat pancreatic acini and murine Swiss 3T3 cells. In one series of analogues, Cys residues in these positions were used for bridging via a disulfide bond. (D)-C-Q-W-A-V-G-H-L-C-NH_2 retained significant binding affinity for rat pancreatic acini cells and was a full amylase releasing agonist (EC_{50} 187 nM). Potency was markedly increased by substituting D-Ala for Gly (EC_{50} 67 nM compared to 10 nM for its linear counterpart) and was decreased by substituting L-Cys for D-Cys in this analogue (EC_{50} 214 nM), thus strongly suggesting stabilization of peptide folding by the D residues. Elimination of the COOH-terminal amino acid produces competitive antagonists in the linear analogues; however, (D)-C-Q-W-A-V-G-H-C-NH_2 was devoid of activity. Likewise, cyclization to position 13 with the 14 amino acids intact to give (D)-C-Q-W-A-V-G-H-C-L-NH_2 resulted in an almost inactive peptide. On the other hand, as in the linear series, the reduced peptide bond analogue, (D)-C-Q-W-A-V-(D)-A-H-L-ψ(CH_2NH)-C-NH_2, was a receptor antagonist (IC_{50} 5.7 mM), albeit much weaker than the corresponding linear analogues, but with no residual agonist activity. Direct head-to-tail cyclization was also tried. Both cyclo[(D)-F-Q-W-A-V-G-H-L-L] (EC_{50} 346 nM) and the shorter cyclo[Q-W-A-V-G-H-L-L] (EC_{50} 1236 nM) were full agonists. Elimination of the COOH-terminal residue in cyclo[(D)-p-Cl-F-Q-W-A-V-(D)-A-H-L] produced an agonist (EC_{50} 716 nM) rather than an antagonist. These results provide support for the proposal that both bombesin agonists and antagonists adopt a folded conformation at their receptor(s). Furthermore, the retention of appreciable potencies using several cyclization strategies and chain lengths suggests that further optimization of these structures both in terms of potency and ring size is possible. Since these peptides have increased conformational restriction, they should begin to serve as useful substrates for NMR and molecular modeling studies aimed at comparing the obviously subtle differences between agonist and antagonist structures.

* This research was supported in part by National Institutes of Health Grant CA-45153. The costs of publication of this article were defrayed in part by the payment of page charges. This article must therefore be hereby marked "*advertisement*" in accordance with 18 U.S.C. Section 1734 solely to indicate this fact.

Competitive receptor antagonists of bombesin (Bn)[1]/GRP peptides have now been created by a number of very different design approaches. Replacement of His in position 12 of Bn (<Q-Q-R-L-G-N-Q-W-A-V-G-H-L-M-NH_2) resulted in the first reported Bn antagonists (1, 2). More potent antagonists were then prepared by replacing the —CONH— peptide bond in position 13-14 by a —CH_2NH— group (3). Moreover, it was discovered that replacement of the 9-10 peptide bond in a similar fashion also resulted in an antagonist, although it exhibited considerably less affinity for guinea pig pancreatic acini cells (3). Elimination (4) of the COOH-terminal Met residue in *N*-Ac-GRP(20-27) (Ac-H-W-A-V-G-H-L-M-NH_2) also gave a receptor antagonist with quite high affinity which was increased substantially by alkylamide, phenalkylamide, and ester modifications at the COOH terminus (4-6). Affinities of both the 13-14 reduced peptide and the desMet analogues were also increased substantially in the Bn series by reducing the chain length to the 6-14 or 6-13 sequences and substituting D-aromatic amino acids in position 6 (7-9). The biological properties of some of these antagonists varied considerably depending on the biological system being employed. Thus, <Q-Q-R-L-G-N-Q-W-A-V-G-H-L-ψ(CH_2NH)-L-NH_2 displayed considerable agonist activity using a frog esophageal peptic cell system (10) and, to a lesser extent, using rat pancreatic acini (8). Even some of the shorter pseudopeptide and peptide desMet[14]-alkylamide analogues were found to have varying degrees of partial or even full agonist activity depending on the structure of the COOH-terminal amino acid or the length of the alkyl substituent (8, 9). In the reduced peptide bond antagonists, COOH-terminal aromatic amino acids had particularly high agonist potency which could, however, be eliminated by halogen substituents on the aromatic side chain (8) or by switching to a D-amino acid. Surprisingly, agonist potency could also be much reduced by a halogen substituent on the D-Phe residue in position 6 (8). Similarly, a 4-Cl-phenylethylamide Bn antagonist displayed little or no agonist activity, whereas the corresponding unsubstituted phenylethylamide had high agonist activity (9).

In more recent studies, it was shown that some of these analogues distinguish Bn receptor subtypes (11). In particular, some reduced peptide bond analogues and various desMet[14] antagonists had much reduced affinity for neuromedin B-preferring Bn receptors on rat esophageal tissue even though their receptors had high affinity for various Bn agonists and neuromedin B itself. Moreover, antagonists based on the D-

[1] The abbreviations used are: Bn, bombesin; HEPES, 4-(2-hydroxyethyl)-1-piperazineethanesulfonic acid; hplc, high performance liquid chromatography; ψ, reduced peptide bond; GRP, gastrin-releasing peptide.

Phe[12] modification retained significant affinity for both types of receptor (11).

This complex series of interacting events triggered by diverse structural modifications suggests several conclusions regarding the mechanism of action of these peptides. Clearly, the COOH-terminal dipeptide unit and hydrogen-bonding points integral to this particular peptide bond are critical for triggering the biological response of the peptide agonists and, indeed, we have hypothesized (1) that intramolecular hydrogen bonding could be an important factor in retaining conformational integrity responsible for agonist activity. It seems likely that the apparently diverse structural alterations which result in antagonist formation exercise their effects ultimately through closely related perturbations in this agonist conformation, thus resulting in destruction of biological activity yet with retention of the ability to bind the receptor.

It is extremely difficult to precisely elucidate these conformational parameters by physicochemical measurements on flexible peptide chains which, at least in the case of bombesin and a D-Phe[12] analogue in recent high resolution NMR and CD studies (12, 13), show little ability to adopt preferred conformations in solution other than some evidence for weak α-helicity in the COOH-terminal region of Bn. A partial solution to this problem with peptides is to develop conformationally restricted analogues which are covalently cyclized while retaining as much affinity for their receptors as possible. Establishing those initial structural leads which enable potency to be retained after cyclization is often difficult; however, early attempts to design cyclic Bn analogues did result in a moderately active agonist when positions 5–14 were joined (14) in a 4–14 structure, thus suggesting the feasibility of this type of approach. In the present study, we were also intrigued by the observations described above in which modifications to NH_2- and COOH-terminal aromatic amino acid residues in Bn(6–14) analogues resulted in similar effects on biological activity. We reasoned that their side chains could be in close proximity while bound to receptors and that possibly cyclization from position 6–14 might be of some interest. A number of cyclization strategies are described utilizing short agonist and antagonist structures as starting points.

EXPERIMENTAL PROCEDURES

Materials

Protected amino acids were obtained from Bachem, Inc., Torrance, CA. Rats were obtained from the Small Animals Section, Veterinary Resources Branch, NIH. HEPES was from Boehringer Mannheim; purified collagenase (type CLSPA, 440 units/mg) from Worthington Biochemicals; sodium borate, soybean trypsin inhibitor, carbamylcholine, theophylline, bacitracin from Sigma; essential vitamin mixture (100× concentrated) from Microbiological Associates, Bethesda, MD; $Na^{125}I$ from Amersham Corp.; Phadebas amylase test reagent from Pharmacia LKB Biotechnology Inc.; bovine plasma albumin (Fraction V) from Miles Laboratories; COOH-terminal octapeptide of cholecystokinin (CCK-8) from Peninsula Laboratories, Belmont, CA; and FURA-2/AM from Molecular Probes, Eugene, OR. Stock cultures of murine Swiss 3T3 cells were kindly provided by Dr. E. Rozengurt, Imperial Cancer Research Fund, London.

The standard incubation solution used in experiments involving pancreatic acini contained 24.5 mM HEPES (pH 7.4), 98 mM NaCl, 6 mM KCl, 2.5 mM NaH_2PO_4, 5 mM sodium pyruvate, 5 mM sodium fumarate, 5 mM sodium glutamate, 2 mM glutamine, 11.5 mM glucose, 0.5 mM $CaCl_2$, 1.0 mM $MgCl_2$, 5 mM theophylline, 1% (w/v) albumin, 0.01% (w/v) trypsin inhibitor, 1% (v/v) amino acid mixture, and 1% (v/v) essential vitamin mixture. The incubation solution was equilibrated with 100% O_2, and all incubations were carried out with O_2 as the gas phase.

Methods

Preparation of Peptides—Automated solid phase syntheses of peptides (Advanced ChemTech Model 200), including introduction of the reduced peptide bond, were carried out by the standard methods recently described by us (3) on methylbenzhydrylamine resin (Advanced ChemTech, Louisville, KY) for COOH-terminal amides and standard Leu-*O*-polystyrene resin for analogues with free carboxyl-terminal COOH groups prior to cyclization. The single analogue containing the reduced peptide bond was synthesized by the method of Sasaki and Coy (15). The crude hydrogen fluoride-cleaved Cys peptide amides were cyclized in 90% acetic acid solution by titration with dilute I_2 solution prior to purification. These materials and peptide-free acids, prior to NH_2- to COOH-terminal cyclization, were purified on a column (2.5 × 90 cm) of Sephadex G-25 which was eluted with 2 M acetic acid followed by preparative medium pressure chromatography on a column (1.5 × 45 cm) of Vydac C18 silica (10–15 μm) which was eluted with linear gradients of acetonitrile in 0.1% trifluoroacetic acid using a Rainin (Woburn, MA) hplc system with a Macintosh computer controller (flow rate approximately 2 ml/min). Analogues were further purified by re-chromatography on the same column with slight modifications to the gradient conditions when necessary. Homogeneity of the peptides was assessed by thin layer chromatography and analytical reverse-phase high pressure liquid chromatography, and purity was 97% or higher. Peptides with free termini were then cyclized in dilute dimethylformamide solution by treatment with a small excess of dicyclohexylcarbodiimide/1-hydroxybenzotriazole or BOP reagent/diisopropylethylamine and monitoring by analytical hplc. They were further purified as already described.

Amino acid analysis of acid hydrolysates of the peptides gave the expected amino acid ratios. The primary structures of the cyclic peptides were further confirmed by fast atom bombardment mass spectrometry, and each gave the expected molecular ion.

Tissue Preparation—Dispersed acini from rat pancreas were prepared as described previously (9).

Amylase Release—Dispersed acini from one rat pancreas were suspended in 150 ml of standard incubation solution, samples (250 ml) were incubated for 30 min at 37 °C, and amylase release was measured as described previously (16, 17). Amylase activity was determined by the method of Ceska *et al.* (18, 19) using the Phadebas reagent. Amylase release was calculated as the percentage of amylase activity in the acini at the beginning of the incubation that was released into the extracellular medium during the incubation.

Effect of Peptides on Bombesin-stimulated Amylase Release—Antagonist activity was determined as described before (9). Various concentrations of peptides were incubated alone or with 0.3 nM bombesin, a concentration that causes half-maximal stimulation which, in the present studies, was a 5.5-fold increase over basal.

Binding of ^{125}I-Labeled [Tyr[4]]Bombesin to Acini or 3T3 Fibroblasts—^{125}I-[Tyr[4]]bombesin (2000 Ci/mmol) was prepared by the method described previously (20). ^{125}I-[Tyr[4]]bombesin was separated from ^{125}I using a Sep-Pak and separated from unlabeled peptide by reverse phase high pressure liquid chromatography on a column (0.46 × 25 cm) of μBondapak C18. The column was eluted isocratically with acetonitrile (22.5%) and triethylammonium phosphate (0.25 M (pH 3.5)) (77.5%) at a flow rate of 1 ml/min. Incubations contained 0.05 nM ^{125}I-[Tyr[4]]bombesin and were for 60 min at 37° C for pancreatic acini and for 30 min at 22° C for 3T3 cells.

Nonsaturable binding of ^{125}I-[Tyr[4]]bombesin was the amount of radioactivity associated with the acini or 3T3 cells when incubation contained 0.05 nM ^{125}I-[Tyr[4]]bombesin plus 1 mM bombesin. All values shown are for saturable binding, *i.e.* binding measured with ^{125}I-[Tyr[4]]bombesin alone (total) minus binding measured in the presence of 1 mM unlabeled bombesin (nonsaturable binding). Nonsaturable binding was <10% of total binding in all experiments.

Effects of Peptides on Cytosolic Calcium in Swiss 3T3 Fibroblasts—Swiss 3T3 cells (3×10^{-6} cells/ml) were loaded with 2 mM FURA-2/AM for 45 min at 37° C in standard incubation buffer without phosphate or essential vitamin mixture. Cytosolic Ca^{2+}, $[Ca^{2+}]_i$, was measured using a Delta PTI Scan-1 spectrofluorimeter (PTI Instruments, Gaithersburg, MD) which had provisions for continuous stirring and temperature control at 37 °C. Fluorescence was measured at 500 nm after excitation at 340 nm and 380 nm. Autofluorescence of the unloaded cells was subtracted, and $[Ca^{2+}]_i$ was calculated by the method of Grynkiewicz *et al.* (21).

RESULTS

When tested at a concentration of 10 mM, 9 of the 12 cyclized Bn analogues stimulated amylase release from the rat acinar cells (Table I). Three analogues, [Cys^{9,14}]Bn, [D-Cys^6,Cys^{13}]Bn(6–13), and [D-Cys^6,D-Ala^{11},Cys^{14},ψ^{13-14}]Bn(6–14) failed to stimulate amylase release (Table I). When each of these peptides was studied for antagonist properties by determining its ability to inhibit Bn-stimulated amylase release, only the latter caused inhibition, whereas the other two were devoid of effect (Table I, right column).

Dose-response curves illustrating the relative abilities of the cyclic analogues and several control peptides to stimulate or inhibit Bn-stimulated amylase release from these cells are shown in Fig. 1 and Fig. 2, respectively, and their ability to inhibit ^{125}I-[Tyr^4]Bn binding to Bn receptors on rat pancreatic acini cells is shown in Fig. 3. The EC$_{50}$ and K_i values calculated from these data are given in Table II. Since all but one of the cyclic structures were based on either the Bn(6–14) sequence (N-Q-W-A-V-G-H-L-M-NH$_2$), the 6–14 sequence containing the reduced peptide bond between positions 13 and 14, on litorin (<Q-Q-W-A-V-G-H-F-M-NH$_2$), which is closely related to Bn(6–14), containing the ψ-bond between position 8 and 9, or the desMet^{14}-(6–13) sequence of Bn, a number of linear control peptides were included to encompass these sequences. These included Bn itself (I, Table II), [Leu^{14}]Bn (II), Bn(6–14) (III), [D-Phe^6]Bn(6–14) (IV), [D-Phe^6,D-Ala^{11},Leu^{14}]Bn (VII), litorin (IX), and [Leu^{8,9}]litorin (X), all of which were potent agonists with high affinities and K_i values ranging from 2–78 nM (Table II). Control representatives of previously described linear antagonists included [D-Phe^6,Leu^{14},ψ^{13-14}]Bn(6–14) (XXIII) (IC$_{50}$ 40 nM), Bn(6–13) (XVIII) (IC$_{50}$ 5.2 mM), [D-Phe^6]Bn(6–13) (XIX) (IC$_{50}$ 0.1 mM), and [Leu^8,desMet^9]litorin (XXI) (IC$_{50}$ 0.77 mM).

All cyclic and control linear peptides, except two cyclic peptides, [D-Cys^6,Cys^{13}]Bn(6–13) (XX) and [Cys^{9,14}]Bn (XVII) and the linear peptide Bn(9–14) (XVI), interacted with Bn receptors to either stimulate or inhibit Bn-stimulated amylase release (Figs. 1–3). In contrast to [D-Cys^6,Cys^{13}]-Bn(6–13) (XX, Table II), the linear peptides [D-Phe^6]Bn(6–13) (XIX) or Bn(6–13) (XVIII) both functioned as receptor antagonists (Fig. 2 and Table II). Agonist activity and binding affinity were restored to XX by the addition of a Leu substituent to position 14 to give [D- Cys^6,Cys^{13},Leu^{14}]Bn(6–14) (XIII) which still had very low affinity and biological potency (EC$_{50}$ 5.5 mM; K_i = 28 mM) compared to the linear peptide [D-Phe^6]Bn(6–14) (EC$_{50}$ 0.0006 mM; Ki = 0.006 mM) (Figs. 1 and 3; Table II). Cyclization between positions 6 and 14 via a disulfide bridge in [D-Cys^6,Cys^{14}]Bn(6–14) (VIII) gave a much more potent agonist analogue (EC$_{50}$ 0.19 mM; K_i = 3.3 mM), and agonist potency was increased still further by the presence of D-Ala in place of Gly^{11} to give [D-Cys^6,D-Ala^{11},Cys^{14}]Bn(6–14) (VI) (EC$_{50}$ 67 nM; K_i = 69 nM) (Figs. 1 and 3; Table II). Potency was partially lost if L-Cys was employed rather than D-Cys in position 6 and [Cys^6,D-Ala^{11},Cys^{14}]Bn(6–14) (V) had an EC$_{50}$ of 0.21 mM and a K_i of 2.1 mM. Cyclization between

TABLE I

Effect of various cyclized Bn analogues on basal and Bn-stimulated amylase release from rat pancreatic acini cells

Pancreatic acini were incubated at 37 °C for 30 min either alone, with 0.3 nM Bn, or a 10 μM concentration of the indicated concentration of the cyclized Bn analogue alone or in combination. Values are means ± 1 S.E. from five separate experiments. Values for amylase release are expressed as the percentage of the total cellular amylase that was released into the extracellular medium during the incubation. NT-agonist = cyclized analogue was not tested for antagonist activity because it had agonist activity.

Peptide added (10 μM)	Amylase release	
	Alone	Plus 0.3 nM Bn
	% total	
None	2.5 ± 0.1	14.6 ± 2.1
[Cys^{6,14},D-Ala^{11}]Bn(6–14)	19.1 ± 0.6^a	NT-agonist
[D-Cys^6,D-Ala^{11},Lys^{14}]Bn(6–14)	18.1 ± 1.0^a	NT-agonist
[D-Cys^6,Cys^{14}]Bn(6–14)	19.9 ± 1.1^a	NT-agonist
Cyclo[D-Phe^1,Leu^{8,9}]Litorin	17.9 ± 1.4^a	NT-agonist
[Cys^{7,14},D-Ala^{11}]Bn(6–14)	17.0 ± 1.9^a	NT-agonist
[D-Cys^6,Cys^{13},Leu^{14}]Bn(6–14)	16.9 ± 1.2^a	NT-agonist
Cyclo[Leu^{14},Bn(7–14)]	20.5 ± 2.5^a	NT-agonist
Cyclo[desGly^{11},Leu^{14}]Bn(7–14)	13.6 ± 0.2^a	NT-agonist
[Cys^{9,14}]Bn	2.7 ± 0.1^a	13.9 ± 1.1
[D-Cys^6,Cys^{13}]Bn(6–13)	2.6 ± 0.2	14.2 ± 0.7
Cyclo[Cpa^1,D-Ala^6,Leu^8,desMet^9]litorin	17.5 ± 1.4^a	NT-agonist
[D-Cys^6,D-Ala^{11},Cys^{14},$\psi^{13,14}$]Bn(6–14)	2.6 ± 0.2	6.8 ± 1.1^b

^{a} Significantly greater than no additions, $p < 0.01$.
^{b} Significantly less than 0.3 nM Bn alone, $p < 0.01$.

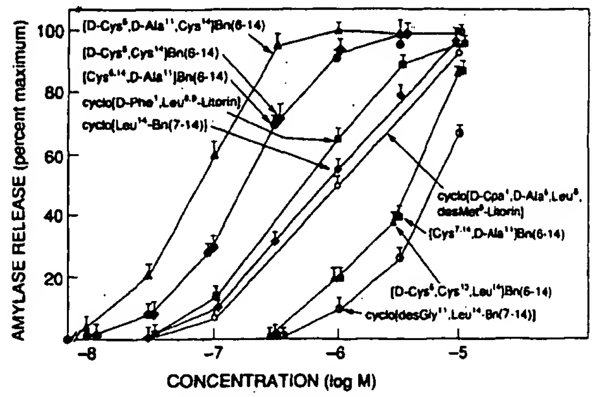

FIG. 1. **Ability of various cyclized Bn-related peptides with agonist activity to stimulate amylase release from dispersed rat pancreatic acini.** Pancreatic acini were incubated with the indicated concentration of the cyclized Bn-related peptide for 30 min at 37 °C. Results are expressed as the percentage of maximal responses by 10 nM Bn. Basal and maximal amylase release was 2.5 ± 0.1% and 19.6 ± 1.8% of total cellular amylase release, respectively. Each *point* is a mean from four separate experiments, and, in each experiment, each value was determined in duplicate. *Vertical bars* represent 1 S.E.

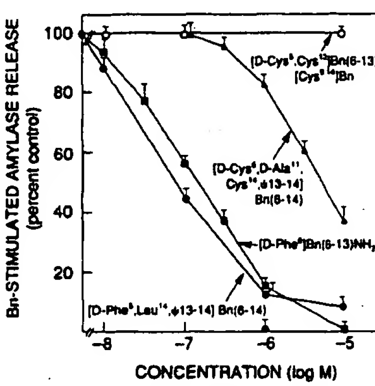

FIG. 2. **Ability of various cyclized and structurally related Bn peptides without agonist activity to inhibit Bn-stimulated amylase release.** Pancreatic acini were incubated with or without 0.3 nM Bn, a half-maximally effective concentration, with the indicated concentrations of the various Bn-related peptides. Results are expressed as the percentage of the stimulated amylase release caused by 0.3 nM alone. Basal and 0.3 nM Bn-stimulated amylase release was 2.6 ± 0.1% and 14.6 ± 2.0% of the total cellular amylase release, respectively. Each *point* is a mean from four separate experiments, and, in each experiment, each value was determined in duplicate. *Vertical bars* represent 1 S.E.

positions 7 and 14 to give [Cys^7,D-Ala^{11},Cys^{14}]Bn(6–14) (XII) resulted in a relatively weakly active agonist (EC$_{50}$ 2.1 mM; K_i = 45 mM) (Figs. 1 and 3; Table II). Cyclization of a D-Phe^1 version of [Leu^{8,9}]litorin via the α-amino group and the COOH-terminal COOH group to give cyclo[D-Phe^1,Leu^{8,9}] litorin (XI) retained almost all of the agonist potency (EC$_{50}$ 0.35 mM; K_i = 1.2 mM) of the former (Table II). The related shorter 7–14 analogue, cyclo[Leu^{14}]Bn(7–14) (XIV) was only a 3 times less potent agonist, and even removal of Gly^{11} in this to give cyclo[desGly^{11},Leu^{14}]Bn(7–14) (XV) resulted in retention of some agonist activity (EC$_{50}$ 6.5 mM; K_i = 25.8 mM) (Figs. 1 and 3; Table II). Elimination of the COOH-terminal Met residue to give cyclo[D-Cpa^1,Leu^{8,9}desMet^9]litorin (XXII) resulted in the most potent agonist of this series (EC$_{50}$ 0.7 mM; K_i = 0.4 mM) (Figs. 1 and 3; Table II).

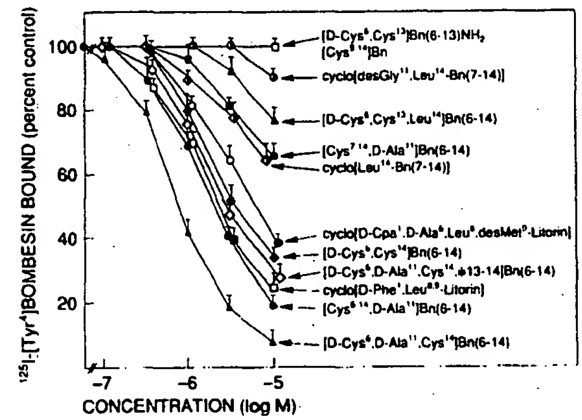

FIG. 3. **Ability of various cyclized Bn-related peptides to inhibit binding of ^{125}I-[Tyr^4]Bn to dispersed rat pancreatic acini.** Pancreatic acini were incubated for 30 min at 30 °C with 50 pM ^{125}I-[Tyr^4]Bn with the indicated concentrations of the cyclized Bn analogues. Results are expressed as the percentage of the saturable binding with no unlabeled cyclized Bn analogue present. Results are means from four separate experiments, and, in each experiment, each value was determined in duplicate. *Vertical bars* represent 1 S.E.

To confirm that the various cyclized Bn analogues that functioned as agonists were actually stimulating amylase release through Bn receptor occupation, the effect of the specific Bn receptor antagonist, [D-Phe^6]Bn(6–13) methyl ester, on stimulation by the most potent cyclic agonist, [D-Cys^6,D-Ala^{11},Cys^{14}]Bn(6–14) was examined (Fig. 4). At a 2 nM dose level, the methyl ester caused half-maximal inhibition of amylase release produced by a 0.1 mM concentration of the cyclic agonist, whereas a 0.1 mM dose produced complete blockade of amylase release. Increasing the cyclic agonist concentration to 1 mM resulted in a typical parallel shift in the dose-reponse inhibition curve, indicating that the agonist/antagonist were interacting in a competitive manner.

Replacement of the position 13–14 peptide bond in the most potent agonist analogue of the Cys-bridged series (VI) by a CH_2NH group to give [D-Cys^6,D-Ala^{11},Cys^{14},ψ^{13-14}]Bn(6–14) (XXIV) resulted in destruction of agonist activity; however, the peptide still retained binding affinity and exhibited a K_i of 2.2 mM (Figs. 1–3; Table II). This peptide was able to inhibit the amylase-releasing response of Bn itself (Fig. 2) with an IC$_{50}$ of 5.7 mM. The inhibitory effect of this cyclic antagonist on Bn-stimulated amylase release was investigated in more detail (Fig. 5) using acini incubated with various doses of Bn. Detectable amylase release occurred with 0.03 nM Bn, half-maximal at 0.3 nM, and maximal at 10 nM. [D-Cys^6,D-Ala^{11},Cys^{14},ψ^{13-14}]Bn(6–14) caused a parallel rightward shift in the dose-response curve for Bn-stimulated amylase release, and this was proportional to the concentration of the analogue used (Fig. 5). There was no change in the maximal Bn response (Fig. 5). Analysis of these data by the Schild

TABLE II

Bioactivities and affinities of cyclized and other structurally related Bn analogues for Bn receptors on rat pancreatic acini cells

K_i values for binding of the various analogues were calculated by the method of Cheng and Prusoff (28) and are from the data shown in Fig. 3. The EC$_{50}$ or IC$_{50}$ values are from the data shown in Figs. 1 and 2 and represent the concentration causing half-maximal amylase release or half-maximal inhibition of Bn-stimulated amylase release, respectively. Each value is the mean ± 1 S.E. of at least four experiments. Abbreviations: Antag = antagonist, Ag = agonist, P. Ag (% max) = partial agonist (percent maximal response), Cpa = *p*-chlorophenylalanine.

	Peptide	Biological activity	EC$_{50}$/IC$_{50}$	K_i
			μM	μM
I	Bn	Ag	0.0002 ± 0.0001	0.004 ± 0.001
II	[Leu^{14}]Bn	Ag	0.0008 ± 0.0002	0.021 ± 0.004
III	Bn(6–14)	Ag	0.0002 ± 0.0001	0.006 ± 0.001
IV	[D-Phe^6]Bn(6–14)	Ag	0.0006 ± 0.0001	0.002 ± 0.001
V	[Cys^{6,14},D-Ala^{11}]Bn(6–14)	Ag	0.21 ± 0.03	2.1 ± 0.3
VI	[D-Cys^6,D-Ala^{11},Cys^{14}]Bn(6–14)	Ag	0.067 ± 0.006	0.69 ± 0.09
VII	[D-Phe^6,D-Ala^{11},Leu^{14}]Bn(6–14)	Ag	0.010 ± 0.002	0.013 ± 0.003
VIII	[D-Cys^6,Cys^{14}]Bn(6–14)	Ag	0.19 ± 0.01	3.3 ± 0.7
IX	Litorin	Ag	0.0004 ± 0.0001	0.006 ± 0.001
X	[Leu^{8,9}]Litorin	Ag	0.49 ± 0.13	0.78 ± 0.41
XI	Cyclo[D-Phe^1,Leu^{8,9}]litorin	Ag	0.35 ± 0.04	1.2 ± 0.1
XII	[Cys$^{7-14}$,D-Ala^{11}]Bn(6–14)	Ag	2.1 ± 0.1	45.2 ± 10.6
XIII	[D-Cys^6,Cys^{13},Leu^{14}]Bn(6–14)	Ag	5.5 ± 0.8	28.2 ± 10.2
XIV	Cyclo[Leu^{14}-Bn(7–14)]	Ag	1.2 ± 0.4	4.0 ± 0.8
XV	Cyclo[des-Gly^{11},Leu^{14}-Bn(7–14)]	Ag	6.5 ± 0.6	25.8 ± 12.2
XVI	Bn(9–14)	None	No activity at 10	>10
XVII	[Cys^{8,14}]Bn	None	No activity at 10	>30
XVIII	Bn(6–13)	Antag	5.2 ± 1.4	9.2 ± 2.5
XIX	[D-Phe^6]Bn(6–13)	Antag	0.10 ± 0.02	0.03 ± 0.01
XX	[D-Cys^6,Cys^{13}]Bn(6–13)	None	No activity at 10	58.4 ± 20.6
XXI	[Leu^8,desMet^9]litorin	Antag	0.7 ± 0.12	0.32 ± 0.15
XXII	Cyclo[Cpa^1,D-Ala^6,Leu^8,desMet^9]litorin	Ag	0.7 ± 0.2	0.4 ± 1.8
XXIII	[D-Phe^6,Leu^{14},ψ^{13-14}]Bn(6–14)	P. Ag (10% max)	0.040 ± 0.012	0.062 ± 0.001
XXIV	[D-Cys^6,D-Ala^{11},Cys^{14},ψ^{13-14}]Bn(6–14)	Antag	5.7 ± 2.7	2.2 ± 0.3

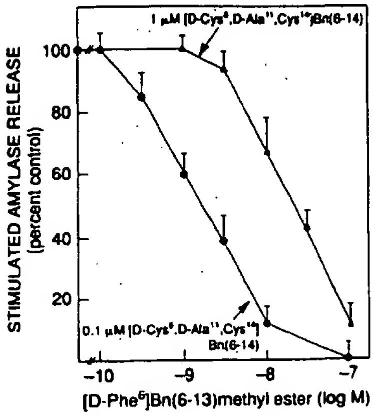

FIG. 4. **Ability of the Bn-receptor antagonist [D-Phe^6]Bn(6–13) methyl ester to inhibit amylase release from rat pancreatic acini stimulated by [D-Cys^6,D-Ala^{11}, Cys^{14}]Bn(6–14).** Pancreatic acini were incubated with or without either 0.1 μM or 1 μM [D-Cys^6,D-Ala^{11},Cys^{14}]Bn(6–14) with the indicated concentrations of [D-Phe^6]Bn(6–13) methyl ester for 30 min at 37 °C. Values are expressed as the percentage of control which is the stimulated amylase release caused by 0.1 μM or 1 μM [D-Cys^6,D-Ala^{11},Cys^{13}]Bn(6–14) alone. Basal, 0.1 μM, or 1 μM [D-Cys^6,D-Ala^{11},Cys^{13}]Bn(6–14) caused 3.6 ± 0.6, 14.6 ± 6.7, and 18.7 ± 2.4% of total cellular amylase. Each value is the mean of three separate experiments, and, in each experiment, each point is determined in duplicate. *Vertical bars* represent 1 S.E.

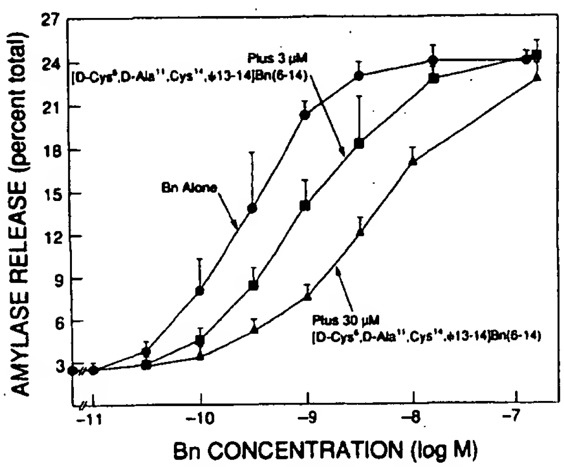

FIG. 5. **Ability of the cyclized analogue [D-Cys^6,D-Ala^{11},Cys^{14},ψ^{13-14}]Bn(6–14)NH_2 to affect Bn-stimulated amylase release.** Pancreatic acini were incubated with or without 3 μM or 30 μM [D-Cys^6,D-Ala^{11},Cys^{14},ψ^{13-14}]Bn(6–14) with the indicated concentrations of Bn for 30 min at 37 °C. Amylase release is expressed as the percentage of the total cellular amylase released during the incubation period. Each value is the mean of three separate experiments, and, in each experiment, each point is determined in duplicate. *Vertical bars* represent 1 S.E.

method gave the regression equation, $y = 1.07(\pm\ 0.05)x + 6.175$ with a correlation coefficient of 0.99 ($p < 0.001$) which has a slope not significantly different from unity and gave a binding affinity of 1.7 ± 0.1 mM. The specificity of the inhibitory activity of [D-Cys^6,D-Ala^{11},Cys^{14},ψ^{13-14}]Bn(6–14) to inhibit the action of a number of agonists that do not interact with Bn receptors was studied (Table III). The analogue did not inhibit amylase release produced by CCK-8, carbachol, or secretin at 10 mM, a concentration which significantly inhibited Bn or neuromedin B-stimulated secretion (Table III).

In previous studies (22), Bn-related peptides have been shown to interact with high affinity receptors on 3T3 cells

TABLE III

Effect of [D-Cys^6,D-Ala^{11},Cys^{14},ψ^{13-14}]Bn(6–14) on the ability of various agents to stimulate enzyme secretion from rat pancreatic acini

Pancreatic acini were incubated for 30 min at 37 °C with the indicated secretagogue either alone or with 10 μM [D-Cys^6,D-Ala^{11},Cys^{14},ψ^{13-14}]Bn(6–14). Results are expressed as the percentage of the total cellular amylase released into the extracellular medium during the incubation. Results are means ± 1 S.E. from five experiments, and in each experiment each value was determined in duplicate.

Secretagogue	Amylase release	
	Alone	Plus 10 μM [D-Cys^6,D-Ala^{11}, Cys^{14},ψ^{13-14}]Bn(6–14)
	% total	
None	4.0 ± 0.5	4.4 ± 0.8
Bn (0.3 nM)	15.0 ± 1.0	7.4 ± 2.0[a]
Neuromedin B (30 nM)	16.4 ± 2.0	5.7 ± 1.2[a]
CCK-8 (0.1 nM)	19.3 ± 2.4	18.6 ± 1.9
Carbachol (0.3 μM)	15.7 ± 2.0	16.7 ± 1.7
Secretin (0.1 μM)	9.1 ± 1.0	12.1 ± 2.0

[a] Significantly different from secretagogue alone, $p < 0.01$.

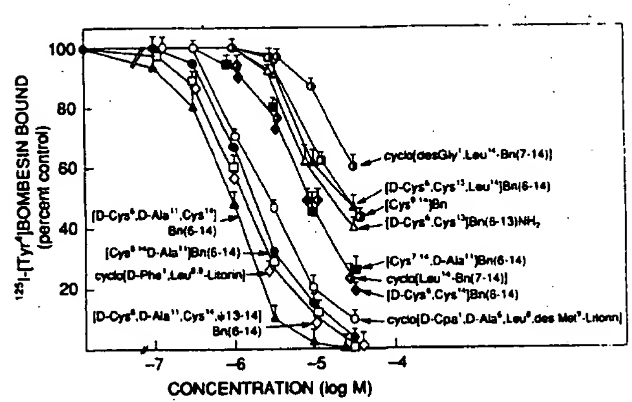

FIG. 6. **Ability of various cyclized Bn-related peptides to inhibit binding of ^{125}I-[Tyr^4]Bn to 3T3 cells.** 3T3 cells were incubated for 30 min at 37 °C with 50 pM ^{125}I-[Tyr^4]Bn with the indicated concentrations of the cyclized analogues. Results are expressed as the percentage of the saturable binding with no unlabeled cyclized analogue present. Results are the means from four separate experiments, and, in each experiment, each value was determined in duplicate. *Vertical bars* represent 1 S.E.

resulting in the activation of phospholipase C, mobilization of calcium, and stimulation of growth. The present cyclic analogues were examined for their ability to displace ^{125}I-[Tyr^4]Bn from intact 3T3 cells (Fig. 6) or alter cytosolic Ca^{2+} in 3T3 cells (Fig. 7). In a similar fashion to Bn receptors on pancreatic acini, [D-Cys^6,D-Ala^{11},Cys^{14}]Bn(6–14) (K_i = 0.95 mM) had the highest affinity of all the cyclic analogues. Furthermore, each of the analogues had the same relative potencies for Bn receptors on both cell types (compare Figs. 3 and 6). [D-Cys^6,D-Ala^{11},Cys^{14},ψ^{13-14}]Bn(6–14) also bound to Bn receptors on 3T3 cells with a 2-fold higher affinity than on rat acinar cells (K_i = 1.0 ± 0.1 *versus* 2.2 ± 0.3 mM, respectively). To investigate whether these analogues were functionally active on 3T3 cells, the abilities of [D-Cys^6,D-Ala^{11},Cys^{14}]Bn(6–14), which functions as an agonist in pancreatic acini, and [D-Cys^6,D-Ala^{11},Cys^{14},ψ^{13-14}]Bn(6–14), which functions as an antagonist in acini, to alter cytosolic Ca^{2+} in 3T3 cells were determined (Fig. 7). The former caused a dose-dependent increase in $[Ca^{2+}]_i$ with a half-maximal effect at 1 mM (Fig. 7, *right*), whereas the latter peptide had no effect at doses up to 30 mM (Fig. 7, *middle*) but caused a dose-depend-

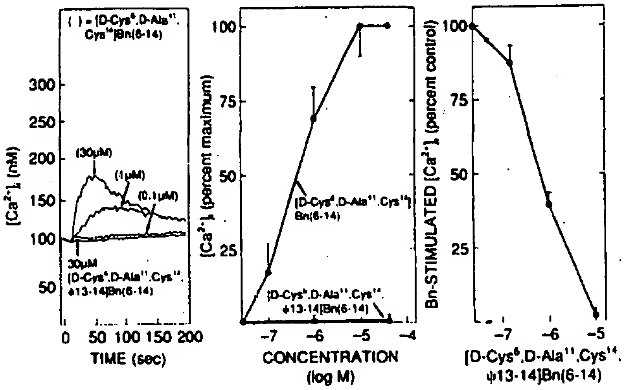

FIG. 7. Ability of [D-Cys^6,D-Ala^{11},Cys^{14}]Bn(6–14) or [D-Cys^6,D-Ala^{11},Cys^{14},ψ^{13-14}]Bn(6–14) to alter cytosolic calcium in 3T3 cells. 3T3 cells were incubated with the indicated concentrations of the cyclized analogues alone (*left* and *center panel*) or with 1 nM bombesin (*right panel*). In the *left panel*, the time of the ability of the indicated concentration of the cyclized Bn analogue to alter cytosolic calcium is shown, and, in the *middle panel*, the results are expressed as the percentage of the maximal response by 30 μM [D-Cys^6,D-Ala^{11},Cys^{14}]Bn(6–14). In these experiments, the control value of cytosolic calcium was 98 ± 9, and the 30 μM [D-Cys^6,D-Ala^{11},Cys^{14}]Bn(6–14) response was 221 ± 4. In the *right panel* is shown the ability of various concentrations of [D-Cys^6,D-Ala^{11},Cys^{14},ψ^{13-14}]Bn(6–14) to inhibit the increase in cytosolic calcium caused by 1 nM bombesin. In these experiments, basal calcium concentration was 113 ± 5, and 1 nM stimulated the cytosolic calcium to 233 ± 5 (n = 5). *Vertical bars* represent 1 S.E.

ent inhibition of the Bn-stimulated increase in $[Ca^{2+}]_i$ with a half-maximal effect at 1 mM (Fig. 7, *right*).

DISCUSSION

Cyclization of normally flexible, linear peptides has become a standard approach in analogue design and can result in interesting effects on biological properties, *in vivo* stability, and specificity and also yield much useful information on the mechanism of action of the ligand which, even in solution, would necessarily have a closer conformational resemblance to its receptor-bound state as long as reasonable affinity was maintained. The technique has been tried on numerous peptide systems and, in particular, work on cyclic enkephalin analogues with disulfide bridges (23), δ receptor specificity, and luteinizing hormone-releasing hormone analogues with multiple amide bridges (24) has resulted in analogues with sufficient rigidity to be useful for NMR conformational studies.

In the present Bn study, the already discussed choice of positions 6 and 14 as cyclization points appears to be sound in that it has resulted in retention of significant binding affinity with (D)-C-Q-W-A-V-G-H-L-C-NH_2 (VIII), although this was roughly 1000 times less than its linear counterpart, [D-Phe^6]Bn(6–14) (IV) for the rat acini cells. The ring size significantly affected affinity because the 7–14 cyclic, N-C-W-A-V-(D)-A-H-L-C-NH2 (XII), underwent a considerably greater loss of affinity, and the 9–14 analogue (XVII) had no activity. The fact that the affinity of VIII could be increased 5-fold by substitution of D-Ala for Gly in position 11 to give (D)-C-Q-W-A-V-(D)-A-H-L-C-NH_2 (VI) is strongly indicative of stabilization of folding by, perhaps, β-turn formation. This position in the linear peptides has previously been proposed (1, 25) as a potential folding site which might be stabilized by D-Ala; however, in the linear peptides, little effect on potency is generally observed. In the present series of peptides, [D-Phe^6,D-Ala^{11},Leu^{14}]Bn (VII) is actually one-half as potent as [D-Phe^6]Bn(6–14) (IV) (Table II), and this can probably be attributed to the Leu^{14} substitution (also compare I and II). The importance of a D-amino acid in position 6 also is illustrated by the over 3-fold loss of potency and binding affinity with C-Q-A-V-(D)-A-L-C-NH_2 (V), thus suggesting the possibility of folding in this region of the peptide backbone as well. High resolution NMR studies are being attempted on the Cys-bridged agonist and antagonist analogues (VI and XXIV, respectively) using peptide solutions in MeOH, dimethyl sulfoxide, and dimethyl sulfoxide/H_2O at various temperatures.[2] The quality of the one-dimensional spectra has generally been poor due to line broadening at all temperatures, making complete structural assignments difficult. The two-dimensional spectra yielded better data, and cyclization between the 2 Cys residues could be shown by NOEs between [Cys^{14}C$^\alpha$H]-[D-Cys^{6}C$^\beta$H] and [Cys^{14}NH$_2$]-[D-Cys^{6}C$^\alpha$H]. However, too few nonsequential NOEs have been observed for the presence of specific turns or conformations to be proposed. It should be emphasized, however, that even when cyclized these quite large sequences still possess relatively little conformational restraint and thus retain much of the flexibility of the linear peptides in solution. Meaningful NMR measurements aimed at elucidating possible receptor-bound conformations thus requires the introduction of much additional structural simplification and restraint for which the present analogues provide a useful basis.

In the present synthetic studies, the disulfide bridge strategy involving linked amino acid side chains was not the only successful method for producing biologically active cyclic analogues. The joining of termini in the Bn(6–14) series or 1–8 litorin series via a normal peptide bond also retained affinity and amylase releasing activity. Cyclo[(D)-F-Q-W-A-V-G-H-L-L] (XI, Table II) was about as potent as its Cys-bridged counterpart (VIII). Shortening the chain to 8 amino acids by removal of 1 NH_2-terminal residue to give cyclo[Q-W-A-V-G-H-L-L] (XIV) resulted in little loss of activity, and even further shortening by removal of the Gly residue to give cyclo[Q-W-A-V-H-L-L] (XV) resulted in the surprising retention of significant potency.

We were also interested in designing constricted Bn receptor antagonists by approaches similar to those used previously (26) in the linear analogues, that is by either removal of the NH_2-terminal amino acid or incorporation of the CH_2NH bond between the 2 COOH-terminal amino acids. Elimination of the COOH-terminal amino acid in the Cys-bridged series with [D-Cys^6,Cys^{13}]Bn(6–13) (XIX) resulted in almost complete loss of affinity for both rat pancreatic acini and 3T3 cells and probably reflects the incompatibility of the position 13 side chain to derivatization in this manner since readdition of the position 14 amino acid in XIII resulted in only a partial regaining of affinity. Elimination of the COOH-terminal amino acid in the head-to-tail cyclics to give cyclo[(D)-p-Cl-F-Q-W-A-V-G-H-L] (XXII) resulted in complete retention of binding affinity and agonist potency. In this structure, however, the position 6 amino acid becomes synonymous with the position 14 residue so that it can be considered to be simply a NH_2-terminally shortened analogue containing a D- amino acid in position 14.

The reduced peptide bond approach using the most potent Cys-bridged cyclic agonist analogue (VI) as the base structure was much more successful in producing an antagonist. Incorporation of a reduced peptide bond between positions 13 and 14 converted it from an agonist to full antagonist (XXIV) with only about a 3-fold loss of binding affinity. A number of observations supported the conclusion that this cyclic peptide was inhibiting the action of Bn by functioning as a Bn-

[2] G. Van Binst and P. Verheyden, personal communication.

receptor antagonist. The inhibitory activity was only observed for the Bn-receptor agonists, Bn and neuromedin B, and not for other pancreatic secretagogues such as CCK-8 and secretin which stimulate secretion through different receptors. A Schild plot of the ability of the cyclic antagonist to inhibit the action of Bn on pancreatic acini gave a slope not significantly different from unity, thus suggesting it was behaving as a classical Bn receptor antagonist. Also, for both 3T3 cells and rat pancreatic acini, the dose-inhibition curves for altering Bn-induced changes in biological activity and inhibiting ^{125}I-labeled Bn extended over the same concentration ranges which demonstrates directly that inhibitory activity is attributable to Bn receptor occupation. Interestingly, this antagonist was devoid of detectable partial agonist activity, whereas its linear counterpart, [D-Phe^6,Leu$^{13}\psi$(CH_2NH)Leu^{14}]Bn(6–14) (XXIII) has been shown to retain partial agonist activity (8).

We have theorized previously (6) that the conversion of an agonist to an antagonist structure by replacement of the 13–14 peptide bond was in some way related to the loss of the normal peptide bond CO group and a concomitant hydrogen bond with a peptide bond NH group present in another part of the peptide chain. This could result in greater rotational freedom at the COOH terminus and destruction of the correct agonist conformation via side chain shifts. It could be argued that antagonist formation by insertion of the pseudopeptide bond in a cyclic peptide in which free rotation is already suppressed by the disulfide bridge does not support this conclusion. However, as already mentioned, these large cyclic peptides still possess much flexibility so that loss of a transannular hydrogen bond could still produce sufficient conformational change for bioactivity to be lost.

In summary, a number of biologically active cyclic bombesin receptor agonist and antagonist analogues have been synthesized and characterized which comprise from 7–9 amino acid residues. The success of a variety of cyclization strategies, chain sizes, and additional conformational restraint via the use of D-amino acid suggests that further structural simplification and potency increases can be obtained. There is much literature precedent for this; for instance, the cyclic somatostatin tetradecapeptide was finally reduced to a 6-residue cyclic structure with much enhanced potency (27) by structure-activity studies and molecular modeling techniques. Such structurally simplified and constrained Bn/GRP analogues would be of great value in elucidating the binding conformations of both agonists and antagonists and might also have improved pharmacological and pharmacokinetic properties.

Acknowledgments—We would like to thank A. Odell, L. Massi, J. Encarnacion, D. LaPage, L. Cooper, and E. Yauger for their expert technical assistance.

REFERENCES

1. Heinz-Erian, P., Coy, D. H., Tamura, M., Jones, S. W., Gardner, J. D., and Jensen, R. T. (1987) *Am. J. Physiol.* **252**, G439–G442
2. Saeed, Z. A., Huang, S. C., Coy, D. H., Jiang, N.-Y., Heinz-Erian, P., Mantey, S., Gardner, J. D., and Jensen, R. T. (1989) *Peptides* **10**, 597–603
3. Coy, D. H., Heinz-Erian, P., Jiang, N.-Y., Sasaki, Y., Taylor, J., Moreau, J.-P., Wolfrey, W. T., Gardner, J. D., and Jensen, R. T. (1988) *J. Biol. Chem.* **263**, 5056–5060
4. Heimbrook, D. C., Saari, W. S., Balishin, N. L., Friedman, A., Moore, K. S., Reiman, M. W., Kiefer, D. M., Rotberg, N. S., Wallen, J. W., and Oliff, A. (1989) *J. Biol Chem.* **264**, 11258–11262
5. Camble, R., Cotton, R., Dutta, A. S., Garner, A., Howard, C. F., More, V. E., and Scholes, P. B. (1989) *Life Sci.* **45**, 1521–1527
6. Wang, L.-H., Coy, D. H., Taylor, J. E., Jiang, N.-Y., Kim, S. H., Moreau, J.-P., Huang, S. C., Mantey, S. A., Frucht, H., and Jensen, R. T. (1990) *Biochemistry* **29**, 616–622
7. Coy, D. H., Taylor, J. E., Jiang, N.-Y., Kim, S. H., Wang, L.-H., Huang, S., Moreau, J.-P., Gardner, J. D., and Jensen, R. T. (1989) *J. Biol. Chem.* **264**, 14691–14697
8. Coy, D. H., Wang, L.-H., Jiang, N.-Y., and Jensen, R. T. (1990) *Eur. J. Pharmacol.* **190**, 31–38
9. Wang, L.-H., Coy, D. H. Taylor, J. E., Jiang, N.-Y., Moreau, J.-P., Huang, S. C., Frucht, H., Haffar, B. M., and Jensen, R. T. (1990) *J. Biol. Chem.* **265**, 15695–15703
10. Dickinson, K. E. J., Uemara, N., Sekar, M. C., McDaniel, H. B., Anderson, W., Coy, D. H., and Hirschowitz, B. I. (1988) *Biochem. Biophys. Res. Commun.* **157**, 1154–1158
11. von Schrenck, T., Wang, L.-H., Coy, D. H., Villanueva, M. L., Mantey, S., and Jensen, R. T. (1990) *Am. J. Physiol.* **259**, G468–G473
12. Di Bello, C., Gozzini, L., Tonellato, M., Corradini, M. G., D'Auria, G., Paolillo, L., and Trivelloni, E. (1989) *Biopolymers* **28**, 421–440
13. Di Bello, C., Scanelli, A., Corradini, M. G., Paolillo, L., Trivelloni, E., Scatturin, A., Vertuani, G., Gozzini, L., and de Castiglioni, R. (1989) *Biochem. Biophys. Res Commun.* **161**, 987–993
14. Knight, M., Burke, T. R., Pineda, J. D., Cohen, S. L., Mahmoud, S., and Moody, T. W (1990) in *Proceedings of the 11th American Peptide Symposium* (Rivier, J., and Marshall, G., eds) pp. 185–187, ESCOM Science Publishers B. V., Leiden, Netherlands
15. Sasaki, Y., and Coy, D. H. (1987) *Peptides* **8**, 119–121
16. Jensen, R. T., Lemp, G. F, and Gardner, J. D. (1982) *J. Biol. Chem.* **257**, 5554–5559
17. Gardner, J. D., and Jackson, M. J. (1979) *J. Physiol. (Lond.)* **270**, 439–454
18. Ceska, M., Birath, K., and Brown, B. (1969) *Clin. Chim. Acta* **26**, 437–444
19. Ceska, M., Brown, B., and Birath, K. (1969) *Clin. Chim. Acta* **26**, 781–784
20. Jensen, R. T., Heinz-Erian, P., Moran, T., Mantey, S. A., James, S. W., and Gardner, J. D. (1988) *Am. J. Physiol.* **254**, G883–G890
21. Grynkiewicz, G., Poenie, M., and Tsien, R. Y. (1985) *J. Biol. Chem.* **260**, 3440–3450
22. Rozengurt, E. (1988) *Ann. N. Y. Acad. Sci.* **547**, 277–292
23. Mosberg, H. I., Hurst, R., Hruby, V. J., Galligan, J. J., Burks, T. F., Gee, K., and Yamamura, H. I. (1982) *Biochem. Biophys. Res. Commun.* **106**, 506–512
24. Rivier, J. E., Rivier, C., Vale, W., Corrigan, A., Porter, J., Gierasch, L. M., and Hagler, A. T. (1990) in *Proceedings of the 11th American Peptide Symposium* (Rivier, J., and Marshall, G., eds) pp. 33–37, ESCOM Science Publishers B. V., Leiden, Netherlands
25. Rivier, J. E., and Brown, M. R. (1978) *Biochemistry* **17**, 1766–1771
26. Jensen, R. T., and Coy, D. H. (1991) *Trends Physiol. Sci.* **12**, 13–19
27. Veber, D. F., Saperstein, R., Nutt, R. F., Freidinger, R. M., Brady, S. F., Curley, P., Perlow, D. S., Paleveda, W. J., Colton, C. D., Zacchei, A. G., Tocco, D. J., Hoff, D. R., Vandlen, R. L., Gerich, J. E., Hall, L., Mandarino, L., Cordes, E. H., Anderson, P. S., and Hirschman, R. (1984) *Life Sci.* **34**, 1371–1378
28. Cheng, Y., and Prusoff, W. H. (1973) *Biochem. Pharmacol.* **22**, 3099–3108

THE JOURNAL OF BIOLOGICAL CHEMISTRY

Vol. 263, No. 11, Issue of April 15, pp. 5056–5060, 1988
Printed in U.S.A.

Probing Peptide Backbone Function in Bombesin

A REDUCED PEPTIDE BOND ANALOGUE WITH POTENT AND SPECIFIC RECEPTOR ANTAGONIST ACTIVITY*

(Received for publication, October 7, 1987)

David H. Coy‡, Peter Heinz-Erian§, Ning-Yi Jiang‡, Yusuke Sasaki‡¶, John Taylor‖, Jacques-Pierre Moreau‖, William T. Wolfrey§, Jerry D. Gardner§, and Robert T. Jensen§

From the ‡Department of Medicine, Peptide Research Laboratories, Tulane University Medical Center, New Orleans, Louisiana 70112, the §Digestive Diseases Branch, National Institute of Diabetes and Digestive and Kidney Diseases, National Institutes of Health, Bethesda, Maryland 20892, and ‖Biomeasure, Inc., Hopkinton, Massachusetts 01748

Each peptide bond CONH group in the most important COOH-terminal octapeptide region of [Leu[14]]bombesin was replaced by a CH_2NH group using recently developed rapid solid-phase methods. The resulting analogues were then examined for amylase releasing activity in guinea pig pancreatic acini and for their ability to inhibit binding of [[125]I-Tyr[4]]bombesin to acinar cells. Replacement of the Trp[8]-Ala[9], Gly[11]-His[12], and His[12]-Leu[13] peptide bonds resulted in about 1000-, 200-, and 300-fold losses in both amylase releasing activity and binding affinity. The Val[10]-Gly[11] replacement, however, retained 30% potency relative to the parent peptide. Ala[9]-Val[10] and Leu[13]-Leu[14] bond replacement analogues exhibited no detectable amylase releasing activity but were still able to bind to acini with K_d values of 1060 and 60 nM, respectively (compared to 15 nM for [Leu[14]]bombesin itself). Subsequently, both analogues were demonstrated to be competitive inhibitors of bombesin-stimulated amylase release with IC_{50} values of 937 and 35 nM, respectively. [Leu[14]-ψ-CH_2NH-Leu[13]]Bombesin exhibits a 100-fold improvement in binding affinity compared to previously reported bombesin receptor antagonists and showed no affinity for substance P receptors. It was also a potent inhibitor of bombesin-stimulated growth of murine Swiss 3T3 cells with an IC_{50} of 18 nM. In terms of a bombesin receptor-binding conformation, these results may aid in the delineation of intramolecular hydrogen-bonding points and the eventual design of improved, conformationally restricted analogues.

There has been considerable interest in the design and development of competitive bombesin receptor antagonists as possible antimitotic agents since the discovery that bombesin (*p*Glu-Gln-Arg-Leu-Gly-Asn-Gln-Trp-Ala-Val-Gly-His-Leu-Met-NH_2) and related peptides (1) act as potent autocrine growth factors in human small cell lung carcinoma systems *in vitro* and *in vivo* (2, 3). These cells also contain high levels of bombesin immunoreactivity (4) and high affinity receptors for the peptide (5, 6).

There have been two published reports concerning peptide analogues capable of blocking the actions of bombesin. The first of these (7) described the ability of a substance P receptor antagonist to prevent bombesin-stimulated pancreatic amylase release with an IC_{50} in the millimolar range. The second (8) report concerned a bombesin analogue in which D-Phe replacement for His[12] resulted in a competitive antagonist. Although this latter compound was specific for pancreatic bombesin receptors, it also had a relatively high IC_{50} of 4 mM.

In the present paper, rather than using the classical side chain modification strategies, we have adopted a more unusual peptide backbone modification approach to bombesin analogue design and antagonist discovery. This was prompted by a recent report (9) in which the tetragastrin pseudopeptide, *t*-butoxycarbonyl-Trp-Leu-ψ[CH_2NH]-Asp-Phe-NH_2, was found to be an effective gastrin receptor antagonist and our own work (10) on ψ-CH_2NH pseudooctapeptide somatostatin analogues which were helpful in examining potential peptide bond involvement in intramolecular hydrogen bonding and peptide conformation. Although the reduced peptide bond is only one of many possible alternatives (11) for altering the CONH linkage, it also has the advantage of being easily incorporated (12) by reductive alkylation with sodium cyanoborohydride and the appropriate protected amino acid aldehyde during the rapid solid-phase synthesis of a peptide. Synthetic work was concentrated on the COOH-terminal half of the bombesin peptide chain which earlier structure-activity studies (13) indicate to be primarily responsible for receptor binding and triggering of the biological signal. To eliminate the readily oxidized Met[14] residue, the analogues described here were based on [Leu[14]]bombesin which retains about 33% of the biological potency and binding affinity of bombesin itself (Table I).

EXPERIMENTAL PROCEDURES

Materials

Protected amino acids and other synthetic reagents were obtained from Advanced ChemTech, Louisville, KY. NIH strain guinea pigs (175–225 g) were obtained from the Small Animals Section, Veterinary Resources Branch, National Institutes of Health. HEPES[1] was from Boehringer Mannheim; purified collagenase (type CLSPA, 440 units/mg) from Worthington; sodium borate, soybean trypsin inhibitor, carbamylcholine, theophylline, bacitracin, and 8-bromo-cAMP from Sigma; essential vitamin mixture (100× concentrated) from Microbiological Associates; glutamine and gastrin-I(2–17) from Research Plus; [125]I-labeled *N*-succinimydyl-3-(4-hydroxyphenyl)propionate (1500 Ci/mmol) and Na[125]I from Amersham Corp.; [[3]H]thymidine from Du Pont-New England Nuclear; Phadebas amylase test reagent from Pharmacia LKB Biotechnology Inc.; bovine plasma albumin (Fraction V) from Miles Laboratories; A23187 from

* The costs of publication of this article were defrayed in part by the payment of page charges. This article must therefore be hereby marked "*advertisement*" in accordance with 18 U.S.C. Section 1734 solely to indicate this fact.

¶ Present address: Tohoku College of Pharmacy, Sendai, Miyagi 983, Japan.

[1] The abbreviations used are: HEPES, 4(2-hydroxyethyl)-1-piperazineethanesulfonic acid; [125]I-BH-SP, [125]I-labeled Bolton-Hunter-substance P; LH-RH, luteinizing hormone-releasing hormone.

Behring Diagnostics; vasoactive intestinal polypeptide and substance P from Peninsula Laboratories. COOH-terminal octapeptide of cholecystokinin was a gift from M. Ondetti, Squibb Institute for Biomedical Research, Princeton, NJ.

The standard incubation solution used in experiments involving pancreatic acini contained 24.5 mM HEPES (pH 7.4), 6 mM, NaCl, 2.5 mM, KCl, 5 mM NaH_2PO_4, 5 mM Na pyruvate, 5 mM, Na fumarate, 5 mM Na glutamate, 2 mM glutamine, 11.5 mM glucose, 0.5 mM $CaCl_2$, 1.0 mM $MgCl_2$, 5 mM theophylline, 1% (w/v) albumin, 0.01% (w/v) trypsin inhibitor, 1% (v/v) amino acid mixture, and 1% (v/v) essential vitamin mixture. The incubation solution was equilibrated with 100% O_2 and all incubations were carried out with O_2 as the gas phase.

Methods

Preparation of Peptides—Solid-phase syntheses, including introduction of each reduced peptide bond, were carried out by the standard methods recently described by Sasaki and Coy (12). The crude hydrogen fluoride-cleaved peptides were purified on a column (2.5 × 90 cm) of Sephadex G-25 which was eluted with 2 M acetic acid, followed by preparative medium pressure chromatography on a column (1.5 × 45 cm) of Vydac C_{18} silica (15–20 μm) which was eluted with a linear gradient of 15–55% acetonitrile in 0.1% trifluoroacetic acid using an Eldex Chromatrol gradient controller (flow rate 1 ml/min). Analogues were further purified by re-chromatography on the same column with slight modifications to the gradient conditions when necessary. Homogeneity of the peptides was assessed by thin layer chromatography and analytical reverse-phase high pressure liquid chromatography, and purity was 97% or higher. Amino acid analysis gave the expected amino acid ratios. The presence of the reduced peptide bond was demonstrated by fast atom bombardment mass spectrometry. Each of the 6 analogues gave good recovery of the molecular ion corresponding to the calculated molecular mass of 1587.

Tissue Preparation—Dispersed acini from guinea pig pancreas were prepared as described previously (14).

Amylase Release—Dispersed acini from one guinea pig pancreas were suspended in 150 ml of standard incubation solution and samples (250 μl) were incubated for 30 min at 37 °C. Amylase activity was determined by the method of Ceska *et al.* (15, 16) using the Phadebas reagent. Amylase release was calculated as the percentage of amylase activity in the acini at the beginning of the incubation that was released into the extracellular medium during the incubation.

Binding of [^{125}I-Tyr^4]Bombesin—[^{125}I-Tyr^4]Bombesin (2000 Ci/mmol) was prepared using a modification (17) of the chloramine-T method of Hunter and Greenwood (18). [^{125}I-Tyr^4]Bombesin was separated from ^{125}I using a Sep-Pak and separated from unlabeled peptide by reverse-phase high pressure liquid chromatography on a column (0.46 × 25 cm) of μBondapak C_{18}. The column was eluted isocratically with acetonitrile (22.5%) and triethylammonium phosphate (0.25 M, pH 3.5) (77.5%) at a flow rate of 1 ml/min. Incubations contained 0.05 nM [^{125}I-Tyr^4]bombesin and were for 30 min at 37 °C. Nonsaturable binding of [^{125}I-Tyr^4]bombesin was the amount of radioactivity associated with the acini when incubation contained 0.05 nM [^{125}I-Tyr^4]bombesin plus 1 mM bombesin. All values shown are for saturable binding, *i.e.* binding measured with [^{125}I-Tyr^4]bombesin alone (total) minus binding measured in the presence of 1 mM unlabeled bombesin (nonsaturable binding). Nonsaturable binding was <20% of total binding in all experiments.

Binding of ^{125}I-Bolton-Hunter-Substance P (^{125}I-BH-SP)—^{125}I-BH-SP (1500 Ci/mmol) was prepared using a modification (19) of the method of Bolton and Hunter (20) and purified by reverse-phase high pressure liquid chromatography on a C_{18} column (21). Binding of ^{125}I-BH-SP to dispersed pancreatic acini was measured as described previously (19). Nonsaturable binding of ^{125}I-BH-SP was the amount of radioactivity associated with the acini when the incubation contained 0.06 nM ^{125}I-BH-SP plus 1 mM unlabeled substance P. All values given are for saturable binding, *i.e.* binding measured with ^{125}I-BH-SP alone (total) minus binding measured with 1 mM unlabeled substance P (nonsaturable). Nonsaturable binding was <20% of total binding in all experiments.

Growth of Swiss 3T3 Fibroblasts—Stock cultures of Swiss 3T3 cells (American Type Culture Collection CCL 92) were grown in Dulbecco's modified Eagle's medium supplemented with 10% fetal calf serum in an atmosphere of 10% CO_2, 90% air at 37 °C. The cells were seeded into 24-well cluster trays and used 4 days after the last change of medium. The cells were arrested in the G_1/G_0 phase of the cell cycle by changing to serum-free medium prior to thymidine uptake determinations.

Assays of DNA Synthesis—3T3 cells were washed twice with 1-ml aliquots of medium (without serum) and then incubated with medium, 0.5 mM [^{3}H]thymidine (20 Ci/mmol), bombesin (1 nM), and several concentrations of bombesin analogue in a final volume of 0.5 ml. After 28 h at 37 °C, [^{3}H]thymidine incorporation into acid-insoluble pools was then determined. Cells were washed twice with ice-cold 0.9% saline (1-ml aliquots) and acid-soluble radioactivity was removed by a 30-min (4°) incubation with 5% trichloroacetic acid. The cultures were washed once with 95% ethanol (1 ml) and solubilized by a 30-min incubation with 0.1 N NaOH. The solubilized material was measured for radioactivity on the scintillation counter.

RESULTS

We were interested in quantitating both the agonist and potential antagonist activity of the 6 analogues which were synthesized. They were, therefore, initially examined for stimulating effects on pancreatic amylase release, which is a major biological activity of bombesin peptides, and the dose-response curves obtained are shown in Fig. 1 in comparison to bombesin and [Leu^{14}]bombesin standards. EC_{50} values calculated from half-maximal stimulation concentration are given in Table I. Only [Val^{10}-ψ-CH_2NH-Gly^{11},Leu^{14}]bombesin retained high potency, being about three times less active than [Leu^{14}]bombesin itself. Analogues with 11–12, 12–13, and, particularly, 8–9 peptide bond replacement were several orders of magnitude less potent, but were full agonists. In contrast, 9–10 and 13–14 bond replacement completely destroyed detectable amylase releasing activity. The analogues were then tested for their abilities to inhibit binding of [^{125}I-Tyr^4]bombesin to pancreatic acini and inhibition curves are shown in Fig. 2 with calculated K_d values given in Table I. All analogues displayed affinities that correlated completely with their biopotencies with the exception of the 9–10 and 13–14 replacement peptides which were able to bind with K_d values of 1060 and 60 nM, respectively, despite having no amylase releasing activity.

The 9–10 and 13–14 replacement peptides were tested for inhibition of the amylase release produced by a 0.2 nM dose of bombesin (Fig. 3). Both gave concentration-dependent inhibition of the activity of bombesin and the calculated IC_{50} values were 937 ± 8 and 35 ± 7 nM, respectively. Finally, the antagonists were examined for their specificity towards bom-

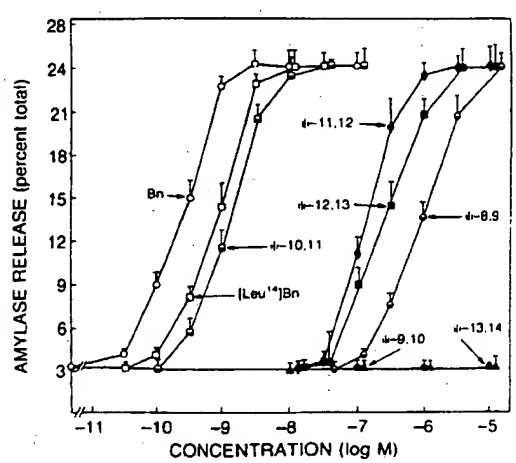

FIG. 1. **Effect of various concentrations of bombesin and [Leu^{14}]bombesin standards and 6 reduced-peptide bond replacement analogues on amylase release from dispersed guinea pig pancreatic acinar cells under conditions described in the text.** Values are the means from five experiments ± standard error.

TABLE I

Comparison of the ability of bombesin and [Leu[14]]peptide bond replacement analogues to stimulate dispersed acinar amylase release and displace [[125]I-Tyr[4]]bombesin from intact cells

K_d values for binding of the analogues were calculated by the method of Cheng and Prusoff (28). The K_d value for bombesin was determined by Scatchard analysis. EC_{50} and IC_{50} values are from data shown in Figs. 2 and 3 and represent concentrations of peptide causing half-maximal amylase release or half-maximal inhibition of 0.2 nM bombesin-stimulated release, respectively. Each value is the mean ± S.E. of five experiments.

Bond replaced	Amylase release (EC_{50})	Binding (K_d)
	nM	
8 9 10 11 12 13 14		
-Trp-Ala-Val-Gly-His-Leu-Met-NH$_2$	0.2 ± 0.1	4.4 ± 0.6
Leu	0.8 ± 0.3	15.1 ± 2.9
~[a]	1060.5 ± 14.5	15500.6 ± 2040
~	ND[b]	1060.7 ± 140.8
~	2.1 ± 0.3	38.9 ± 5.9
~	140.6 ± 20.5	2410.8 ± 154.5
~	251.8 ± 36.6	4512.6 ± 1132.3
~	ND[c]	59.6 ± 5.8

[a] ~, Peptide bond replaced.
[b] Antagonist, IC_{50} = 937 ± 8 nM.
[c] Antagonist, IC_{50} = 35 ± 7 nM (see Fig. 3).

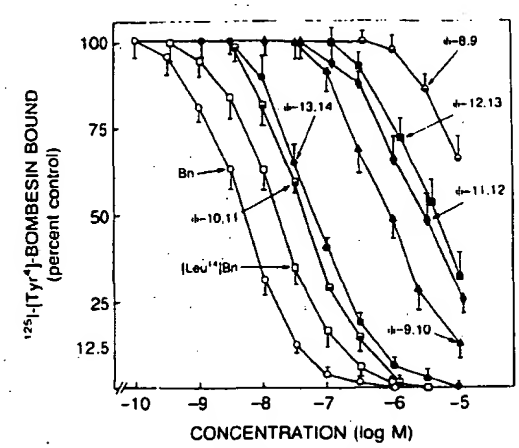

FIG. 2. Displacement of [125]I-labeled bombesin from intact guinea pig pancreatic acinar cells by various concentrations of bombesin, [Leu[14]]bombesin, and 6 peptide bond replacement analogues under conditions described in the text. Values are the means from five experiments ± standard error.

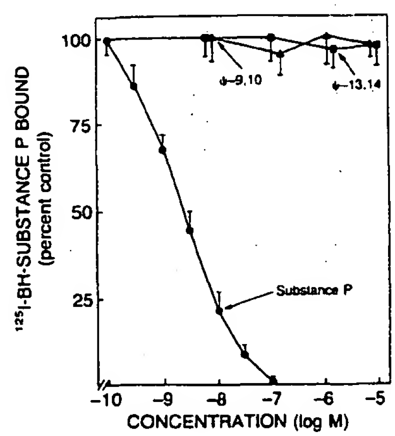

FIG. 4. Displacement of [125]I-labeled Bolton-Hunter-substance P from guinea pig pancreatic acinar cells by a substance P standard and [Leu[13]-ψ-CH$_2$NH-Leu[14]]- and [Ala[9]-ψ-CH$_2$NH-Val[10]]bombesin under conditions described in the text. Values are the means from five experiments ± standard error.

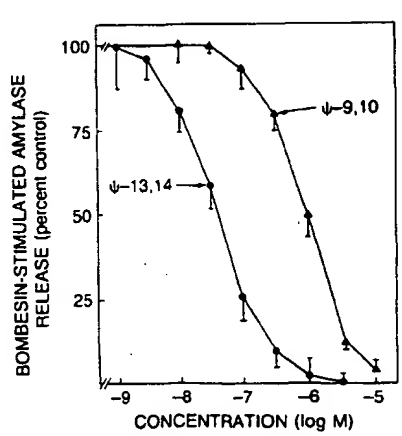

FIG. 3. Inhibitory effects of various concentrations of [Leu[13]-ψ-CH$_2$NH-Leu[14]]- and [Ala[9]-ψ-CH$_2$NH-Val[10]]bombesin on guinea pig pancreatic acinar amylase release stimulated by 0.2 nM bombesin under conditions described in the text. Values are the means from five experiments ± standard error.

besin receptors. Importantly, no inhibition of the binding of [125]I-labeled substance P could be achieved at concentrations up to 10 mM (Fig. 4). No inhibition of amylase release stimulated by substance P, cholecystokinin 8, vasoactive intestinal polypeptide, 8-bromo-cAMP, or A21837 was evident at the concentrations tested (Table II). The dose-response curve for bombesin-stimulated amylase release was shifted in a parallel fashion to the right by increasing concentrations of either the 13–14 (data not shown) or 9–10 bond replacement peptide. Schild plots for both peptides demonstrated a slope not significantly different from unity with a K_d of 22 ± 6 nM for the 13–14 and 473 ± 60 nM for the 9–10 bond replacement analogue.

The antagonist activity of [Leu[13]-ψ-CH$_2$NH-Leu[14]]bombesin was also examined in a totally different biological system, murine Swiss 3T3 fibroblast cells, the growth of which is stimulated by bombesin agonists (22) and which are known to contain bombesin receptors (23). Excellent inhibition of bombesin-stimulated growth was demonstrated and data from three experiments based on [^{3}H]thymidine incorporation are shown in Fig. 5. An average IC_{50} of 18 nM (Table III) was obtained from these experiments, which agrees very well with that derived from the acinar cell system. For comparison, a

TABLE II

Effect of [Leu^{13}-ψ-CH_2NH-Leu^{14}]- and [Ala^9-ψ-CH_2NH-Val^{10}, Leu^{14}]bombesin on guinea pig pancreatic acinar amylase release stimulated by various agents

Secretagogue	Amylase release: Alone	+0.3 mM 13–14 analogue	+10 mM 9–10 analogue
		% total[a]	
None	3.9 ± 0.7	4.1 ± 0.3	4.0 ± 0.2
Bombesin (0.2 nM)	17.1 ± 2.3	4.3 ± 0.3[b]	5.1 ± 1.0[b]
Substance P (3 nM)	10.3 ± 1.1	10.8 ± 0.3	11.2 ± 0.7
Cholecystokinin 8 (0.1 nM)	35.6 ± 2.2	33.9 ± 2.1	36.7 ± 3.0
Carbachol (10 mM)	28.4 ± 2.2	28.0 ± 2.9	30.0 ± 3.6
Vasoactive intestinal polypeptide (0.1 nM)	20.2 ± 2.4	20.4 ± 0.9	22.1 ± 1.1
8-Bromo-cAMP (1 mM)	24.0 ± 2.1	23.8 ± 2.5	25.1 ± 7.3
A21837 (3 mM)	13.2 ± 1.9	12.3 ± 0.3	13.0 ± 1.3

[a] Results are the means ± S.E. from five separate experiments.
[b] $p < 0.01$ compared to bombesin alone.

TABLE III

Comparison of the effectiveness of inhibition of 3T3 cell growth by two bombesin antagonists and a substance P antagonist

Peptide	IC_{50}
	nM
[D-Phe^{12}]Bombesin	>5000
[D-Arg^1, D-Pro^2, D-Trp^{7,9}, Leu^{11}] Substance P	2900
[Leu^{13}-ψ-CH_2NH-Leu^{14}]Bombesin	18 ± 12[a]

[a] Calculated from the data shown in Fig. 5.

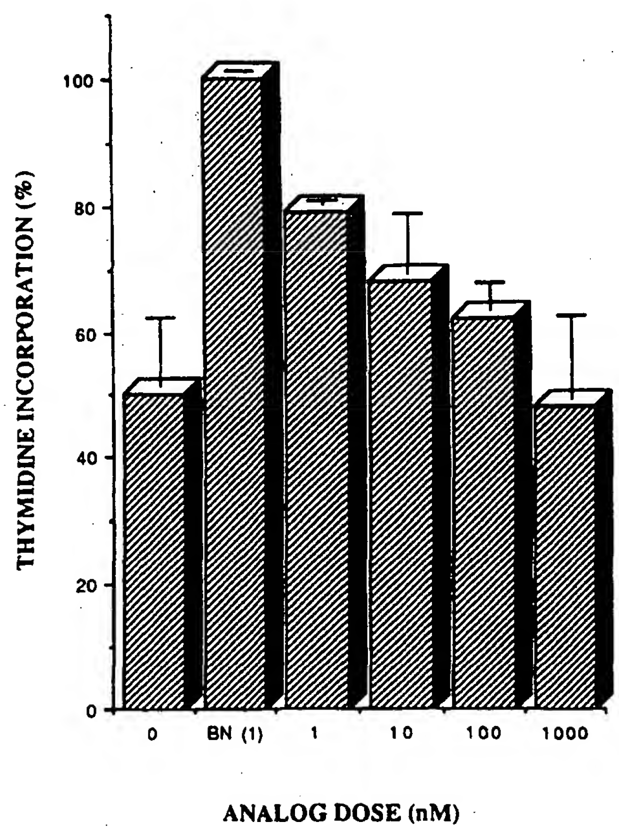

FIG. 5. **[Leu^{13}-ψ-CH_2NH-Leu^{14}]Bombesin inhibition of bombesin-stimulated [^{3}H]thymidine incorporation into murine Swiss 3T3 cells in culture.** Values are the means from three experiments ± standard error.

substance P receptor antagonist exhibited an IC_{50} of 2600 nM and our previous [D-Phe^{12}]bombesin antagonist was not effective at concentrations up to 5000 nM.

DISCUSSION

Although modifications to a peptide bond have long been considered an interesting approach to structure-activity relationships, it was not until recently that the chemistry for introducing one of them, the CH_2NH group, was simplified by adapting it to rapid solid-phase methods (12). Therefore, we are only just beginning to build a sufficiently large data base for this type of analogue with which to eventually derive some indication of what can be expected in terms of effects on biological activity generally. Thus far, reduced peptide bond somatostatin (10), gastrin (9), and bombesin analogues have not yielded any compounds with increased biopotency caused by increased receptor affinity. Likewise, in a reduced peptide bond series of luteinizing hormone-releasing hormone (LH-RH) antagonists (24), no analogues were found with improved antagonist activity. On the other hand, both the gastrin and the present bombesin studies resulted in the discovery of more than one antagonist analogue in each case. It is tempting to conclude, therefore, that this may be the design approach of choice for antagonist discovery.

Generally, the tendency for loss of potency in a peptide agonist series is probably explained by the profound effects which elimination of a peptide bond CO group will have on conformation due to both loss of a potential intramolecular hydrogen-bonding point and increased rotation about the C–N bond. In a folded peptide conformation, hydrogen bonding is a prime factor stabilizing the structure and in our previously reported somatostatin octapeptide series (10), for which much physicochemical data existed, replacement of hydrogen bonds not involved in this process tended to retain the most activity.

With [Leu^{13}-ψ-CH_2NH-Leu^{14}]bombesin it is entirely possible that the 13–14 peptide bond CO group, although clearly not necessary for binding, is directly responsible for triggering the receptor response. However, this does not account for the antagonist activity also produced by 9–10 bond replacement. We suggest that another explanation could reside in destabilization of a folded, extensively hydrogen-bonded conformation similar to those present in somatostatin analogues (25), LH-RH (26), and several other peptides. Fig. 6 attempts to show this. We have placed the beginning of a β-turn at Val^{10} so that Gly^{11} occupies a pivotal position. The rest of the chain, modeled on the known solution conformation of conformationally restricted somatostatin octapeptides (25), is arranged in the form of an antiparallel β-pleated sheet. It should be

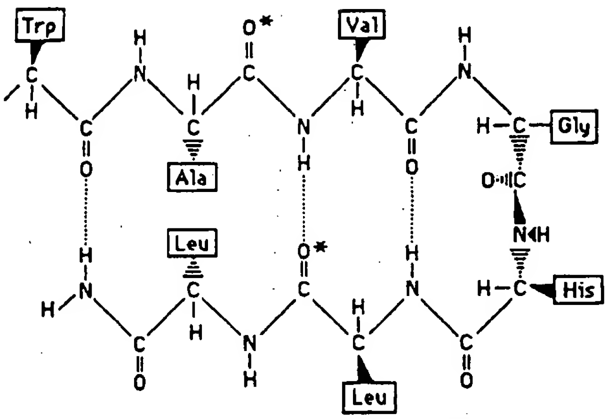

FIG. 6. **Possible conformation for the COOH-terminal octapeptide region of [Leu[14]]bombesin with a type II′ β-bend involving the Val-Gly-His-Leu tetrapeptide.** Carbonyl groups (*) which produce antagonists when replaced by CH_2 and putative intramolecular hydrogen bonding interactions along the chain are shown.

noted that Gly[11] in bombesin can be replaced by D-Ala with complete retention of activity, which prompted Rivier and Brown (13) and, more recently, Erne and Schwyzer (27) to discuss a similar β-bend. Also, the β-bends in somatostatin and LH-RH are similarly characterized by residues (Trp and Gly in positions 8 and 6, respectively) which can be replaced by D-amino acids with, in these cases, actual improvements in potency. In the β-pleated sheet area of the model, hydrogen bonding between the Leu[13]-Leu[14]-CO group and the Ala[9]-Val[10]-NH group assumes some importance and we propose that its destruction in the 13–14 analogue could result in a conformational shift responsible for loss of biological activity. Additionally, the 9–10 NH group would be adjacent to the Ala[9]-CO group which, when replaced by CH_2 also results in an antagonist. It is thus conceivable that the same hydrogen bond could also be inhibited by the 9–10 peptide bond replacement since bond angles and rotational freedom would all be significantly affected. Also noteworthy in relation to this model are the loss of activity caused by replacement of the Trp[8]-CO group which, could also be involved in another hydrogen bond, and the previously described importance of the COOH-terminal amide (13) which would also contribute to the same interaction. There is also loss of activity, although much less dramatic, associated with the Val[10]-CO replacement which constitutes part of the hydrogen bond integral to the β-bend. It should be emphasized that no direct physicochemical evidence from solution studies exists to support this hypothesis and, indeed, a recent infrared spectroscopic study of bombesin in phospholipid bilayer membranes (27) points to a α-helical structure in this environment. However, as Erne and Schwyzer (27) point out, the helical structure of the membrane-bound peptide could actually facilitate a second conformational transition caused by interaction with the receptor which could well involve the proposed β-turn and hydrogen bonding points. In any event, the model does provide a useful starting point for the design of additional, conformationally covalently restricted linear and cyclic analogues in the future.

An additional advantage to this type of analogue design strategy appears to lie in the absence of multiple side chain modifications which are so often needed for development of potent antagonists by standard approaches. This can often result in the introduction of undesirable properties, such as the loss of specificity with the substance P antagonists (7), introduction of enhanced histamine releasing activity with the LH-RH antagonists (28), and the poor solubility properties of the [D-Phe[12]]bombesins. In contrast, both of the present antagonists exhibited physical properties almost identical to bombesin and thus far both appear to be highly specific for bombesin receptors.

It is encouraging that the high antagonist activity of [Leu[13]-ψ-CH_2NH-Leu[14]]bombesin extended to an assay system examining bombesin-stimulated cellular growth where it is about 200 times more potent than the substance P inhibitor spantide, which is the only other compound reported capable of blocking the actions of bombesin in the 3T3 cell system. This indicates that there are no significant differences in receptor recognition requirements between acinar and 3T3 cells and suggests that the probability of this antagonist inhibiting bombesin-stimulated growth of human small cell lung carcinoma strains should be quite good. The development of a bombesin receptor antagonist with useful therapeutic properties may require additional synthetic work aimed at improving receptor affinity even further and particularly at improving *in vivo* pharmacokinetic properties. The present compound offers an excellent lead structure for this type of research.

REFERENCES

1. Erspamer, V. (1980) in *Gastrointestinal Hormones* (Glass, G. B. J., ed) pp. 343–361, Raven Press, New York
2. Minna, J. D., Carney, D. N., Cuttitta, F., Gazdar, A. F., Ihde, G. C., Mulshine, J., and Nau, M. (1984) in *Adjuvant Therapy of Cancer IV* (Jones, S. E., and Salmon, S. E., eds) pp. 168–182, Grune and Stratton, New York
3. Cuttitta, F., Carney, D. N., Mulshine, J., Moody, T. W., Fedorko, J., Fischler, A., And Minna, J. D. (1985) *Nature* **316**, 823–826
4. Moody, T. W., Pert, C. B., Gadzer, A. F., Carney, D. N., and Minna, J. D. (1981) *Science* **214**, 1246–1248
5. Moody, T. W., Bertness, V., and Carney, D. N. (1983) *Peptides* **4**, 683–686
6. Moody, T. W., Carney, D. N., Cuttitta, F., Quattroochi, K., and Minna, J. D. (1985) *Life Sci.* **37**, 105–113
7. Jensen, R. T., Jones, S. W., Folkers, K., and Gardner, J. D. (1984) *Nature* **309**, 61–63
8. Heinz-Erian, P., Coy, D. H., Tamura, M., Jones, S. W., Gardner, J. D., and Jensen, R. T. (1987) *Am. J. Physiol.* **252**, G439–G442
9. Martinez, J., Bali, J. P., Rodriguez, M., Castro, B., Magous, R., Laur, J., and Ligon, M. F. (1985) *J. Med. Chem.* **28**, 1874–1879
10. Sasaki, Y., Murphy, W. A., Heiman, M., Lance, V. A., and Coy, D. H. (1987) *J. Med. Chem.* **30**, 1162–1166
11. Spatola, A. F. (1983) in *Chemistry and Biochemistry of Amino Acids and Proteins* (Weinstein, B., ed) pp. 267–357, Marcel Dekker, Basel
12. Sasaki, Y., and Coy, D. H. (1986) *Peptides* **8**, 119–121
13. Rivier, J. E., and Brown, M. R. (1978) *Biochemistry* **17**, 1766–1771
14. Jensen, R. T., Lemp, G. F., and Gardner, J. D. (1982) *J. Biol. Chem.* **257**, 5554–5559
15. Ceska, M., Birath, K., and Brown, B. (1969) *Clin. Chim. Acta* **26**, 437–444
16. Ceska, M., Brown, B., and Birath, K. (1969) *Clin. Chim. Acta* **26**, 445–453
17. Jensen, R. T. T., Moody, T., Pert, C., Rivier, J. E., and Gardner, J. D. (1978) *Proc. Natl. Acad. Sci. U. S. A.* **75**, 6139–6143
18. Hunter, W. M., and Greenwood, F. C. (1962) *Nature* **194**, 495–496
19. Jensen, R. T., Jones, S. W., Lu, Y-A., Xu, J-C., Folkers, K., and Gardner, J. D. (1984) *Biochim. Biophys. Acta* **804**, 181–191
20. Bolton, A. E., and Hunter, W. M. (1973) *Biochem. J.* **133**, 529–539
21. Shults, C. W., Find, R., Jensen, R. T., Moody, T. W., O'Donohue, T. L., and Chase, T. M. (1982) *Peptides* **3**, 1073–1075
22. Rozengurt, E., and Sinnet-Smith, J. (1983) *Proc. Natl. Acad. Sci. U. S. A.* **80**, 2936–2940
23. Zachary, I., and Rozengurt, E. (1985) *Proc. Natl. Acad. Sci. U. S. A.* **82**, 7616–7620
24. Hocart, S. J., Nekola, M. V., and Coy, D. H. (1988) in *Peptides: Chemistry and Biology, Proceedings of the 10th American Peptide Symposium* (Marshall, G. R., ed) ESCOM Science Publishers, Leiden, The Netherlands, in press
25. Wynants, C., Van Binst, G., and Loosli, H. R. (1985) *Int. J. Peptide Protein Res.* **25**, 615–621
26. Monahan, M. W., Amoss, M. S., Anderson, H. A., and Vale, W. (1973) *Biochemistry* **12**, 4616–4620
27. Erne, D., and Schwyzer, R. (1987) *Biochemistry* **26**, 6316–6319
28. Morgan, J. E., O'Neil, C. E., Coy, D. H., Hocart, S. J., and Nekola, M. V. (1986) *Int. Arch. Allergy Appl. Immun.* **80**, 70–75

CCK-A Receptor Selective Antagonists Derived from the CCK-A Receptor Selective Tetrapeptide Agonist Boc-Trp-Lys(Tac)-Asp-MePhe-NH_2 (A-71623)†

Elizabeth E. Sugg,*,‡ Millard J. Kimery,‡ Jian Mei Ding,§ Deborah C. Kenakin,|| Laurence J. Miller,⊥ Kennedy L. Queen,|| and Thomas J. Rimele||

Departments of Medicinal Chemistry, Bioanalytical and Structural Chemistry, and Cellular Biochemistry, Glaxo Research Institute, 5 Moore Drive, Research Triangle Park, North Carolina 27709, and Center for Digestive Diseases, Mayo Clinic, Rochester, Minnesota 55905

Received August 24, 1994®

Analogs of the CCK-A receptor selective agonist Boc-Trp-Lys(Tac)-Asp-MePhe-NH_2 (A-71623) were prepared in which the lysine residue was replaced with L-4-aminophenylalanine and D- or L-3-aminophenylalanine. These new analogs were moderately potent antagonists of CCK-8 in the isolated guinea pig gallbladder with exceptional CCK-A receptor selectivity as evaluated in membrane preparations from CHO K1 cells stably transfected with human CCK-A and CCK-B receptors.

Cholecystokinin (CCK) is a gastrointestinal hormone and neurotransmitter first isolated from porcine intestine.[1] CCK is released from intestinal endocrine cells in response to nutrient ingestion.[2] While a variety of molecular forms of CCK have been identified, the C-terminal octapeptide (CCK-8, H-Asp-Tyr(SO_3H)-Met-Gly-Trp-Met-Asp-Phe-NH_2) retains full bioactivity, interacting with two receptor subtypes. CCK-A receptors predominate in the periphery (gallbladder, pancreas, pyloric sphincter, and vagal afferent fibers) but are also found in discrete regions of the brain.[3] CCK-B or gastrin receptors predominate in the brain and gastric glands.[4,5] The physiological role of CCK-8 is to aid digestion of nutrients through the induction of gallbladder contraction, pancreatic secretion, and delayed gastric emptying.[3,5] Exogenous CCK decreases meal size in a variety of species including lean[6] and obese[7] humans. This satiety effect of CCK requires an intact vagal afferent nerve and appears to be mediated by peripheral CCK-A receptors.[8]

The high molecular weight, the acid lability of the Tyr(SO_3H) residue, and the metabolic instability of CCK-8 provided the impetus for numerous chemical modifications.[9] In 1990, scientists at Abbott reported a series of unique CCK analogs derived by replacement of the methionine residue of Boc-CCK-4 (Boc-Trp-Met-Asp-Phe-NH_2) with side-chain-substituted Lys derivatives.[10,11] Boc-Trp-Lys(Tac)-Asp-MePhe-NH_2 (A-71623) was functionally equivalent to CCK-8 with remarkable CCK-A receptor selectivity (1200-fold), enhanced metabolic stability, and potent anorectic activity in rats,[12,13] mice, dogs, and monkeys.[14]

The tetrapeptide Boc-Trp-Lys(Tac)-Asp-Phe-NH_2 was approximately 3-fold less potent and less CCK-A receptor selective than the *N*-MePhe derivative.[11] In this series, the side-chain-truncated analog Boc-Trp-Orn-(Tac)-Asp-Phe-NH_2 had 170-fold reduced CCK-A receptor affinity, was a weak partial agonist in stimulating phophatidylinositide (PI) hydrolysis, and had 380-fold reduced efficacy in stimulating amylase release from isolated guinea pig pancreatic acini.[11] In contrast, the side-chain-extended analog Boc-Trp-hLys(Tac)-Asp-Phe-NH_2 had only 24-fold reduced CCK-A receptor affinity, was a full agonist in the PI hydrolysis assay, and had only 10-fold reduced efficacy in stimulating amylase release from isolated guinea pig pancreatic acini.[11]

This dependence of functional activity on the length of the methylene bridge between the urea moiety and the peptide backbone prompted our investigation of additional analogs of Boc-Trp-Lys(Tac)-Asp-MePhe-NH_2 in which the methylene bridge of the lysine residue was replaced by an aromatic ring. We now report the synthesis and biological activity of analogs of Boc-Trp-Lys(Tac)-Asp-MePhe-NH_2 in which the lysine residue was replaced by L-4-aminophenylalanine (L-4-Amf) and L- or D-3-aminophenylalanine (L-3-Amf or D-3-Amf). Side-chain-substituted (*o*-tolylamino)carbonyl (Tac) or [(*o*-chlorophenyl)amino]carbonyl (Cpac) urea derivatives of Lys and 4-Amf were prepared. Since we and others[15] have found that the N-terminal acetyl derivative was essentially equipotent to the N-terminal *tert*-butyloxycarbonyl derivative, all analogs were prepared as *N*-acetyl derivatives. The tetrapeptide Ac–Trp-Phe-Asp-MePhe-NH_2 was also prepared to evaluate the role of the urea substituent in these new analogs.

Methods

The urea-substituted amino acids were prepared by reaction of the corresponding *N*-α-Boc derivatives of L-Lys or L-4-Amf with *o*-tolyl isocyanate or *o*-chlorophenyl isocyanate in water or aqueous acetonitrile. *N*-α-Boc-D,L-3-aminophenylalanine was prepared by catalytic reduction of *N*-α-Boc-D,L-3-nitrophenylalanine[16,17] and converted to the urea derivative in a similar manner. Analogs 1–4 and 7 were prepared by automated solid-phase peptide synthesis and acetylated prior to cleavage and deprotection.

The peptides containing D- or L-3-Amf were prepared as a mixture of diastereomers and cleaved from the resin prior to acetylation. The diastereomeric amino terminal peptides were separated by preparative RP-HPLC. A

† Abbreviations: 4-Amf, 4-aminophenylalanine; 3-Amf, 3-aminophenylalanine; Boc, *tert*-butyloxycarbonyl; Cpac, [(*o*-chlorophenyl)amino]carbonyl; DCC, dicyclohexylcarbodiimide; HOBt, *N*-hydroxybenzotriazole; Tac, (*o*-tolylamino)carbonyl; hLys, homolysine;

* To whom correspondence should be addressed.
‡ Department of Medicinal Chemistry.
§ Department of Bioanalytical and Structural Chemistry.
|| Department of Cellular Biochemistry.
⊥ Center for Digestive Diseases.

® Abstract published in *Advance ACS Abstracts*, December 1, 1994.

Table 1. Functional Activity of Tetrapeptides Ac-Trp-NH-CHR-CO-Asp-MePhe-NH$_2$

			GPGB			
Analog	R	Stereo	pEC$_{50}$[a]	%mCCK-8[b]	pA$_2$[c]	Slope[d]
1	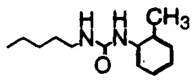	L	8.8 ± 0.2 (4)	105%		
2	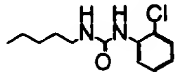	L	9.3 + 0.6 (4)	117%		
3	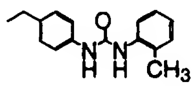	L		i.a.[e]	7.4 (8.5 - 6.9)	1.2 (1.6 - 0.8)
4	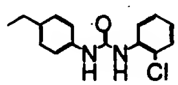	L		i.a.[e]	7.1 (7.9 - 6.6)	1.4 (1.9 - 0.9)
5	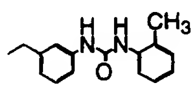	L		i.a.[e]	7.2 (8.4 - 6.6)	0.9 (1.3 - 0.6)
6	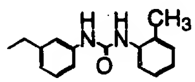	D		i.a.[e]	7.4 (7.7 - 7.1)	1.5 (1.2 - 1)
7	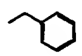	L		i.a.[e]		

[a] −log of the EC$_{50}$ ± SD (number of determinations). In the same assay, CCK-8 had a pEC$_{50}$ of 9.41 ± 0.15 (4). [b] % mCCK-8, percent contraction induced by test compound at 30 μM, normalized to the percent contraction induced by 1 μM CCK-8. [c] pA$_2$, −log of the concentration required to shift the CCK-8 concentration−response curve 2-fold; 95% confidence limits in parentheses. [d] Slope of the Schild plot; 95% confidence limits in parentheses. [e] i.a., inactive at 30 μM.

portion of each amino terminal peptide was treated with leucine aminopeptidase (16 h at 37 °C), and the resultant mixtures were monitored by LC-MS. The diastereomer completely degraded by enzyme treatment was assigned L-stereochemistry. The diastereomer which was resistant to enzymatic degradation was assigned D-stereochemistry. The remaining samples of the purified amino terminal diastereomeric peptides were treated with acetic anhydride/pyridine to obtain the *N*-acetyl derivatives, **5** and **6**.

Analogs **1**−**7** were purified to homogeneity (>98%) by preparative RP-HPLC, and the lyophiles were characterized by analytical RP-HPLC, ^{1}H-NMR spectroscopy, and high-resolution fast-atom bombardment (FAB) mass spectrometry. Analogs were evaluated for functional activity in the isolated guinea pig gallbladder (GPGB, Table 1). Receptor binding affinities were measured on membrane preparations from CHO K1 cell lines stably transfected with cDNA for human CCK-A[18] or CCK-B[19] receptors (Table 2).

Results and Discussion

While the lysine-substituted derivatives **1** and **2** were full agonists in the isolated GPGB (Table 1), the Amf derivatives **3**−**6** were moderately potent antagonists of CCK-8 in the GPGB, with pA$_2$ values ranging from 7.1 to 7.4. The D-3-Amf analog **6** was slightly more potent than the L-3-Amf analog **5**. Analog **6** also blocked the agonist activity of **1** in the GPGB with a pA$_2$ of 6.9 (6.5−7.7), suggesting that these analogs were interacting with the same CCK receptor as CCK-8 in the isolated GPGB preparation. The L-Phe analog, **7**, was completely inactive in the GPGB, confirming that the antagonist activity observed with **3**−**6** was related to the urea side-chain substituent.

The receptor affinities and subtype selectivities of these new analogs for human CCK-A and CCK-B

Table 2. Receptor Binding Affinities of Tetrapeptides for Human CCK-A and CCK-B Receptors

	pIC$_{50}$[a]		
analog	CCK-A	CCK-B	B/A[b]
1	7.7 ± 0.4 (3)	5.3 ± 0.2 (5)	251
2	8.3 ± 0.1 (3)	6 ± 0.05 (3)	200
3	7.5 ± 0.1 (3)	4.0 ± 0.3 (3)	3162
4	7.0 ± 0.02 (3)	4.2 ± 0.1 (3)	631
5	7 ± 0.1 (5)	5 ± 0.1 (3)	100
6	7.2 ± 0.2 (5)	4.3 ± 0.2 (3)	794
7	<4 (3)	5.4 ± 0.01 (3)	<0.04
CCK-8	9.4 ± 0.1 (3)	9.5 ± 0.4 (9)	0.8
CCK-8NS	5.7 ± 0.8 (4)	8.3 ± 0.4 (3)	0.003
MK-329	9.6 ± 0.5 (9)	7 ± 0.2 (3)	398
L 365,260	6.8 ± 0.4 (4)	8.2 ± 0.2 (2)	0.04

[a] −log of the concentration displacing 50% of [^{125}I]Bolton Hunter CCK-8 from membrane preparations isolated from CHO K1 cells stably transfected with cDNA of human CCK-A and CCK-B receptors. ±SD. Number of determinations are in parentheses. [b] CCK-A receptor selectivity. IC$_{50}$(CCK-B)/IC$_{50}$(CCK-A).

receptors are reported in Table 2. It should be noted that all of the standards reported in Table 2 show slightly better CCK-B affinity and receptor selectivity on the human receptors than has been reported[10,21,22] for comparisons with membrane preparations from rat pancreatic acinar cell (CCK-A) and guinea pig cerebral cortical (CCK-B) membranes.

The rank order of human CCK-A receptor affinities for **1**−**6** paralleled the rank order of potencies (pED$_{50}$ or pA$_2$) seen in the isolated GPGB. Lys derivatives **1** and **2** were 200-fold CCK-A receptor selective, with the Cpac derivative **2** having slightly higher CCK-A receptor affinity than the Tac derivative **1**. The L-4-Amf derivatives **3** and **4** were even more CCK-A receptor selective (3100- and 630-fold, respectively), with the Tac derivative **3** having slightly higher CCK-A receptor affinity than the Cpac derivative **4**. The D-3-Amf analog **6** had similar CCK-A receptor affinity but better CCK-A

receptor selectivity than the corresponding L-3-Amf analog **5**. Despite being equipotent to **3** in the GPGB assay, the D-3-Amf analog **6** had lower CCK-A receptor affinity and selectivity than the L-4-Amf analog **3**. The control tetrapeptide **7** had weak affinity for the human CCK-B receptor but did not bind the human CCK-A receptor (up to 10 μM), demonstrating the critical role of the urea substituent for CCK-A receptor recognition.

The ability of analogs **1** or **6** to influence intracellular calcium was evaluated with the stably transfected CHO K1 cells loaded with FURA2-AM (n = 1). Lysine derivative **1** was a full agonist on both the hCCK-A (ED_{50} = 4.2 nM) and hCCK-B (ED_{50} = 530 nM) receptor-containing cell lines, while the D-3-Amf analog **6** was inactive as an agonist. However, as predicted from the human receptor binding affinities, a single 1 μM concentration of analog **6** blocked the agonist activity of **1** in the human CCK-A receptor-containing cell line (15.6-fold shift; pK_B = 7.2) but not in the human CCK-B receptor-containing cell line.

In summary, analogs of Boc-Trp-Lys(Tac)-Asp-MePhe-NH_2 were prepared in which the methylene bridge between the urea substituent and the peptide backbone was replaced with a four-carbon (L-4-Amf) or three-carbon (L- and D-3-Amf) aromatic linker. To our surprise, these modifications produced moderately potent antagonists, with CCK-A receptor selectivity equal to or better than the lysine-substituted derivatives. In addition to altering the bridge length between the urea substituent and the peptide backbone, substitution of an aromatic ring would be expected to increase the steric bulk and hydrophobicity and decrease the conformational mobility of the urea-substituted amino acid. Moreover, substitution of an aniline for an alkylamine could alter the electronics and preferred conformation of the urea. The few compounds reported here do not provide a sufficient database to define which, if any, of these steric and/or electronic factors contribute to this remarkable conversion of functional activity.

Experimental Section

All chemicals and solvents were reagent grade unless otherwise specified. CCK-8 and nonsulfated CCK-8 (CCK-8NS) were purchased from Sigma (St. Louis, MO). MK-329[20] and L 365,260[21] were obtained from Merck & Co. (Rathway, NJ).

The ^{1}H-NMR spectra were recorded on either a Varian VXR-300 or a Varian Unity-300 instrument. Chemical shifts are expressed in parts per millon (ppm, δ units). Coupling constants are in units of hertz (Hz). Splitting patterns are designated as s, singlet; d, doublet; q, quartet; m, multiplet; br, broad. Low-resolution mass spectra (MS) were recorded on a JOEL JMS-AX505HA, JOEL SX-102, or SCIEX-APIII spectrometer. All mass spectra were taken in the positive ion mode under electrospray ionization (ESI) or fast-atom bombardment (FAB) methods. Reactions were monitored by thin-layer chromatography on 0.25 μm silica gel plates (E. Merck, 60F-254), visualized with UV light, 7% ethanolic phosphomolybdic acid, or p-anisaldehyde solution.

N-α-Boc-L-lysine[(N^ϵ-o-tolylamino)carbonyl]. o-Tolyl isocyanate (6.7 g, 50 mmol) was added to a solution of N-α-Boc-L-lysine (12.3 g, 50 mmol) dissolved in 1 N aqeuous sodium hydroxide (50 mmol). The reaction mixture was stirred at room temperature for 3 h, acidified with 1 N aqueous HCl, and extracted into ethyl acetate (6 × 50 mL). The combined organic extracts were washed with brine (1 × 30 mL), dried ($MgSO_4$), and concentrated in vacuo to give the crude urea (18 g, 94%) which was used without further purification: ^{1}H-NMR (300 MHz, DMSO-d_6) δ 1.36 (s, 13H), 3.83 (m, 1H), 2.15 (s, 3H), 3.05 (d, J = 5.13 Hz, 2H), 6.51 (t, J = 4.88 Hz, 1H), 6.83 (t, J = 7.33 Hz, 1H), 7.08 (m, 3H), 7.58 (s, 1H), 7.81 (d, 1H); MS (FAB) m/z 380 (MH^+); TLC (9:1 $CHCl_3$:CH_3OH) R_f = 0.06. Anal. ($C_{19}H_{29}N_3O_5$), C, H, N.

N-α-Boc-L-lysine[[N^ϵ-(o-chlorophenyl)amino]carbonyl]. Via N-α-Boc-L-lysine (5.0 g, 20.5 mmol) and o-chlorophenyl isocyanate (3.69 g, 24 mmol), the title compound (4.41 g, 54%) was prepared as previously described: ^{1}H-NMR (300 MHz, $CDCl_3$) δ 1.4 (s, 9H), 1.55 (m, 2H), 1.75 (m, 2H), 1.85 (m, 2H), 3.2 (br s, 2H), 4.23 (m, 1H), 5.3 (br d, 1H), 6.83 (br t, 1H), 7.1−7.3 (m, 3H), 8.05 (d, 1H); MS (FAB) m/z 400 (MH^+); TLC (9:1 $CHCl_3$:CH_3OH) R_f = 0.08. Anal. ($C_{18}H_{26}N_3O_5Cl$) C, H, N.

N-α-Boc-4-L-aminophenylalanine[(N^ϕ-o-tolylamino)-carbonyl]. Via N-α-Boc-4-L-aminophenylalanine (5.6 g, 20 mmol) and o-tolyl isocyanate (3.2 g, 24 mmol), the title compound (4.1 g, 49%) was prepared as previously described and used without further purification: ^{1}H-NMR (300 MHz, CD_3OD) δ 1.4 (s, 9H), 2.25 (s, 3H), 2.88 (dd, 1H), 3.1 (dd, 1H), 4.3 (dd, 1H), 7.03 (m, 1H), 7.18 (m, 4H), 7.38 (d, 2H), 7.63 (d, 1H); MS (FAB) m/z 414 (MH^+); TLC (9:1 $CHCl_3$:CH_3OH) R_f = 0.52. Anal. ($C_{22}H_{27}N_3O_5$) C, H, N.

N-α-Boc-4-L-aminophenylalanine[[N^ϕ-(o-chlorophenyl)amino]carbonyl]. Via N-α-Boc-4-L-aminophenylalanine (5.6 g, 20 mmol) and o-chlorophenyl isocyanate (3.69 g, 24 mmol), the title compound (6.2 g, 72%) was prepared as previously described and used without further purification: ^{1}H-NMR (300 MHz, CD_3OD) δ 1.4 (s, 9H), 2.88 (dd, 1H), 3.13 (dd, 1H), 4.33 (dd, 1H), 6.95−7.45 (m, 7H), 8.1 (dd, 1H); MS (FAB) m/z 434 (MH^+); TLC (9:1 $CHCl_3$:CH_3OH) R_f = 0.8. Anal. ($C_{21}H_{24}N_3O_5Cl$) C, H, N.

N-α-Boc-3-D/L-aminophenylalanine. N-α-Boc-3-D/L-nitrophenylalanine[16,17] (8.9 g, 18 mmol) and 10% Pd/C (0.8 g) in methanol (100 mL) were shaken under hydrogen (45 psi) overnight. The mixture was filtered through Celite, and the filtrate was evaporated in vacuo to give the title compound (8.7 g, 18 mmol) which was used without further purification: ^{1}H-NMR (300 MHz, CD_3OD) δ 1.4 (s, 9H), 2.83 (dd, 1H), 3.05 (dd, 1H), 4.33 (dd, 1H), 6.65 (m, 3H), 7.05 (m, 1H); MS (FAB) m/z 281 (MH^+); TLC (9:1 $CHCl_3$:CH_3OH) R_f = 0.14. Anal. ($C_{14}H_{20}N_2O_4$) C, H, N.

N-α-Boc-3-D/L-aminophenylalanine[(N^ϵ-o-tolylamino)-carbonyl]. Via N-α-Boc-3-D/L-aminophenylalanine (4.7 g, 16.7 mmol) and o-tolyl isocyanate (2.7 g, 20 mmol), the title compound (5.1 g, 74%) was prepared as previously described and used without further purification: ^{1}H-NMR (300 MHz, CD_3OD) δ 1.4 (s, 9H), 2.3 (s, 3H), 2.9 (dd, 1H), 3.15 (dd, 1H), 4.23 (m, 1H), 6.85−7.25 (m, 6H), 7.43 (d, 1H), 7.63 (d, 1H); MS (FAB) m/z 414 (MH^+); TLC (9:1 $CHCl_3$:CH_3OH) R_f = 0.54. Anal. ($C_{22}H_{27}N_3O_5$) C, H, N.

Peptide Synthesis. Analogs were prepared by automated solid-phase peptide synthesis (ABI 430) on p-methylbenzhydrylamine resin[22] (Peptides International, Louisville, KY). N-α-$tert$-Butyloxycarbonyl (Boc) amino acid derivatives were purchased from Bachem Biosciences (Philadelphia, PA) or Applied Biosystems Inc. (Foster City, CA). DCC/HOBt single coupling protocols were utilized for the N-α-Boc-MePhe-OH, N-α-Boc-Lys(N^ϵ-Tac)-OH, N-α-Boc-Lys(N^ϵ-Cpac)-OH, N-α-Boc-4-Amf-(N^ϕ-Tac)-OH, N-α-Boc-4-Amf(N^ϕ-Cpac)-OH, N-α-Boc-D/L-3-Amf-(N^ϵ-Tac)-OH, and N-α-Boc-Trp-OH. DCC/HOBt double coupling protocols were utilized for N-α-Boc-Asp(benzyl). Peptides were cleaved from the resin, and all protecting groups were removed by treatment at 0 °C for 1 h with anhydrous liquid HF (10 mL/g of resin) containing dithioethane (1 mL/g of resin) and anisole (1 mL/g of resin). The HF was removed in vacuo, and the resin was washed with cold diethyl ether and filtered. Peptides were extracted from the resin with aqueous acetic acid (30%). The crude peptides obtained by lyophilization were purified to homogeneity by preparative reversed-phase high-pressure liquid chromatography (RP-HPLC) using a Waters Model 3000 Delta Prep column equipped with a Delta-pak radial compression cartridge (G18, 300 A, 15 μm, 47 mm × 300 mm) as the stationary phase. The mobile phase employed 0.1% aqueous TFA with acetonitrile (Burdick and Jackson) as the organic modifier. Linear gradients were used in all cases, and the flow rate was 100 mL/min (t_0 − 5 min). Appropriate

Table 3. Physical Data for Analogs 1–7

analog	empirical formula	HRMS[a] calculated	HRMS[a] found	t_R, min (% CH_3CN/30 min)[b]	purity[c]
1	$C_{41}H_{50}N_8O_8$	783.3830	783.3833	19.4 (30–48%)	98.7
2	$C_{40}H_{47}N_8O_8Cl$	803.3284	803.3297	15.4 (33–51%)	98.1
3	$C_{44}H_{48}N_8O_8$	817.3673	817.3663	18.1 (33–51%)	98.2
4	$C_{43}H_{45}N_8O_8Cl$	837.3127	837.3135	21.6 (33–51%)	98.5
5	$C_{44}H_{48}N_8O_8$	817.3673	817.3679	16 (36–54%)	99.3
6	$C_{44}H_{48}N_8O_8$	817.3673	817.3687	15.8 (36–54%)	99.0
7	$C_{36}H_{41}N_6O_7$	669.3037	669.3039	21.6 (24–42%)	98.4

[a] MH^+, obtained in positive ion mode, utilizing FAB ionization on an AMD 604 double focusing magnetic sector mass spectrometer. [b] Analytical retention time on a Vydac C18 column (5 μm, 4.6 mm × 200 mm), utilizing a linear gradient of acetonitrile and a flow rate of 1.5 mL/min. [c] Purity assessed by integration at $\lambda = 214$ nm.

fractions were combined and lyophilized to obtain the target peptide analogs. Analytical purity was assessed by RP-HPLC using a Waters 600E system equipped with a Waters 990 diode array spectrometer (λ range 200–400 nm). The stationary phase was a Vydac C18 column (5 μm, 4.6 mm × 200 mm). The mobile phases were the same as above, linear gradients were again utilized, and the flow rate was 1.5 mL/min (t_0 = 2.8 min). Analytical data (Table 3) is reported as retention time, t_R, in minutes (% acetonitrile over time). High-resolution mass spectra (Analytical Instrument Group, Raleigh, NC) were recorded in the positive ion mode on a AMD-604 (AMD Intectra GmbH) high-resolution double focusing mass spectrometer under FAB conditions (Table 3).

H-Trp-3-D,L-Amf[(N^ϵ-tolylamino)carbonyl]-Asp-MePhe-NH$_2$. This compound was prepared as a mixture of diastereomers containing D,L-3-Amf(Tac) and cleaved from the resin prior to N-terminal acetylation. Separation by preparative RP-HPLC afforded the individual diastereomeric analogs in greater than 98% purity. H-Trp-L-3-Amf[(N^ϵ-*o*-tolylamino)-carbonyl]-Asp-MePhe-NH$_2$: $C_{42}H_{46}N_8O_7$; MS (FAB) *m/z* 775 (MH^+); t_R = 20.3 min (27–45%/30 min); H-Trp-D-3-Amf[(N^ϵ-*o*-tolylamino)carbonyl]-Asp-MePhe-NH$_2$: $C_{42}H_{46}N_8O_7$; MS (FAB) *m/z* 775 (MH^+); t_R = 22.3 min (27–45%/30 min). The individual diastereomeric peptides were converted to the *N*-acetyl derivatives **5** and **6** by treatment with acetic anhydride (0.01 mL) and pyridine (0.02 mL) in DMF (3 mL) at ambient temperature for 30 min. The reaction mixture was diluted with aqueous TFA (10%, 50 mL) and lyophilized to a solid. Purification by RP-HPLC afforded the *N*-acetyl derivatives in >99% purity.

Assignment of Stereochemistry. Each diastereomeric peptide were incubated at 37 °C for 16 h with leucine aminopeptidase (Sigma; 1:50) in 100 μL of 50 mM NH_4HCO_3 (pH 8.5) solution. The hydrolysis reactions were terminated by the addition of TFA (1 μL), and the reaction mixtures were reduced almost to dryness by lyophilization and then reconstituted with 0.05% aqueous TFA (100 μL) to a final concentration of 10 μM. About 100 pmol of peptide hydrolysate was used for each LC/MS experiment. Samples were analyzed on a Vydac C18 column (5 μm, 320 μm × 30 cm) conditioned to a flow rate of 7 μL/min. The mobile phase was 0.1% aqueous TFA (10% B to 60% B) with acetonitrile as the organic modifier. Masses were detected with a Sciex API-III triple quadrupole electrospray mass spectrometer. The collision gas used for MS/MS was Ar with 10% N_2. Digested peptides were analyzed from *m/z* 300 to 1000 using repetitive scans at a rate of 3.5 s/scan.

Guinea Pig Gallbladder Tissue Preparation. Gallbladders were removed from male Hartley guinea pig sacrificed with CO_2 atmosphere. The isolated gallbladders were cleaned of adherent connective tissue and cut into two rings from each animal (2–4 mm in length). The rings were suspended in organ chambers containing a physiological salt solution (118.4 mM NaCl, 4.7 mM KCl, 1.2 mM $MgSO_4$, 2.5 mM $CaCl_2$, 1.2 mM KH_2PO_3, 25 mM $NaHCO_3$, 11.1 mM dextrose). The bathing solution was maintained at 37 °C and aerated with 95% O_2/5% CO_2 to maintain pH 7.4. Tissues were connected via gold chains and stainless steel mounting wires to isometric force displacement transducers (Grass, Model FT03 D). Responses were then recorded on a polygraph (Grass, Model 7E). One tissue from each animal served as a time/solvent control and did not receive test compound. Rings were gradually stretched (over a 120 min/period) to a basal resting tension of 1 g which was maintained throughout the experiment. During the basal tension adjustment period, the rings were exposed to acetylcholine (10^{-6} M) four times to verify tissue contractility. The tissues were then exposed to a submaximal dose of sulfated CCK-8 (Sigma; 3×10^{-9} M). After obtaining a stable response, the tissues were washed out three times rapidly and every 5–10 min for 1 h to reestablish a stable base line.

Agonist ED$_{50}$'s. Compounds were dissolved in dimethyl sulfoxide (DMSO) and then diluted with water and assayed via a cumulative concentration–response curve to test compound (10^{-11}–3×10^{-5} M) followed by a concentration–response curve to sulfated CCK-8 (10^{-10}–10^{-6} M) in the presence of the highest concentration of the test compound. As a final test, acetylcholine (1 mM) was added to induce maximal contraction. A minimum of three determinations of activity was made for each test compound.

Antagonist p*A*$_2$'s. Gallbladder tissues from at least three different animals were incubated for 60 min with a given concentration (three to five concentration per analog) of the antagonist followed by a cumulative concentration–response curve with CCK-8 or compound **1**. One paired tissue from each animal did not receive the antagonist and served as the time/solvent control used to calculate the concentration ratio for the rightward shift in the CCK-8 concentration response. p*A*$_2$'s were determined by Schild analysis for a given number of observations.[23] Upper and lower 95% confidence limits and slopes of the Schild plot are given for each p*A*$_2$.

Establishment of Stable CCK Receptor-Bearing Cell Lines. The cDNA clones for the human CCK-A[18] or CCK-B[19] receptors were ligated into cDNA1-Neo vector from Invitrogen Corp. (San Diego, CA) for direct transfection. DNA was prepared by the alkaline lysis method and transfected into CHO K1 cells (ATCC, Rockville, MD) using the Lipofectin reagent[24] (Gibco BRL, Gaithersberg, MD). Stable transfectants were initially selected by the use of Geneticin (Gibco BRL), and receptor-bearing resistant cells were enriched by fluorescence-activated cell sorting based on binding of Fluorescein-Gly-[Nle28,31]-CCK-8. Clonal lines were subsequently established by the limiting dilution method.

Cell Membrane Preparation. CHO K1 cells stably transfected with human CCK-A or CCK-B receptor cDNA were grown at 37 °C under a humidified atmosphere (95% O_2/5% CO_2) in Ham's F12 medium supplemented with 5% heat-inactivated fetal bovine serum. The cells were passaged twice weekly and grown to a density of 2–4 million cells/mL. The cells were collected by centrifugation (600*g*, 15 min, 4 °C) and resuspended in buffer (20 mL, pH 7.4) containing Tris-HCl (25 mM), EDTA (5 mM), EGTA (5 mM), phenylsulfonyl fluoride (0.1 mM), and soybean trypsin inhibitor (100 μg/mL). Cells were disrupted with a motorized glass teflon homogenizer (25 strokes), and the homogenate was centrifuged at low speed (600*g*, 10 min, 4 °C). The supernatant was collected and centrifuged at high speed (500000*g*, 15 min 4 °C) to pellet the particulate fraction. The low-speed pellet was processed three additional times. High-speed particulate fractions were combined and resuspended in buffer (1–5 mg of protein/mL) and frozen at −80 °C. Protein concentration was determined according to manufacturer's directions using BioRad reagent and bovine serum albumin as standard.

Receptor Binding Assays. [^{125}I]Bolton Hunter CCK-8 (Amersham; 2000 Ci/mmol) was dissolved in binding buffer (pH 7.4, 100 000 cpm/25 μL) containing HEPES (20 mM), NaCl (118 mM), KCl (5 mM), $MgCl_2$ (5 mM), and EGTA (1 mM). Nonspecific binding was determined with MK-329[20] (10 μM, CCK-A) or L 365,260[21] (10 μM, CCK-B). Test compounds were dissolved in DMSO at a stock concentration of 100 times the final assay concentration and diluted to appropriate concentrations with binding buffer. Binding assays were performed in triplicate using 96-well plates to which the following were added sequentially: test compound (25 μL), [^{125}I]Bolton Hunter CCK-8 (25 μL), buffer (pH 7.4, 150 μL), and receptor preparation (50 μL). The final concentration of DMSO was 1% in all assay wells. After 3 h at 30 °C, the incubation was terminated by rapid filtration of the mixture onto glass filters (Whatman GF/B) with subsequent washing to remove unbound ligand. Bound radioactivity was quantified by γ counting.

Intracellular Calcium Measurements. Cells grown on glass coverslips to 75–90% confluency were loaded for 50 min in serum-free culture medium containing 5 μM FURA2-AM and 2.5 mM probenecid. A JASCO CAF-102 calcium analyzer was used to measure changes in intracellular calcium concentration by standard ratiometric techniques using excitation wavelengths of 340 and 380 nm. Cells were perfused with increasing concentrations of compound **1** ($n = 1$) until a plateau in the 340/380 ratio was achieved. A washout/recovery period of at least 10 min was allowed between successive stimulations. Following collections of control agonist responses, cells were perfused for 60 min with analog **6** (1 μM, $n = 1$) and a second set of responses to compound **1** was collected. The single concentration K_B was calculated according to the formula,

$$K_B = \frac{[\text{test compound}]}{(\text{CR-1})}$$

where CR is the fold-shift of the concentration response curve to **1** in the presence of the antagonist, **6**.

Acknowledgment. The authors would like to thank Simon Tate (Glaxo Research and Development, Greenford, U.K.) for providing the human CCK-B receptor cDNA clone and acknowledge NIH Grant DK-32878 (L.J.M.) for partial support of this work.

References

(1) Jorpes, J. E.; Mutt, V. Cholecystokinin and Pancreozymin, One Single Hormone? *Acta Physiol. Scand.* **1966**, *66*, 196–202.
(2) Liddle, R. A.; Green, G. M.; Conrad, C. K.; Williams, J. A. Proteins But Not Amino Acids, Carbohydrates, or Fats Stimulate Cholecystokinin Secretion in the Rat. *Am. J. Physiol.* **1986**, *251*, G243–G248.
(3) Silvente-Poirot, S.; Dufresne, M.; Vaysse, N.; Fourmy, D. The Peripheral Cholecystokinin Receptors. *Eur. J. Biochem.* **1993**, *215*, 513–529.
(4) Makovec, F. CCK-B/Gastrin Receptor Antagonists. *Drugs Future* **1993**, *18*, 919–931.
(5) McHugh, P. R.; Moran, T. H. The Stomach, Cholecystokinin, and Satiety. *Fed. Proc.* **1986**, *45*, 1384–1390.
(6) Kissileff, H. R.; Pi-Sunyer, F. X.; Thornton, J.; Smith, G. P. C-Terminal Octapeptide of Cholecystokinin Decreases Food Intake in Man. *Am. J. Clin. Nutr.* **1981**, *34*, 154–160.
(7) Pi-Sunyer, X.; Kissileff, H. R.; Thornton, J.; Smith, G. P. C-Terminal Octapeptide of Cholecystokinin Decreases Food Intake in Obese Men. *Physiol. Behav.* **1982**, *29*, 627–630.
(8) Dourish, C. T.; Ruckert, A. C.; Tattersall, F. D.; Iversen, S. D. Evidence That Decreased Feeding Induced by Systemic Injection of Cholecystokinin is Mediated by CCK-A Receptors. *Eur. J. Pharmacol.* **1989**, *173*, 233–234.
(9) Hermkens, P. H. H.; Ottenheijm, H. C. J.; van der Werf-Pieters, J. M. L.; Broekkamp, C. L. E.; de Boer, T.; van Nispen, J. W. CCK-A Agonists: Endeavours Involving Structure-Activity Relationship Studies. *Recl. Trav. Chim. Pays-Bas* **1993**, *112*, 95–106.
(10) Shiosaki, K.; Lin, C. W.; Kopecka, H.; Craig, R.; Wagenaar, F. L.; Bianchi, B.; Miller, T.; Witte, D.; Nadzan, A. M. Development of CCK-Tetrapeptide Analogues as Potent and Selective CCK-A Receptor Agonists. *J. Med. Chem.* **1990**, *33*, 2952–2956.
(11) Shiosaki, K.; Lin, C. W.; Kopecka, H.; Tufano, M. D.; Bianchi, B. R.; Miller, T. R.; Witte, D. G.; Nadzan, A. M. Boc-CCK-4 Derivatives Containing Side-Chain Ureas as Potent and Selective CCK-A Receptor Agonists. *J. Med. Chem.* **1991**, *34*, 2837–2842.
(12) Asin, K. E.; Gore, P. A., Jr.; Bednarz, L.; Holladay, M.; Nadzan, A. M. Effects of Selective CCK Receptor Agonists on Food Intake After Central or Peripheral Administration in Rats. *Brain Res.* **1992**, *571*, 169–174.
(13) Asin, K. E.; Bednarz, A. L.; Nikkel, A. L.; Gore, P. A., Jr.; Montana, W. E.; Cullen, M. J.; Shiosaki, K.; Craig, R.; Nadzan, A. M. Behavorial Effects of A-71623, a highly selective CCK-A Agonist Tetrapeptide. *Am. J. Physiol.* **1992**, *263*, R125–R135.
(14) Asin, K. E.; Bednarz, L.; Nikkel, A. L.; Gore, P. A.; Nadzan, A. M. A-71623, A Selective CCK-A Receptor Agonist, Suppresses Food Intake in the Mouse, Dog and Monkey. *Pharmacol. Biochem. Behav.* **1992**, *42*, 699–704.
(15) Elliott, R. L.; Kopecka, H.; Bennett, M. J.; Shue, Y.-K.; Craig, R.; Lin, C.-W.; Bianchi, B. R.; Miller, T. R.; Witte, D. G.; Stashko, M. A.; Asin, K. E.; Nikkel, A.; Bednarz, L.; Nadzan, A. M. Tetrapeptide CCK Agonists: Structure Activity Studies on Modifications at the N-terminus. *J. Med. Chem.* **1994**, *37*, 309–313.
(16) Chung, J. Y. L.; Tufano, M. D.; May, P. D.; Shiosaki, K.; Nadzan, A. M.; Garvey, D. S.; Shue, Y. K.; Brodie, M. S.; Holladay, M. W. Preparation of Tetrapeptide Type-B CCK Receptor Ligands. Eur. Pat. Appl. 405506, 1991, 38–39.
(17) Knittel, J. J.; He, X. Q. Synthesis and Resolution of Novel 3'-Substituted Phenylalanine Amides. *Pept. Res.* **1990**, *3*, 176–181.
(18) Ulrick, C. D.; Ferber, I.; Holicky, E.; Hadac, E.; Buell, G.; Miller, L. J. Molecular Cloning and Functional Expression of the Human Gallbladder Cholecystokinin A Receptor. *Biochem. Res. Commun.* **1993**, *193*, 204–211.
(19) Lee, Y.-M.; Beinborn, M.; McBride, E. W.; Lu, M.; Kolakowski, L. F., Jr.; Kopin, A. S. The Human Brain Cholecystokinin B/Gastrin Receptor. *J. Biol. Chem.* **1993**, *268*, 8164–8169.
(20) Evans, B. E.; Bock, M. G.; Rittle, K. E.; Dipardo, R. M.; Whitter, W. L.; Veber, D. L.; Anderson, P. S.; Freidinger, R. M. Design of Potent, Orally Effective, Nonpeptidyl Antagonists of the Peptide Hormone Cholecystokinin. *Proc. Natl. Acad. Sci. U.S.A.* **1986**, *83*, 4918–4922.
(21) Bock, M. G.; Dipardo, R. M.; Evans, B. E.; Rittle, K. E.; Whitter, W. L.; Veber, D. F.; Anderson, P. S.; Freidinger, R. M. Benzodiazepine Gastrin and Brain CCK Receptor Ligands, L365,260. *J. Med. Chem.* **1989**, *32*, 16–23.
(22) Orlowski, R. C.; Walter, R.; Winkler, D. Study of Benzhydrylamine-Type Polymers. Synthesis and Use of p-Methoxybenzhydrylamine Resin in the Solid-Phase Synthesis Preparation of Peptides. *J. Org. Chem.* **1976**, *41*, 3702–3706.
(23) Arunlakshana, O.; Schild, H. O. Some Quantitative Uses of Drug Antagonists. *Br. J. Pharmacol.* **1959**, *14*, 48–58.
(24) Felgner, P. L.; Gadek, T. R.; Holm, M.; Roman, R.; Chan, H. W.; Wenz, M.; Northrup, J. P.; Ringold, G.; Danielsen, M. Lipofection: a Highly Efficient, Lipid-Mediated DNA-Transfection Procedure. *Proc. Natl. Acad. Sci. U.S.A.* **1987**, *84*, 7413–7417.

JM940558F

Pergamon

Bioorganic & Medicinal Chemistry Letters, Vol. 4, No. 7, pp. 867-872, 1994

0960-894X/94 $6.00+0.00

0960-894X(94)E0066-N

NOVEL CHOLECYSTOKININ RECEPTOR LIGANDS: OXOPIPERAZINES DERIVED FROM BOC-CCK-4

Andrzej R Batt, David A Kendrick, Elizabeth Mathews, David P Rooker, Hamish Ryder*, Graeme Semple and Michael Szelke

Ferring Research Institute, Southampton University Research Centre, Chilworth, Southampton SO1 7NP, U.K.

Abstract: Replacement of the C-terminal dipeptide amide of Boc-CCK-4 (1) with oxopiperazines yields a series of weak CCK-receptor ligands. Further modifications result in more potent and receptor subtype selective compounds.

The rational design of novel ligands for the cholecystokinin (CCK) and gastrin receptors, based upon the C-terminal tetrapeptide fragment common to the two hormones, has received substantial attention in recent years. Boc-CCK-4 (1) has high (nM) affinity for CCK-B/gastrin receptors but weaker (µM) affinity for CCK-A receptors.[1] Simple derivatives of this potent gastrin/CCK-B agonist, such as the phenethylamide 2[2] and the aminomethylene pseudopeptide 3[3], are moderately active gastrin antagonists. Replacement of the methionine residue of Boc-CCK-4 with lysine derivatives has, on the other hand, resulted in a series of potent and selective CCK-A agonists exemplified by A-71623 (4).[1, 4, 5] Several studies have indicated that gastrin and CCK peptides adopt a turn conformation at the C-terminus,[6-8] which brings the aromatic side chains of tryptophan and phenylalanine into close proximity. The best evidence that the bioactive conformation is non-extended comes from the work of Horwell et al.,[9] who have shown that modest CCK-B receptor binding affinity was retained by the dipeptide Boc-Trp-Phe-NH_2. This lead compound has subsequently been developed to yield the potent CCK-B receptor antagonist CI-988 (5).[10, 11]

Boc-Trp-Met-Asp-Phe-NH_2 1

Boc-Trp-Leu-Asp-NH-$(CH_2)_2$Ph 2

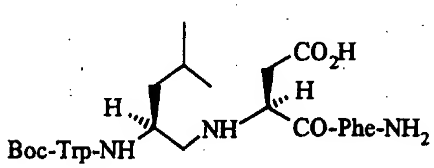

3

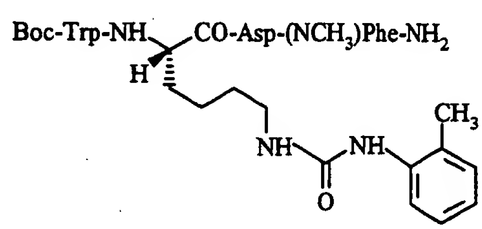

4

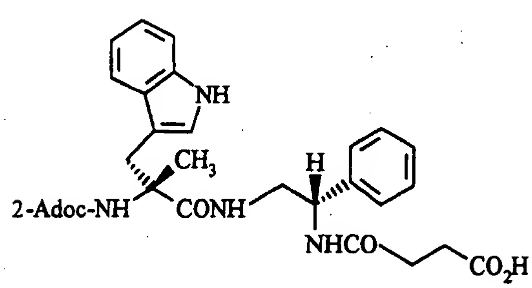

5

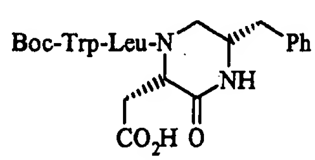

6

As part of our programme aimed at the development of non-peptidic gastrin and CCK antagonists we have introduced a series of conformational restrictions to the peptide backbone of Boc-CCK-4 analogues, with the expectation that one or more of these constrained compounds might mimic the bioactive conformation. It was found that compound **6**, obtained by replacement of the C-terminal dipeptide with an oxopiperazine moiety,[12] retained weak affinity for the CCK-B receptor and had rather stronger affinity for the CCK-A receptor. Herein we describe the manipulation of this lead to yield compounds of varying selectivity and potency for CCK-A and CCK-B receptors. The synthesis of compounds of this type was straightforward and utilised standard procedures. The synthesis of **6** (Scheme 1) is a typical example.

Scheme 1

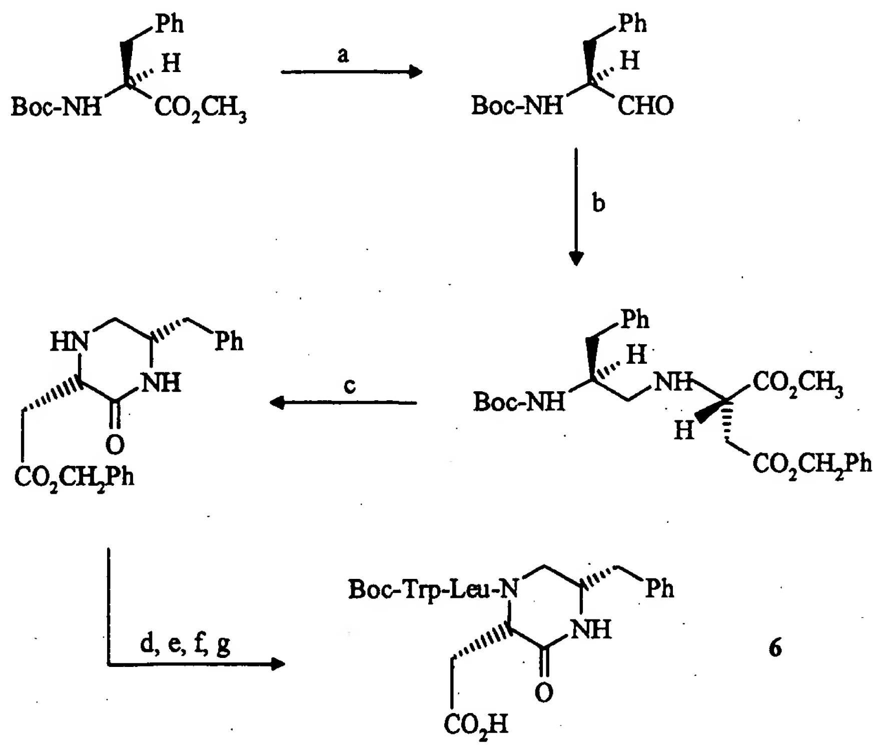

6

Reagents: (a) DIBAL, $PhCH_3$, 80% (b) $NaCNBH_3$, MeOH, AcOH, H-Asp(OBzl)OMe, 77% (c) 4M HCl, Dioxan then base work-up, 90% (d) BOP-Cl, Boc-Leu-OH, 65% (e) 4M HCl, Dioxan, 100% (f) Boc-Trp-OH, HOBt, WSCI, 82% (g) H_2, Pd/C, 90%.

A brief investigation of structure-activity relationships at the C-terminal oxopiperazine moiety of **6** revealed compounds with improved potency for both CCK-A and CCK-B receptors (Table I). Stereochemical inversion of the carboxymethyl side-chain of **6** yields an 8-fold increase in CCK-B receptor affinity (compound **7**), whereas the removal of this side-chain (**12**) results in a compound with improved CCK-A binding affinity. Inversion of the remaining side-chain gave **13**, the most potent CCK-A ligand in this series and one which displays excellent selectivity for the CCK-A over the CCK-B receptor.

Table I: Effect on CCK Receptor Binding Affinities of Substitution and Stereochemistry of Oxopiperazine

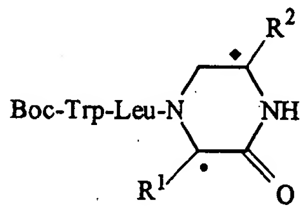

Compound	R^1	R^2	stereochemistry ●	stereochemistry ◆	IC_{50} (μM)[a] CCK-A	IC_{50} (μM)[a] CCK-B	A/B ratio
6	CH_2CO_2H	CH_2Ph	S	S	0.84 (0.824 - 0.853)	61 (49.6 - 72.4)	0.014
7	CH_2CO_2H	CH_2Ph	R	S	2.8 (2.65 - 3.03)	7.4 (6.56 - 8.39)	0.38
8	CH_2CO_2H	CH_2Ph	S	R	3.6 (3.51 - 3.61)	17 (13.2 - 21.5)	0.21
9	CH_2CO_2H	CH_2Ph	R	R	6.3 (5.36 - 7.22)	70 (53.4 - 86.9)	0.09
10	CH_2CO_2H	Ph	S	S	9.4 (9.02 - 9.86)	9.4 (7.51 - 11.3)	1.0
11	CH_2CO_2H	$(CH_2)_2Ph$	S	S	0.63 (0.425 - 0.833)	8.2 (7.35 - 9.10)	0.077
12	H	CH_2Ph	-	S	0.27 (0.262 - 0.269)	37 (31.7 - 42.5)	0.0073
13	H	CH_2Ph	-	R	0.046 (0.0445 - 0.0480)	39 (36.2 - 42.7)	0.0012

Note a: IC_{50} represents the concentration producing half-maximal inhibition of specific binding of [^{125}I] CCK-8 to CCK receptors on mouse pancreatic membranes (CCK-A) and mouse forebrain membranes (CCK-B). Figures given are the mean and range of two determinations. Binding assays were carried out according to published methods.[13]

Modification of the N-terminal dipeptide portion of **6** yields compounds with improved potency and selectivity for the CCK-B receptor (Table II). In particular, removing the steric bulk of the N-terminal blocking group (**14**, **15**) reverses receptor selectivity. Optimisation of the length of the indole linker and replacement of the leucine residue with the aminohexanoic acid residue yields compound **17** which has micromolar affinity and displays moderate selectivity for the CCK-B receptor. The receptor binding affinities of the literature[2] antagonist **2** are included for comparison.

Table II: Effect on CCK Receptor Binding Affinities of N-terminal Dipeptide Modification

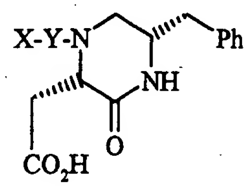

			IC_{50} (μM)[a]		
Compound	X	Y	CCK-A	CCK-B	A/B ratio
6	Boc-Trp	Leu	0.84 (0.824 - 0.853)	61 (49.6 - 72.4)	0.014
14	H-Trp	Leu	51 (51.1 - 51.7)	15 (7.05 - 22.9)	3.4
15	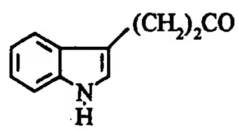	Leu	56 (53.4 - 58.9)	8.9 (7.96 - 9.85)	6.3
16	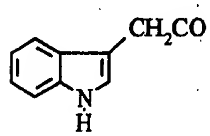	Leu	13 (12.9 - 13.9)	2.5 (1.79 - 3.27)	5.2
17	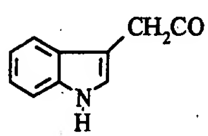	Aha	7.2 (6.76 - 7.69)	1.2 (1.19 - 1.28)	6.0
18	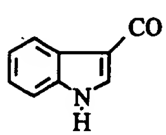	Aha	1.4 (1.17 - 1.64)	>100	-
2			3.5	0.35	10

Variation of the N-terminus of the monosubstituted series (Table III) reveals that, in contrast to CCK-B binding, CCK-A receptor affinity increases with the size of the N-terminal blocking group. Thus benzyloxycarbonyl (**20**) is more potent than *tert*-butyloxycarbonyl (**12**), which is in turn more potent than ethoxycarbonyl (**21**). Interestingly, replacement of the tryptophan residue of **12** with phenylglycine (**23**) reverses receptor selectivity. Combination of the benzyloxycarbonyl with the R-oxopiperazine yields the most potent and selective CCK-A ligand in this series (**24**).

Table III: Modification of the N-terminus of Monosubstituted Oxopiperazines

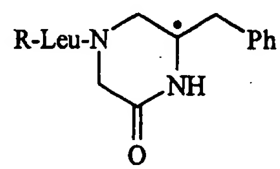

Compound	R	Stereochemistry at •	IC_{50} (μM)[a] CCK-A	CCK-B	A/B ratio
12	Boc-Trp	S	0.27 (0.262 - 0.269)	37 (31.7 - 42.5)	0.0073
19	Boc-DTrp	S	5.5 (5.35 - 5.56)	>100	-
20	$PhCH_2OCO$-Trp	S	0.064 (0.0594 - 0.0687)	18 (16.8 - 18.8)	0.0036
21	CH_3CH_2OCO-Trp	S	0.43 (0.415 - 0.450)	38 (20.2 - 56.0)	0.011
22	PhCH=CHCO-Trp	S	0.52 (0.443 - 0.597)	>100	-
23	Boc-Phg	S	24 (22.7 - 25.3)	10 (9.37 - 10.6)	2.4
13	Boc-Trp	R	0.046 (0.0445 - 0.0480)	39 (36.2 - 42.7)	0.0012
24	$PhCH_2OCO$-Trp	R	0.014 (0.0131 - 0.0146)	15 (14.9 - 15.1)	0.0009

In summary, we have shown that rational manipulation of Boc-CCK-4 can lead to both CCK-A and CCK-B selective ligands with reduced peptide character.

The more potent and selective of these ligands are currently being utilised as the leads for the development of highly potent non-peptidic CCK-A and CCK-B receptor antagonists. This work will be reported in due course.

Acknowledgement:

We thank Yamanouchi Pharmaceutical Co Ltd for their generous support of this work.

References:

1. Shiosaki, K.; Lin, C.W.; Kopecka, H.; Craig, R.; Wagenaar, F.L.; Bianchi, B.; Miller, T.; Witte, D.; Nadzan, A.M. *J. Med. Chem.* **1990**, *33*, 2950.

2. Martinez, J.; Rodriguez, M.; Bali, J.-P.; Laur, J. *Int. J. Peptide Protein Res.* **1986**, *28*, 529.

3. Martinez, J.; Bali, J.-P.; Rodriguez, M.; Castro, B.; Magous, R.; Laur, J.; Lignon, M.-F. *J. Med. Chem.* **1985**, *28*, 1874.

4. Shiosaki, K.; Lin, C.W.; Kopecka, H.; Tufano, M.D.; Bianchi, B.R.; Miller, T.R.; Witte, D.G.; Nadzan, A.M. *J. Med. Chem.* **1991**, *34*, 2837.

5. Shiosaki, K.; Lin, C.W.; Kopecka, H.; Craig, R.A.; Bianchi, B.R.; Miller, T.R.; Witte, D.G.; Stashko, M.; Nadzan, A.M. *J. Med. Chem.* **1992**, *35*, 2007.

6. Peggion, E.; Foffani, M.T. *Biopolymers* **1985**, *24*, 647.

7. Peggion, E.; Foffani, M.T.; Mammi, S. *Bio-organic Chemistry in Healthcare and Technology*, Pandit, U.K. and Alderweireldt, F.C. Eds.; Plenum Press: New York, 1991, 121.

8. Pincus, M.R.; Carty, R.P.; Chen, J.; Lubowsky, J.; Avitable, M.; Shah, D.; Scheraga, H.A.; Murphy, R.B. *Proc. Natl. Acad. Sci. USA* **1987**, *84*, 4821.

9. Horwell, D.C.; Beeby, A.; Clark, C.R.; Hughes, J. *J. Med. Chem.* **1987**, *30*, 729.

10. Horwell, D.C.; Hughes, J.; Hunter, J.C.; Pritchard, M.C.; Richardson, R.S.; Roberts, E.; Woodruff, G.N. *J. Med. Chem.* **1991**, *34*, 404.

11. Horwell, D.C. *Neuropeptides* **1991**, *19*, 57.

12. Oxopiperazines have previously been reported as structural templates in the design of CCK-B agonists. The compounds prepared (e.g. 25) use a 2,5-dioxopiperazine to restrict the conformational freedom of the N-terminal tryptophan of CCK-4. See: Shiosaki, K.; Craig, R.; Lin, C.W.; Barrett, R.W.; Miller, T.; Witte, D.; Wolfram, C.A.W.; Nadzan, A.M. in "Peptides: Chemistry, Structure and Biology", ESCOM, Leiden, 1990, p. 978.

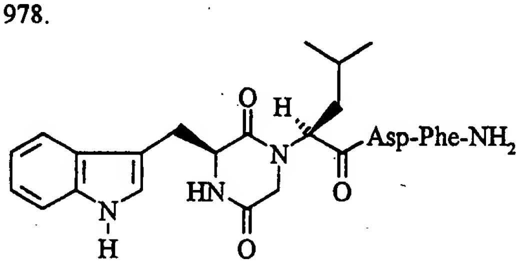

25

13. Wennogle, L.P.; Steel, D.J.; Petrack, B. *Life Sciences* **1985**, *36*, 1485.

(*Received in Belgium* 2 *December* 1993; *accepted* 15 *February* 1994)

Peptide Chemistry 1993: Y.Okada(Ed.)
Protein Research Foundation, Osaka (1994)

Structure–Function Relationship of Heat–Stable Enterotoxin (ST)
–Steric Requirements at Position 12 for Receptor Binding–

Takehiro Okumura, Takashi Sato, Hiroshi Ozaki, Akihiro Wada, Yuji Hidaka, Jun Okuda#, Yoshifumi Takeda#, and Yasutsugu Shimonishi

Institute for Protein Research, Osaka University, Yamadaoka 3–2, Suita, Osaka 565
#Faculty of Medicine, Kyoto University, Yoshida–Konoe, Sakyo–ku, Kyoto 606

Introduction

It is well known that some of enteric bacteria produce a heat–stable enterotoxin (ST) which causes acute diarrheal symptom [1]. This physiological response is followed by the binding of ST to its receptor protein on the intestinal epithelial cells. STs characterized so far share a highly conserved sequence which consists of thirteen amino acid residues with three intramolecular disulfide linkages. The tridecapeptide has a comparable toxicity to the native toxin and forms "toxic domain" of ST [2, 3], in which –Asn–Pro–Ala– located in the central region is completely conserved in ST family members (Fig. 1).

The molecular structure of [Mpr^5]STp(5–17) corresponding to a toxic domain of STp, which is produced by a pathogenic strain of *Eschrichia coli*, was determined by x–ray analysis [6]. The results suggested that three amino acid residues, Asn^{11}, Pro^{12}, and Ala^{13}, are involved in the receptor binding [6, 7]. Furthermore, we demonstrated that the substitution for Ala^{13} by Leu or

Toxic domain

STh Asn–Ser–Ser–Asn–Tyr–Cys–Cys–Glu–Leu–Cys–Cys–***Asn–Pro–Ala***–Cys–Thr–Gly–Cys–Tyr

STp Asn–Thr–Phe–Tyr–Cys–Cys–Glu–Leu–Cys–Cys–***Asn–Pro–Ala***–Cys–Ala–Gly–Cys–Tyr

[Mpr^5]STp(5–17) Mpr–Cys–Glu–Leu–Cys–Cys–***Asn–Pro–Ala***–Cys–Ala–Gly–Cys

Mpr: 3–mercaptopropionic acid

Fig. 1. *Primary Structures of ST and ST Analog; STh in ref. 4 and STp in ref. 5.*

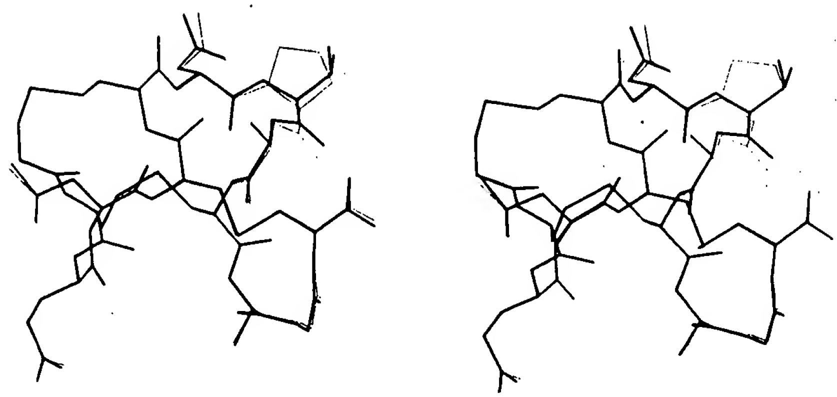

Fig. 2. *Stereo-diagram of the molecule of [Mpr^5,Val^{12}]STp(5-17) (thick line) and [Mpr^5]STp(5-17) (thin line). The former molecule was superimposed on the latter by least-squares fitting of 52 main-chain atoms.*

Gly greatly decreased the enterotoxicity and binding ability though the molecular structures of the analogs were scarcely affected by the substitutions [8, 9]. These findings suggest that the specific receptor for ST sharply recognizes the bulkiness of the side-chain at position 13.

To elucidate the mechanism of molecular recognition of ST by its receptor protein, we examined the effect of substitutions for Pro^{12} by aliphatic amino acids with different shapes on the receptor binding abilities and the molecular structure of one of these analogs by x-ray crystallography. Here, we report the structure-function relationship of ST and discuss the steric requirements of amino acid at position 12 for the receptor binding based on the molecular structure determined by x-ray analysis.

Results and Discussion

Design for ST Analogs : For estimating the contributions of methylenes of the Pro^{12} side-chain to the receptor binding, four ST analogs, [Mpr^5]STp(5-17), [Mpr^5,Val^{12}]STp(5-17), [Mpr^5,Ala^{12}]STp(5-17), [Mpr^5,Gly^{12}]STp(5-17), were synthesized by the solid-phase method with Boc-strategy. In addition to these, [Mpr^5,Ile^{12}]STp(5-17) was prepared to examine the effect of opening the Pro-pyrrolidine ring and of adding the branched γ-methyl group of substituted Val residue.

X-ray Analysis : In the analogs substituted for Pro^{12}, [Mpr^5,Val^{12}]STp(5-17) gave a suitable crystal for high-resolution x-ray analysis by macro seeding method. The molecular structure was solved at 0.91 Å resolution as previously described [6], and refined to a final R value of 0.094 for 4897 reflections. The refined structure had an enough quality to discuss the conformation of the side-chain as well as the main-chain. This structure was compared with that of [Mpr^5]STp(5-17) which was analyzed at 0.89 Å resolution [6]. Figure 2 shows the superposition of [Mpr^5,Val^{12}]STp(5-17) on [Mpr^5]STp(5-17). The main-chain and side-chain conformation of [Mpr^5,Val^{12}]STp(5-17) was almost identical with that of [Mpr^5]STp(5-17) and the rms distance value between 52 main-chain atoms was 0.15 Å (Fig. 2). This result suggests that the conformations of ST analogs examined here would be little affected by the substitutions at position 12. This consideration is compatible with our previous observation that the substitutions of Ala^{13} had little effect on the conformation of ST [8].

Tablel 1. *Biological Properties of ST Analogs*

Analogs	Receptor Binding Ability		Enterotoxicity	
	Ki (M)[a]	RA[b]	MED (pmol)[c]	RE[d]
$[Mpr^5]STp(5-17)$	$(3.4 \pm 0.3) \times 10^{-8}$	1.0	1.0	1.0
$[Mpr^5,Ile^{12}]STp(5-17)$	$(3.7 \pm 0.3) \times 10^{-8}$	0.92	1.1	0.91
$[Mpr^5,Val^{12}]STp(5-17)$	$(5.7 \pm 0.3) \times 10^{-8}$	0.60	2.0	0.50
$[Mpr^5,Ala^{12}]STp(5-17)$	$(1.1 \pm 0.3) \times 10^{-7}$	0.31	4.1	0.24
$[Mpr^5,Gly^{12}]STp(5-17)$	$(1.8 \pm 0.3) \times 10^{-6}$	0.019	33	0.030

[a] Values denote inhibition constant (*Ki*) with its standard deviation calculated from equilibrium binding data (n = 3) by the computer program "LIGAND". [b] RA: Relative binding affinity. [c] MED: Minimum effective dose. [d] RE: Relative enterotoxicity

Receptor Binding Assay : Five ST analogs were assayed for their enterotoxicities in suckling mice and for their binding abilities to rat intestinal membrane. All analogs bound to the receptor in a dose-dependent fashion and displaced $[^{125}I\text{-}Tyr^4]STh(5-18)$ completely. The inhibition constant (*Ki*) values of these analogs were calculated using a nonlinear least-squares curve fitting method [10] (Table 1). The difference in enterotoxicities among five ST analogs reflected the difference in their binding abilities, which decreased as the loss of the methylenes of the side-chain at position 12. From the evidence that substitution of Pro^{12} had little effect on the molecular structure of ST, it is considered that the difference in the binding ability is only attributed to the difference in the shape of the aliphatic side-chain at position 12.

Structure-Function Relationship : $[Mpr^5,Ile^{12}]STp(5-17)$ showed the same *Ki* value as $[Mpr^5]STp(5-17)$ within its experimental error. This indicates that the effects of opening the pyrrolidine ring and of adding the branched γ-methyl group on the receptor binding ability canceled each other. Therefore, the apparent contribution of β-, γ-, and δ-methylenes of the Pro^{12} side-chain to the receptor binding could be estimated by comparing the binding abilities of $[Mpr^5,Gly^{12}]STp(5-17)$, $[Mpr^5,Ala^{12}]STp(5-17)$, $[Mpr^5,Val^{12}]STp(5-17)$, and $[Mpr^5]STp(5-17)$. The contribution of the whole side-chain of Pro^{12} to the apparent binding energy of ST and its receptor protein was estimated to be approximately 2.4 kcal mol^{-1} calculated from the *Ki* values of $[Mpr^5]STp(5-17)$ and $[Mpr^5,Gly^{12}]STp(5-17)$ [11]. Similarly, those of β-, γ-, and δ-methylenes were estimated to be approximately 1.7, 0.4, and 0.3 kcal mol^{-1} from the *Ki* values of $[Mpr^5,Ala^{12}]STp(5-17)$ and $[Mpr^5,Gly^{12}]STp(5-17)$, $[Mpr^5,Val^{12}]STp(5-17)$ and $[Mpr^5,Ala^{12}]STp(5-17)$, and $[Mpr^5]STp(5-17)$ and $[Mpr^5,Val^{12}]STp(5-17)$, respectively. The contribution of the β-methylene to the apparent binding energy is about 70% of that of the whole side-chain of Pro^{12}, suggesting that the β-methylene plays an important role for the receptor binding. This result is compatible with the fact that the β-methyl group of Ala^{13} which is adjacent to the β-methylene of Pro^{12} in the tertiary structure of the ST molecule is also important for the receptor binding [8, 9]. Therefore, it is considered that a site formed by the β-methylene of Pro^{12} and the β-methyl of Ala^{13} binds to the ST receptor protein and a site formed by γ- and δ-methylenes of Pro^{12} is not so closely involved in the binding as β-methylene of Pro^{12}.

Conclusion

The x-ray analysis of [Mpr^5,Val^{12}]STp(5–17) demonstrated that its molecular structure is almost identical with that of [Mpr^5]STp(5–17) and suggested that the molecular structures of three ST analogs, [Mpr^5,Ile^{12}]STp(5–17), [Mpr^5,Ala^{12}]STp(5–17), and [Mpr^5,Gly^{12}]STp(5–17), are the same as that of [Mpr^5]STp(5–17). Based on the results from x-ray analysis and receptor binding assay, we estimated that the β-methylene of Pro^{12} takes 70% of the side-chain contribution of Pro^{12} to the apparent binding energy and that the shares of γ- and δ-methylenes are 20 and 10%, respectively. The results take us consider that ST receptor protein binds to a site formed by the β-methylene of Pro^{12} and the β-methyl group of Ala^{13} and provide a molecular basis for the interaction between ST and its receptor protein.

Acknowledgments

This work is supported in part by the Yamada Science Foundation. We wish to thank Prof. Yukiteru Katsube of the Institute for Protein Research, Osaka University for facilitating the use of x-ray diffraction apparatus. Use of the facility at the Radioisotope Research Center of Osaka University is acknowledged.

References

1. H. W. Smith and C. L. Gyles, *J. Med. Microbiol.*, **3**, 387–401 (1970).
2. S. Aimoto, T. Takao, Y. Shimonishi, S. Hara, T. Takeda and T. Miwatani, *Eur. J. Biochem.*, **129**, 257–263 (1982).
3. S. Yoshimura, H. Ikemura, H. Watanabe, S. Aimoto, Y. Shimonishi, S. Hara, T. Takeda, T. Miwatani and Y. Takeda, *FEBS Lett.*, **181**, 138–142 (1985).
4. S. Aimoto, T. Takao, Y. Shimonishi, S. Hara, T. Takeda and T. Miwatani, *Eur. J. Biochem.*, **129**, 257–263 (1982).
5. T. Takao, T. Hitouji, S. Aimoto, Y. Shimonishi, S. Hara, T. Takeda, Y. Takeda and T. Miwatani, *FEBS Lett.*, **152**, 1-5 (1983).
6. H. Ozaki, T. Sato, H. Kubota, Y. Hata, Y. Katsube and Y. Shimonishi, *J. Biol. Chem.*, **226**, 5934-5941 (1991).
7. Y. Takeda, S. Yamasaki, T. Hirayama and Y. Shimonishi, In "*Molecular Pathogenesis of Gastrointestinal Infections*", eds. T. Wadstrom *et al.*, (Plenum Press, New York) pp.125–138 (1991).
8. T. Sato, H. Ozaki, Y. Kitagawa, Y. Hata, Y. Katsube and Y. Shimonishi, In "*Peptide Chemistry 1991*", ed. A. Suzuki, (Protein Research Foundation, Osaka) pp.93–98 (1992).
9. A. Wada, T. Hirayama, J. Fujisawa, Y. Hidaka and Y. Shimonishi, In "*Peptide Chemistry 1992*", ed. N. Yanaihara, (ESCOM, Leiden) pp.350–352 (1993).
10. P. J. Munson and D. Rodbard, *Anal. Biochem.*, **107**, 220–239 (1980).
11. The procedure will be reported elsewhere entitled "Probing the side-chain contribution to peptide-protein interaction" by T. Sato, T. Okumura and Y. Shimonishi.

Available online at www.sciencedirect.com

SCIENCE DIRECT®

Tetrahedron Letters 45 (2004) 3117–3121

Tetrahedron Letters

ELSEVIER

Pyridine-based receptors with high affinity for carbohydrates. Influence of the degree of steric hindrance at pyridine nitrogen on the binding mode

Monika Mazik[a,*] and Willi Sicking[b]

[a]*Institut für Organische Chemie der Technischen Universität Braunschweig, Hagenring 30, 38106 Braunschweig, Germany*

[b]*Institut für Organische Chemie der Universität Duisburg-Essen, Universitätsstraße 5, 45117 Essen, Germany*

Received 4 February 2004; revised 16 February 2004; accepted 17 February 2004

Abstract—Remarkable changes in the binding affinity and selectivity of pyridine-based receptors toward monosaccharides have been observed when the degree of steric hindrance at pyridine nitrogen atom decreases.

The molecular recognition of carbohydrates by synthetic receptors forms an area of high current interest, arising from the extreme importance of sugar molecules within biological systems. Carbohydrates actively control a whole range of biological processes including cell growth and differentiation. A range of carbohydrate binding proteins mediate the interactions of cells with their environment, primarily via interactions with the carbohydrates on the surfaces of cell.[1] Thus, the carbohydrates play fundamental roles in cell–cell recognition and other interactions processes. The protein–carbohydrate interactions involve the hydrogen bonding, metal coordination, van der Waals forces, and hydrophobic interactions.[1,2] These interactions have inspired the development of a number of different artificial receptor structures for the recognition of carbohydrates.[3] Particularly, many representatives of hydrogen bonding receptors have been obtained and studied.[4,5] However, the selective and effective molecular recognition of carbohydrates by a synthetic receptor is still a challenging goal in artificial receptor chemistry.

In this paper we describe the remarkable changes in the affinity as well as selectivity of pyridine-based receptors when the degree of steric hindrance at pyridine nitrogen atom decreases. The acyclic receptors **1** and **2**,[6] compared to the previously reported receptor **3**,[5b] reflect the change from α,α- to the α,β- or α,γ-disubstituted pyridine groups. The presence of an unsubstituted α-position in the pyridine ring is a typical feature of the receptors **1** and **2**. Consequently, the pyridine units are sterically less hindered at nitrogen and can be involved much easier and effective in the binding interactions. These receptors contain neighboring acceptor/donor groups (pyridine-N/amide-NH), which are able to participate in cooperative hydrogen bonds with the sugar hydroxyls. As shown by our earlier studies, the property of cooperativity is of particular importance in the area of synthetic carbohydrate receptors.[4i,5] Although, the structural variation of the receptor structure is minimal, the binding properties of the new receptors change dramatically.

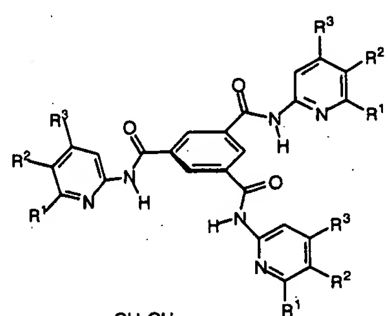

1: $R^1 = R^2 = H$, $R^3 = CH_3$
2: $R^1 = R^3 = H$, $R^2 = CH_3$
3: $R^1 = CH_3$, $R^2 = R^3 = H$

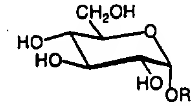

4: $R = C_8H_{17}$, **4a**: $R = CH_3$

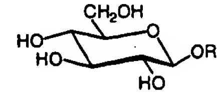

5 : $R = C_8H_{17}$

Keywords: Molecular recognition; Carbohydrate receptors; Hydrogen bonding.

* Corresponding author. Tel.: +49-531-391-5266; fax: +49-531-391-8185; e-mail: m.mazik@tu-bs.de

0040-4039/$ - see front matter © 2004 Elsevier Ltd. All rights reserved.
doi:10.1016/j.tetlet.2004.02.087

The evidence for the particularly strong complexation of monosaccharides with the receptors **1** and **2** was obtained by the NMR spectroscopy and extraction experiments. The crystal structures of the receptors **1** and **2** are shown in Figure 1.

All ^{1}H NMR titration experiments were carried out in the concentration range, in which the receptors do not self-aggregate ([**1**] or [**2**] < 0.0015 mol/L). The concentration range was estimated on the basis of a series of dilution experiments. The ^{1}H NMR titrations show that the addition of only 0.5 equiv of α-glucopyranoside **4** leads to practically complete complexation of host **1**. The signal due to amide NH of **1** shifted downfield by 1.10 ppm and the aromatic phenyl proton peak moved upfield by 0.40 ppm. Both the stoichiometry observed by fitting the binding isotherm and the molar ratio plots verify that host **1** forms 2:1 receptor:sugar complexes with α-glucopyranoside. A clear break in the molar ratio plot indicates that the formation of a complex with high stability constant is taking place.[8] Additionally, receptor **1** is able to extract 0.5 equiv of methyl-α-D-glucopyranoside (**4a**) from the solid state into a $CDCl_3$ solution.

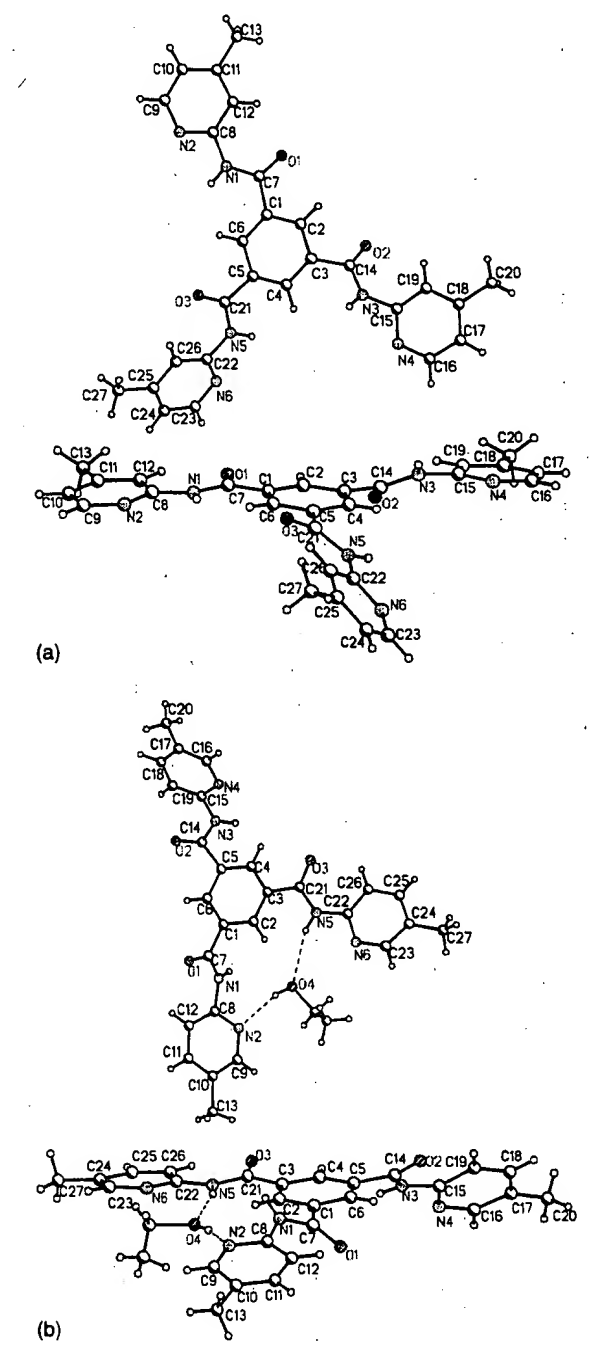

Figure 1. Crystal structure of **1** (a) and **2** (b),[7] top and side views.

The binding affinity toward α-glucopyranosides **4–4a** obtained with receptor **1** is comparable to that obtained with the host **2**. The complexation between **4** and receptor **2** is again evidenced by several changes in the ^{1}H NMR spectra, particularly by the significant downfield shifts of the receptor amide protons ($\Delta\delta_{max} = 1.10$ ppm) and upfield shifted resonances for the aromatic phenyl protons of **2** ($\Delta\delta_{max} = 0.37$ ppm), as shown in Figure 2a. After 0.5 equiv of octyl α-D-glucopyranoside (**4**) had been added, almost no change was observed in the NMR spectra.

The plot of the observed and calculated downfield chemical shifts of the NH resonances of **2** as a function of added sugar **4** is illustrated in Figure 3a.[9] The graph rises linearly with increasing the sugar concentration until $\Delta\delta_{max}$ is reached at 1:0.5 receptor:sugar stoichiometry. In the first part of the titration curve the receptor is the excess component and sugar the minor component, thus the 1:1 complex is formed followed by the immediate formation of a strong 2:1 receptor–sugar complex.

The data from titrations of **1** or **2** versus α-glucopyranoside **4** suggested a very large value of the overall formation constants and were impossible to follow for precisely binding constant calculations. In order to determine the binding constants, additional inverse titrations were carried out in which the concentration of glycoside **4** was held constant and that of receptor **1** or **2** varied. In these titrations, the motion of the signal due to anomeric CH proton of **4**, which is shifted significantly downfield, was monitored. The typical titration curves are shown in Figure 3c and d. In the first part of the titration curves, the sugar is now the excess component and the receptor the minor component. The anomeric CH proton exhibits chemical shift changes of 0.55 and 0.50 ppm ($\Delta\delta_{max}$) during complexation with **1** and **2** (Fig. 2c), respectively. These shifts are significantly larger in comparison to those reported usually for the anomeric CH in the literature (mostly $\Delta\delta_{max} = 0.05$–0.15 ppm), indicating an important contribution of this unit to the stability of the complexes **4·1** and **4·2**. On the basis of the inverse titrations the binding constants of **4** and receptor **1** were found to be 3640 (K_{a1}) and 82,450 M^{-1} (K_{a2}), while the binding constants for **4·2** amount to 2100 (K_{a1}) and 47,600 M^{-1} (K_{a2}).[9] The stronger binding of **1** in comparison to **2** can be attributed both to the different basicity of the pyridine recognition units (the increase in pK_a is somewhat greater for γ- than for β-methyl substituted pyridine[10]) and to

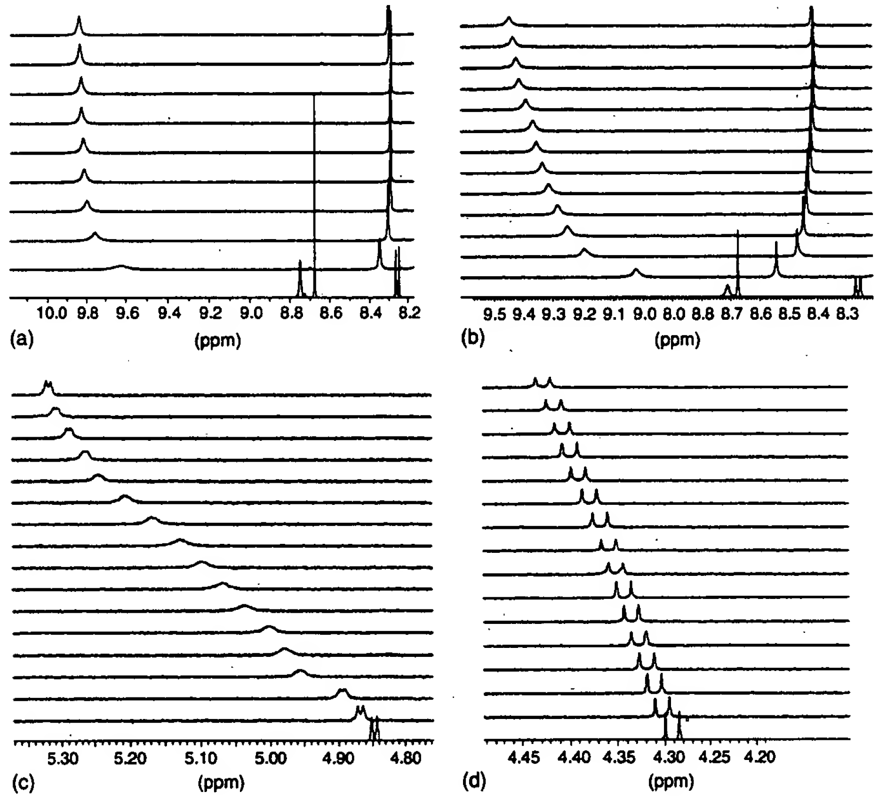

Figure 2. (a) ^{1}H NMR spectra ($CDCl_3$, 25 °C) of receptor **2** (the shifts of the NH and CH_{Ph} resonances are shown) after addition of (from bottom to top) 0.00, 0.39, 0.59, 0.80, 0.99, 1.19, 1.40, 1.59, 1.99, and 2.39 equiv of α-glucopyranoside **4** ([**2**]=1.33 mM). (b) ^{1}H NMR spectra of receptor **2** (the shifts of the NH and CH_{Ph} resonances are shown) after addition of 0.00, 0.25, 0.50, 0.63, 0.75, 0.88, 1.00, 1.13, 1.26, 1.51, 1.76, 2.00, 2.26, and 2.52 equiv of **5** ([**2**]=1.03 mM). (c) The downfield chemical shifts of the anomeric CH resonances of α-anomer **4** during the titration with receptor **2** ([**4**]=0.61 mM, [**2**]=0.10–2.50 mM). (d) The downfield chemical shifts of the anomeric CH resonances of β-anomer **5** during the titration with receptor **2** ([**5**]=0.61 mM, [**2**]=0.10–2.50 mM).

the different sterical effects. The 2:1 receptor:sugar binding mode is also supported by molecular modeling. A possible strutcture of the 2:1 and 1:1 complexes of **2** and **4** is shown in Figure 4.

In contrast to α-anomer **4**, the β-anomer **5** showed lower affinity to **1** and **2**. The ^{1}H NMR titration of **1** or **2** versus **5** also produced several spectral changes (Fig. 2b). The largest complexation-induced shifts were observed for the NH-signal (downfield shift of 0.85 and 0.80 ppm for **1** and **2**, respectively,) and for the phenyl CH-signal of the receptors (upfield shift of 0.35 ppm for **1** and 0.30 ppm for **2**). Comparison of Figure 3a and b clearly shows that the process of complexation is not reflected by these chemical shifts upon binding with α- or β-anomer in the same way. Whereas after the addition of 0.5 equiv of α-anomer almost no change was observed in the chemical shift of receptor signals, with the β-anomer chemical shift changes continue to higher receptor:sugar ratios. Nevertheless, for all systems the stoichiometry observed by fitting the binding isotherm is in agreement with that determined by the ratio method, which indicates the formation of 1:2 sugar:receptor complexes. The best fit of the titration data was obtained again with the 'mixed' 1:1 and 2:1 receptor:sugar binding models. The association constants of 660 (K_{a1}) and 24,200 M^{-1} (K_{a2}) were determined for **5·1** (Table 1), whereas the binding constants for **5·2** amount to 440 (K_{a1}) and 22,600 M^{-1} (K_{a2}). The association constants obtained from these experiments (typical titration curve is shown in Fig. 3e) are identical within the limits of uncertainty to those determined from titrations where the role of host and guest **5** was reversed. As shown in Figure 2d, the peak for the anomeric CH proton of **5** is affected significant weakly by complexation (0.18 and 0.15 ppm by complexation with **1** and **2**, respectively) than that of **4** (Fig. 2c), indicating a weaker binding again.

Notably, the observed α/β-anomer selectivities of **1** and **2** differ from those observed for the hydrogen-bonding host molecules described so far, which usually show higher affinity toward β-anomer. This preference has been ascribed to the hydrogen-bonding abilities of sugar hydroxyl groups. As discussed in Refs. 4f and 11 the axial 1-alkoxy group in α-anomer can form intramolecular hydrogen bonds with 2-OH group more easily than equatorial 1-alkoxy substituent in β-anomer can do. In this context, the 2-OH in β-glucopyranoside **5** is relatively free from intramolecular hydrogen bonding and can interact with receptor molecules more strongly. The strong binding of **4** with **1** or **2** indicates that the intermolecular host–guest H-bonding compete effectively with the intramolecular H-bonding network in

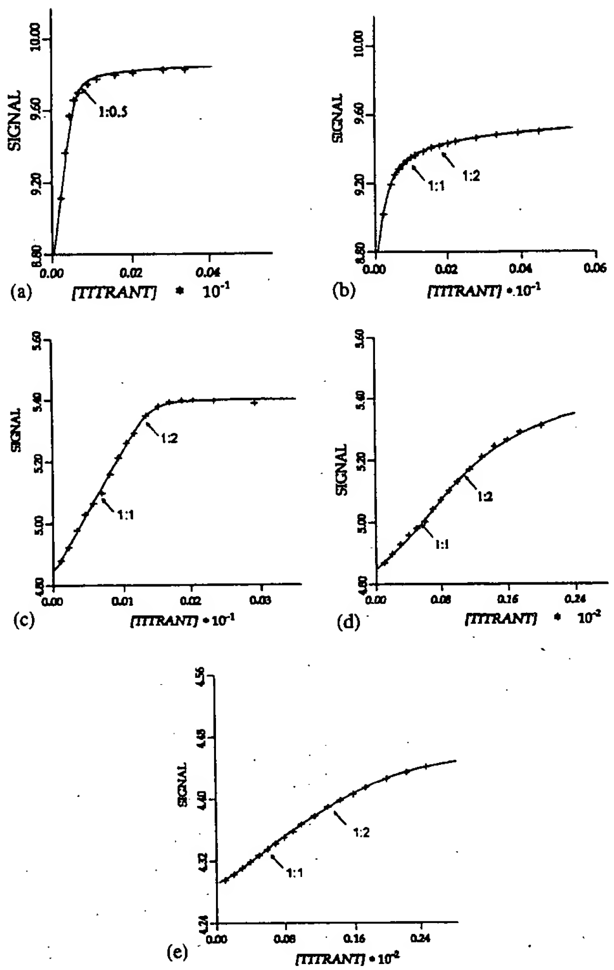

Figure 3. Plot of the observed (×) and calculated (—) downfield chemical shifts of the NH resonances of **2** as a function of added α-glucopyranoside **4** (a) or β-glucopyranoside **5** (b). The [receptor]/[sugar] ratio is marked (a–b). Plot of the downfield chemical shifts of the anomeric CH resonances of sugar **4** as a function of added **1** (c) or **2** (d), respectively. Plot of the downfield chemical shifts of the anomeric CH resonances of sugar **5** as a function of added **2** (e). The [sugar]/[receptor] ratio is marked (c–e).

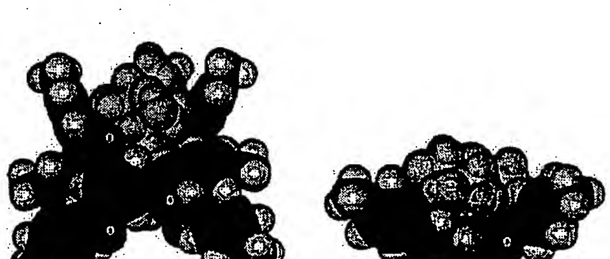

Figure 4. Energy-minimized structure of the 2:1 (left) and 1:1 (right) complexes formed between receptor **2** and glucopyranoside **4** (MacroModel V.6.5, Amber* force field, Monte Carlo conformational searches, 50,000 steps).

carbohydrates. The intramolecular bond is replaced by enough intermolecular H-bonds during the binding process. Molecular modeling studies suggest the existence of hydrogen bonds between OHs of **4** and the amide-NH/pyridine-N of **1** or **2**, including cooperative hydrogen bonds (OH···N-pyr, HO···HN-amide), in which the hydroxyl group acts simultaneously as a hydrogen bond donor and acceptor. The hydrogen bonds are supplemented by interactions of sugar CH moieties with the phenyl and pyridine groups of the receptors. Both sides of the pyranoside ring (α- and β-face) are involved in the stacking interactions with aromatic residues of the two receptor molecules in 2:1 receptor:sugar complexes. Furthermore the complex of **4** is also stabilized by weak CH···N-pyr and CH···O=C hydrogen bonds. These intermolecular interactions were also evidenced by the observed changes of chemical shifts in the NMR spectra of the complexes. In comparison with **4**, the CHs of sugar **5** participate in less intermolecular interactions (as indicated by molecular modeling, **5** is less favorable positioned in the cavity between the two receptors). The 2:1 receptor:sugar complexes display also hydrogen bonding between the two receptor molecules (two amide-NH···N-pyr hydrogen bonds).

Table 1. Association constants K_a[a] (M^{-1}) and corresponding free energy changes ΔG° ($kJ\,mol^{-1}$) for receptors **1–2** and glucopyranosides **4–5**

Host–guest complex	K_{a1} (ΔG°)	K_{a2}[b] (ΔG°)	$\Delta\delta_{max}$ (ppm)
1·4	3640 (−20.3)	82,450 (−28.0)	0.55[c]/1.10[d]
2·4	2100 (−18.9)	47,600 (−26.7)	0.50[c]/1.10[d]
1·5	660 (−16.1)	24,200 (−25.0)	0.18[c]/0.85[d]
2·5	440 (−15.1)	22,600 (−24.8)	0.15[c]/0.80[d]

[a] Average K_a values from multiple titrations ($CDCl_3$, stored over activated molecular sieves and deacidified with Al_2O_3), values provided by HOSTEST.[9] The reproducibility of the K_a values was ±10–15%. Uncertainty in a single K_a estimation was ±2–10%. Dilution experiments show that receptors do not self-aggregate in the used concentration range.

[b] 2:1 Receptor:sugar complex.

[c] Complexation-induced shifts observed for the anomeric CH of sugar (titrations of sugar vs receptor, inverse titrations).

[d] Complexation-induced shifts observed for the NH of receptor (titrations of receptor vs sugar).

In contrast to receptors **1** and **2**, receptor **3**, in which both pyridine α-positions are blocked, shows significantly lower affinity to both anomers and the formation of 1:1 complexes. The binding constant for α-anomer **4** and receptor **3** was found to be $4000\,M^{-1}$, the one for β-anomer **5** and host **3** amounts to $8700\,M^{-1}$.[5] Thus, the binding properties of the new receptors **1** and **2** apparently indicate that the steric interactions involving the pyridine substituents significantly affect the binding properties. These results reflect clearly the great importance of hydrogen-bonding interactions with the pyridine nitrogen atom for the binding affinity of the receptors. According to molecular modeling the steric effects from the α-position of the pyridine rings of **3** hinder the formation of intermolecular interactions, which are typical for 2:1 receptor:sugar complexes between **1/2** and glucopyranosides. The decreased degree of steric hindrance at the pyridine nitrogen allows for

the development of much stronger host:guest hydrogen-bonding interactions in the complexes. This knowledge may also enable the design of further hydrogen-bonding receptors, which may lead to the development of new chemosensors. Structures of type **1** or **2** can be incorporated into more sophisticated architectures to create a range of receptors, which should be able to form energetically favorable 1:1 complexes with sugar derivatives. Studies to synthesis of new receptors of this type are in progress.

Acknowledgements

This work was supported by the Deutsche Forschungsgemeinschaft (SFB 452). We thank Prof. Roland Boese and Dieter Bläser for performing the X-ray measurements, and Prof. Craig Wilcox for giving access to the HOSTEST program.

References and notes

1. (a) Osborn, H.; Khan, T. *Oligosaccharides. Their synthesis and biological roles*; Oxford, University Press: New York, 2000; (b) Lis, H.; Sharon, N. *Chem. Rev.* **1998**, *98*, 637–674.
2. (a) Weiss, W. I.; Drickamer, K. *Ann. Rev. Biochem.* **1996**, *65*, 441; (b) Quiocho, F. A. *Pure. Appl. Chem.* **1989**, *61*, 1293–1306; (c) Lemieux, R. U. *Chem. Soc. Rev.* **1989**, *18*, 347–374.
3. (a) Davis, A. P.; Wareham, R. S. *Angew. Chem., Int. Ed.* **1999**, *38*, 2978–2996; (b) Hartley, J. H.; James, T. D.; Ward, C. J. *J. Chem. Soc., Perkin Trans. 1* **2000**, 3155–3184; (c) For a recent review on boronic acid based receptors, see: James, T. D.; Shinkai, S. *Top. Curr. Chem.* **2002**, *218*, 159–200.
4. Some recent examples: (a) Welti, R.; Abel, Y.; Gramlich, V.; Diederich, F. *Helv. Chim. Acta* **2003**, *86*, 548–562; (b) Welti, R.; Diederich, F. *Helv. Chim. Acta* **2003**, *86*, 494–503; (c) Dukh, M.; Saman, D.; Lang, K.; Pouzar, V.; Cerny, I.; Drasar, P.; Kral, V. *Org. Biomol. Chem.* **2003**, *1*, 3458–3463; (d) Ishi-I, T.; Mateos-Timoneda, M. A.; Timmerman, P.; Crego-Calama, M.; Reinhoudt, D. N.; Shinkai, S. *Angew. Chem., Int. Ed.* **2003**, *42*, 2300–2305; (e) Lecollinet, G.; Dominey, A. P.; Velasco, T.; Davis, A. P. *Angew. Chem., Int. Ed.* **2002**, *41*, 4093–4096; (f) Tamaru, S.; Shinkai, S.; Khasanov, A. B.; Bell, T. W. *Proc. Natl. Acad. Sci. U.S.A.* **2002**, *99*, 4972–4976; (g) Ladomenou, K.; Bonar-Law, R. P. *Chem. Commun.* **2002**, 2108–2109; (h) Liao, J.-H.; Chen, C.-T.; Chou, H.-C.; Cheng, C.-C.; Chou, P.-T.; Fang, J.-M.; Slanina, Z.; Chow, T. J. *Org. Lett.* **2002**, *4*, 3107–3110; (i) Mazik, M.; Radunz, W.; Sicking, W. *Org. Lett.* **2002**, *4*, 4579–4582, and references cited therein.
5. (a) Mazik, M.; Sicking, W. *Chem. Eur. J.* **2001**, *7*, 664–670; (b) Mazik, M.; Bandmann, H.; Sicking, W. *Angew. Chem., Int. Ed.* **2000**, *39*, 551–554.
6. Compounds **1** and **2** were synthesized from benzene-1,3,5-tricarbonyl chloride and 2-amino-4-methyl-pyridine or 2-amino-5-methyl-pyridine, respectively (CH_2Cl_2 or THF, NEt_3, room temperature). *N,N′,N″*-Tris-(4-methylpyridin-2-yl)benzene-1,3,5-tricarbonamide (**1**): ^1H NMR ($CDCl_3$): $\delta = 2.40$ (s, 9H, $3\times CH_3$), 6.93 (d, $3H_{pyr}$, $J = 5.2$ Hz), 8.17 (d, $3H_{pyr}$, $J = 5.2$ Hz), 8.20 (s, $3H_{pyr}$), 8.68 (s, $3H_{Ph}$), 8.82 (s, 3H, $3\times NH$). ^{13}C NMR ($CDCl_3$): $\delta = 21.35$, 114.98, 121.51, 129.38, 135.70, 147.58, 150.07, 151.27, 163.94. HR-MS, calcd for $C_{27}H_{24}N_6O_3$: 480.1910. Found: 480.1903. *N,N′,N″*-Tris-(5-methyl-pyridin-2-yl)benzene-1,3,5-tricarbon-amide (**2**): ^1H NMR (200, $CDCl_3$): $\delta = 2.32$ (s, 9H, $3\times CH_3$), 7.58 (dd, $3H_{pyr}$, $J = 8.6/2.20$ Hz), 8.13 (d, $3H_{pyr}$, $J = 2.2$ Hz), 8.25 (d, $3H_{pyr}$, $J = 8.6$ Hz), 8.67 (s, $3H_{Ph}$), 8.73 (s, 3H, $3\times NH$). ^{13}C NMR ($CDCl_3$): $\delta = 17.87$, 113.84, 129.17, 129.83, 135.73, 139.07, 147.96, 148.97, 163.38. HR-MS, calcd for $C_{27}H_{24}N_6O_3$: 480.1910. Found: 480.1907.
7. Crystals of **1** were obtained from THF/heptane solution, crystals of **2** from ethanol solution (one hydrogen-bonded ethanol molecule is shown). Crystallographic data for the structures reported in this paper have been deposited with the Cambridge Crystallographic Data Centre as supplementary publication no CCDC-229363 (**1**) and 229364 (**2**).
8. (a) Schneider, H.-J.; Yatsimirsky, A. *Principles and Methods in Supramolecular Chemistry*; John Wiley & Sons: Chichester, 2000, p 148; (b) Tsukube, H.; Furuta, H.; Odani, A.; Takeda, Y.; Kudo, Y.; Inoue, Y.; Liu, Y.; Sakamoto, H.; Kimura, K. In *Comprehensive Supramolecular Chemistry*; Atwood, J. L., Davis, J. E. D., MacNicol, D. D., Vögtle, F., Eds.; Pergamon: Oxford, UK, 1996; Vol. 8, p 425.
9. Wilcox, C. S.; Glagovich, N. M. Program HOSTEST 5.6, University of Pittsburgh.
10. Katritzky, A. R.; Pozharski, A. F. *Handbook of Heterocyclic Chemistry*; Pergamon: Amsterdam, The Netherlands, 2000; p 178.
11. (a) Cuntze, J.; Owens, L.; Alcazar, V.; Seiler, P.; Diederich, F. *Helv. Chim. Acta* **1995**, *78*, 367–390; (b) Huang, C.-Y.; Cabell, L. A.; Anslyn, E. V. *J. Am. Chem. Soc.* **1994**, *116*, 2778–2792.

Design and Synthesis of Sialyl Lewis^x Mimics as E- and P-Selectin Inhibitors

Neelu Kaila, Bert E. Thomas IV§

Department of Chemical Sciences and Biological Chemistry, WYETH,
200 Cambridge Park Drive, Cambridge, Massachusetts

Abstract: The selectins are a family of cell-adhesion proteins that mediate the rolling of leukocytes on activated endothelial cells through the recognition of the carbohydrate epitope sialyl Lewis^x (sLe^x). Control of the leukocyte-endothelial cell adhesion process may prove useful in cases where excess recruitment of leukocytes can contribute to acute diseases such as stroke and reperfusion injury and chronic diseases such as psoriasis and rheumatoid arthritis. The development of molecules that block the interactions between sLe^x and the selectins has become an active area of research. In this review, we will highlight the various approaches taken toward the development of sLe^x mimetics as antagonists of E- and P-selectin, including the use of structural information about the selectins and their interactions with sLe^x that have been revealed through the use of NMR, protein crystallography and molecular modeling. Med Res Rev, 22, No. 6, 566–601, 2002; Published online in Wiley InterScience (www.interscience.wily.com). DOI 10.1002/med.10018

Key words: selectins; inflammation; antagonist; structural biology

1. *INTRODUCTION*

The selectins are a family of three (i.e., P-, E-, and L-selectin) calcium-dependent, cell-adhesion molecules. They are transmembrane glycoproteins containing an amino-terminal lectin domain, an epidermal growth factor domain and a variable number of complement regulatory-like repeats. There is greater than 50% homology between the lectin domains among the human selectins. P-selectin is stored in secretory granules of endothelial cells and platelets. It is rapidly expressed on the surface after stimulation with cytokines.[1,2] E-selectin is expressed on activated endothelial cells.[3] L-selectin is constitutively expressed on the surface of most leukocytes.[4,5] Once injury occurs, there are four important steps in the transfer of leukocytes from the blood stream to the injury site: (a) attachment and rolling, (b) activation, (c) adherence, and (d) transendothelial

§ The Current address of Bert E. Thomas is Guilford Pharmaceuticals.
Correspondence to: Neelu Kaila, Department of Chemical Sciences, WYETH, 200 Cambridge Park Drive, Cambridge, MA 02140. (E-mail:nkaila@wyeth.com)

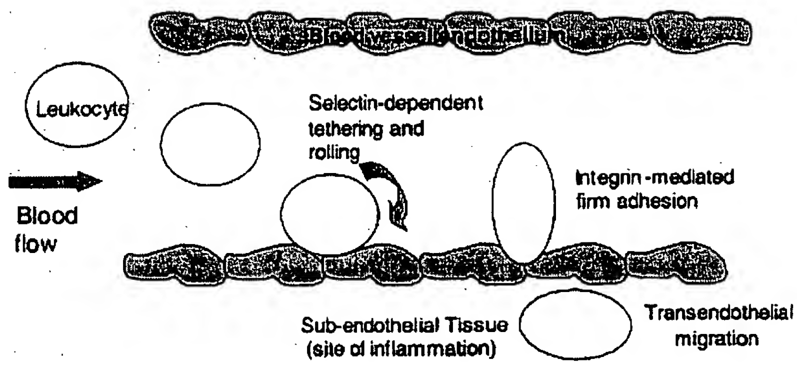

Figure 1. Transfer of leukoctes from the blood stream to the injury site. [Color figure can be viewed in the online issue, which is available at www.interscience.wiley.com]

migration (Fig. 1).[6] In a productive immune response, this leads to seclusion of infection. However, overzealous transfer of leukocytes causes widespread tissue damage leading to several disease states such as reperfusion injury, cardiovascular diseases, and allergic diseases. Therefore, the development of selectin antagonists is an attractive therapeutic target.

The first step in the adhesion cascade, attachment and rolling, is mediated by the interactions between carbohydrate epitopes on the leukocytes and E- and P-selectins.[7,8] P-selectin mediates attachment and is translocated to the surface of the endothelium within minutes of activation. E-selectin mediates slow rolling and is expressed after several hours on the activated cell surface. Although several selectin counter receptors have been proposed, the best characterized is the physiological ligand for P-selectin, P-selectin glycoprotein ligand-1 (PSGL-1). It is a disulfide-bonded homodimer with two 120-kDa subunits. It is expressed on all leukocytes[9–11] and binds P-selectin via an anionic amino-terminal peptide sequence (Fig. 2).

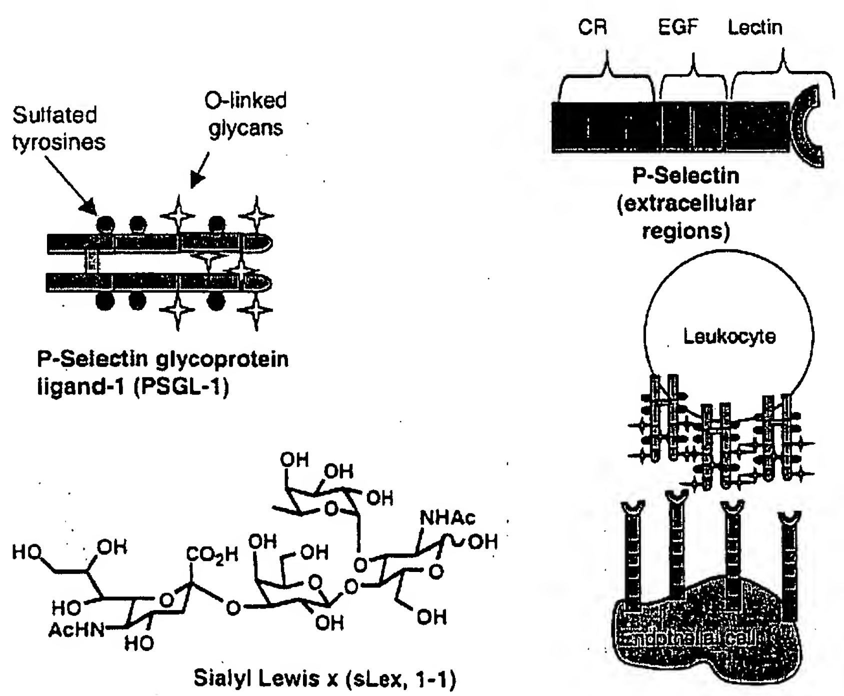

Figure 2. Selectin counter receptors.

The carbohydrate epitope (*O*-linked glycans) on PSGL-1 is the tetrasaccharide sialyl Lewis^x (sLe^x, **1-1**, Fig. 2). sLe^x binds to E- and P-selectin with low-affinity, having a K_D of 0.5 and 8 mM, respectively.[5] PSGL-1 binds to P-selectin with high affinity and requires both the sLe^x containing *O*-glycan and one or more tyrosine sulfates. PSGL-1 binds weakly to E-selectin. The importance of the selectins in inflammation is borne-out in selectin deficient mice. The P-selectin knockout[12,13] and the P/E selectin double knockout show elevated levels of neutrophils in the blood.[14,15] These knockout mice exhibit impaired DTH response and delayed TIP response.

The known biology of the selectins suggests that inhibiting the selectin-sLe^x interaction, which is the initial event in the adhesion cascade, is an effective approach for treating a variety of disease states such as: (a) reperfusion injury during myocardial infarction, organ transplantation, and traumatic shock; (b) cardiovascular diseases such as atherosclerosis and peripheral vascular disease, and (c) allergic diseases such as bronchial asthma and rhinitis.[16–19] The first half of this review will discuss the use of structural information about the selectins and their interactions with sLe^x that have been revealed through the use of NMR, protein crystallography, and molecular modeling. The second half of this review documents the attempts made toward a small molecule E- and P-selectin inhibitor and some of the issues related to biological evaluation of these antagonists.

2. STRUCTURE AND MODELING OF SELECTINS

A complete knowledge of the biology of the selectins requires a comprehensive understanding of the three-dimensional structure of the selectins, their ligands, and their complexes. Experiments ranging from binding studies of modified sLe^x analogues to structure determination using NMR and protein crystallography have been utilized by numerous groups. Early information revealed by these experiments was crucial to the development of models of the interactions between the selectins and sLe^x. While many of these models failed to correctly predict all of the interactions between sLe^x and the selectins that were recently deduced from the crystal structures of the sLe^x bound to E- and P-selectin,[20] they were a driving force behind the design of selectin antagonists and further structure determination experiments discussed in this review. In this section, a general overview of these structure-related experiments will be presented, starting with a discussion of the protein crystallography experiments, followed by a discussion of binding studies of modified sLe^x analogues, NMR experiments and finally an overview of the various hypothetical complex structures and the molecular modeling experiments.

A. Selectin Structure

The selectins consist of five domains: a N-terminal, calcium-dependent lectin domain, an epidermal growth factor domain (EGF), a variable number of complement regulatory-like units (CR), a transmembrane domain, and an intracellular tail. The sLe^x binding site has been localized on the lectin domain.[21] The role of the EGF and CR domains in ligand binding is still unclear. There is data to suggest that both domains play a role in binding, but in the case of E-selectin the data is conflicting.[22–28] Because most, if not all, of the drug design efforts that have been published to date are directed towards antagonists that bind to the lectin domain, we will concentrate our discussions on structural work regarding the lectin domain and selectin ligands.

B. Protein Crystallography

The crystal structure of an oligosaccharide bound to rat mannose-binding protein A (MBP-A) was the first crystal structure to directly impact the development of selectin antagonists.[29] There is ~30% identity between the lectin domains of MBPs and selectins. It was the first structure of an

oligosaccharide bound to a C-type lectin domain. One of the required calcium ions was shown to bind directly to the oligosaccharide, in contrast to previous crystal structures of lectin-oligosaccharide complexes, where the calcium or manganese ions were critical to maintaining the structural integrity of the binding site but did not directly interact with the oligosaccharide.[30–33]

The calcium ion in MBP-A interacts directly with the 3- and 4-hydroxyls of mannose, which are in equatorial positions. MBP-A also binds L-fucose which has an axial 4-hydroxyl and an equatorial 2-hydroxyl. Superimposing the 2- and 3-hydroxyl of L-fucose onto the 4- and 3- hydroxyls of D-mannose, respectively, allows the sugars to occupy the same space when binding the calcium ion with their equatorial hydroxyls and allows for the third hydroxyl of each sugar to overlay and interact with the protein. D-galactose is not bound by MBP-A. Overlaying the calcium-binding hydroxyls of D-galactose onto D-mannose suggests that the interaction of the third hydroxyl is critical for binding as the third hydroxyl of D-galactose is not in position to interact with the protein. These observations became the basis for most of the hypothetical models of sLe^x binding to the selectins, where the required calcium binds to the 2- and 3-hydroxyls of the L-fucose unit of sLe^x. While this was a perfectly rational assumption to make based on the data in hand at that time, it was later shown to be incorrect.

Graves et al. provided the first look at the sLe^x binding site when they solved the crystal structure of the lectin and EGF domains of E-selectin.[34] When compared to the MBP-A complex structure it was apparent that the lectin domain of E-selectin has some important differences. The most apparent difference was the loss of the second calcium binding site. In addition, only four conserved residues are used to bind the calcium (Glu80, Asn82, Asn105, and Asp106) by E-selectin. The fifth conserved residue used by MBP-A is replaced by a water in E-selectin due to a change in the position and orientation of the conserved residue. Other differences were also identified and are generally related to insertions and deletions in the sequences. Solving the crystal structure of E-selectin provided the foundation for defining the sLe^x binding site and a launching pad for a number of hypothetical models of sLe^x bound to E-selectin.

Subsequently, Ng and Weis solved the crystal structure of sLe^x bound to a selectin-like mutant of MBP-A.[35] Residues 211–213 were mutated to the corresponding Lys-Lys-Lys sequence found in lectin domain of E-selectin. In this complex structure, the 2- and 3-hydroxyls of fucose complex calcium, as had been predicted based on the earlier MBP-A complex structures.[29] The 4-hydroxyl of galactose interacts directly with Lys211 (MBP-A), while the 6-hydroxyl of galactose interacts with Lys211 (MBP-A) through a water mediated hydrogen bond. The most interesting aspect of this crystal structure was that the carboxylate of sialic acid did not interact with the protein. This was surprising since sialic acid had been shown to be important to binding. The authors proposed two possible explanations: (1) that sLe^x binds in a different orientation to E-selectin than to the MBP-A triple mutant or (2) that the structure was consistent with the known data and that the importance of the carboxylate of the sialic acid may not be directly related to a specific interaction with E-selectin.

The latest and most significant crystallographic experiments involve solving the structure of sLe^x bound to E-selectin and P-selectin and the structure of the PSGL-1 N-terminus bound to P-selectin by Somers et al.[20] The structure of sLe^x bound to E-selectin, shown in Figure 3, provided a few surprises. The majority of the interactions are electrostatic in nature. The buried surface area is a relatively small 549 Å.[21] The calcium is bound by the 3- and 4-hydroxyls of fucose. The majority of the proposed hypothetical models had predicted that the 2- and 3- hydroxyls of fucose would bind to the calcium ion. In addition, some of the other specific interactions between sLe^x and E-selectin were unexpected based on previous crystal structures and predictions.

The primary interactions between sLe^x and E-selectin are given in Table I and Figure 4. The 3- and 4-hydroxyls of fucose make additional interactions with protein sidechains that also bind the calcium ion. The 4-hydroxyl of galactose binds to the sidechain of Tyr94 while the 6-OH binds to the sidechain of Glu92. The sialic acid makes two interactions in the E-selectin crystal structure, one to the sidechain of Arg97 and the other to the sidechain of Tyr48. In P-selectin, Arg97 is mutated to a

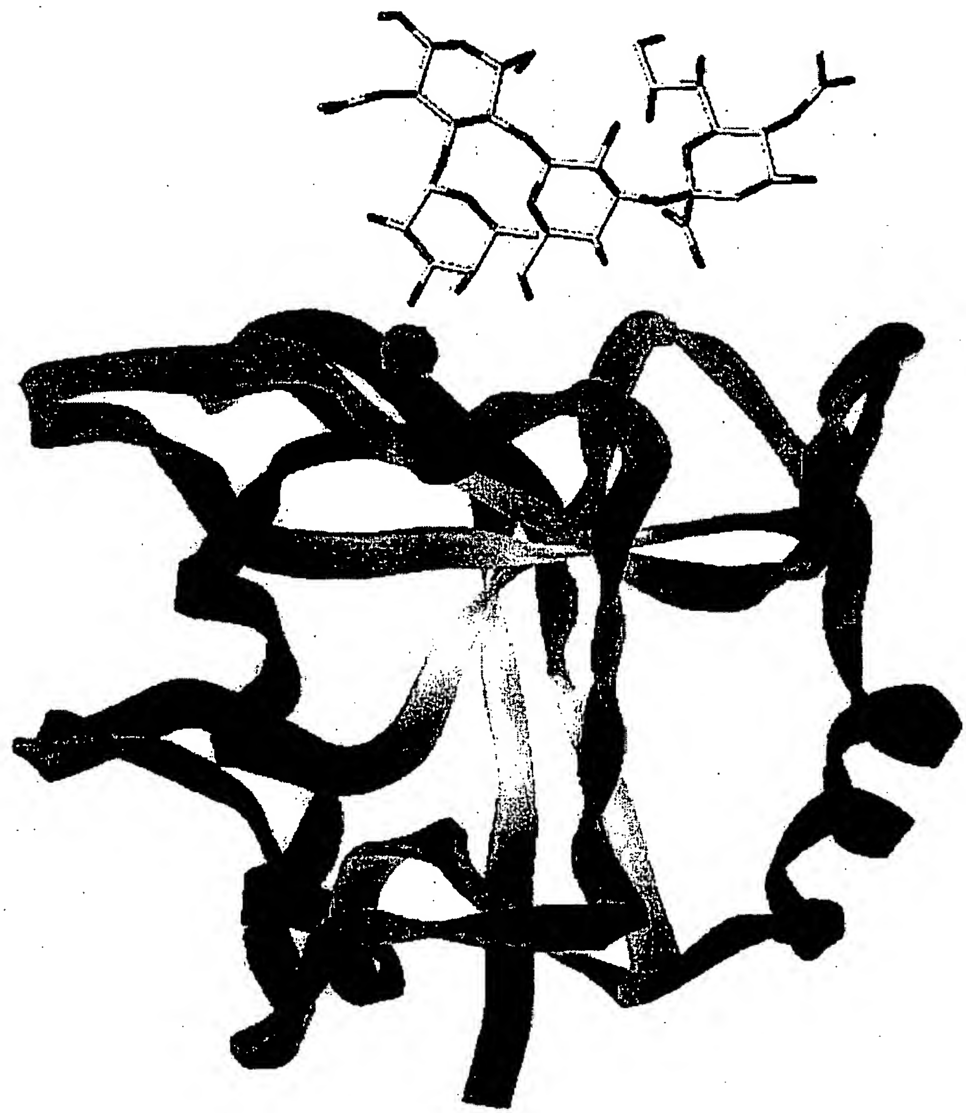

Figure 3. The crystal structure of sLe^x bound to lectin domain of E-selectin. The structure of E-selectin is represented with a ribbon, colored by a secondary structure (yellow—a-helix; purple—b-sheet; cyan—random coil), outlined to protein backbone. The bound calcium is represented by a green sphere and sLe^x is shown in a capped stick model.

serine, eliminating an ion–ion interaction. The superior interactions of sialic acid with E-selectin may provide a partial rationalization for the ~15 fold greater affinity of sLe^x for E-selectin over P-selectin.

While many theoretical models of sLe^x-selectin complexes predicted the interaction of sialic acid with Arg97, most of the other interactions were incorrectly predicted, although the general location and orientation of sLe^x in the binding site was reasonable. This points out the difficulty in predicting the structure of a protein–ligand complex, particularly when the interaction between the protein and the ligand is weak.

The crystal structure of the PSGL-1 N-terminus bound to P-selectin has also been solved. The peptide contained the 28 N-terminal amino acids, including three tyrosines that are sulphated. Each of the sulfated tyrosines were shown to contribute to binding.[20] From a drug design prespective, this

Table 1. Interaction Distances Between sLe^x and E-Selectin and the Bound Calcium and E-Selectin Obtained From the Somers' Crystal Structure of sLe^x Bound to E-Selectin

Interaction	*Distance (Å)*
Ca^{2+}–Fuc O_3	2.39
Ca^{2+}–Fuc O_4	2.59
Glu80 sc–Fuc O_4	2.64
Asn82 sc–Fuc O_4	2.98
Tyr94 sc–Gal O_4	2.89
Glu92 sc–Gal O_6	2.54
Arg94 sc–Gal O_1	3.10
Tyr48 sc–NeuAc CO_2H	2.54
Arg97 se–NeuAc CO_2H	2.79
Ca^{2+}–Glu80 sc	2.56
Ca^{2+}–Asn82 sc	2.43
Ca^{2+}–Asn83 sc	2.35
Ca^{2+}–Asn105 sc	2.37
Ca^{2+}–Asp106 bb	2.48
Ca^{2+}–Asp 106 sc	2.35

Distances (in Angstroms) are measured heavy atom to heavy atom.
bb, backbone; sc, sidechain.

structure is very important because it defines a second binding site that is proximal to the sLe^x binding site that may be ameniable to inhibitor design. Two of the three sulfated tyrosines are visible in the crystal structure. Tys7 of PSGL-1 has a well defined binding site, interacting with a number of residues through electrostatic (Ser46, Ser47, Lys112, His114) and non-polar interactions (Ser47, Lys113). Tys10 of PSGL-1 packs against Leu8 and Leu13 of PSGL-1 directing the Tys10 sulfate so that it interacts with Arg85. Other interesting features of this complex structure are a conformational change of P-selectin around the calcium binding site and a change in the orientation of the lectin domain with respect to the EGF domain.

C. Modified SLe^x

Many groups have chemically modified the structure of sLe^x, shown in Figure 5, in a systematic way to identify the minimal required structural binding elements for sLe^x binding to the selectins.

The fucose moiety of sLe^x has four substituents, three hydroxyls and a methyl group, that can potentially interact with the selectins upon binding. Based on homology to mannose-binding protein, the fucose moiety was correctly assumed to function as the calcium recognition unit of sLe^x.

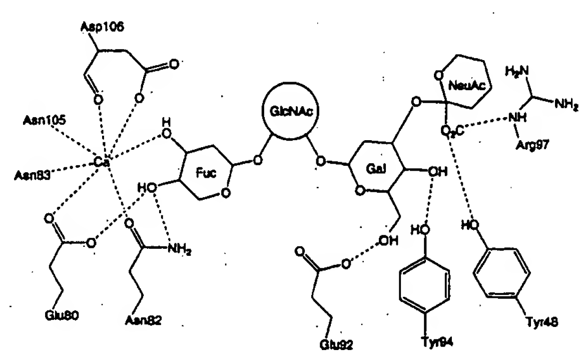

Figure 4. A schematic depicting the interactions between sLe^x, E-selectin, and the bound calcium.

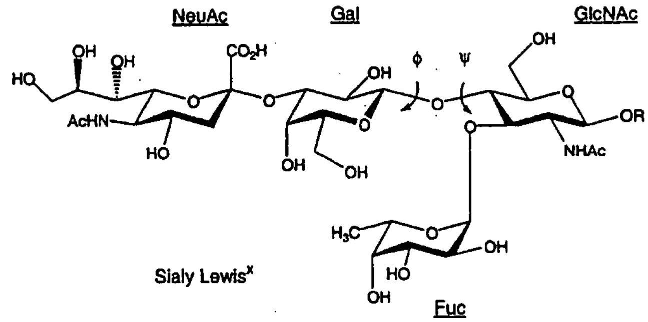

Figure 5. Structure of sialyl Lewis^x. Sugars are designated by abbreviations.

Ramphal et al. replaced each of the substituents with a hydrogen to determine their importance for the binding of sLe^x to E-selectin.[36] The replacement of any of the hydroxyl groups resulted in a complete loss of binding, while replacement of the methyl group with hydrogen (replacement of fucose with arabinose) resulted in a molecule five times less active than sLe^x. Hasegawa et al. looked at replacement of each of the hydroxyls in the fucose of sLe^x and found them to be crucial for binding to E- and L-selectin.[37] In the case of P-selectin, they found that only the 3-hydroxyl was critical for sLe^x binding. It was assumed by analogy to MBP-A and latter confirmed by the determination of sLe^x bound to E- and P-selectin that two of the fucose hydroxyls coordinate the calcium. While it is somewhat surprising that the other calcium coordinating hydroxyl was not found to be critical for binding, it should be noted that sLe^x binds most weakly to P-selectin and the interactions between the 2- and 4-hydroxyls of fucose may not be as optimal when sLe^x binds to P-selectin as compared to binding to E-selectin. Henrichsen showed that replacement of the 2-hydroxyl of fucose with a methoxy group eliminated binding to E-selectin.[38]

The galactose moiety of sLe^x has three hydroxyl substituents that can potentially interact with the selectins upon binding. Stahl et al. examined the role of the 4- and 6-hydroxyls by synthesizing deoxy sLe^x analogues where the hydroxyl was replaced by a hydrogen and in the case of the 4-hydroxyl also replaced by a fluorine.[39] Preliminary assay results were alluded to which indicated that the analogues all bound more weakly to E-selectin than sLe^x, suggesting that these substituents are important but not crucial to binding. The Novartis group recently published a study on the modification of the 6-hydroxyl of the galactose moiety in two sLe^x mimetics which had better IC_{50}s than sLe^x for E-selectin.[40] Diverse sets of substituents were employed. All of the analogues of the mimetics were inactive. The authors suggested that the galactose 6-hydroxyl is optimal.

The sialic acid moiety has four substituents, a glycerol sidechain, one hydroxyl, a carboxylate, and an amide, that can potentially interact with the selectins upon binding. Hasegawa et al. studied the role of most of these substituents. Various modifications of the glycerol sidechain resulted in little to no effect on binding to E-selectin.[37,41] Removal of the *N*-acetyl group also has little effect on binding.[37] Replacement of the carboxylate by different charged groups resulted in similarly active molecules.[37,42]

The GlcNAc moiety has three substituents, two hydroxyls and an amide, that can potentially interact with the selectins upon binding. Ohmoto et al. studied sLe^x analogues where the 1-hydroxyl of GlcNAc was replaced by hydrogen and the 2-position remains a NHAc as in sLe^x or substituted with a hydroxyl or a hydrogen. Each analogue was tested against E-, P-, and L-selectin and showed a unqiue specificity profile. The authors suggested that removal of the 1-hydroxyl of the GlcNAc moiety increased the hydrophobicity of the analogue and, based on models of the complex of these analogues with P-selectin, increase binding affinity through a hydrophobic interaction between the GlcNAc ring and His108. This interaction is not available to sLe^x. Most studies have suggested that the role of GlcNAc is to preorganize the moieties of sLe^x.[43–45]

D. NMR Spectroscopy

The use of NMR spectroscopy to study the conformation of sLe^x in solution and bound to the selectins has been prolific. For the purposes of this review, a general overview of the area will be provided to highlight the efforts of many different research groups. Early work in this area was directed at defining the conformation of sLe^x in solution. Three independent studies reported conformations that were in general agreement, suggesting a single conformation of sLe^x in solution.[46–48] Subsequent NMR and molecular dynamics studies of sLe^x in solution indicated that the Gal-NeuAc linkage was flexible, opening the possibility that sLe^x exists as an ensemble of low energy conformations in solution.[49,50] Poppe et al. found evidence that the Gal-NeuAc linkage samples three different conformation, but that data suggested that the other glycosidic linkages were in single conformations.[51] Recently, Homans et al. reinvestigated the conformation of sLe^x in solution using 13C-enriched sLe^x and 3D ROESY-HSQC experiments.[52] These experiments allowed for the determination of a much greater number of conformational restraints than had previously been determined. Time-average restrained molecular dynamics simulations suggest that the three glycosidic linkages are much more flexible than previously thought. During the course of the short simulation, a second conformation of sLe^x was accessed for a significant amount of time, indicative of the flexibility of the linkages.

Cooke et al. utilized differences in the tNOEs of sLe^x bound and unbound E-selectin to study the complex.[49] They suggested that the bound conformation of sLe^x was not the same as the unbound conformation of sLe^x. Hensley et al. reported just the opposite that the bound conformation of sLe^x was identical to the solution conformation of sLe^x.[53] This finding was disputed by Scheffler et al.,[54,55] who obtained similar results to that of Cooke with more extensive NOESY experiments. Poppe et al. published data on the conformation of sLe^x bound to E- and P-selectin.[51] The bound conformation of sLe^x is similar in both cases, though the largest difference is in the Gal-NeuAc linkage, which is the most flexible glycosidic linkage in solution. These results differed from those of Scheffler in the conformation about Fuc-GlcNAc linkage. Most recently, Homans et al. reported 3D NOESY-HSQC experiments using 13C-enriched sLe^x to determine the bound conformation of sLe^x bound to E-selectin.[52] Their structure of bound sLe^x had differences from that of Scheffler in the galactosyl-sialyl linkage and that of Poppe in the Fuc-GlcNAc linkage. The dihedral angles for ϕ and ψ about each glycosidic linkage as determined by NMR experiments are given in Table II, along with the values obtained from the Somers' crystal structures for comparison.

Table II. Dihedral Angles for ϕ and ψ About Each Glycosidic Linkage of sLe^x Bound to a Selectin is Given as Determined by NMR and Protein Crystallography

		NeuAc-Gal		*Gal-GlcNAc*		*GlcNAc-Fuc*	
Model	*Selectin*	ϕ	ψ	ϕ	ψ	ϕ	ψ
Scheffler	E	−76 ± 10	6 ± 10	39 ± 10	12 ± 6	38 ± 7	26 ± 6
Poppe	E	−58 ± 5	−22 ± 5	24 ± 5	34 ± 3	71 ± 3	14 ± 2
	P	−85 ± 11	−4 ± 12	45 ± 4	18 ± 4	61 ± 10	26 ± 6
Homans	E	−43	−12	45	19	29	41
Somers	E	−65	−11	33	16	43	22
	P	−65	−8	40	8	40	16
	P[a]	−55	−11	40	16	70	20

Dihedral angles are given in degrees and standard errors are provided where available.
[a]Measurements made on the sLe^x moiety of PSGL-1 when bound to P-selectin.

Table III. Ineraction Between sLe^x, E- and P-Selectin and the Bound Calcium as Defined in Various Hypothetical Models

Residue	*Kogan*[a]	*Poppe*[a]	*Kondo*[b]	*Kolb*[a]
Fuc O_2	Ca^{2+} Asn105 sc	Ca^{2+}		Ca^{2+} Asn105 sc
Fuc O_3	Ca^{2+} Gln80 sc Asn82 sc	Ca^{2+}	Ca^{2+} Glu80 sc	Ca^{2+}
Fuc O_4				Asn82 sc
GlcNAc O_6			Lys111 sc	
GlcNAc Amide			Asn82 sc	
Gal O_4		Tyr94 sc		Asn105 sc
Gal O_6	Tyr94 sc		Tyr94 sc Asn105 sc	Tyr94 sc
NeuAc CO_2H	Arg97 sc	Tyr48 sc	Lys 113 sc	Arg97 sc
Ca^{2+}	Glu80 sc Asn82 bb Asn105 sc Asp106 bb Asp106 sc		Glu80 sc	Glu80 sc Asn105 sc Asp106 bb Asp106 bb

[a]model of sLe^x bound to E-selectin.
[b]model of sLe^x bound to P-selectin.
bb, backbone; sc, sidechain.

E. Hypothetical Models of SLe^x Bound to the Selectins

A large number of models of sLe^x bound to E-selectin and P-selectin have been developed over the years. In this section, the models that have been described in some detail will be discussed to show the variety of hypotheses that exist in the field, highlighting the success and failures when compared to the recently published complex structures. Table III gives the important interactions predicted to occur between sLe^x and E-selectin or P-selectin as compiled from the models discussed below.

Kogan et al. published a model of sLe^x binding to E-selectin.[56] The model was constructed using the crystal structure of E-selectin and the complex structure of mannose bound to MBP-A. The conformation of sLe^x that was docked to E-selectin was based on the NMR experiments of Cooke. MBP-A was superimposed onto E-selectin. sLe^x was initially overlayed onto mannose as it binds to MBP-A, requiring that the 2- and 3-hydroxyls of fucose interact with the bound calcium. The MBP-A structure was removed and energy minimizations for sLe^x bound to E-selectin were carried out. No constraints or solvation models were used in the calculations. The minimization relaxed high-energy non-bonded interactions. The resulting model had the 6-hydroxyl of galactose bound to Tyr94 and the sialic acid bound to Arg97.

A model for sLe^x bound to P-selectin was presented by Kondo et al.[44] A homology model of P-selectin was developed based on homology to and the crystal structure of E-selectin. After residues were manually changed to the appropriate P-selectin residues, a molecular dynamics simulation was performed to let the protein to relax any poor non-bonded interactions in the initial model and to allow for any reorganization of loops and sidechains resulting from the newly mutated residues. The final model of sLe^x binding to the P-selectin has some interesting features. Consistent with modified sLe^x experiments, only the 3-hydroxyl of fucose binds to the calcium. The 6-OH of GlcNAc interacts with Lys111, while the carbonyl of the *N*-acetyl group of GlcNAc interacts with Asn82. These are novel interactions not predicted in any of the sLe^x-E-selectin models. The 6-OH of galactose binds to Tyr94 and Asn105, while the sialic acid binds to Lys113.

Poppe discussed a model of sLe^x bound to E-selectin and P-selectin based on their NMR experiments of sLe^x complexed.[51] The models were generated using their preferred conformation of sLe^x docked to the E-selectin crystal structure or a homology model of P-selectin. In each case, the 2- and 3-hydroxyls of fucose was situated to bind to the calcium. The conformation of sLe^x was constrained and a 2000 step rigid-body minimization was performed. The resulting structure was subjected to 10 ps of molecular dynamics at 300 K and subsequently minimized for an additional 2000 steps. In each case, the 4-hydroxyl of galactose interacts with Tyr 94 and the sialic acid binds to Tyr48.

The most recent model of sLe^x bound to E-selectin was presented by Kolb et al.[57] The generation of this model was not described explicitly. The 2- and 3-hydroxyls of fucose bind to calcium. In addition, the 2-hydroxyl interacts with Asn105 and the 3-hydroxyl interacts with Glu80. The 4-hydroxyl of fucose binds to Asn82. The 4-hydroxyl of galactose interacts with Asn105 and the 6-hydroxyl interacts with Tyr94. Lastly, the sialic acid is predicted to bind to Arg97.

As can be seen looking at Table III, each of the models has interactions correctly predicted and incorrectly predicted. The most common mistake was the interactions of fucose with the bound calcium and its binding site. The use of the 3- and 4-hydroxyls to bind calcium was unexpected based, in part, on the crystal structures of MBP-A. The fact that the predictions of the remaining interactions were wrong concerning different interactions demonstrates the difficulty in predicting the crystal structure of a ligand bound to a receptor, particularly when the biological interaction is relatively weak.

F. Molecular Modeling

The molecular modeling efforts directed toward drug design and discovery can be split into two groups. The first group is based solely on the structure of the ligand without the direct involvement of the receptor structure in the calculations. The ligand based efforts, which can be further broken down to conformational analysis and pharmacophore searches, will be discussed first. The second group is receptor-based modeling where efforts are directed toward understanding and optimizing the interactions between the ligand and the receptor. The receptor-based efforts will be discussed second.

Kolb et al. published a number of papers based on a Monte Carlo conformational analysis method they developed for the rapid generation of a Boltzman weighted ensemble of states.[58–60] Included in the methodology is the utilization of an implicit water model (GB/SA) to allow for a more realistic computational representation of the ligand of interest as it would exist in a biological environment. An example of the use of this methodology was recently published where Ernst et al. were attempting to get improved affinity by designing mimetics that improved preorganization of the important pharmacophoric elements. The replacements of GlcNAc by (R,R)-cyclohexan-1,2-diol and sialic acid by glycolic acid or cyclohexyl lactic acid were evaluated. Compound **2-1**, shown in Figure 6, samples a wider range of conformations than sLe^x samples in solution, but **2-1** still sampled a conformation similar to the bound conformation of sLe^x, just with a lower frequency than sLe^x in solution does. Replacement of glycolic acid with (S)-cyclohexyl lactic acid (**2-2**) lead to a compound that sampled conformations similar to the conformation of bound sLe^x with greater frequency than sLe^x does in solution, whereas (R)-cyclohexyl lactic acid (**2-3**) lead to a compound that never sampled the appropriate conformation for binding to E-selectin. This lead the authors to correctly predict that **2-2** would be more active than **2-1** or **2-3** (see Section 3B) because it contained a higher level of conformational preorganization than the other ligands. The conformation of **2-2** bound to E-selectin was determined by NMR and shown to be the same as that of sLe^x.

Information obtained from molecular dynamics simulations that are described later in this review was used to develop a pharamacophore model for an E-selectin inhibitor.[61] A 3D-pharmacophore search of the ACD-3D database was done using the pharmacophore, as shown in

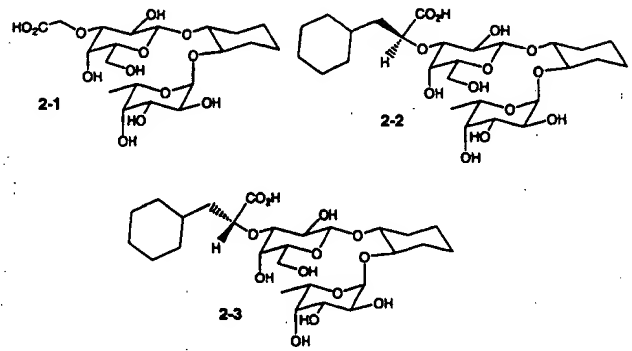

Figure 6. Structures of three sLe^x mimetics studied by Kolb et al. using a Monte Carlo conformational analysis methodology.

Figure 7. No hits were found using the pharmacophore, so the pharmacophore was modified by replacing the fucose moiety with a carboxylate, the sulfonic acid with a carboxylate, and the branched alkyl chain with a single alkyl chain. Using the modified pharmacophore, **2-4A** was identified as an inhibitor. Further optimization using conformational analysis and medicinal chemistry resulted in a potent inhibitor **2-4B** (see Section 3D).

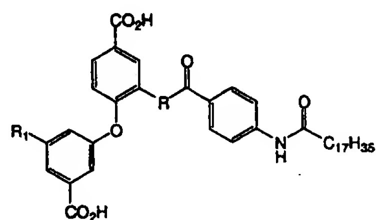

	R	R_1
2-4A	HN—C(=O)—CH_2	CO_2H
2-4B	NH	H

Structure 2–4

Rao et al. also used a pharmacophore search based on the bound conformation of sLe^x to identify potential inhibitors.[62] The pharmacophore was based on the three vicinal hydroxyls of the fucose and the carboxylate of the sialic acid, which in their model were separated by 10–12 Å. The

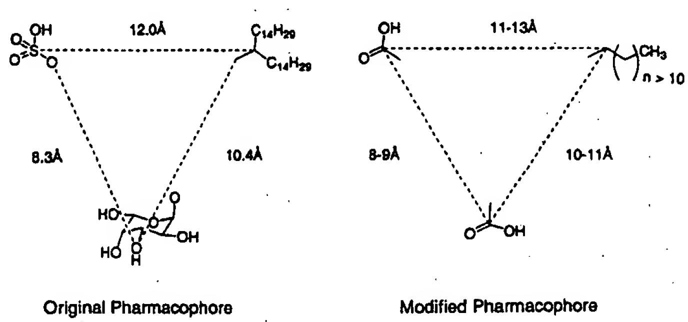

Figure 7. The original pharmacophore resulting from the model of sLe^x bound to E-selectin derived from molecular dynamics simulations and the modified pharmacophore that was successfully used to search the ACD for selectin antagonists.

initial 2D search of the FCD database, which contained ~75,000 compounds at the time, yielded almost 400 hits. Using the pharmacophore with the distance constraints reduced the number of hits to 23, which was further reduced to 9 hits upon visual examination. Three of the compounds assayed showed activity. These compounds are shown in Figure 8. One of the hits, glycyrrhizin, is a natural product with known anti-inflammatory properties. It blocked binding of sLe^x in a dose-dependent fashion. It had an IC_{50} of < 0.5 mM against P-selectin. Cariminic acid also blocked selectin binding at concentrations comparable to those of glycrrihizin. A-Hedrin was less active (IC50 = 2–3 mM).

Kogan et al. designed a series of sLe^x mimetics using mannose attached to a biphenyl moiety that contained a carboxylate, with the intention of including the hydroxyls of the sLe^x fucose and the carboxylate of the sLe^x sialic acid.[63] Using their previously described model of sLe^x bound to E-selectin, a mannose-biphenyl unit was superimposed onto the fucose of sLe^x. This allowed for the evaluation of many substitutents at various positions on the biphenyl ring. The optimal substituent was a carboxylate that was predicted to interact with Arg97 (see Section 3C).

Tsujishita et al. studied a model of GSC-150 (**2-5**), bound to E-selectin using molecular dynamics simulations.[64] Based on the molecular dynamics simulations, three critical interactions were identified: calcium binding by the 2- and 3-hydroxyls of the fucose moiety, sulfate binding to the basic protein residues, and an extended hydrophobic interaction between the long-branched alkyl chains and the protein surface. The molecular dynamics simulations indicated that the interaction between the sugar and the calcium was weak, while the hydrophobic interaction was strong. The two hydrophobic areas on the protein surface are predicted to be (1) Tyr44, Pro46, and Tyr48 and (2) Ala9, Leu114, and the alkyl portions of the Lys111, Lys112, and Lys113 sidechains. Another interesting side of these simulations was the transitity of the interaction between the 2-hydroxyl of the fucose and the calcium. While the interaction between the 3-hydroxyl and the calcium is tight throughout the molecular dynamics simulation, the interaction between the 2-hydroxyl and the calcium fluctuated greatly. GSC-150 was found to be more potent than sLe^x against E- and P-selectin in an competitive binding assay.

Kondo et al. designed a series of antagonists using modified serine-glutamic acid dipeptides.[65] Molecular dynamics simulations of **2-6**, **2-7**, **2-8**, and **2-9**, shown in Table IV, were undertook to evaluate the effect of differences in the peptide stereochemistry on binding. Initial models were generated by binding the 2- and 3-hydroxyls groups of the fucose to the bound calcium. In the case

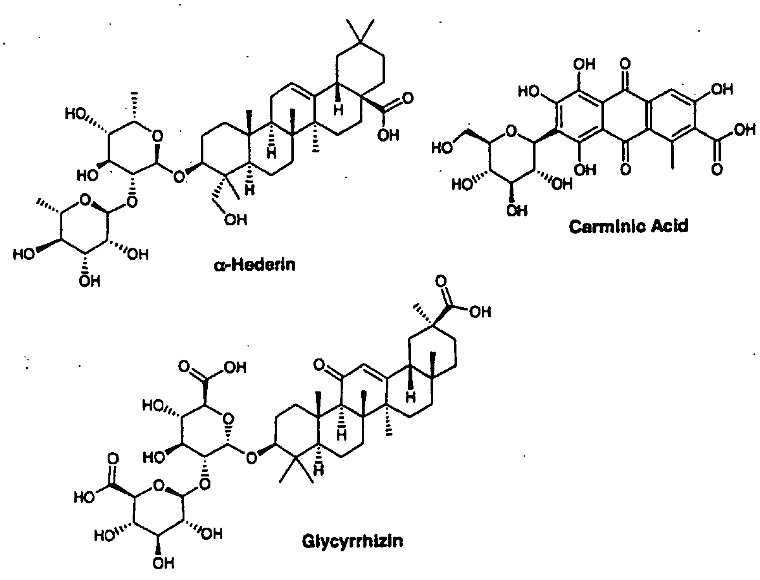

Figure 8. Three active selectin antagonist identified using a 3D pharmacophore to search the ACD database.

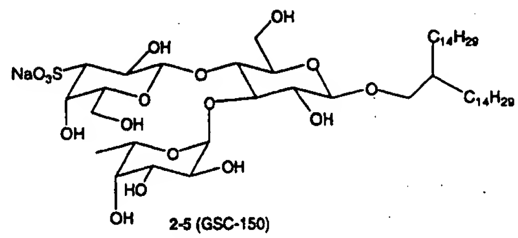

Structure 2–5

of 2-6, the D-Glu was directed towards Arg97, whereas for 2-7 the L-Glu was directed towards Lys111. The hydrophobic chains were situated close to a previously defined hydrophobic binding region. The 200-ps molecular dynamics simulations using explicit water were performed on each complex. The final form of 2-6 was a type II β-turn which was not present in the initial structure. In the case of 2-7, the initial and final structures were characterized by a type II' β-turn. Models for 2-8 and 2-9 bound to E-selectin were not stable over the course of the simulations. These results were used to choose the starting templates for further chemical optimization.[66]

Kondo et al. also found that a five-membered fucose ring can replace a six-membered fucose as the calcium binding moiety in their dipeptide inhibitors.[67] Average structures from molecular dynamics simulations of model complexes of 2-7 and 2-11 bound to E-selectin indicate that the 2- and 3-hydroxyls of the 5-membered fucose of 2-11 overlay well with those of the 6-membered fucose of 2-7. Both 2-10 and 2-11 showed good activity in an E-selectin assay (Table IV).

Taylor et al. designed a sLe^x mimetic based on a model of the complex of sLe^x bound to E-selectin.[68] Using a method similar to that of Kogan et al., the Taylor model was constructed by docking sLe^x, in a conformation defined by the NMR experiments of Scheffler, to the E-selectin crystal structure of Graves. The 2- and 3-hydroxyls of fucose were required to bind to the calcium. This put the sialic acid in proximity of Arg97. sLe^x was minimized to eliminate any steric clashes. Multiple conformers of 2-12, a tetralin with a *O*-linked fucose and an alkyl-linked carboxylate, were generated and subsequently superimposed onto the fucose of sLe^x. It was found that one of the low energy conformers of 2-12 placed its carboxylate in proximity of Arg97, mimicking the fucose, and

Table IV. IC_{50}'s (μM) of Serine-Glutamic Acid Dipeptide Based Inhibitors of Tsukida et al. against E-, P-, and L-Selectin

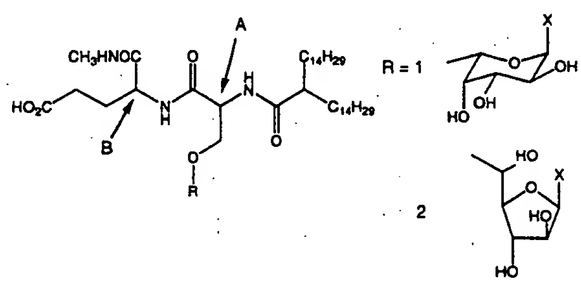

Compound	*A*	*B*	*R*	*E-selectin*	*P-selectin*	*L-selectin*
2–6	L	D	1	13	0.5	6.0
2–7	D	L	1	5.5	0.7	9.4
2–8	L	L	1	> 1000	1.9	39
2–9	D	D	1	> 1000	2.1	18
2–10	L	D	2	3.1		
2–11	D	L	2	4.3		

sialic acid of sLe^x. This was the most active compound in their assay, 2-fold more active than sLe^x. Unusual activity was seen for compound **2-13.** Modeling studies indicated that this compound could occupy the active site with a potential interaction between the acid group and the guanidino group of Arg97 but that the interaction vector differed from the interaction vector utilized by the sialic acid of sLe^x. No activity was seen in compounds without a fucose or a carboxylic acid group (**2-14**).

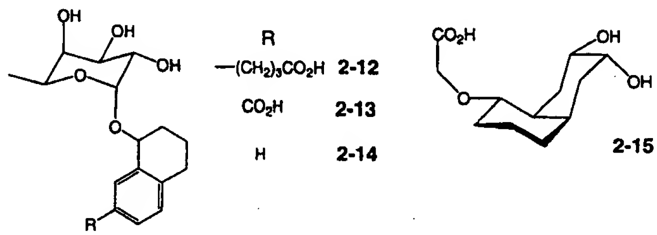

Structure 2–12 to 2–15

Gravel et al. took a similar approach to evaluate a cis-decalinic mimetic of sLe^x.[69] After generating a model similar to Kogan et al., **2-15** was superimposed onto the fucose of sLe^x. Compound **2-15** was minimized in the binding site, using constraints on the interactions between the fucose hydroxyls and the bound calcium. The carboxylate of **2-15** was predicted to interact with Tyr94 as well as Arg97. This requires the carboxylate of **2-15** to interact with Arg97 from a different orientation than the sialic acid of sLe^x, allowing an interaction with Tyr94 that is accounted for by the 4-OH of galactose in the crystal structure complex of sLe^x and E-selectin. Compound **2-15** had the same activity as sLe^x for both E- and P-selectin.

Slee et al. recently published on imidazole-based selectin inhibitors.[70] Compounds were manually docked onto a model of P-selectin. These structures were energy minimized followed by a Monte Carlo protocol. The resulting structures have a carboxylate binding to the calcium, the imidazole ring proximal to Lys111 and Lys113 and an amide moiety interacting with Ser97 and Ser99. In the case of **2-16**, one of the more potent compounds, a second carboxylate binds to Lys112. This compound showed good activity in all in-vitro assays. In the mouse TIP model it reduced the inflammatory response in a dose-dependent manner, causing a 30–50% reduction in cell infiltration at doses of 10–50 mg/kg i.v.

Kaila et al. designed and synthesized β-C-mannosides as E-selectin antagonists (also see Section 3C).[71] They used the proposed structure of Poppe et al.[51] as a starting point for modeling the bound structures of mannosides **2-17** and **2-18** to E-selectin, respectively. The mannose ring of **2-17** and **2-18** were overlaid onto the L-fucose in the proposed complex structure. The glutamate side chains of **2-17** and **2-18** were then orientated such that they were pointed in the general direction of the sialic acid binding site. The structures were energy minimized followed by a Monte Carlo simulation. Instead of the mannose moiety remaining overlayed on the fucose moiety in the Poppe sLe^x structure, it relaxed onto the surface of E-selectin, optimizing the non-bonded interactions. Using the lowest energy, Monte Carlo structure of **2-18** bound to E-selectin as a starting point, a

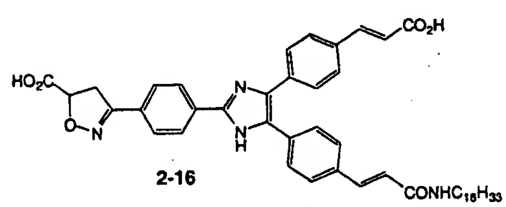

Structure 2–16

virtual library that corresponds to derivatization of C-6 of mannose was generated in the presence of E-selectin. Each initial structure was minimized, followed by a Monte Carlo simulation. The low energy structure of each construct was retained, ranked, and used to choose reagents.

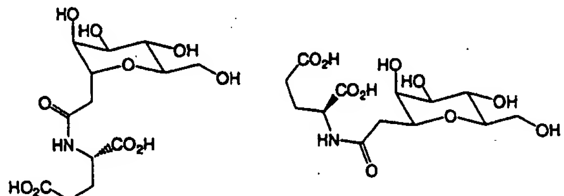

2-17 2-18

Structure 2–17 to 2–18

3. SMALL MOLECULE SELECTIN ANTAGONISTS

Sialyl Lewis^x and other tetrasaccharide analogs have been prepared both for study of structure-function relationships and use as drug candidates.[17,57,72–78] The use of sLe^x itself as a drug candidate has proven to be unsuccessful. Cytel Corporation announced in 1999 that CY1503 (cylexin, a sLe^x pentasaccharide) showed no benefit over the placebo in phase II/III clinical trials for treatment of reperfusion injury although it blocks selectin activity in a variety of animal models.[79] The likely reason for the failure is low bioavailabilty and poor stability to degradative enzymes. Low biological affinity is another factor; the K_d values for E- and P-selectin binding to sLe^x are 0.5 and 8 mM respectively. An additional obstacle towards study and use of sLe^x analogs as drug candidates is the difficulty in synthesis. Sialyl Lewis^x has been synthesized using chemical and enzymatic techniques. Wong et al. previously discussed these in a review.[17] Large-scale production of sLe^x is most effectively accomplished using a multienzyme system.[47] Thus, like other carbohydrates, sLe^x and its analogs seem to suffer from poor pharmacokinetic properties, low binding affinity and complexity of synthesis.

In recent years several research groups focused on searching for orally available, high affinity, low molecular weight selectin inhibitors. The most frequently used strategy has been the substitution of the sugars in sLe^x with other moieties such that the key interactions are retained. Our discussion mimics this approach by sorting the selectin inhibitors on the basis of number of sugars present in the molecule.

A. MImics Containing Three Sugars

Sialic acid (NeuAc) is the most expensive sugar in sLe^x. There is ample evidence in literature that it can be successfully replaced by anionic functionalities. Sulfated Lewis^x trisaccharide **3-A1** does exist, as a natural analog of sLe^x, and shows superior binding to E-selectin.[80] Several groups replaced sialic acid with a sulfate group.[37,81] Martin-Lomas et al.[82] prepared a sulfated trisaccharide derivative. The synthesis of their potential ligand **3-A2** was made easier by substituting the less important *N*-acetyl glucosamine with glucose, so they can start with the readily available lactose unit. No activities were reported for these compounds. Glycomed patented sulfated-lactose derivatives as selectin antagonists.[83] Kiessling's group prepared Le^a sulfated trisaccharides **3-A3** where the *N*-acetyl group of glucose has been removed.[84] These compounds showed activity against E-selectin. Compound **3-A3.1** was 20-fold more potent than **3-A3.2** in an E-selectin ELISA assay. The 1-deoxy-3′-*O*-sulfo Lex analogs **3-A4** prepared by Hasegawa[85] were found to be less potent than sLe^x in their E-selectin assay but showed increased potency against P-selectin in a competitive

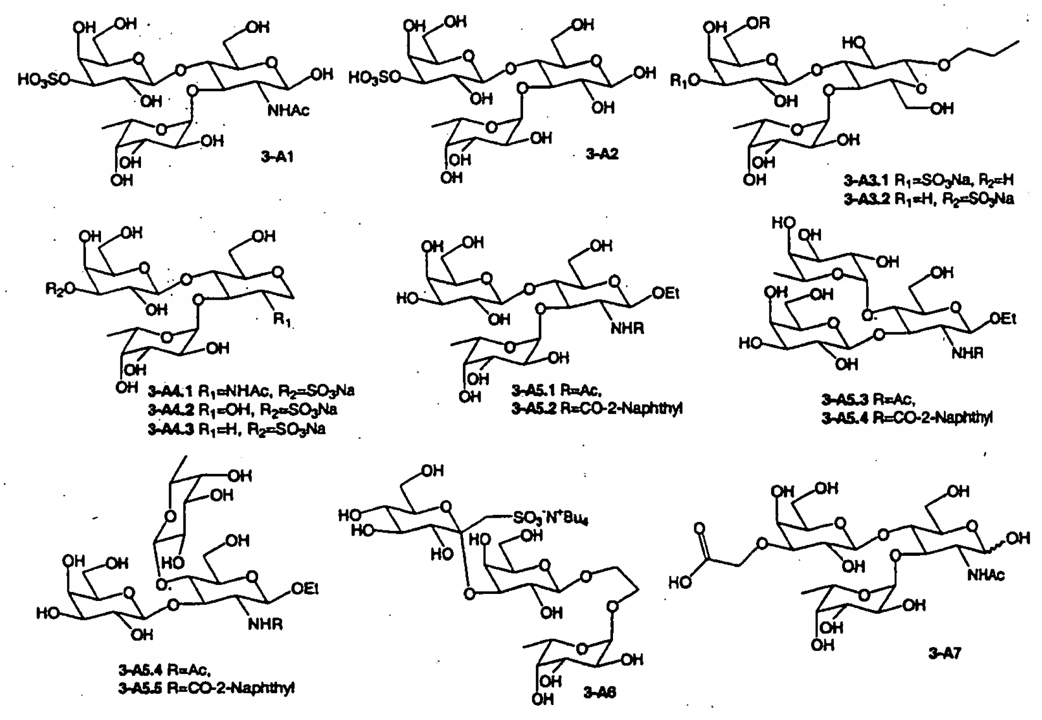

Structure 3-A1 to 3-A7

binding assay (IC_{50} 0.56 mM for **3-A4.2**, 0.67 mM for **3-A4.3**, 1 mM for sLe^x). Some other groups also prepared non-sialylated trisaccharide sLe^x mimics. Non-sialylated *N*-modified analogs of sLe^x and sLe^a (**3-A5**) were prepared by Imazaki and found to be equipotent to sLe^x in an in vitro E-selectin assay.[86] In an in vivo lipoteichoic acid (LTA)-induced murine pleursy model compounds **3-A5.1** and **3-A5.2** showed 51 and 62% inhibition, respectively, at an i.v. dose of 30 mg/kg. Herczegh and Liptak prepared a sulfonic-acid type mimic (**3-A6**) of sLe^x for which no activity was reported.[87,88] NeuAc has also been successfully replaced with phosphate groups.[85,89] The 3′-O′-phospho Le^a analog synthesized by Bertozzi et. al. was found to be 20-fold more active than the 3′-sulfo Le^x derivative against E-selectin in an ELISA assay.

The 3′-carboxymethyl substituted analog **3-A7** has similar antagonist affinity as sLe^x.[90] This is the most frequently used sialic acid replacement. A more rigid sialic acid mimic was used in compound **3-A8**[91] by Thoma and collaborators where the carboxylic acid is fixed in the equatorial position of a six-membered acetal to mimic the solution phase conformation of sLe^x. Analog **3-A8** was found to be inactive in an E-selectin assay. Other rigid NeuAc mimics that have been used in the literature are lactic acid derivatives. These resulted in very active E-selectin inhibitors. For example, Thoma's group prepared several 1,2-deoxyglucose derivatives (**3-A9**).[92–95] Compound **3-A9.1**, where NeuAc was replaced with a cyclohexyllactic acid and GlcNAc with a glucal-derived building block was thirty times more potent than sLe^x in a static E-selectin assay. Another hypothesis put forward by some workers in the field suggests a complimentary lipophilic binding site on the E-selectin surface. In an effort to target this site, Thoma et al. prepared derivatives **3-A9.2** where they modified the glucal derived moiety. The activity profile did not support the presence of a lipophilic site. Two of the inhibitors **3-A9.1** and **3-A9.3** when tested in vivo in a murine model of acute inflammation, showed an ED_{50} of 15 mg/kg.

Some work has been reported where the *N*-acetyl glucosamine has been replaced with other more stable functionalities, keeping the other three sugar units intact. Hanessian's group[74] replaced

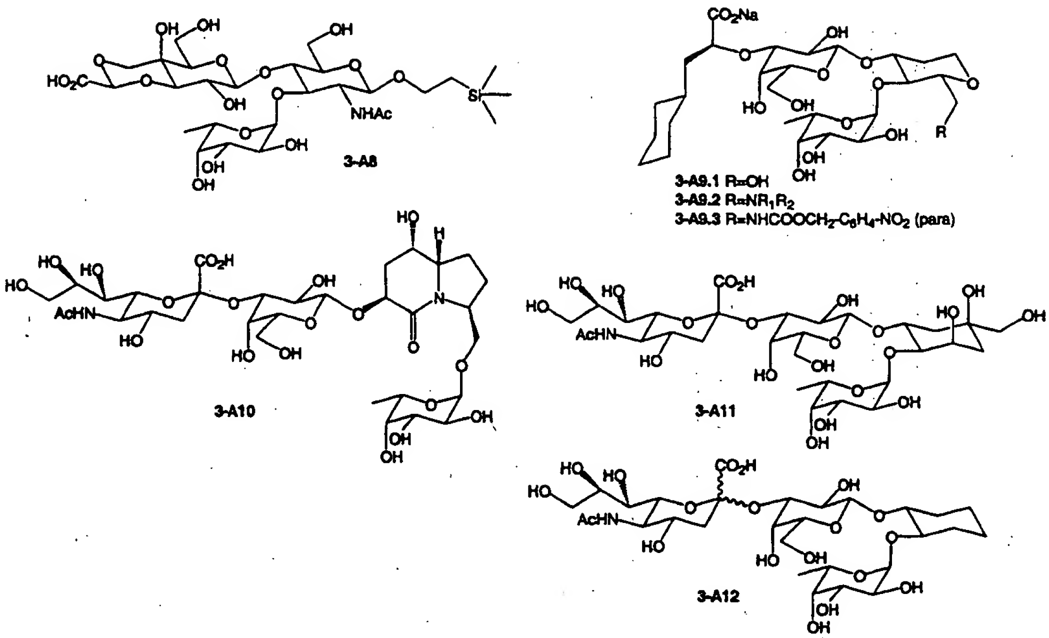

Structure 3-A8 to 3-A12

the GlcNAc monosaccharide with an indolizidinone type unit (**3-A10**). Compound **3-A10** was found to be inactive in an E-selectin cell free assay, but was more active than sLe^x in a P-selectin assay. This group also used quinic acid as a glucosamine replacement (**3-A11**).[96] The cyclohexyl ring of quinic acid should be more stable than a sugar. Compound **3-A11** was found to be as active as sLe^x. Toepfer and coworkers substituted glucose with trans-1,2 cyclohexanediol unit (**3-A12**).[97] This compound exhibited good activity in E- and P-selectin cell based assays. It was three times more potent than sLe^x.

In summary, while the mimics with three sugar units generally possess activity comparable or better than sLe^x they are more useful for studying structure-activity relationships than as potential inhibitors. They suffer from most of the same issues as tetrasaccharide sLe^x analogs, those being cost, stability, and rapid metabolism.

B. Mimics Containing Two Sugars

It has been shown that the *N*-acetyl glucosamine unit is merely a linker between fucose and galactose in sLe^x (see Section 2). There have been several attempts to simplify the sLe^x structure by replacing GlcNAc with groups that will keep the core conformation of sLe^x unchanged. These mimics used either carboxymethyl or alkylated carboxymethyl as sialic acid surrogates. Ragan and Cooper[98] used a simple two-carbon tether to link the galactose, fucose, and a carboxymethyl group as a sialic acid mimic in their dissacharide **3-B1**. Compound **3-B1** displayed weak inhibition in a static E-selectin assay. Mimetics prepared by Wong and collaborators contain ethylene glycol (**3-B1**), butane, cis-olefin, and epoxide as spacers between galactose and fucose (**3-B2**).[99–101] Conformational flexibility of the tethers was blamed for their lack of activity. Prodger's group was one of the first to use 1,2-diols as a glucose replacement.[102–105] They also used the carboxymethyl unit as a sialic acid replacement in their derivatives **3-B3**. Only one compound (**3-B3.2**) where a rigid cyclohexanediol was used as a mimic was found to be equipotent to sLe^x in their E-selectin assay. The diols used contained diverse functional groups and different levels of torsional constraint. Kolb et al. replaced *N*-acetyl glucosamine with R,R-1,2 cyclohexanediol, but used L-phenyl lactic

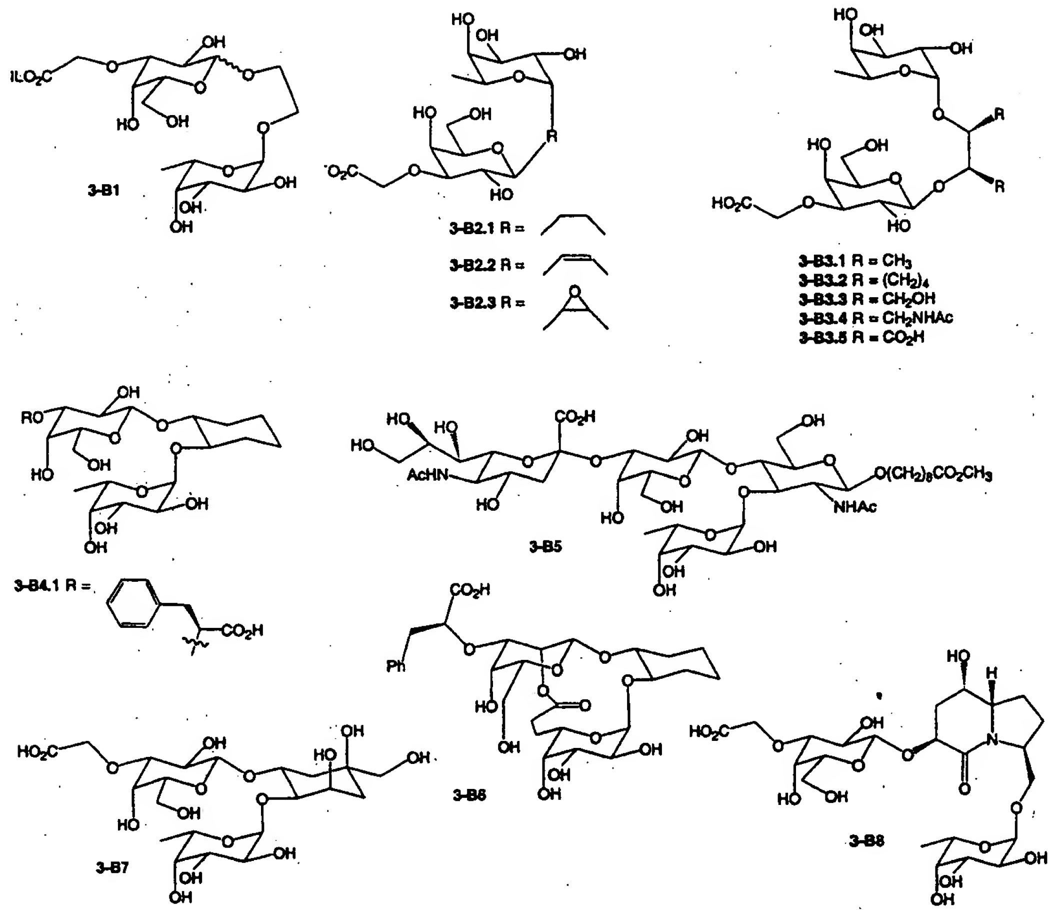

Structure 3-B1 to 3-B8

acid (**3-B4.1**) or L-cyclohexyl lactic acid (**2-2**) as a sialic acid replacement. In their cell free ELISA assay, **3-B4.1** and **2-2** were found to be three and twelve times more potent than a sLe^x derivative (**3-B5**), respectively. Compound **2-2** is a selective E-selectin inhibitor *in vivo*. Following treatment with **2-2**, there was an increase in the leukocyte rolling velocity in TNF-α stimulated mouse cremaster.[106] Encouraged by the positive results, this group prepared several derivatives where the six position of the galactose was modified in compounds **3-B4.1** and **3-B4.2**.[40] Unfortunately, all the compounds were inactive. ($IC_{50} > 10$ mM). They also rigidified compound **3-B4.1** by linking the 6-position of fucose to the 2-position of galactose. The rigid macrocycle **3-B6** was found to be three times less active than **3-B5**.[60] Hanessian's group prepared mimetics where they replace the GlcNAc unit with a quinic acid **3-B7**[96] and indolizidinone-type **3-B8**[74] template. In these compounds, a carboxymethyl group was used to replace the sialic acid residue. Neither of the inhibitors showed any appreciable activity against E-selectin.

Wong's group[107,108] synthesized the 1,1-linked dissacharide **3-B9** using the mannose sugar as a surrogate for fucose due to its better chemical stability and ease of availability. Compound **3-B9** was five times more active than sLe^x in their cell-free E-selectin assay. Encouraged by this result, they modified the **C-6** position of mannose.[109] In the above compounds, the flexible carboxymethyl group was used as a NeuAc substitute. They also synthesized spiro 1,1-galactosyl mannosides **3-B10** in order to put constraints on the orientation of the carboxyl group.[110] Compound **3-B10.2**, where the carboxyl group has a well-defined orientation, was found to be more potent than the more flexible dissacharide **3-B9** against P-selectin.

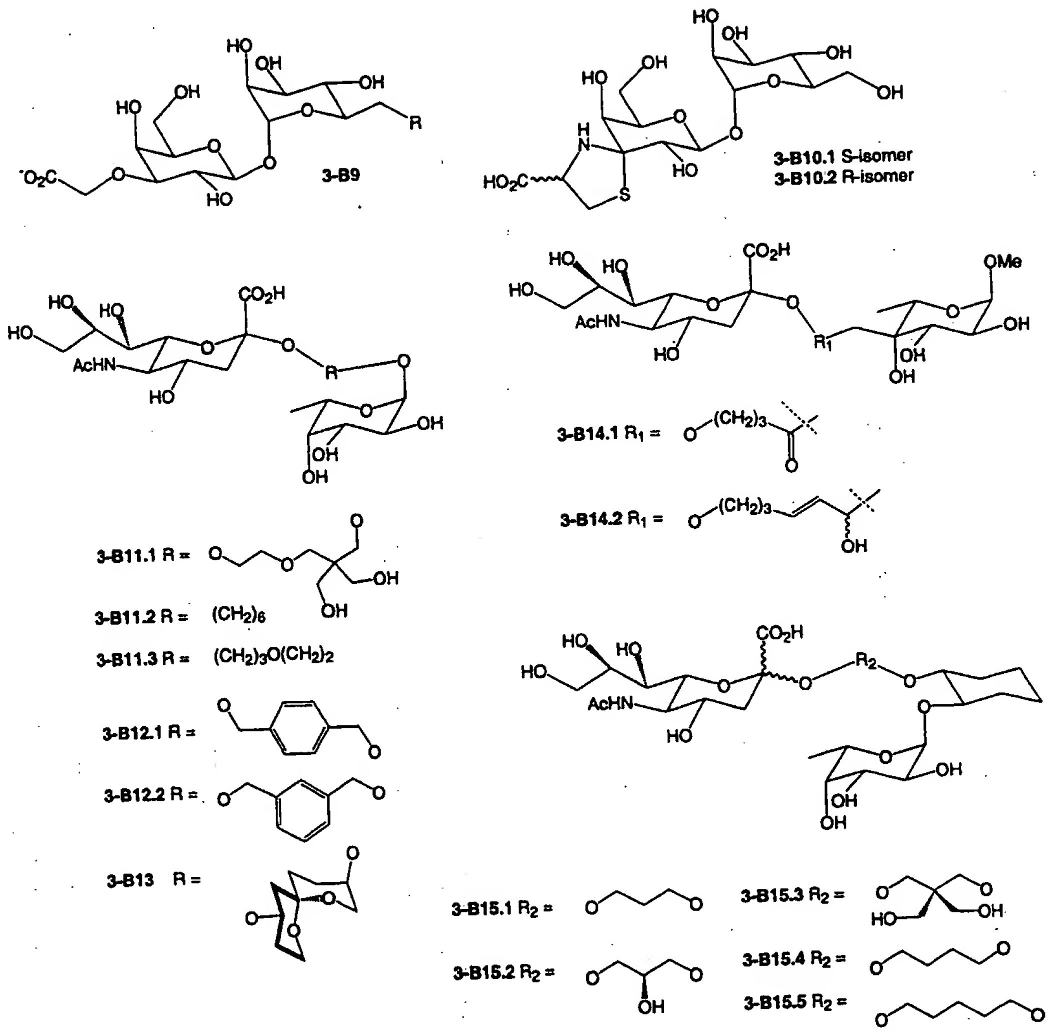

Structure 3-B9 to 3-B15

Another approach is to replace the galactose-*N*-acetylglucosamine disaccharide portion with a linker that will position sialic acid and fucose in a spatially similar arrangement as sLe^x. Some of the spacers used were flexible alkyl chains, as seen in **3-B11.1**,[111] **3-B11.2**,[112] and **3-B11.3**.[113] To date, the unfunctionalized flexible linkers have shown disappointing biological activity. Some groups have argued that the entropic penalty resulting from the extreme flexibility of a simple saturated spacer is the reason for lack of activity. Use of a rigid benzenedimethanol moiety resulted in compounds that were 20-fold less active than sLe^x in a static E-selectin assay (**3-B12**).[114] Prodger and coworkers used an inflexible spiroketal scaffold (**3-B13**).[115] Glycoside **3-B13** showed low levels of inhibition of E-selectin. One factor that could contribute to poor potency in the rigid linkers is the lack of functionalities that imitate the 4- and 6-hydroxyls of galactose, which are also necessary for activity (see Section 2). Allanson and associates used 6-atom chains (**3-B14**) hoping to create a mimic that would not only be a spacer but could also be used to introduce functionality to represent galactose.[116,117] These compounds were either inactive or showed weak binding to activated endothelial cell cultures. Toepfer et al. also observed loss of activity in E- and P-selectin cell based assays when they used propanediol-cyclohexane moieties to substitute for Gal-GlcNAc (**3-B15**).[97]

In summation, mimics for the dissaccharide Gal-GlcNac have delivered disappointing results. Inhibitors that contain fucose and galactose sugars, but use a cyclohexane diol as GlcNAc and phenyl or cyclohexyl lactic acid as a NeuAc replacement have proven to be the most effective. Some of these potent compounds have shown efficacy in animal models. Whether the PK profile of these compounds containing two sugar units will permit their use as orally active drugs remains to be seen.

C. *Mimics Containing One Sugar*

All of the fucose hydroxyls are involved in the binding of sLe^x to the selectins (see Section 2). Since the focus is to reduce the carbohydrate nature of the mimics several efforts have been made to design and synthesize compounds that contain only the fucose sugar bound to an appropriate scaffold to which a carboxyl group is attached. Hanessian prepared some fucosides where the stable carbocycle quinic acid was used as a D-galactose mimic, with a conformationally biased ethylenedioxy tether and a glycolic ether as glucose and sialyl carboxylate mimics, respectively (**3-C1**).[96] Both the compounds were not active against E-selectin. As mentioned earlier, this group has also incorporated β-turn like motifs indolozidinone (**3-C2**) and γ-lactam (**3-C3**)[74] scaffolds in fucosides. Since the use of trans-1,2-cyclohexandiol moiety as a replacement for GlcNAc has met with some success, Toepfer and coworkers used this functionality to prepare a series of mimetics. Their malonic acid derivatives (**3-C4**)[118] showed better activity than the piperidine carboxylic acid compounds (**3-C5**).[119,120] Inhibitors **3-C4.2** and **3-C5.1** showed inhibition of leukocyte adhesion in rat mesenteric venules at 3 mg/kg. The Liu[121] and Banteli[122] groups used aryl-cyclohexyl ether as a replacement for the galactose-glucosamine unit. All of the mimics prepared (**3C-6** and **3-C7**), except **3-C6.4**, were found to be inactive against E-selectin. The authors feel that the use of an aromatic spacer instead of galactose probably does not allow for the preorganization of the molecules needed to fit the binding site.

Wong and coworkers used α-*O*-fucosyl-aminocyclohexanol and α-*O*-fucosyl-threonine as a core structure for the synthesis of some *O*-fucopeptides (**3-C8.1** and **3-C8.2**). In these inhibitors, aminocyclohexanol and threonine are the GlcNAc equivalent with the functionality in the amino acids substituting for the interactions made by the 4- and 6-hydroxyls of galactose. These compounds also have a carboxylate or sulphate containing R group that mimics the NeuAc. A large amount of work done with this class of compounds at the Scripps Research Institute resulted in some very potent selectin inhibitors.[123–129] A new synthetic strategy was developed for the parallel synthesis of some of the fucopeptides. These libraries were prepared by solid phase synthesis using para-acyloxymethylenzlidene acetal as an anchoring group. Wong and collaborators[130] also prepared some glycopeptides (**3-C9**) where L-galactose was used to mimic the L-fucose residue. A series of unnatural amino acids were used to replace the D-galactose of sLe^x. A side chain containing a carboxylate group replaced the sialic acid. The unnatural amino acids used were prepared enzymatically or synthetically. Compound **3-C9.2** was the best mimic (two-fold more active than sLe^x). Researchers from Japan also prepared some *O*-fucosyl peptides (**3-C10**) that show selectin activity.[131]

Researchers at Glycomed[132–134] patented glycosides (mainly fucosides) with naphthyl, flavonoid, and phenyl backbones. Some investigators prepared conformationally rigid analogs of sLe^x which contain fucose bound directly to tetralin,[68,135] naphthalene,[68,134] anthraquinone,[136] or anthracene.[136] Wong and Huang[100] designed **3-C11** where a D-tartaric acid derivative represents the glucosamine and a linear five-carbon spacer linked to a carboxylate replaces the NeuAc-Gal unit. Compound **3-C11** was 10-fold less active than sLe^x against E-selectin.

The use of a mannose residue over fucose was first done by Kogan and co-workers[63] because of considerations of cost, ease of synthesis and better fit in the E-selectin/sLe^x model. The sialic acid was replaced with a carboxymethyl group, and a rigid biphenyl spacer was used in place of the

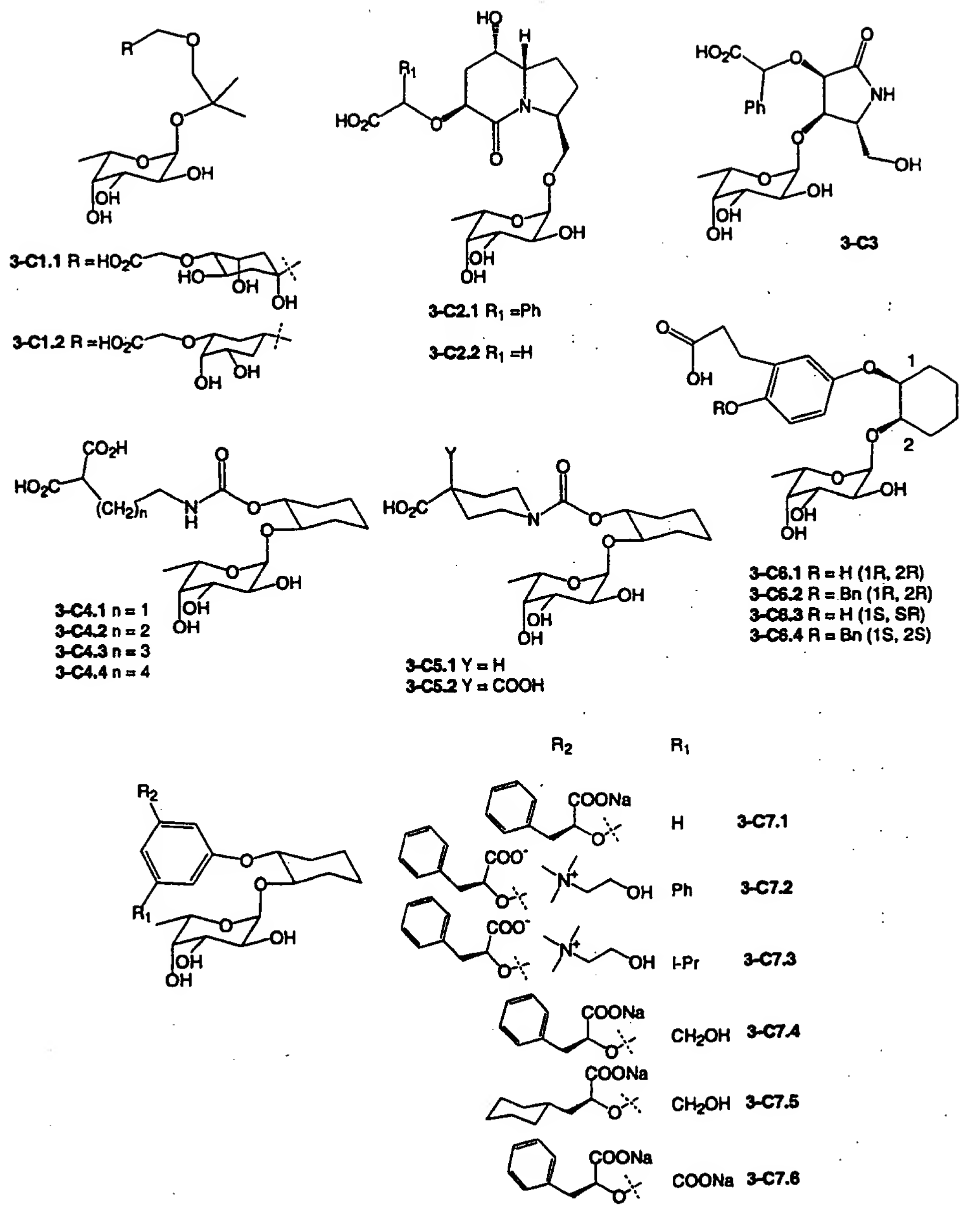

Structure 3-C1 to 3-C7

Gal-GlcNAc dissacharide. A series of (α-D-mannopyranosyloxy)biphenyl-substituted carboxylic acids were prepared. One of the compounds **3-C12.1**, which has only one sugar and is half the molecular weight of sLe^x, was found to be more potent than sLe^x against E- and P-selectin. It lacks functionality to mimic the hydroxyl groups of galactose. The attachment of the mannose ring was varied,[137] which resulted in compounds **3-C12.2** and **3-C12.3**. Both inhibitors showed improved binding compared to sLe^x and **3-C12.1**. Parekh and workers had isolated oligosaccharides containing extended sialyl di-Lewis^x (Sle^x Le^x) from human neutrophils.[138] Hence, Kogan et al.[139] incorporated an additional mannose unit via an appropriate spacer in **3-C12.1** to mimic the sLe^x Le^x unit. Several variations in the arrangement and the number of mannose residues and carboxylic acid groups were made. Modifications in length or atom type in the linker were also studied for a series of

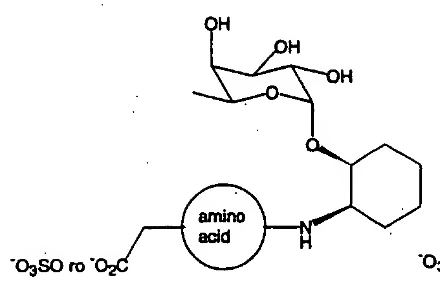

3-C8.1

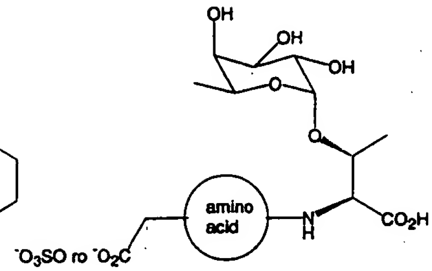

3-C8.2

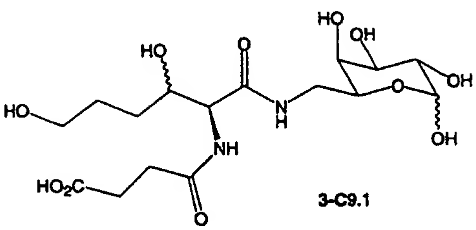

3-C9.1

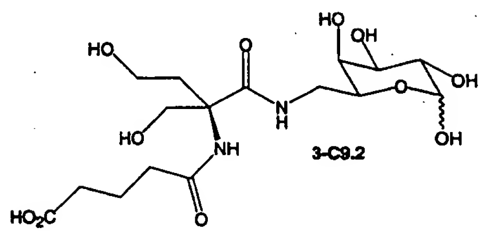

3-C9.2

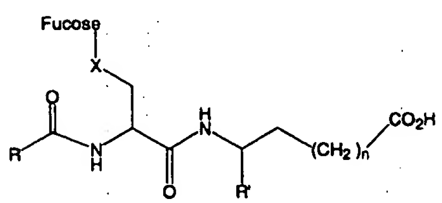

3-C10 X = O or S

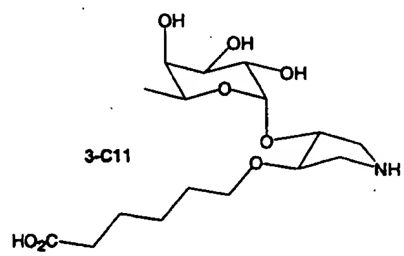

3-C11

Structure 3-C8 to 3-C11

dimer and trimer compounds. Dimer **3-C12.4** (TBC1269) was found to be 6-fold and 50-fold more active than sLe^x in its ability to inhibit the binding of sLe^x expressing HL-60 cells to E- and P-selectin IgG fusion proteins, respectively. The authors suggested that the SAR of the divalent structures indicate that both mannose units bind to the same lectin domain. TBC-1269 is a phase II clinical candidate of Texas Biotechnology for the potential treatment of asthma, reperfusion injury, and psoriasis.[140] Toepfer and Kretzschmar[119] also prepared some piperidine carboxylic acid mannosides **3-C13**. Both compounds were less active than sLe^x against E- and P-selectin. Wong and coworkers prepared some mannosyl phosphonate derivatives (**3-C14**) using enzymatic aldol condensations. These compounds showed moderate inhibition against E- and P-selectin.[141,142] The *O*-glycoside mimetic **3-C14.1** was more active than C-glycoside **3-C14.2**.

Wong and collaborators[101,129] realized that the use of C-glycosides in place of *O*-glycosides would increase the stability of the selectin antagonists towards endogenous glycodidases. Initially, they designed and synthesized fucopeptides[99,101] where the galactose residue was substituted with an amino acid either 4-hydroxy threonine (**3-C15.1**) or threonine (**3-C15.2**). A two or three carbon tether was then used to link the fucose to the amino acid via an amide or ester bond. Only compound **3-C15.1** (X=NH, n = 2) showed inhibition comparable to sLe^x in an E-selectin assay. On a positive note, these compounds were resistant to α-fucosidase and β-galactosidase. This group also used the four component Ugi reaction to prepare a library of C-glycopeptides (**3-C16**).[143] Carbon linked D-mannose or L-fucose replaced the *O*-fucose of sLe^x. Some of the mimics were more active than sLe^x

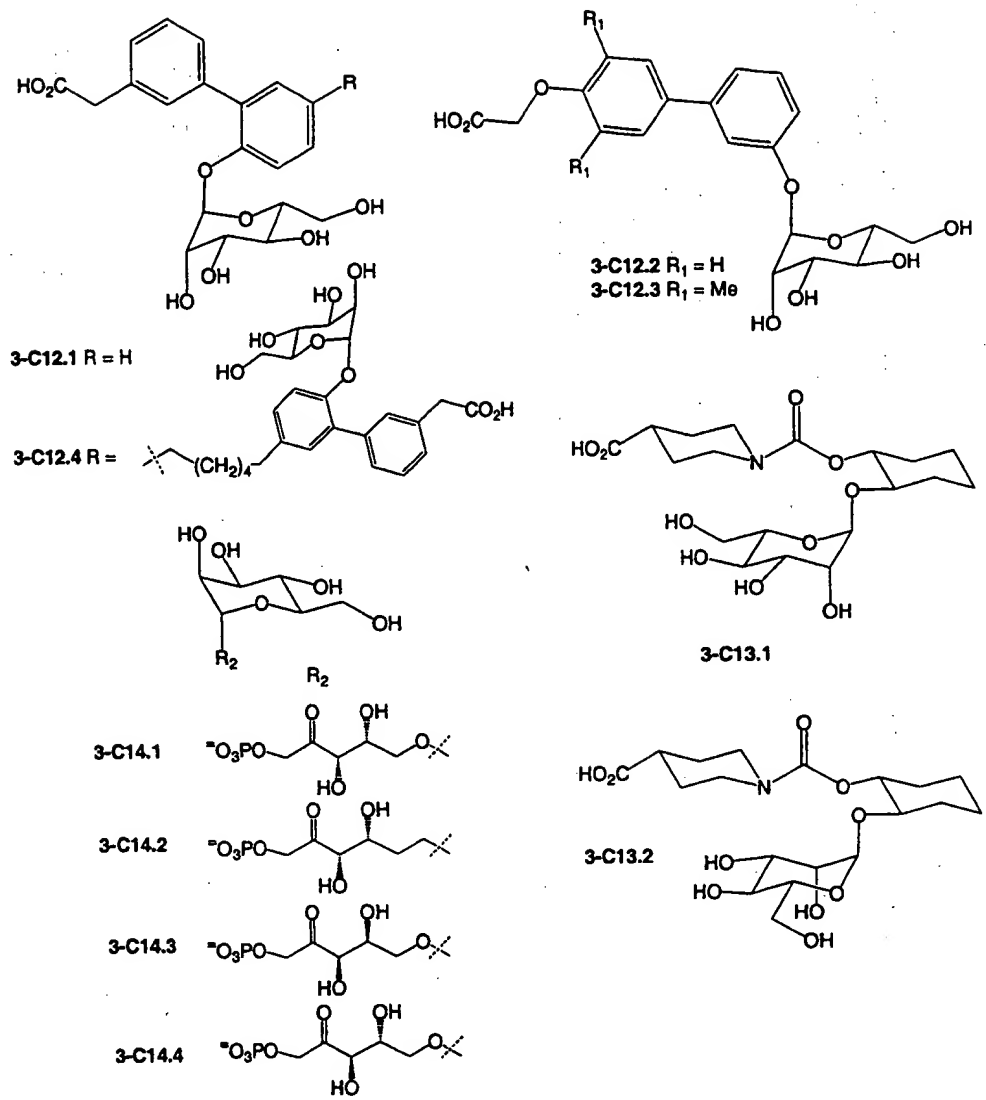

Structure 3-C12 to 3-C14

against P-selectin, but this was not the case for E-selectin. One of the compounds, **3-C17.1**, was found to be fifteen times more potent than sLe^x for P-selectin. A cyclic sLe^x mimic (**3-C17.2**) containing all the functionalities of **3-C17.1** was synthesized at Scripps recently and found to be a 100-fold more active at inhibiting P-selectin.[144] The synthesis of glycomimetic candidates using the Ugi reaction was first accomplished by Armstrong.[145] Some C-linked fucopeptides were patented by Kunz et. al.[146] Aryl C-linked glycosides were designed and synthesized by several groups.[147–151] The aromatic ring functions as a scaffold on which the acid and fucose residues can be placed. Kretzschmar[147] used a flexible saturated chain to link the aryl group to fucose. The aryl group contains functionalities that mimic the NeuAc and the galactose residues. Compound **3-C18** showed comparable inhibition to sLe^x in E- and P-selectin assays. This compound showed 43% inhibition in an *in vivo* leukocyte adhesion assay at 3 mg/kg i.v.[152,153] Satoh[148] attached the aryl ring with carboxylic acid functionality directly to the sugar (**3-C19**). A diverse set of carboxylic acids and sugars were used. These β-C-glycosides were found to be potent inhibitors of P-selectin in a competitive cell-free ELISA assay, showing IC_{50} in the low Micro Molar range. Preparation and use

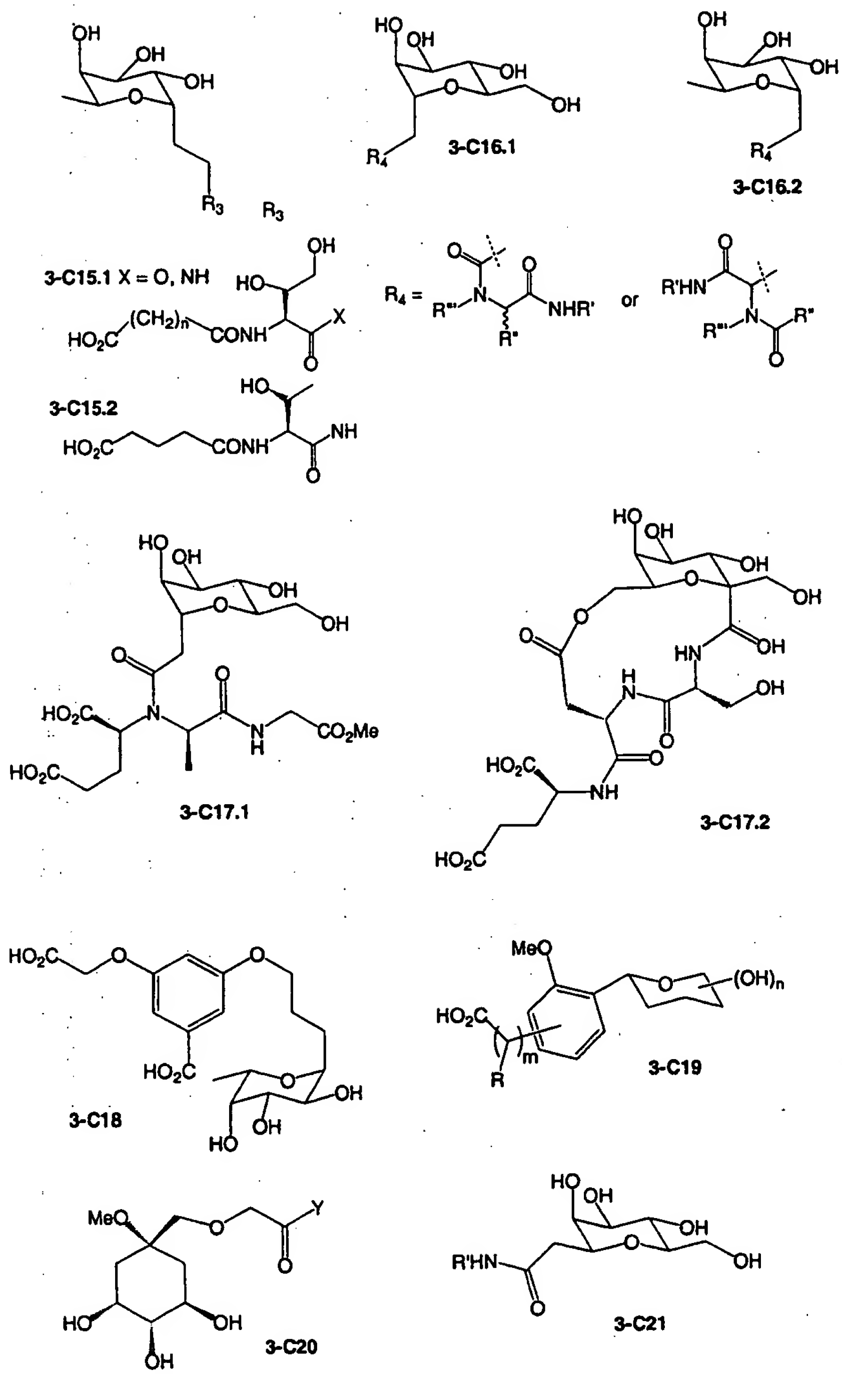

Structure 3-C15 to 3-C21

of benzyl, aryl, and *N*-hydroxyaminoalkyl C-glycoside as selectin antagonists was also reported by other Japanese groups.[150,151,154] Some quinic acid derivatives with the general structure **3-C20**, where Y can be an amino acid or hydroxyl, have shown selectin inhibition.[155] These cyclohexane derivatives should be physiologically more stable.

Researchers at Novartis[156] tried to mimic the conformation of sLe^x by preparing spatially restricted (R)- and (S)-aminoethyl-α-C-mannosides as building blocks for selectin inhibitors. Wong's group used the C-mannose core to produce several selectin antagonists.[133,157] They found α-mannosyl glutamate 2–17 to be five times more potent than sLe^x. Based on modeling results (see section 2) Kaila et al. used the β-mannose scaffold to produce E-selectin inhibitors **3-C21**.[71] Compounds that contained phenyl substituents at the **C-6** position were found to have increased potency. Their most potent compound was five times less potent than sLe^x in an E-selectin ELISA assay.

The activities observed for compounds containing only one carbohydrate unit suggest that non-carbohydrate antagonists of E- and P-selectin are a feasible alternative to sugar-based analogs. TBC 1269 (**3-C12.4**), which is active in several animal models, is the most advanced drug candidate at the moment.

D. High Molecular Weight Selectin Antagonists

This class of compounds will be mentioned only briefly, since the focus of this manuscript is small molecular weight selectin inhibitors. There are several reviews of this area in the literature.[17,158–165] Some of the papers published after the Wong review are cited here. Due to the hetrogeneity of the selectin interactions the most active inhibitors come from this class of compounds. The more potent selectin inhibitors so far are carbohydrates carrying lipophilic tails, high molecular weight charged aggregates, peptides, complex derivatives, and conjugates of the tetrasaccharide sLe^x and its mimetics. All these compounds are unfit for oral drug formulations. Sugar conjugates carrying lipophillic chains and charged aggregates share common structural features with detergents and are dependent on dosage, molecular weight and negative charge distribution/density.[166–169] These may be acting by distortion of the cell membranes in vivo. Kondo's group, in continuation of their work on sLe^x mimetics, synthesized long chain fucofuranosyl Ser-Glu dipeptide and mannosyl Ser-Glu dipeptide that are active against the selectins.[66,67,170] Recently they also developed a pharmacophore model of a sLe^x/E-selectin complex (see Section 2, Fig. 7)[61] and used it to identify a non-carbohydrate selectin inhibitor. Further optimization of the inhibitor resulted in **2-4B**, which was 7-fold more potent than sLe^x toward E-selectin. Slee et al. reported non-carbohydrate imidazole based selectin inhibitors.[70] Based on modeling studies, the authors proposed that these compounds bind in the sLe^x site (see Section 2).

Since the selectin-ligand interactions are multivalent, inhibitors presented in a multivalent form should posses increased potency. This has indeed been the case. Polymers, liposomes, and protein conjugates containing sLe^x or similar carbohydrates have shown increased binding to E- and P-selectins relative to their monomeric derivatives. Recently, Nagy and coworkers demonstrated that addition of anionic groups to the liposome matrix containing polyvalent displays of sLe^x-like oligosacccharide groups has a favorable effect on inhibition.[171] Researchers from Bristol-Myers Squibb showed that malonate substituted galactocerebrosides have a high affinity for P-selectin. They act by mimicking binding to the sLe^x binding pocket.[172] Researchers in Japan recently produced several sLe^x-polysaccharide conjugates and investigated their potential for drug delivery to inflammmatory lesions.[173] Some multivalent polylysine conjugates of **3-A9.1** prepared by Thoma and collaborators showed a 700-fold improvement in potency (compared to **3-A9.1**) against E-selectin in an in vitro cell-based rolling assay.[174]

A peptide-based approach to selectin inhibitors has been examined, since the carbohydrate-protein interactions are weak. Several groups have used phage peptide libraries to isolate and identify peptides that bind successfully to receptors expressed in a tissue specific manner. Fukuda et al. recently screened peptides for their binding to anticarbohydrate antibodies that recognize E-selectin carbohydrate ligands. Using this approach, they successfully identified a heptapeptide that binds to all members of the selectin family.[175] When i.v. injected, this peptide, IELLQAR, inhibited the lung colonization of mouse **B16** melanoma and human lung tumor cells expressing sLe^x. Around

the same time Blaszczyk-Thurin and coworkers isolated a dodecapeptide that might be a selectin inhibitor.[176] Statistically significant reduction of neutrophil recruitment into the intraperitoneal cavity was observed upon administration of this peptide in a murine acute inflammation model *in vivo*. A carbon-fucosylated derivative of the natural substance glycyrrhizin is active against E- and P-selectin in in-vitro assays.[177] In conclusion, even though the molecules in this class are extremely potent selectin inhibitors, they are not ideal candidates for oral drug development.

4. IN VITRO BIOLOGICAL EVALUATION OF SMALL MOLECULES

Since the selectins are involved in the attachment and rolling of leukocytes on the vascular surface, under the influence of shear forces, it gives them some unusual properties. They exhibit fast binding kinetics. The selectins make few interactions with their counter receptors. These contacts are for the most part electrostatic in nature. The overall affinity is weak. The consequence of the natural ligand binding weakly to the receptor necessitates the use of a multimeric presentation of the receptor or the ligand in the assays. For example, it is necessary to utilize avidity in the ELISA-based assays. A multimeric presentation ensures sufficient interactions survive wash steps and produce adequate signal to measure differences in inhibition of binding. A draw back to this approach is that mutimeric interactions lead to inconsistent complex formation, which in turn leads to larger assay variability than typical biological assays. As a result, there are false positives in these non-equilibrium avidity type assays. Also static cell adhesion assays with long interaction times can show in vitro binding that may not be relevant in the flow situations *in vivo*. A variety of assays have been used. These are summarized in Wongs review.[17] Workers at Wyeth/Genetics Institute[20] use a new assay, the Biacore (surface plasmon resonance) inhibition assay for P-selectin. In this assay the sensitivity of the Biacore instrument allows for measurement of the weak monomeric selectin interactions in real time, under equilibrium flow conditions, and therefore, avoids the pitfalls of the avidity assays. The Biacore instrument measures changes in the angle of light reflected from a sensor chip. This measured change is proportional to the mass at the sensor chips surface. Monomeric biotinylated ligand, PSGL-1, is immobilized on a streptavidin (SA) Biacore sensor chip. Soluble P-selectin, at the K_D concentration for the interaction, is flowed over the chip with and without small molecule antagonist (Fig. 9). This assay gives fewer false positives and increases reproducibility.

The use of a biophysical method like NMR is also a valuable tool to avoid some of the described difficulties with traditional assays. In transfer NOE experiments, molecules exhibit strong negative trNOEs when bound to the protein and can be differentiated from non-binding molecules with weak positive NOEs.[178]

Due to the problem with the reproducibility of assay results and the absence of a universal assay, we have not given absolute IC_{50} values for inhibitors in this review. We have tried to express inhibitor potency relative to sLe^x, so that the binding affinities for inhibitors from different groups can be qualitatively compared.

In general, cell interaction assays incorporating physiologically relevant shear forces (e.g., in flow chambers) are more realistic. The in vitro flow assay developed by Patton et al. at Glycotech monitors the rolling of PMN on stimulated human umbilical vein endothelium cells (HUVEC) in a Flow chamber.[93] Video records of bright-field microscopic regions of rolling and arrested cells are analyzed to quantitate inhibition.

Another problem has been encountered in cases where acidic ion exchange resins are used during sLe^x mimetics synthesis. Small amounts of polyanions released from the resin were found to be potent selectin inhibitors especially P-selectin. These polyanions are difficult to remove by chromatography (silica gel, biogel, sephadex, etc.) and not detectable by routine analysis. Several encouraging improvements observed for P-selectin antagonists should be considered with caution.

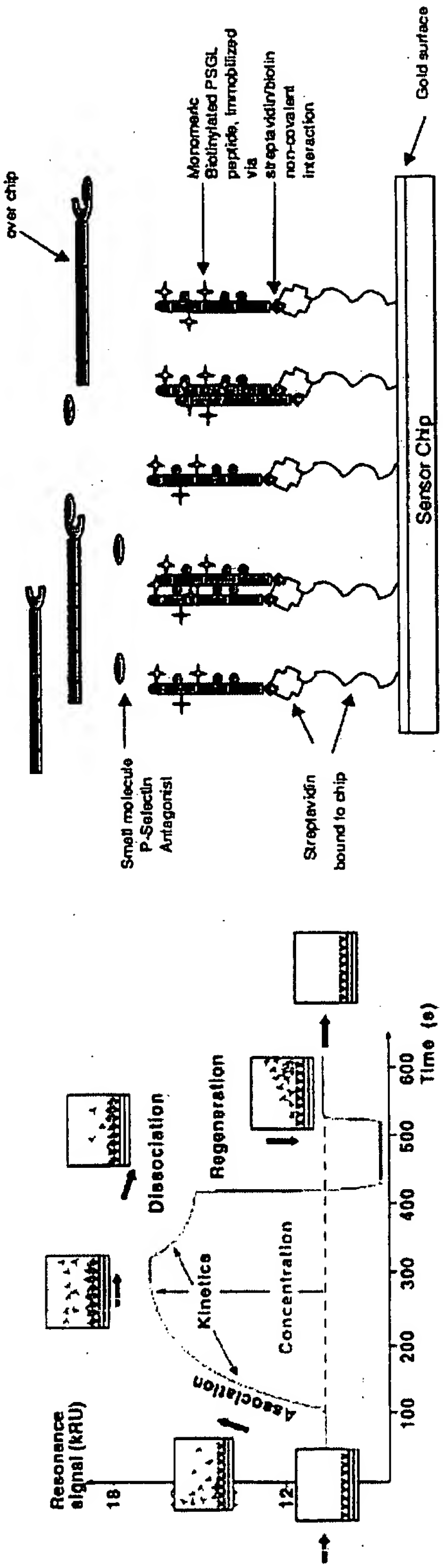

Figure 9. Characterstics of a sensogram, the readout of the Biacore instrument. Inset picture shows events at the sensor chip surface.

This was discussed by Kretzschmar et al. in their paper.[179] Thus, a consequence of the weak selectin—sLe^x binding is variability in assays and one must keep in mind the importance of assay conditions used when identifying potential ligands.

5. CONCLUSIONS

One strategy for the development on novel anti inflammatory therapeutics is the interruption of the leukocyte endothelium interaction. Clearly the disruption of the initial step in the cascade, i.e., attachment and rolling of leukocytes mediated by PSGL-1 (sLe^x) and the selectins is a viable approach. Sialyl $Lewis^x$ is a good starting point for the design of selectin antagonists and has been used by several groups to design selectin inhibitors with low molecular weight, modified physical properties, decreased synthetic complexity, and a reduced carbohydrate nature. Unfortunately, none of these sLe^x mimics have yet been developed into an approved drug. There are several reasons for this. The sLe^x binding site is flat and generally hydrophilic, particularly when compared to a typical drug target. The interactions between the ligand and receptor are primarily electrostatic in nature, with few other contacts being made. The inherent low affinity of sLe^x for the selectins is required by the role it plays in the attachment and rolling process, which suggests that the binding site has evolved to optimize the specificity and the weakness of the interactions with sLe^x. It may be reasonable to assume that the development of high-affinity antagonists for a binding site that has been evolved for weak interactions with a readily degradable ligand may be more difficult than the traditional drug target. In addition, carbohydrate-based molecules are generally prone to rapid metabolism and elimination. Finally, the lack of general testing protocols applicable in different research laboratories creates issues with biological evaluation.

The recently determined X-ray crystal structures of human LE-P-selectin with sLe^x and with a truncated human PSGL-1, as well as human LE-E-selectin with sLe^x, provide new insight into the nature of the interactions that result in the reduction of leukocyte rolling. This new information concerning the interactions between sLe^x and the selectins, along with the knowledge that a second potentially drugable binding site exists proximal to the sLe^x binding site, should be the impetuous for the design and development of novel selectin inhibitors. One could envision the design of novel non-carbohydrate based inhibitors specifically directed towards the PSGL-1 peptide binding site.

At present no inhibitors of selectin-mediated cellular adhesion are on the market. In 1998, a phase IIA clinical trial studying the intravenous use of TBC-1269 in asthma was completed In this study, TBC-1269 demonstrated statistically significant improvements over placebo as measured by eosinophil recruitment. An inhaled formulation of TBC-1269 is currently in a phase I clinical trial. A recombinant soluble PSGL-1 chimera (rPSGL-Ig) is currently in Phase II clinical trials for acute myocardial infarction. Recombinant PSGL-1 comprises the first 47 amino acids from the N-terminal end of the extracellular domain of mature PSGL-1 fused at the hinge region of IgG1. The search for an orally administered selectin-based prophylactic type treatment for inflammation is still ongoing.

ACKNOWLEDGMENT

We thank Patty Bedard of WYETH for Figures 1 and 9.

REFERENCES

1. Geng JG, Bevilacqua MP, Moore KL, McIntyre TM, Prescott SM, Kim JM, Bliss GA, Zimmerman GA, Mcever RP. Rapid neutrophil adhesion to activated endothelium mediated by GMP-140. Nature 1990;343:757–760.

2. Hattori R, Hamilton KK, Fugate RD, McEver RP, Sims PJ. Stimulated secretion of endothelium von Willebrand factor is accompanied by rapid redistribution to the cell surface of the intracellular granule membrane protein GMP-140. J Biol Chem 1989;264:7768–7771.
3. Bevilacqua MP, Pober JS, Mendrick DL, Cotran RS, Gimbrone MA Jr. Identification of an inducible endothelial-leukocyte adhesion molecule. Proc Natl Acad Sci USA 1987;84:9238–9242.
4. Gallatin WM, Weissman IL, Butcher EC. A cell-surface molecule involved in organ-specific homing of lymphocytes. Nature 1983;304:30–34.
5. Lewinsohn DM, Bargatze RF, Butcher EC. Leukocyte-endothelial cell recognition: Evidence of a common molecular mechanism shared by neutrophils, lymphocytes, and other leukocytes. J Immunol 1987;138:4313–4321.
6. Jung U, Norman KE, Ramos CL, Scharffetter-Kochanek K, Beaudet AL, Ley K. Transit time of leukocytes rolling through venules controls cytokine-induced inflammatory cell recruitment in vivo. J Clin Invest 1998;102:1526–1533.
7. Springer TA. Traffic signals for lymphocyte recirculation and leukocyte emigration: The multistep paradigm. Cell 1994;76:301–314.
8. Vestweber D, Blanks JE. Mechanisms that regulate the function of the selectins and their ligands. Physiol Rev 1999;79:181–213.
9. Pouyani T, Seed B. PSGL-1 recognition of P-selectin is controlled by a tyrosine sulfation consensus at the PSGL-1 amino terminus. Cell 1995;83:333–343.
10. Sako D, Comess KM, Barone KM, Camphausen RT, Cumming DA, Shaw GD. A sulfated peptide segment at the amino terminus of PSGL-1 is critical for P-selectin binding. Cell 1995;83:323–331.
11. Wilkins PP, Moore KL, McEver RP, Cummings RD. Tyrosine sulfation of P-selectin glycoprotein ligand-1 is required for high affinity binding to P-selectin. J Biol Chem 1995;270:22677–22680.
12. Ley K, Bullard DC, Arbones ML, Bosse R, Vestweber D, Tedder TF, Beaudet AL. Sequential contribution of L- and P-selectin to leukocyte rolling in vivo. J Exp Med 1995;181:669–675.
13. Mayadas TN, Johnson RC, Rayburn H, Hynes RO, Wagner DD. Leukocyte rolling and extravasation are severly compromised in P-selectindeficient mice. Cell 1993;74:541–554.
14. Bullard DC, Kunkel EJ, Kubo H, Hicks MJ, Lorenzo I, Doyle NA, Doerschuk CM, Ley K, Beaudet AL. Infectious susceptibility and severe deficiency of leukocyte rolling and recruitment in E-selectin and P-selectin double mutant mice. J Exp Med 1996;183:2329–2336.
15. Frenette PS, Mayadas TN, Rayburn H, Hynes RO, Wagner DD. Susceptibility to infection and altered hematopoiesis in mice deficient in both P- and E-selectins. Cell 1996;84:563–574.
16. Klaus L. Functions of selectins. Results Probl Cell Differ 2000;33:177-200. (For recent reviews in the area of selectins see references 8, 16–19.)
17. Simanek EE, McGarvey GJ, Jablonowski JA, Wong C-H. Selectin-carbohydrate interactions: From natural ligands to designed mimics. Chem Rev 1998;98:833–862.
18. Ebnet K, Vestweber D. Molecular mechanisms that control leukocyte extravasation: The selectins and the chemokines. Histochem Cell Biol 1999;112:1–23.
19. Dasgupta F. Selectin antagonists. High throughput screening for novel anti-inflammatories 2000;123–144.
20. Somers WS, Tang J, Shaw GD, Camphausen RT. Insight into the molecular basis of leukocyte tethering and rolling revealed by structures of P- and E-selectin bould to sLe^x and PSGL-1. Cell 2000;103:467–479.
21. Erbe DV, Wolitzky BA, Presta LG, Norton CR, Ramos RJ, Burns DK, Rumberger JM, Rao BNN, Foxall CR, Brandley BH, Lasky LA. Identification of an E-selectin region critical for carbohydrate recognition and cell adhesion. J Cell Biol 1992;119:215–227.
22. Siegelman MH, Cheng IC, Weissman IL, Wakeland EK. The mouse lymph node homing receptor is identical with the lymphocyte cell surface marker Ly-22: Role of the EGF domain in endothelial binding. Cell 1990;61:611–622.
23. Watson SR, Imai Y, Fennie C, Geoffrey J, Singer M, Rosen SD, Lasky LA. The complement binding-like domains of the murine homing receptor facilitate lectin activity. J Cell Biol 1991;115:235–243.
24. Kansas GS, Saunders KB, Ley K, Zakrzewicz A, Gibson RM, Furie BC, Furie B, Tedder TF. A role for the epidermal growth factor-like domain of P-selectin in ligand recognition and cell adhesion. J Cell Biol 1994;124:609–618.

25. Li SH, Burns DK, Rumberger JM, Presky DH, Wilkinson VL, Anostario M Jr, Wolitzky BA, Norton CR, Familleti PC, Kim KJ, Goldstein AL, Cox DC, Huang K-S. Consensus repeat domains of E-selectin enhance ligand binding. J Biol Chem 1994;269:4431–4437.
26. Bartgatze RF, Kurk S, Watts G, Kishimoto TK, Speer CA, Jutila MA. In vivo and in vitro functional examination of a conserved epitope of L- and E-selectin crucial for leukocyte-endothelial cell interactions. J Immunol 1994;152:5814–5825.
27. Gibson RM, Kansas GS, Tedder TF, Furie B, Furie BC. Lectin and epidermal growth factor domains of P-selectin at physiologic density are the recognition unit for leukocyte binding. Blood 1995;85:151–158.
28. Kolbinger F, Patton JT, Geisenhoff G, Aenis A, Li X, Katopodis AG. The carbohydrate-recognition domain of E-selectin is sufficient for ligand binding under both static and flow conditions. Biochemistry 1996;35:6385–6392.
29. Weis WI, Drickamer K, Hendrickson WA. Structure of a C-type mannose-binding protein complexed with an oligosaccharide. Nature 1992;360:127–134.
30. Wright CS. Refinement of the crystal structure of wheat germ agglutinin isolectin 2 at 1.8 A resolution. J Mol Biol 1987;194:501–529.
31. Bourne Y, Rouge P, Cambillau C. X-ray structure of a (alpha-Man(1-3)beta-Man(1-4)GlcNAc)-lectin complex at 2.1-A resolution. The role of water in sugar-lectin interaction. J Biol Chem 1990;265:18161–18165.
32. Shaanan B, Lis H, Sharon N. Structure of a legume lectin with an ordered N-linked carbohydrate in complex with lactose. Science 1991;254:862–866.
33. Naismith JH, Emmerich C, Habash J, Harop SJ, Helliwell JR, Hunter WN, Rafetery J, Kalb AJ, Yariv J. Refined structure of concanavalin A complexed with methyl α-D-mannopyranoside at 2.0. ANG. resolution and comparison with the saccharide-free structure. Acta Crystallogr 1994;D50:847–858.
34. Graves BJ, Crowther RL, Chandram C, Rumberger JM, Li S, Huang K-S, Presky DH, Familletti PC, Wolitzky BA, Burns DK. Insight into e-selectin/ligand interaction from the crystal structure and mutagenesis of the lec/EGF domains. Nature 1994;367:532–538.
35. Ng KK-S, Weis WI. Structure of a selectin-like mutant of mannose-binding protein complexed with sialylated and sulfated Lewis^x oligosaccharides. Biochemistry 1997;36:979–988.
36. Ramphal JY, Zheng Z-L, Perez C, Walker LE, DeFrees SA, Gaeta FCA. Structure-activity relationships of sialyl lewis x-containing oligosaccharides. 1. Effect of modifications of the fucose moiety. J Med Chem 1994;37:3459–3463.
37. Brandley BK, Kiso M, Abbas S, Nikrad P, Srivasatava O, Foxall C, Oda Y, Hasegawa A. Structure-function studies on selectin carbohydrate ligands. Modifications to fucose, sialic acid, and sulphate as a sialic acid replacement. Glycobiology 1993;3:633–639.
38. Henrichsen D, Ernst B, Magnani JL, Wang W-T, Meyer B, Peters T. Bioaffinity NMR spectroscopy: Identification of an E-selectin antagonist in a substance mixture by transfer NOE. Angew Chem Int Ed Engl 1999;38:98–102.
39. Stahl W, Sprengard U, Kretzschmar G, Kunz H. Synthesis of deoxy sialyl Lewis^x analogues. Potential selectin antagonists. Angew Chem Int Ed Engl 1994;22:2096–2098.
40. Banteli R, Ernst B. Synthesis of sialyl Lewis^x mimics. Modifications of the 6-position of galactose. Bio Med Chem Lett 2001;11:459–462.
41. Tyrrell D, James P, Rao N, Foxall C, Abbas S, Dasgupta F, Nashed M, Hasegawa A, Kiso M, Asa D, Kidd J, Brandley BK. Structural requirements for the carbohydrate ligand of E-selectin. Proc Natl Acad Sci USA 1991;88:10372–10376.
42. Ohmoto H, Nakamura K, Inoue T, Kondo N, Inoue Y, Yoshino K, Kondo H, Ishida H, Kiso M, Hasegawa A. Sudies on selectin blockers. 1. Structure-activity relationships of sialyl Lewis^x analogs. J Med Chem 1996;39:1339–1343.
43. DeFrees SA, Gaeta FCA, Lin YC, Ichikawa Y, Wong C-H. Ligand recognition by E-selectin: Analysis of conformation and activity of synthetic monomeric and bivalent sialyl Lewis X analogs. J Am Chem Soc 1993;115:7549–7550.
44. Hiramatsu Y, Tsujishita H, Kondo H. Studies on selectin blockers. 3. Investigation of the carbohydrate ligand sialyl Lewis^x recognition site of P-selectin. J Med Chem 1996;39:4547–4553.

45. Wada Y, Saito T, Matsuda N, Ihmoto H, Yoshino K, Ohashi M, Kondo H, Ishida H, Kiso M, Hasegawa A. Studies on selectin blockers. 2. Novel selectin blocker as potential therapeutics for inflammatory disorders. J Med Chem 1996;39:2055–2059.
46. Ball GE, O'Neill RA, Schultz JE, Lowe JB, Weston BW, Nagy JO, Brown EG, Hobbs CJ, Bednarski MD. Synthesis and structural analysis using 2-D NMR of sialyl Lewis X (SLex) and Lewis X (Lex) oligosaccharides: Ligands related to E-selectin [ELAM-1] binding. J Am Chem Soc 1992;114:5449–5451.
47. Ichikawa Y, Lin C-Y, Dumas DP, Shen G-J, Garcia-Junceda E, Williams MA, Bayer R, Ketcham C, Walker LE, Paulson JC, Wong C-H. Chemical-enzymatic synthesis and conformational analysis of sialyl Lewis X and derivatives. J Am Chem Soc 1992;114:9283–9298.
48. Lin C-Y, Hummel CW, Huang D-H, Ichikawa Y, Nicolaou KC, Wong C-H. Conformational studies of sialyl Lewis X in aqueous solution. J Am Chem Soc 1992;114:5452–5454.
49. Cooke RM, Hale RS, Lister SG, Shah G, Weir MP. The conformation of the sialyl Lewis^x ligand changes upon binding to E-selectin. Biochemistry 1994;33:10591–10596.
50. Rutherford TJ, Spackman DG, Simpson, PJ, Homans SW. 5 nanosecond molecular dynamics and NMR study of conformational transitions in the sialyl-Lewis X antigen. Glycobiology 1994;4:59–68.
51. Poppe L, Brown GS, Philo JS, Nikrad PV, Shah BH. Conformation of sLe^x tetrasaccharide, free in solution, and bound to E-, P-, and L-selectin. J Am Chem Soc 1997;119:1727–1736.
52. Harris R, Kiddle, GR, Field RA, Milton MJ, Ernst B, Magnani JL, Homans SW. Stable-isotope-assisted NMR stidues on ^{13}C-enriched sialyl Lewis^x in solution and bound to E-selectin. J Am Chem Soc 1999;121:2546–2551.
53. Hensley P, McDervitt PJ, Brooks I, Trill JJ, Field JA, McNulty DE, Connor JR, Griswold DE, Kumar NV, Kopple KD, Carr SA, Dalton BJ, Johanson KJ. The soluble form of E-selectin is an asymmetric monomer. Expression, purification, and characterization of the recombinant protein. J Biol Chem 1994;269:23949–23958.
54. Scheffler K, Ernst B, Katopodis A, Magnani JL, Wang WT, Weisemann R, Peters T. Determination of the bioactive conformation of the carbohydrate ligand in the E-selectin/sialyl Lewis^x complex. Angew Chem Int Ed Engl 1995;34:1841–1844.
55. Scheffler K, Brisson J-R, Weisemann R, Magnani JL, Wong WT, Ernst B, Peters TJ. Application of homonuclear 3D NMR experiments and 1D analogs to study the conformation of sialyl Lewis^x bound to E-selectin. Biomol NMR 1997;9:423–436.
56. Kogan TP, Revelle BM, Tapp S, Scott D, Beck PJ. A single amino acid residue can determine the ligand specificity of E-selectin. J Biol Chem 1995;270:14047–14055.
57. Ernst B, Dragic Z, Marti S, Müller C, Wagner B, Jahnke W, Magnani JL, Norman KE, Oehrlein R, Peters T, Kolb HC. Design and synthesis of E-selectin antagonists. Chimia 2001;55:268–274.
58. Kolb HC, Ernst B. Development of tools for the design of selectin antagonists. Chem Eur J 1997;3:1571–1578.
59. Kolb HC, Ernst B. Recent progress in the glycodrug area. Pure Applied Chem 1997;69:1879–1884.
60. Kolb HC. Design and synthesis of a macrocyclic E-selectin antagonist. Bio Med Chem Lett 1997;7:2629–2634.
61. Hiramatsu Y, Tsukida T, Nakai Y, Inoue Y, Kondo H. Study on selectin blocker. 8. Lead discovery of a non-sugar antagonist using a 3D-pharmacophore model. J Med Chem 2000;43:1476–1483.
62. Rao BNN, Anderson MB, Musser JH, Gilbert JH, Schaefer ME, Foxall C, Brandley BK. Sialyl Lewis^x mimics derived from a pharmacophore search are selectin inhibitors with anti-inflammatory activity. J Biol Chem 1994;269:19663–19666.
63. Kogan TP, Dupre B, Keller, KM, Scott IL, Bui H, Market RV, Beck PJ, Voytus JA, Revelle BM, Scott D. Rational design and synthesis of small molecule, non-oligosaccharide selectin inhibitors: (α-D-mannosepyranosyloxy)biphenyl-substituted carboxylic acids. J Med Chem 1995;38:4976–4984.
64. Tsujishita H, Hiramatsu Y, Kondo N, Ohmoto H, Kondo H, Kiso M, Hasegawa A. Selectin-ligand interactions revealed by molecular dynamics simulation in solution. J Med Chem 1997;40:362–369.
65. Tsukida T, Hiramatsu Y, Tsujishita H, Kiyoi T, Yoshida M, Kurokawa K, Moriyama H, Ohmoto H, Wada Y, Saito T, Kondo H. Studies on selectin blockers. 5. Design, synthesis, and biological profile of sialyl Lewis^x mimetics based on modified serine-glutamic acid dipeptides. J Med Chem 1997;40:3534–3541.

66. Tsukida T, Moriyama H, Kurokawa K, Achiha T, Inoue Y, Kondo H. Studies on selectin blockers. 7. Structure-activity relationships of sialyl Lewis^x mimetics based on modified ser-glu dipeptides. J Med Chem 1998;41:4279–4287.
67. Hiramatsu Y, Moriyama H, Kiyoi T, Tsukida T, Inoue Y, Kondo H. Studies on selectin blockers. 6. Discovery of homologous fucose sugar unit necessary for E-selectin binding. J Med Chem 1998;41: 2302–2307.
68. Murphy PV, Hubbard RE, Manallack DT, Wills RE, Montana JG, Taylor RJK. The design, synthesis, and evaluation of novel conformationally rigid analogues of sialy Lewis^x. Bio Med Chem Lett 1998;6:2421–2439.
69. De Vleeschauwer M, Vaillancourt M, Goudreau N, Guindon Y, Gravel D. Design and synthesis of a new sialyl Lewis^x mimetic: How selective are the selectin receptors? Bio Med Chem Lett 2001;11:1109–1112.
70. Slee DH, Romano S, Yu J, Nguyen TN, John JK, Raheja NK, Axe FU, Jones TK, Ripka WC. Development of potent non-carbohydrate imidazole-based small molecule selectin inhibitors with anti-inflammatory activity. J Med Chem 2001;44:2094–2107.
71. Kaila N, Thomas BE, Thakker P, Alvarez JC, Camphausen RT, Crommie D. Design and synthesis of sialyl Lewis^x mimics as E-selectin inhibitors. Bio Med Chem Lett 2001;11:151–155.
72. DeFrees SA, Gaeta FCA, Gaudino JJ, Zheng Z, Hayashi M. Sialyl Lewis^x analogues as inhibitors of cellular adhesion. Unites States Patent 5604207. 1997. (See reference 17 and for recent references see 79–86.)
73. Ida T, Oohira Y, Preparation of fluorine-containing sialyl lewis^x derivative having activity of inhibiting selectin cell adhesion and its intermediates. Jpn Kokai Tokkyo Koho JP 09052902 A2. 1997.
74. Hanessian S, Huynh HK, Reddy GV, McNaughton-Smith G, Ernst B, Kolb HC, Magnani J, Sweeley C. Exploration of β-turn scaffolding motifs as components of sialyl lewis^x mimetics and their relevance to P-selectin. Bioorg Med Chem Lett 1998;8:2803–2808.
75. Wong C-H, Lin C-C, Woltering TJ, Weitz-Schmidt G. Preparation of liposomic sialyl lewis^x mimetics as selectin inhibitors. PCT Int Appl WO9910359. 1999.
76. Matta KL, Jain RK. Synthetic core 2-like branched structures as ligands for selectins. European Patent 0919563A2. 1999.
77. Xia J, Alderfer JL, Matta KL. Chemical Synthesis of a core 2 branched pentasaccharide containing a carboxylate group. Bioorg Med Chem Lett 2000;10:2485–2487.
78. Kuznik G, Unverzagt C, Horsch B, Kretzschmar G. Chemical and enzymatic synthesis of modified sialyl lewis^x tetrasaccharides with high affinity for E- and P-selectin. J Prakt Chem 2000:342:745–752.
79. Lefer DJ. Pharmacology of selectin inhibitors in ischemia/reperfusion states. Ann Rev Pharmacol Toxicol 2000;40:283–294.
80. Yuen C-T, Bezouska K, O'Brien J, Stoll M, Lemoine R, Lubineau A, Kiso M, Hasegawa A, Bockovich NJ, Nicolaou KC, Feizi T. Sulfated blood group Lewis^a. J Biol Chem 1994;269:1595–1598.
81. Koenig A, Jain R, Vig R, Norgard-Sumnicht KE, Matta KL, Varki A. Selectin inhibition: Synthesis and evaluation of novel sialylated, sulfated and fucosylated oligosaccharides, including the major capping group of GlyCAM-1. Glycobiology 1997;7:79–93.
82. Singh K, Fernandez-Mayoralas A, Martin-Lomas M. Synthesis of oligosaccharides structurally related to E-selectin ligands. J Chem Soc Chem Commun 1994;775–776.
83. Abbas SA, Falguni D, Darwin A, Musser JH, Nashed MA. Substituted lactose derivatives. United States Patent 5591835. 1997.
84. Manning DD, Bertozzi CR, Pohl NL, Rosen SD, Kiessling LL. Selectin-saccharide interactions: Revealing structure-function relationships with chemical synthesis. J Org Chem 1995;60:6254–6255.
85. Ohmoto H, Nakamura K, Inoue T, Kondo N, Inoue Y, Yoshino K, Kondo H. Studies on selectin blockers. 1. Structure-activity relationships of sialyl lewis^x analogs. J Med Chem 1996;39:1339–1343.
86. Imazaki N, Koike H, Miyauchi H, Hayashi M. Stereoselective synthesis of Lewis-associated trisaccharides as E-selectin inhibitors. Bioorg Med Chem Lett 1996;6:2043–2048.
87. Borbas A, Szabovik G, Antal Z, Herczegh P, Agocs A, Liptak A. Sulfonomethyl analogues of aldos-2-ulosonic acids. Synthesis of a new sialyl lewis^x analogue. Tetrahedron Lett 1999;40:3639–3642.
88. Borbas A, Szabovik G, Antal Z, Feher K, Csavas M, Szilagyi L, Herczegh P, Liptak A. Sulfonic acid analogues of the sialyl lewis^x tetrasaccharide. Tetrahedron: Assym 2000;11:549–566.

89. Manning DD, Bertozzi CR, Rosen SD, Kiessling LL. Tin-mediated phosphorylation: Synthesis and selectin binding of a phospho lewis[a] analog. Tetrahedron Lett 1996;37:1953–1956.
90. Musser JH, Rao N, Nashed M, Dasgupta F, Abbas S, Nematalla A, Date V, Foxall C, Asa D. (Trends in drug research, Chapter 3.) Pharmacochem Libr 1993;20:33–40.
91. Thoma G, Schwarzenbach F, Duthaler RO. Synthesis of a sialyl lewis[x] mimic with fixed carboxylic acid group: Chemical approach toward the elucidation of the bioactive conformation of sialyl lewis[x]. J Org Chem 1996;61:514–524.
92. Thoma G, Kinzy W, Burns C, Patton JT, Magnani JL, Banteli R. Synthesis and biological evaluation of a potent E-selectin antagonist. J Med Chem 1999;42:4909–4913.
93. Bantelli R, Herold P, Bruns C, Patton JT, Magnani JL, Thoma G. Potent E-selectin antagonists. Helv Chim Acta 2000;83:2893–2907.
94. Thoma G, Magnani JL, Patton JT. Synthesis and biological evaluation of a sialyl lewis[x] mimic with significantly improved E-selectin inhibition. Bioorg Med Chem Lett 2001;11:923–925.
95. Thoma G, Banteli R, Kinzy W. Derivatives of sialyl lewis[x] and a, in which the natural neuraminic acid residue and the natural *N*-acetylglucosamine monomer are replaced. Intenational Patent WO 06730. 1998.
96. Hanessian S, Reddy GV, Huynh HK, Pan J, Pedatella S. Design and synthesis of sialyl Le[x] mimetics based on carbocyclic scaffolds derived from (–) quinic acid. Bioorg Med Chem Lett 1997;7:2729–2734.
97. Toepfer A, Kretzschmar G, Bartnik E. Synthesis of novel mimetics of the sialyl lewis[x] determinant. Tetrahedron Lett 1995;36:9161–9164.
98. Ragan JA, Cooper K. Synthesis of a galactose-fucose disaccharide mimic of sialyl lewis[x]. Bioorg Med Chem Lett 1994;4:2563–2566.
99. Uchiyama T, Vassilev VP, Kajimoto T, Wong W, Huang H, Lin C-C, Wong C-H. Design and Synthesis of sialyl lewis[x] mimetics. J Am Chem Soc 1995;117:5395–5396.
100. Huang H, Wong C-H. Synthesis of biologically active sialyl lewis[x] mimetics. J Org Chem 1995;60:3100–3106.
101. Uchiyama T, Woltering TJ, Wong W, Lin C-C, Kajimoto T, Takebayashi M, Weitz-Schmidt G, Asakura T, Noda M, Wong C-H. Design and synthesis of C-linked fucosides as inhibitors of E-selectin. Bioorg Med Chem 1996;4:1149–1165.
102. Prodger JC, Bamford MJ, Gore PM, Holmes DS, Saez V, Ward P. Synthesis of a novel sialyl lewis[x]. Tetrahedron Lett 1995;36:2339–2342.
103. Prodger JC, Bamford MJ, Bird MI, Gore PM, Holmes DS, Priest R, Saez V. Mimics of the sialyl lewis[x] tetrasaccharide. Replacement of the *N*-acetylglucosamine sugar with simple C_2-symmetric 1,2-diols. Bioorg Med Chem 1996;4:793–801.
104. Bamford MJ, Bird MI, Gore PM, Holmes DS, Priest R, Prodger JC, Saez V. Synthesis and biological activity of conformationally constrained sialyl Lewis[x] analogues with reduced carbohydrate character. Bioorg Med Chem Lett 1996;6:239–244.
105. Kolb H. Diglycosylated 1,2-diols as mimetics of sialyl Lewis[x] and sialyl Lewis a. International Patent WO 01569. 1997.
106. Norman KE, Anderson GP, Kolb HC, Ley K, Ernst B. Sialyl Lewis x (sLe[x]) and an sLe[x] mimetic, CGP69669A, disrupt E-selectin-dependent leukocyte rolling in vivo. Blood 1998;91:475–483.
107. Hiruma K, Kajimoto T, Weitz-Schmidt G, Ollmann I, Wong C-H. Rational design and synthesis of a 1,1-linked dissacharide that is 5 times as active as Sialyl Lewis[x] in binding to E-selectin. J Am Chem Soc 1996;118:9265–9270.
108. Cheng X, Khan N, Mootoo DR. Synthesis of the C-glycoside analogue of a novel sialyl Lewis X mimetic. J Org Chem 2000;65:2544–2547.
109. Hiruma K, Kanie O, Wong C-H. Synthesis of analogs of 1,1-linked galactosyl mannoside as mimetics of sialyl Lewis[x] tetrasaccharide. Tetrahedron 1998;54:15781–15792.
110. Shibata K, Hiruma K, Kanie O, Wong C-H. Synthesis of 1,1-linked galactosyl mannosides carrying a thiazine ring as mimetics of sialyl Lewis[x] antigen: Investigation of the effect of carboxyl group orientation on P-selectin inhibition. J Org Chem 2000;65:2393–2398.
111. Hanessian S, Prabhanjan H. Design and synthesis of glycomimetic prototypes-A model sialyl Lewis[x] ligand for E-selectin. Synlett 1994;868–870.
112. Dekany G, Wright K, Ward P, Toth I. Synthesis of sialyl Lewis[x] analogues. J Carbohydrate Chem 1996;15(4):383–398.

113. Dasgupta F, Musser JH, Levy DE, Tang PC. Sialic acid/fucose based medicaments. United States Patent 5658880. 1997.
114. Kaila N, Yu H-A, Xiang Y. Design and synthesis of novel sialyl Lewis^x mimics. Tetrahedron Lett 1995;36:5503–5506.
115. Birkbeck AA, Ley SV, Prodger JC. Spiroketal glycomimetics: The synthesis of a conformationally restrained sialyl Lewis^x mimic. Bioorg Med Chem Lett 1995;5:2637–2642.
116. Allanson NM, Davidson AH, Martin FM. A novel mimic of the sialyl Lewis^x determinant. Tetrahedron Lett 1993;34:3945–3948.
117. Allanson NM, Davidson AH, Floyd CD, Martin FM. The synthesis of novel mimics of the sialyl Lewis^x determinant. Tetrahedron: Asymmetry 1994;5:2061–2076.
118. Toepfer A, Kretzschmar G, Schuth S, Sonnentag M. Malonic acid derivatives as sialyl Lewis^x mimetics. Bioorg Med Chem Lett 1997;7:1317–1322.
119. Toepfer A, Kretzschmar G. Piperidine carboxylic acid derivatives as sialyl Lewis^x mimetics. Bioorg Med Chem Lett 1997;7:1311–1316.
120. Toepfer A, Kretzschmar G, Schoelkens B, Klemm P, Huels C, Seiffge D. Carbohydrate conjugates of piperidine and pyrrolidine derivatives as leukocyte adhesion inhibitors. Ger Offen. DE 19537334 A1. 1997.
121. Liu A, Dillon K, Cmpbell RM, Cox DC, Huryn DM. Synthesis of E-selectin inhibitors: Use of an arylcyclohexyl ether as a disaccharide scaffold. Tetrahedron Lett 1996;37:3785–3788.
122. Bantelli R, Ernst B. Synthesis of sialyl Lewis^x mimics: Replacement of galactose by aromatic spacers. Tetrahedron Lett 1997;38:4059–4062.
123. Wang R, Wong C-H. Synthesis of sialyl Lewis^x mimetics: Use of O-a-Fucosyl-(1R,2R)-2-aminocyclohexanol. Terahedron Lett 1996;37:5427–5430. (This class of compounds are discussed in detail in reference 17.)
124. Lin C-C, Shimazaki M, Heck M-P, Aoki S, Wang R, Kimura T, Ritzen H, Takayama S, Wu S-H, Weitz-Schmidt G, Wong C-H. Synthesis of sialyl Lewis^x mimetics and related structures using the glycosyl phosphite methodology and evaluation of E-selectin inhibition. J Am Chem Soc 1996;118:6826–6840.
125. Lin C-C, Kimura T, Wu S-H, Weitz-Schmidt G, Wong C-H. Liposome-Like fucopeptides as sialyl Lewis^x mimetics. Bioorg Med Chem Lett 1996;6:2755–2760.
126. Wu S-H, Shimazaki M, Lin C-C, Qiao L, MoreeWJ, Weiz-Schmidt G, Wong C-H. Synthesis of fucopeptides as sialyl Lewis^x mimetics. Angew Chem Int Ed 1996;35:88–90.
127. Lampe TFJ, Wetz-Schmidt G, Wong C-H. Parallel synthesis of sialyl Lewis^x mimetics on a solid phase: Access to a library of fucopeptides. Angew Chem Int Ed 1998;37:1707–1711.
128. Wong C-H, Lampe TFJ. Fucopeptides mimetics. United States Patent 6111084. 2000.
129. Wong C-H, Lin C-C, Kajimoto T. Sialyl Lewis^x mimetics incorporating fucopeptides. United States Patent 5962660. 1999.
130. Cappi MW, Moree WJ, Qiao L, Marron TG, Wetz-Schmidt G, Wong C-H. Synthsis of novel 6-amido-6-deoxy-L-galactose derivatives as sialyl Lewis^x mimetics. Bioorg Med Chem 1997;5:283–296.
131. Tsukida T, Kiyoi T, Achiha T, Moriyama H, Kurokawa K, Ohmoto H, Nakamura K, Kondo H, Wada Y, Saito T, Fucose derivatives, drugs containing the same as active ingredient, and intermediates for producing the same. International patent WO97/15585. 1997.
132. Anderson MB, Levy DE, Tang PC, Musser JH, Rao N. Sialyl Lewis^x mimetics containing flavanoid backbones. International patent WO97/31007. 1997.
133. Anderson MB, Levy DE, Tang PC, Musser JH, Rao N, Cui JR. Sialyl Lewis^x mimetics containing phenyl backbones. International patent WO97/30984. 1997.
134. Anderson MB, Levy DE, Tang PC, Musser JH, Rao N. Sialyl Lewis^x mimetics containing naphthyl backbones. United States patent 5837689. 1998.
135. Manallack DT, Montana JG, Murphy PV, Hubbard RE, Taylor RJK. Design, synthesis, and testing of novel inhibitors of cell adhesion. Mol Model Predict Bioact 2000;371–372.
136. Rao N, Tang PC, Musser JH. Anthraquinone and anthracene derivatives as inhibitors of the cell-adhesion molecules of the immune system. International Patent WO94/18189. 1994.
137. Dupre B, Bui H, Scott IL, Market RV, Keller KM, Beck PJ, Kogan TP. Glycomimetic selectin inhibitors: (α-D-mannopyranosyloxy)methylbiphenyls. Bioorg Med Chem Lett 1996;6:569–572.

138. Patel TP, Goelz SE, Lobb RR, Parekh RB. Isolation and characterization of natural protein-associated carbohydrate ligands for E-selectin. Biochemistry 1994;33:14815–14824.
139. Kogan TP, Dupre B, Bui H, McAbee KL, Kassir JA, Scott IL, Xin H. Novel synthetic inhibitors of selectin-mediated cell adhesion: Synthesis of 1,6-Bis[3-(3-carboxymethylphenyl)-4-(2-α-D-mannopyranosyloxy)phenyl]hexane(TBC1269). J Med Chem 1998;41:1099–1111.
140. Pardella L. TBC-1269 Texas biotechnology corp. Anti-inflammatory immunomodulatory Invest. Drugs 1999;1:56–60.
141. Lin C-C, Moris-Varas F, Weitz-Schmidt G, Wong C-H. Synthesis of sialyl Lewis^x mimetics as selectin inhibitors by enzymatic aldol condensation reactions. Bioorg Med Chem 1999;7:425–433.
142. Wong C-C, Moris-Varas F, Hung S-C, Marron TG, Lin C-C, Gong KW, Weitz-Schmidt G. Small molecules as structural and functional mimics of sialyl Lewis^x tetrasaccharide as selectin inhibition: A remarkable enhancement of inhibition by additional negative charge and/or hydrophobic group. J Am Chem Soc 1997;119:8152–8158.
143. Tsai C-Y, Park WKC, Weitz-Schmidt G, Ernst B, Wong C-H. Synthesis of sialyl Lewis^x mimetics using the Ugi four-component reaction. Bioorg Med Chem Lett 1998;8:2333–2338.
144. Tsai C-H, Huang X, Wong C-H. Design and synthesis of cyclic sialyl Lewis^x mimetics: A remarkanle enhancement of inhibition by pre-organizing all essential functional groups. Terahedron Lett. 2000;41: 9499–9503.
145. Sutherlin DP, Stark TM, Hughes R, Armstrong RW. Generation of C-glycoside peptide ligands for cell surface carbohydrate receptors using a four-component condensation on solid support. J Org Chem 1996;61:8350–8354.
146. Schmidt W, Sprengard U, Kretzschmer G, Kunz H. Preparation of glycomimetics as selectin antagonists and anti-inflammatory agents. Eur Pat Appl EP761661A1. 1997.
147. Kretzschmar K. Synthesis of novel sialyl Lewis^x glycomimetics as selectin antagonists. Tetrahedron 1998;54:3765–3780.
148. Kuribayashi T, Ohkawa N, Satoh S. Aryl C-glycosides: Physiologically stable glycomimetics of sialyl Lewis^x. Bioorg Med Chem Lett 1998;8:3307–3310.
149. Anderson MB, Kobayashi Y, Holme KR, Peto CF, Wang L, Vazir H. Sialyl Lewis^x and sialyl Lewis a glycomimetics. International Patent WO99/29705. 1999.
150. Sato S, Shinozuka T, Ito K. Preparation of benzyl C-glycosides as selectin inhibitors. Jpn Kokai Tokkyo Koho JP 11302272 A2. 1999.
151. Ito M, Imazaki N, Mihauchi H. Preparation of aryl-c-glycosides as selectin inhibitors. Jpn Kokai Tokkyo Koho JP 11269162 A2. 1999.
152. Kretzschmar G, Toepfer A. Preparation and use of benzoic acid derivatives as selectin antagonists and cell-adhesion inhibitors. Ger Offen DE 19648681 A1. 1998.
153. Schmidt W, Sprengard U, Kretzschmar G, Klein R, Kunz H. New glycomimetics as selectin antagonists and antiinflammation pharmaceutical compositions. European Patent EP0771795 A1. 1997.
154. Imazaki N, Miyauchi H, Goto N, Hashimoto K, Tojo S. Preparation of *N*-hydroxyaminoalkyl C-glycosides derivatives as selectin inhibitors. Pct Int Appl WO9929681. 1999.
155. Yuri M, Miyauchi H. Quinic acid derivatives, pharmaceutical compositions containing them, and cyclohexane deivatives as their intermediates. Jpn Kokai Tokkyo Koho JP 11246503 A2. 1999.
156. Roche D, Bantelli R, Winkler T, Casset F, Ernst B. Synthesis of benzylated (R)- and (S)-aminoethyl-C-α-D-mannosides as conformationally restricted building blocks for the preparation of E- and P-selectin antagonists. Tetrahedron Lett 1998;39:2545–2548.
157. Marron TG, Woltering TJ, Weitz-Schmidt G, Wong C-H. C-Mannose derivatives as potent mimics of sialyl Lewis^x. Tetrahedron Lett 1996;37:9037–9040.
158. Sakagami M, Horie K, Nakamoto K, Kawaguchi T, Hamana H. Sialyl Lewis^x-polysaccharide conjugates: Targeting inflammatory lesions. Bioorg Med Chem Lett 1998;8:2783–2786.
159. Sears P, Wong C-H. Carbohydrate mimetics: A new strategy for tackling the problem of carbohydrate-mediated biological recognition. Angew Chem Int Ed 1999;38:2300–2324.
160. Thoma G, Patton JT, Magnani JL, Ernst B, Ohrlein R, Duthaler RO. Versatile functionalization of polyysine: Synthesis, characterization, and use of neoglycoconjugates. J Am Chem Soc 1999;12:5919–5929.
161. Stahn R, Schaefer H, Kernchen F, Schreiber J. Multivalent sialyl Lewis^x ligands of definite structures as inhibitors of E-selectin mediated cell adhesion. Gycobiology 1998;8:311–319.

162. Roy R. Syntheses and some applications of chemically defined multivalent glycoconjugates. Curr Opin Struct Biol 1996;6:692–702.
163. Kiessling LL, Pohl NL. Strength in numbers: Non-natural polyvalent carbohydrate derivatives. Chem Biol 1996;3:71–77.
164. Mammen M, Choi S-K, Whitesides GM. Polyvalent interactions in biological systems: Implications for design and use of multivalent ligands and inhibitors. Angew Chem Int Ed 1998;37:2754–2794.
165. Gardiner JM. The therapeutic potential of synthetic multivalent carbohydrates. Exp Opin Invest Drugs 1998;7:405–410.
166. Golik J, Dickey JK, Todderud G, Lee D, Alford J, Huang S, Klohr S, Eustice D, Aruffo A, Agler ML. Isolation and structure determination of sufonoquinovosyl dipalmitoyl glyceride, a P-selectin receptor inhibitor from the Alga Dictyochloris Fragrans. J Nat Prod 1997;60:387–389.
167. Woltering TJ, Weitz-Schmidt G, Wong C-H. Tetrahedron Lett 1996;37:9033–9036.
168. Manning DD, Hu X, Beck P, Kiessling LL. J Am Chem Soc 1997;119:3161–3162.
169. Kretzschmar G, Toepfer A, Sonnentag M Short synthesis of sulfatide- and SQDG-Mimetics as small molecular weight selectin inhibitors. Tetrahedron 1998;54:15189–15198.
170. Kurokawa K, Kumihara H, Kondo H. A solid-phase synthesis forb-turn mimetics of sialyl Lewis^x. Bioorg Med Chem Lett 2000;10:1827–1830.
171. Bruehl RE, Dasgupta F, Katsumoto TR, Tan JH, Bertozzi CR, Spevak W, Ahn DJ, Rosen SD, Nagy JO. Polymerized liposome assemblies: Bifunctional macromolecular selectin inhibitors mimicking physiological selectin ligands. Biochemistry 2001;40:5964–5974.
172. Marinier A, Martel A, Bachand C, Plamondon S, Turmel B, Daris J-P, Banville J, Lapointe P, Ouellet C, Dextraze P, Menard M, Wright JJK, Alford J, Lee D, Stanley P, Nair X, Todderud G, Tramposch KM. Novel mimics of sialyl Lewis^x: Design, synthesis, and biological activity of a series of 2- and 3-malonate substituted galactoconjugates. Bioorg Med Chem 2001;9:1395–1427.
173. Sakagami M, Horie K, Nakamoto K, Kawaguchi T, Hamana H. Synthesis of sialyl Lewis^x—Polysaccharide conjugates. Chem Pharm Bull 2000;48:1256–1263.
174. Thoma G, Duthaler RO, Magnani JL, Patton JT. Nanomolar E-selectin inhibitors: 700-fold potentiation of affinity by multivalent ligand presentation. J Am Chem Soc 2001;123:10113–10114.
175. Fukuda MN, Ohyama C, Lowitz K, Matsuo O, Pasquaini R, Ruoslahti E, Fukuda M. A peptide mimic of E-selectin ligand inhibits sialyl Lewis^x-dependent lung colonization of tumor cells. Cancer Res 2000;60:450–456.
176. Insug O, Kieber-Emmons T, Otvos L, Blaszczyk-Thurin M. Peptide mimicking sialyl Lewis^x with anti-inflammatory activity. Biochem Biophys Res Comm 2000;268:106–111.
177. Kim M-K, Brandley BK, Anderson MB, Bochner BS. Anatogonism of selectin-dependent adhesion of human eosinophils and neutrophils by glycomimetics and oligosaccharide compounds. Am J Respir Cell Mol Biol 1998;19:836–841.
178. Kaila N, Chen L, Thomas IV BE, Tsao D, Tam S, Bedard PW, Camphausen RT, Alvarez JC, Ullas G. β-C-Mannosides as selectin inhibitors. J Med Chem 2002;45:1563–1566.
179. Kretzschmar G, Toepfer A, Huls C, Krause M. Pitfalls in the synthesis and biological evaluation of sialyl Lewis^x mimetics as potential selectin antagonists. Tetrahedron 1997;53:2485–2494.

Dr. Neelu Kaila *received her Ph.D. in chemistry at Hunter College, City University of New York in 1991 under the supervision of Prof. Richard W. Franck. After two and a half years of post-doctoral research with Prof. Richard W. Franck, she joined Genetics Institute in 1993. At present, she is a senior research scientist II in the chemical sciences department at WYETH, where she has been leading a research team of medicinal chemists for the last 4 years aimed at the design and synthesis of selectin inhibitors.*

Dr. Bert E. Thomas IV *received his BS in chemistry from Butler University in 1987, then completed his Ph.D. at the University of California at Los Angeles under the direction of Professor Ken Houk. This was followed by 2 years of postdoctoral research at the University of California at San Francisco in the laboratories of Prof. Peter Kollman. Since then he has held various positions in the pharmaceutical industry and is currently located at Guilford Pharmaceuticals working on CNS related research.*

Current Status of Selective Estrogen Receptor Modulators (SERMs)

Suzanne D. Conzen

Selective estrogen receptor modulators (SERMs) are a class of several structurally diverse molecules, including steroid hormones, that differentially bind to and modulate the estrogen receptor (ER) in a tissue-specific manner. Because of a SERM's ability to act as an estrogen antagonist in breast tissue, these molecules can be potent anticancer agents and have been studied extensively in both the prevention and the treatment of breast cancer. However, the concomitant action of SERMs as potential estrogen agonists in nonbreast tissue, such as bone and endometrium, results in variable effects by individual SERMs on the development of osteoporosis and uterine cancer. On a molecular level, we are only beginning to understand why an individual SERM can act as an ER agonist in one tissue and as an antagonist in another,[1] but it is likely that the change in ER conformation that follows binding by the SERM results in variable interactions with cofactors required for ER-mediated gene regulation.[2] This discovery has led to a resurgence of interest in developing an "ideal" SERM that might have potent antiestrogenic effects in the breast and endometrium and pro-estrogenic effects in the bone and central nervous system. At the same time, the development of

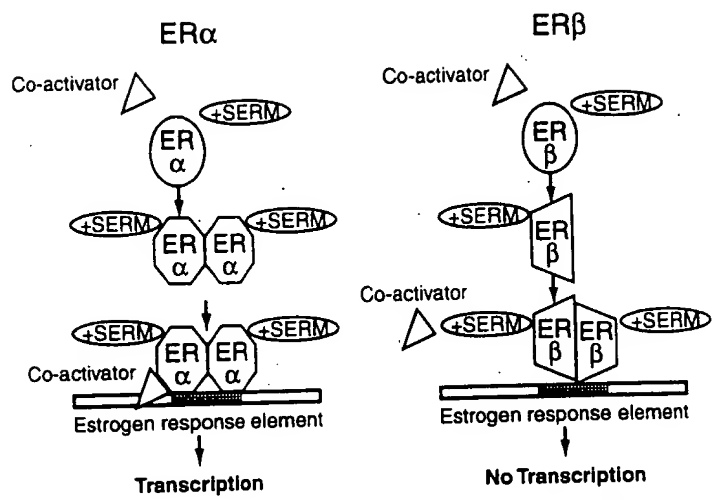

FIGURE 10.1 Model of the molecular basis of the potential differential effects of selective estrogen receptor modulators (SERMs) on estrogen receptor-α (ER-α) versus ER-β. In this conceptual model, binding of a SERM to ER-α creates a conformational change in the ER that favors coactivator binding and results in gene transcription. However, the same SERM can bind to ER-β and result in an alternative conformational change that does not favor ER-β interaction with the coactivator; therefore, no gene transcription results. Differential effects of individual SERMs on ER binding can also result in varied affinities of the ER for corepressors. In addition, the ratio of corepressor to coactivator expression can vary in different target cell types, resulting in cell type–specific gene expression profiles.

aromatase inhibitors (AIs) is challenging the traditional role of SERMs as the gold standard endocrine treatment for early and advanced breast cancer in postmenopausal women.

MOLECULAR MECHANISMS OF SERM ACTION

In the 1970s, tamoxifen was the first SERM to be studied thoroughly in the laboratory and the first to be used in the treatment of breast cancer. As is true with all SERMs, tamoxifen has mixed antagonistic and agonistic effects on the ER. The consequence of tamoxifen binding to an individual ER depends on the ER (α or β isoform) and on the cell type. In fact, within a certain cell type, tamoxifen can act as an estrogen agonist on some genes and an estrogen antagonist on others. This complexity reflects the nature of the interaction of SERMs with ER-α or ER-β; the resulting change in the conformation of the ER on binding to the SERM appears to vary, depending on what cellular environment and specific gene target is being considered (Fig. 10.1).

Our molecular understanding of SERM mechanisms of action has recently increased dramatically because of the knowledge gained from the solution of the ER's three-dimensional structure and because of our better understanding of the mechanisms of ER-mediated gene regulation. In 1998, the structures of the hormone-binding domain of ER-α complexed to estradiol, diethylstilbestrol (DES), tamoxifen, and raloxifene were solved and revealed that the nature of

TABLE 10.1 Overall Efficacy of SERMs in Tamoxifen-Resistant and Hormone-Sensitive Advanced Breast Cancer

Drug	Tamoxifen-Resistant (Phase II)	Hormone-Sensitive or First-Line Therapy (Phase II or III)
	ORR (%)	ORR (%)
Tamoxifen	NA	25.3[a]
Toremifene	0–14	24.0[a]
Droloxifene	15	30–51
Idoxifene	9	20
Arzoxifene	3–10	30–36
Raloxifene	0	19
EM-800	14	NA
Fulvestrant	37	17.5–20.7

ORR, overall response rate (complete response + partial response); NA, not available.
[a]Meta-analysis averages (Ref. 16).

these ligands determines the overall change in structure of the receptor after binding.[3,4] The resulting shape of the receptor-SERM complex, in turn, determines the precise interaction of the ER with coactivators and corepressors that are important for individual gene expression. The structure of the ER that is bound to tamoxifen revealed that coactivator binding can be blocked by tamoxifen due to helix 12 of the ER hormone-binding domain moving over and blocking access of the coactivator to the ER. Similarly, the comparative structures of the ER bound to estradiol versus raloxifene revealed that these two compounds bind to the same site within the core of the LBD but demonstrate different binding effects on helix 12. More recently, it was demonstrated that the conformational shape imposed by a specific SERM differs in outcome for a particular gene target depending upon whether the SERM binds to ER-α or ER-β (Fig. 10.1). This implies that a different interaction with the same coactivator or corepressor can result depending on the specific ER isoform that is targeted by an individual SERM.[2] Thus, the emerging picture is that of SERMs binding to ER-α and/or ER-β and producing alternative shapes in the ER binding interfaces with coactivators and corepressors depending on the specific cell type milieu.

The differential gene induction of various SERMs has resulted in a group of drugs that when bound to a receptor have variable effects on a complement of ER-regulated genes. Furthermore, the ability of the ER to interact with a large array of transcriptional regulatory proteins is important because it implies that SERMs can induce differential effects on genes in different cellular contexts based on variable interactions with corepressors and coactivators. It seems likely that the net balance of corepressors and coactivators in a cell as well as the relative proportions of ER-α and ER-β will determine the overall activity of a SERM in any individual cell type (Table 10.1). Therefore, designing SERMs that act as an-

tagonists in breast tissue and in the endometrium and as agonists in brain and bone is the goal of several active pharmaceutical and academic drug discovery programs. Such a compound may have an advantage over the "pure estrogen antagonist" SERMs and the AIs because they could have the beneficial effects of estrogen (e.g., increasing bone density) on some tissues and antagonistic effects in the breast and the uterus.

Because SERMs can act as estrogen antagonists in certain tissues and estrogen agonists in others, a great deal of effort is being placed on understanding and predicting how these molecules achieve their specific effects on different tissues. A SERM that has antiestrogenic effects on the breast but proestrogenic effects on the brain and bone would be ideal. Despite their imperfections, the current SERMS are very effective in their use in ER-positive breast cancer because they act as antagonists to the generally pro-proliferative effects of the ER in mammary epithelial cells. Tamoxifen, the first SERM to gain widespread clinical use and by far the best-studied SERM in clinical conditions, remains the gold standard SERM against which all others are compared.

PHARMACOLOGY OF SERMS

High-Dose Estrogens

DES and other high-dose estrogens were first studied in the late 1970s. The mechanism whereby achieving very high serum concentrations of estrogens inhibits breast cancer growth is not understood, but it may be related to effects that high-dose estrogens have on nuclear receptors other than ER-α and ER-β.[5] The largest study compared DES with tamoxifen in 143 patients being treated for metastatic breast cancer.[6] The 20-year updated results of this trial were recently published and showed that DES ($N = 74$) and tamoxifen ($N = 69$) responses were approximately equal. The overall objective response was 42% for DES and 34% for tamoxifen ($P = .31$), and the median duration of response was 11.8 months for DES and 9.9 months for tamoxifen ($P = .38$). The median survival was 3.0 years for DES, versus 2.4 years for tamoxifen. Thus, duration of response and progression-free survival were not found to be significantly different between DES and tamoxifen. Despite equivalent responses and a favorable duration of response for DES, treatment with DES is more commonly associated with toxicities such as nausea, edema, vaginal bleeding, and cardiac problems. Therefore, tamoxifen currently remains the preferred SERM for the treatment of metastatic breast cancer.

TRIPHENYLETHYLENE SERMS

Tamoxifen

Tamoxifen is a triphenylethylene that was developed more than 30 years ago as a breast cancer treatment.[7] In addition to its anti-estrogenic effects in the breast, tamoxifen lowers cholesterol and increases bone mineral density in post-

menopausal women.[8] The National Surgical Adjuvant Breast and Bowel Project (NSABP) P-1 trial showed that tamoxifen was an effective preventive of breast cancer but that there are increased risks of endometrial cancer and thrombosis.[9] Tamoxifen alters the shape of the ER on binding; depending on the cellular context, this change leads to the activation or the repression of ER target genes. Tamoxifen's main mechanism of action in breast tissue is thought to be antagonism of several growth-promoting genes and the induction of a delay in the G_1 phase of the cell cycle in breast epithelial cells.[10]

Tamoxifen acts as an estrogen antagonist in cells of the central nervous system and in the vaginal mucosa, resulting in potentially unpleasant side effects, including hot flashes and vaginal dryness and/or discharge. In addition, tamoxifen is associated with life-threatening complications, such as an increased incidence of blood clots and subsequent pulmonary emboli, presumably due to the pro-estrogenic effects of tamoxifen on the vascular endothelium. For example, the results of the NSABP P-1 trial found that relatively healthy postmenopausal patients receiving tamoxifen ($N = 6681$) versus placebo ($N = 6707$) experienced a significantly greater incidence of deep vein thromboses ($N = 35$ versus 22), pulmonary embolism ($N = 18$ versus 6), and stroke ($N = 38$ versus 24). An increased incidence of endometrial cancers and cataracts was also noted in the tamoxifen-treated patients.

Perhaps the most frequently debilitating symptom exacerbated by tamoxifen's anti-estrogenic effects is frequent hot flashes that interrupt a patient's normal activities and sleep cycles. A recent phase III study using the antidepressant medication fluoxetine for the treatment of hot flashes in postmenopausal patients has shown an objective reduction in hot flashes.[11] This trial used a double-blind, randomized, two-period (4 weeks per period), cross-over methodology to study the efficacy of fluoxetine (20 mg/day) for treating hot flashes in women with a history of breast cancer or a concern regarding the use of estrogen (because of breast cancer risk). Another randomized study of a popular treatment for hot flashes, soy, did not result in a significant difference in hot flashes,[12] even though statistically significant levels of genistein, the compound thought to be the active agent in soy milk, was found in the experimental group. Similar results had been noted in an earlier randomized trial of soy tablets versus placebo for the treatment of hot flashes in breast cancer survivors.[13] A randomized trial of black cohosh versus placebo also failed to find a significant effect in alleviating hot flashes.[14] An ongoing Cancer and Leukemia Group B (CALGB) clinical trial is currently evaluating the role of isoflavones and soy in the prevention of hot flashes in women with a history of breast cancer who are receiving concurrent tamoxifen treatment.

Toremifene

Toremifene is similar to tamoxifen in that the only structural difference is a single chlorine atom at position 4 (Fig. 10.2). The inability of toremifene to form DNA adducts in the rat liver may explain why it is not a hepatocarcinogen.[15] As

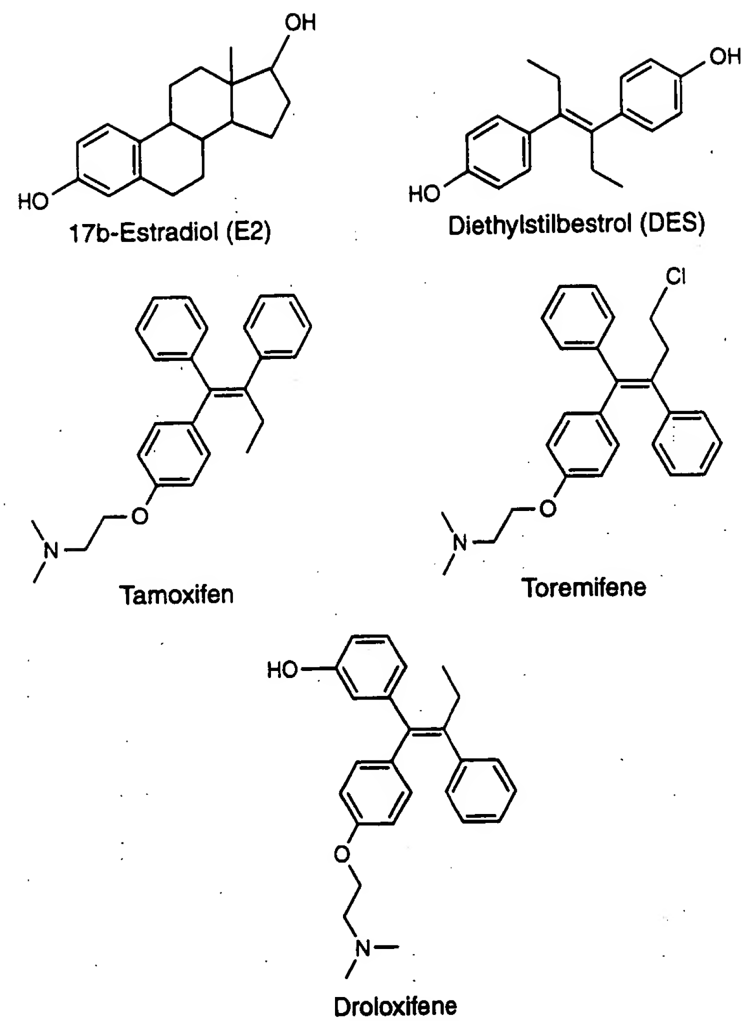

FIGURE 10.2 Chemical structures of estradiol, diethylstilbestrol (DES), and tamoxifen-like selective estrogen receptor modulators (SERMs).

a first-line endocrine therapy for metastatic breast cancer, toremifene has been shown to have response rates that are very similar to those of tamoxifen, ranging from 21% to 38%, in five phase III trials comparing tamoxifen (20–40 mg) with toremifene (40–60 mg).[16] In all studies, toremifene has shown efficacy equivalent to that of tamoxifen for effective response rate, stable disease, time to progression, and overall survival. A recent meta-analysis of 1421 patients from these trials confirmed the lack of difference between tamoxifen and toremifene response rates. Although these studies did not address the question of carcinogenicity from toremifene versus tamoxifen, a Finnish study (N = 899 patients evaluable for safety) assessing the efficacy and safety of toremifene versus tamoxifen in the adjuvant setting for 3 years has found no significant differences in the number of secondary cancers at a short follow-up of 3.4 years.[17] Slightly more vascular complications (deep vein thromboses, cerebrovascular events, and pulmonary embolisms) occurred in tamoxifen-treated patients (5.9%) than in toremifene-

treated patients (3.5%) ($P = .11$), whereas bone fractures and vaginal leukorrhea were slightly more common in the toremifene group. The International Breast Cancer Study Group is currently conducting two randomized adjuvant trials evaluating 5 years of toremifene therapy (60 mg/day) versus 5 years of tamoxifen therapy (20 mg/day). Toremifene is approved for the treatment of metastatic breast cancer in the United States and in Europe.

Droloxifene

Droloxifene is 3-hydroxytamoxifen; it has a higher relative binding affinity than tamoxifen for the ER.[18] However, an increased affinity of a SERM for either ER-α or ER-β does not necessarily determine its clinical efficacy. Data on droloxifene and other novel SERMs suggest that a SERM's efficacy is more likely to be determined by its specific effect on ER interactions and that specific cofactors regulate gene transcription. For droloxifene, initial phase I/II studies suggested a 15% response rate in patients who had previously failed to respond to tamoxifen, suggesting that droloxifene exhibits significant non–cross-resistance with tamoxifen, In addition, an early phase II study of droloxifene as a first-line agent showed a response rate of 51% and a median time to progression of 8 months.[19] However, because two randomized phase III studies comparing droloxifene to tamoxifen showed less activity than tamoxifen in hormone-sensitive breast cancer, development of droloxifene has been dropped.[20]

Idoxifene

Idoxifene, like raloxifene, is structurally similar to tamoxifen and has an increased binding affinity for ER-α due to a pyrrolidine side chain with an iodine atom at the 4 position (Fig. 10.2). Pre-clinical experiments were encouraging because idoxifene inhibited the MCF 7 cancer cell line xenograft growth in nude mice more than tamoxifen[21] while showing reduced uterine stimulation.[22] Unfortunately, clinical trials have revealed an increased incidence of uterine prolapse and polyps in idoxifene-treated women, and no major difference in clinical efficacy has been found for idoxifene compared to tamoxifen.[23] Further development of this drug as a breast cancer treatment has therefore been dropped.[24]

SUMMARY OF TAMOXIFEN DERIVATIVES

Although there has been intense interest in developing a tamoxifen-like derivative with less uterine side effects and better efficacy in breast cancer, the ultimate outcome of these attempts has thus far been disappointing. For example, it does not appear that an individual SERM's relatively high affinity for the ER improves its efficacy as an anticancer drug; similarly, a reduced agonist profile in preclinical studies (e.g., less uterine proliferation in a rat uterotrophic model) does not necessarily predict a better safety profile in clinical studies. Conversely, the

knowledge that we have gained in the past few years about the structure of ER-α and -β when they are bound to a SERM may allow the rational development of drugs that minimize the pro-proliferative action of the SERMs in the uterus and may maximize the pro-estrogenic effects in the brain and bone.

FIXED-RING SERMS

Raloxifene

Raloxifene is a "fixed-ring" SERM that has a binding affinity for the ER similar to that of tamoxifen (Fig. 10.3). Preclinical studies with raloxifene showed an anti-estrogen effect on rat mammary tumor growth that is equal to that of tamoxifen, but significantly less action as an estrogen in the uterus. However, clinical trials subsequently showed no activity in tamoxifen-resistant patients,[25] and a recent phase II clinical study of raloxifene in metastatic breast cancer showed only a 33% clinical benefit, compared with the 44% occurring with tamoxifen.[26] Thus, raloxifene is not being considered as a treatment for existing breast carcinoma. Instead, it is being developed and marketed as a drug for osteoporosis, which, unlike estrogen, has less pro-estrogenic effects on the breast and uterus. In addition, raloxifene is currently being examined in a breast cancer chemopreventive trial called the Study of Tamoxifen and Raloxifene (STAR) trial.

Arzoxifene (LY-353381)

Arzoxifene is a benzothiophene analogue of raloxifene that has a more favorable therapeutic and safety profile than raloxifene in preclinical studies. Specifically, arzoxifene has exhibited more potent and beneficial effects on bone metabolism than raloxifene and has inhibited the growth of ER-positive breast cancer cells in vitro more potently that raloxifene.[27] Phase II data have revealed relatively low arzoxifene response rates for tamoxifen-resistant patients (10%), although there is a 30% response rate in hormone-sensitive patients and a 17% stable disease rate.[28,29] Based on these data, the use of arzoxifene, 20 mg/day, versus tamoxifen, 20 mg/day, is currently being studied in a large multicenter European phase III clinical trial as a first-line therapy in metastatic breast cancer.

EM-800

EM-800 is a prodrug of the active benzopyrene derivative EM-652 (SCH 57068). EM-652 has an ER binding affinity that is significantly greater than that of tamoxifen or raloxifene. Preclinical studies showed strong antiproliferative effects of EM-800 compared with tamoxifen, and when it was administered to ovariectomized animals, EM-800 prevented bone loss and lowered serum cholesterol and triglyceride levels.[30] A phase II study of 43 women who had not responded to tamoxifen was encouraging and showed a 14% response rate and a 23% rate

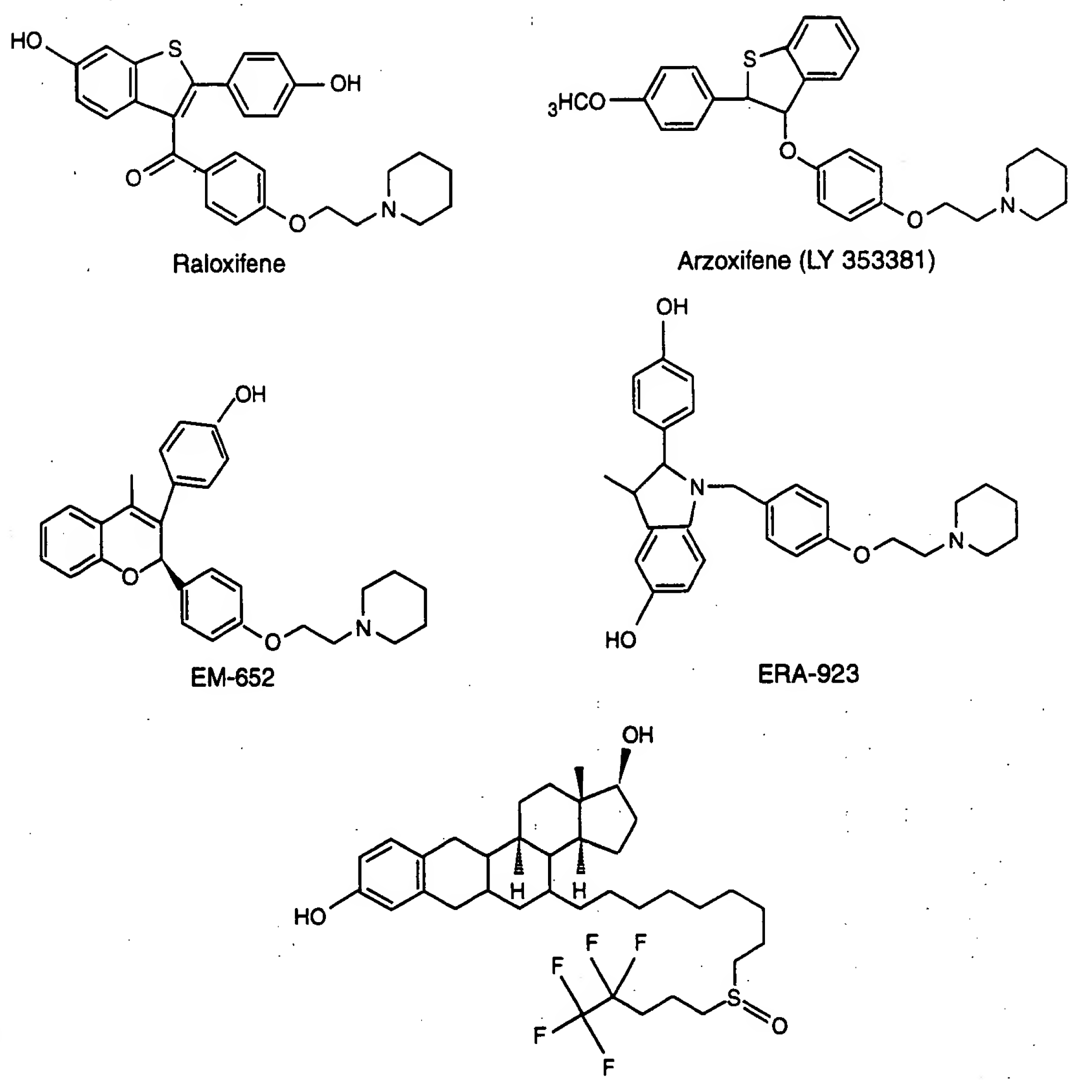

FIGURE 10.3 Chemical structures of second- and third-generation selective estrogen receptor modulators (SERMs).

of stable disease.[31] However, a randomized phase III study in patients with tamoxifen-resistant breast cancer compared EM-800 with the third-generation AI anastrozole; this study has been halted because response rates with EM-800 were lower than those of anastrozole.[24]

ERA-923

ERA-923 is a novel fixed-ring SERM that also has a favorable preclinical profile in comparison with tamoxifen and raloxifene.[32] Unlike tamoxifen, droloxifene, or raloxifene, ERA-923 is not uterotropic in immature rats or ovariectomized mice. A recent pharmacokinetic trial that evaluated the safety and tolerability of once-daily oral ERA-923 (10–200 mg) versus placebo found that subjects taking ERA-

923 had no uterine or ovarian changes, as indicated by transvaginal ultrasound after 28 days of therapy.[33] ERA-923 is currently being evaluated in phase II trials in tamoxifen-resistant breast cancer and as a first-line treatment in ER-positive patients with metastatic breast cancer.[34]

STEROIDAL SERMS ("PURE ANTAGONIST")

Fulvestrant (Faslodex, formerly ICI 182, 780)

Fulvestrant is a derivative of estradiol with a long hydrophobic side chain (Fig. 10.3) and is completely able to block transactivation by the ER. Because of the long bulky side chain at the 7α positions, receptor dimerization appears to be sterically hindered. This drug also appears to induce the degradation of the ER, depleting it from cellular extracts. Furthermore, fulvestrant decreases the number of ER molecules in the nucleus and thus is oftem referred to as an ER "down-regulator." The overall result is that the fulvestrant can block tamoxifen and estrogen induction of several common genes. A benefit to fulvestrant is that it is anti-estrogenic in both the breast and the uterus, presumably because instead of causing a conformational change in the ER, fulvestrant initiates the degradation of the ER. The mechanism by which fulvestrant causes the increased degradation is not well understood, but it may be related to the known susceptibility of the ER to ubiquitin-mediated degradation by the proteasome. Degradation may be accelerated on fulvestrant binding because fulvestrant may effect the folding of the ER; misfolded proteins are often targeted for degradation. The end result appears to be a complete suppression of all ER-activated genes.

Fulvestrant is not available as an oral formulation but instead as a long-acting monthly intramuscular injection. Early phase I and II trials suggested that unlike other SERMs, fulvestrant is active in tamoxifen-resistant disease. For example, a small trial of 19 patients with hormone-refractory disease showed that 13 patients had a clinical benefit with a median duration of 25 months, and two demonstrated a partial response and six achieved stable disease.[35] Furthermore, comparison with an historical control group of patients receiving megestrol acetate (Megace) suggested a longer duration of response with fulvestrant (26 versus 14 months, $P = .04$).[36] Two multicenter phase III studies have suggested that fulvestrant is at least as effective as the AI anastrozole in time to disease progression in women with metastatic disease progression who were receiving or had received endocrine therapy.[37,38] Fulvestrant was approved in the United States for metastatic breast cancer in 2002.

SERMS IN BREAST CANCER PREVENTION AND TREATMENT

Prevention Studies

Tamoxifen The first three major chemoprevention trials examining tamoxifen were performed in Britain (Marsden Hospital Trial), Italy (Italian Tamoxifen Pre-

vention Study), and the United States (NSABP Breast Cancer Prevention Trial). Although the Marsden Hospital[39] and the Italian trials[40] do not show a difference between breast cancer prevention in the placebo and tamoxifen arms, the United States trial does. However, several important differences between the trials may help explain their different outcomes.

The British trial was originally designed as a feasibility study to determine the tolerability of tamoxifen in healthy women with a family history of breast cancer. Thus, the trial was relatively small, involving 2494 women of a median age of 47 who received tamoxifen or placebo for up to 8 years. Only 34% of the women were postmenopausal, and these women were allowed the use of estrogen replacement therapy. Estrogen replacement therapy was used during 13% of the tamoxifen medication period. Mean follow-up time in the study was 70 months, and the overall frequency of breast cancers was equivalent.

The Italian trial included healthy hysterectomized women aged 35–70 years and enrolled a total of 5408 women (2708 placebo and 2700 tamoxifen treated). The preliminary study suggests that there was no difference in the incidence of breast cancer between the placebo (22 cases) and the tamoxifen (19 cases) arm.[41] In the 390 women (14%) receiving placebo and receiving hormone-replacement therapy (HRT), eight cases of breast cancer occurred, suggesting that the use of HRT increased the risk of breast cancer. A recent follow-up showed that HRT users who were randomly assigned to tamoxifen therapy had a rate of breast cancer that was close to that of those who had never received tamoxifen, suggesting a benefit for tamoxifen in HRT users but not in hysterectomized women.[41]

The largest trial to date, performed in the United States by the NSABP, showed that tamoxifen reduces the incidence of ipsilateral and contralateral breast cancer by approximately 50%. A total of 13,388 women participated in this trial. Eligibility requirements included women >35 years of age at high risk for developing breast cancer, women > 60 years of age without additional risk factors other than age, and women with a history of lobular carcinoma in situ. No estrogen replacement therapy was permitted. An interim analysis was published in 1998 after a median follow-up of 54.6 months and showed that the tamoxifen-treated group had 86 fewer breast cancers than the placebo group. The data monitoring committee considered that the highly significant reduction in early incidence of breast cancer at the time of this analysis justified the termination of the trial. The greatest levels of benefit were seen in women with lobular carcinoma in situ (relative risk = 0.44) and atypical ductal hyperplasia (relative risk = 0.14), most of whom were premenopausal. The rate of endometrial cancer was increased in the tamoxifen group (risk ratio = 2.53; 95% confidence interval = 1.35–4.97); this increased risk occurred predominantly in women aged 50 years or older. All uterine cancers in the tamoxifen group were stage I (localized disease), and no endometrial cancer deaths had occurred in this group at the time of analysis in 1998. The rates of stroke, pulmonary embolism, and deep-vein thrombosis were also elevated in the tamoxifen treatment group; these events also occurred more frequently in women aged 50 years or older. A recent risk-

benefit analysis of this trial concluded that given the side effect profile and characteristics of the subgroup that benefited most in terms of risk reduction, tamoxifen is most beneficial for younger women who have an elevated risk of breast cancer.[42]

In a more recent study, the International Breast Cancer Intervention Study randomized over 7144 women to receive tamoxifen or placebo.[43] Women enrolled had to have an overall increase in risk of two- to threefold based on family history and other risk factors. After a median follow-up of 50 months, 69 breast cancers had been diagnosed in 3578 women in the tamoxifen group and 101 in 3566 in the placebo group (a risk reduction of 32% [95% confidence interval 8–50]; P = .013). In this trial, age, degree of risk, and use of hormone-replacement therapy did not affect the reduction. Endometrial cancer was not significantly increased, but thromboembolic events were significantly increased, compared with tamoxifen (particularly after surgery).

In summary, the overall evidence generated by recent prevention trials appears to support a reduction in the incidence of breast cancer in women who are at increased risk, but whether this benefit outweighs the risks and side effects associated with tamoxifen use remains uncertain. Continued follow-up analysis of the ongoing placebo-controlled studies (Marsden, Italian, International Breast Cancer Intervention Study) will allow further analysis of the long-term risks and benefits of tamoxifen in the prevention setting.

Raloxifene Raloxifene is a SERM that was originally developed as a treatment to prevent osteoporosis, but analysis of treatment has suggested a preventive role in breast cancer treatment. In a large North American trial examining the effect of raloxifene on postmenopausal women with osteoporosis as a major endpoint,[44] postmenopausal women with osteoporosis (N = 7705) were enrolled in the Multiple Outcomes of Raloxifene Evaluation (MORE) trial and were randomly assigned to receive placebo, raloxifene at 60 mg/day, or raloxifene at 120 mg/day for 4 years. Breast cancer risk was analyzed by the following baseline characteristics indicative of estrogen exposure: previous hormone replacement therapy, prevalent vertebral fractures, estradiol level, bone mineral density, body mass index, and age at menopause. The trial was originally designed with a primary endpoint to measure bone fractures, and the conclusions on the secondary endpoint of examining breast cancer incidence are less powered. At the relatively early follow-up of 3 years, the MORE study results are consistent with the NSABP P-1 trial, showing a significant decrease in the incidence of ductal carcinoma in situ and invasive breast cancer in patients taking tamoxifen. In addition, both studies show a reduction in fracture incidence, an increase in thromboembolic events, and a slight increase in stroke. Neither the NSABP P-1 study nor the raloxifene study showed an impact on cardiovascular mortality in this group of women.

A recent update of the analysis of the MORE trial shows that raloxifene significantly reduces breast cancer risk in both the low-estrogen and the high-estrogen subgroups for all risk factors examined. For example, women with the

highest body mass index and those with a family history of breast cancer experienced a significantly greater therapy benefit with raloxifene, compared with the two thirds of patients with a lower body mass index or those without a family history, respectively.[45] These findings imply that increased risk imposed by excessive body fat (presumably due to greater fat-generated estrogen levels) or family history result in a greater benefit from SERM treatment.

In the ongoing STAR trial, raloxifene is being directly compared with tamoxifen. In this study, high-risk postmenopausal women are randomly assigned to either tamoxifen (20 mg/day) or raloxifene (60 mg/day) for 5 years. Results should be available in 2005. The STAR trial should provide a definitive answer about the benefits and side effect profile of these two agents. Ongoing molecular biology projects designed to derive the crystal structure of tamoxifen and raloxifene bound to the ER with peptide structures of cofactors will also shed light on how these drugs can act as mixed agonists and antagonists in various tissues.

In summary, one of the major preventive effects of both tamoxifen and raloxifene is that both of them reduce the incidence of in situ and invasive carcinomas in women who are at relatively high risk for breast cancer. The effects of SERMs appear to be only on ER-positive cells, consistent with the initial findings of a reduction in ER-positive breast cancers and not ER-negative cancers. Further efforts are needed to develop agents that may act as chemoprevention for ER-negative breast cancers.

Adjuvant Treatment of Early Breast Cancer (Ductal Carcinoma In Situ and Invasive Cancers)

The NSABP B-24 involved 1804 women and tested the hypothesis that in ductal carcinoma in situ patients with or without positive tumor specimen margins, lumpectomy, radiation therapy, and tamoxifen would be more effective than lumpectomy, radiation therapy, and placebo in preventing invasive and noninvasive ipsilateral breast tumor recurrences, contralateral breast tumors, and tumors at metastatic sites. This study demonstrated that the administration of tamoxifen after lumpectomy and radiation therapy results in a significant decrease in the rate of all breast cancer events, particularly in invasive cancer.[46] The Early Breast Cancer Trialists Collaborative examined information on 37,000 women in 55 trials comprising about 87% of the worldwide evidence.[41] For trials of tamoxifen treatment for 1, 2, and 5 years of adjuvant tamoxifen, the proportional recurrence reductions produced among these 30,000 women during 10 years of follow-up were 21%, 29%, and 47% respectively, with a highly significant trend toward greater effect with longer treatment. The corresponding proportional mortality reductions were 12%, 17%, and 26%, respectively, and again the test for trend was significant. The benefits appear to be largely irrespective of age, menopausal status, and tamoxifen dose (generally 20 mg/day) and to be unrelated to whether chemotherapy is given. The incidence of endometrial cancer approximately doubled in trials of 1 or 2 years of tamoxifen therapy and

approximately quadrupled in trials of 5 years of tamoxifen therapy. Tamoxifen had no apparent effect on the incidence of colorectal cancer or, after exclusion of deaths from breast or endometrial cancer, on any of the other main categories of cause of death. Thus, the overall conclusions of this updated overview are that some years of tamoxifen treatment substantially improve the 10-year survival of both pre- and postmenopausal women with ER-positive tumors.

Recently, a large randomized trial compared the use of the third-generation AI anastrozole (Arimidex) to tamoxifen in the adjuvant setting.[47] The ATAC (Arimidex, Tamoxifen Alone or in Combination) trial was activated in 1996 and closed in 1999 with 9366 postmenopausal breast cancer patients. Postmenopausal patients with invasive operable breast cancer who had completed primary therapy and were eligible to receive adjuvant hormone therapy were randomly assigned to receive anastrozole, tamoxifen, or combination therapy. Median follow-up was 33.3 months, and 7839 (84%) patients were known to be hormone receptor–positive. Disease-free survival at 3 years was 89.4% in patients taking anastrozole and 87.4% in those taking tamoxifen, whereas results with the combination were not significantly different from those with tamoxifen alone. The improvement in disease-free survival with anastrozole occurred in the subgroup of hormone receptor–positive patients, but not the receptor-negative patients. The incidence of contralateral breast cancer was significantly lower with anastrozole than with tamoxifen (odds ratio, 0.42 [0.22–0.79], $P = .007$). Anastrozole caused significantly less endometrial cancer, vaginal bleeding and discharge, cerebrovascular events, venous thromboembolic events, and hot flashes than tamoxifen. However, tamoxifen caused significantly fewer musculoskeletal disorders and fractures than anastrozole. Because the follow-up time is relatively short, the American Society of Clinical Oncologists has recommended that no change be made in the current recommendations for the use of adjuvant tamoxifen unless tamoxifen use is contraindicated (e.g., in a patient with a history of thromboembolic events).[48] The American Society of Clinical Oncologists panel states that they were influenced by the "compelling, extensive, and long-term data available on tamoxifen." Overall, the panel considered the results of the ATAC trial and the extensive supporting data to be very promising but insufficient to change the standard practice from adjuvant treatment with tamoxifen to adjuvant anastrozole. However, in September 2002, the United States Food and Drug Administration approved a supplemental new drug application for anastrozole for the adjuvant treatment of hormone receptor–positive early breast cancer in postmenopausal women.

Metastatic Disease

Three SERMs are approved for the treatment of metastatic breast cancer in the United States: tamoxifen, toremifene, and fulvestrant. Overall, approximately 30% of women treated with these drugs respond to therapy. Interestingly, this benefit applies to both postmenopausal women and premenopausal women with

ER-positive breast cancers. The additional treatment of premenopausal women with ovarian suppression (ovariectomy or luteinizing hormone–releasing hormone agonists) and tamoxifen conferred an advantage over treatment with tamoxifen alone in a meta-analysis of four randomized trials.[49] With a median follow-up of 6.8 years, there was a significant survival benefit and progression-free survival benefit in favor of the combined treatment. The overall response rate was also significantly higher on combined endocrine treatment (stratified Mantel-Haenszel test, $P = 0.03$; odds ratio, 0.67).

Tamoxifen The largest trial to evaluate tamoxifen in advanced breast cancer was conducted by the Australian New Zealand Breast Cancer Trials Group and was begun in 1978. This trial randomly assigned 339 patients to tamoxifen alone, chemotherapy with doxorubicin (50 mg/m^2 intravenously) and cyclophosphamide (750 mg/m^2 intravenously) × six 21-day cycles, or tamoxifen plus chemotherapy.[50] The response rate (complete and partial) for tamoxifen was 22.1%, for chemotherapy alone was 45.1%, and for tamoxifen plus chemotherapy was 51.3%. Despite the differences in response rates, median survival rates were not significantly different ($P = 0.49$).

More recently, the development of AIs has led to comparison of tamoxifen with these agents for treatment of metastatic breast cancer in postmenopausal women. Three clinical trials have already compared tamoxifen with second-generation triazole AIs in large randomized trials. A fourth trial is ongoing, comparing tamoxifen with the steroidal third-generation AI exemestane, a compound that is able to inactivate aromatase completely.

In the first trial, the International Letrozole Study Group trial compared tamoxifen with letrozole in 907 postmenopausal women with advanced breast cancer.[51] The patients had to have ER-positive, PR-positive or ER/PR-unknown tumors to be eligible. Patients may have undergone a single prior endocrine therapy for advanced disease. The overall response rate was (30% versus 20% $P = 0.0006$) in favor of letrozole. Letrozole also had a superior median time to progression (41 weeks versus 26 weeks, $P = 0.0001$). No survival data have been reported.

Two additional large randomized trials have compared tamoxifen, 20 mg daily, with anastrozole, 1 mg daily, for the treatment of metastatic breast cancer. One trial was conducted in Europe, Australia, New Zealand, South America, and South Africa (Tamoxifen or Arimidex Randomized Group Efficacy and Tolerability [TARGET] trial) and the other in the United States and Canada (the North American trial). The international TARGET study randomly assigned 688 postmenopausal women with metastatic breast cancer who were hormone receptor–positive or whose receptor status was unknown.[52] Patients who had undergone previous adjuvant tamoxifen therapy were permitted to enter the trial if the therapy had been stopped at least 12 months earlier; however, no previous hormone therapy for metastatic disease was allowed. Objective response rates were similar: 32.9% for anastrozole and 32.6% for tamoxifen. Clinical benefit rates (complete response + partial response stabilization rates of greater than 24

weeks) were equivalent. Median times to progression were also similar: 8.3 months for tamoxifen and 8.2 months for anastrozole.

The second large randomized trial (the North American Trial) comparing the two drugs also showed equivalent results, except that anastrozole had a greater clinical benefit (59% versus 46%).[37] Anastrozole also had a longer median time to progression (11.1 vs 5.6 months, $P = .005$). Overall, both treatments were well tolerated; however, thromboembolic events (4.1% vs 8.2%) and vaginal bleeding (1.2% vs 3.8%) were reported in fewer patients in the anastrozole group than in the tamoxifen group. Of the 119 patients on this trial whose disease progressed after initial anastrozole therapy and received subsequent tamoxifen, 38 achieved disease stabilization for 24 weeks or more. These data suggest that tamoxifen may be successful after AI treatment, although additional studies need to be performed to address the question of optimal sequencing of hormone therapy in advanced disease.

Neoadjuvant Treatment

Neoadjuvant hormone therapy has recently gathered much support because of the publication of a well-designed, multi-institutional trial comparing tamoxifen with the AI letrozole.[53] The Letrozole 024 Neoadjuvant Trial involved 337 postmenopausal women in 55 centers who had ER- or PR-positive locally advanced breast cancer. Patients were randomly assigned to receive letrozole, 2.5 mg/day, or tamoxifen, 30 mg/day, in a double-blinded study. Letrozole responses occurred in 55% of patients, compared with only 36% of patients taking tamoxifen ($P < .001$). In addition, more patients underwent breast-conserving surgery after treatment with letrozole (45%) compared with tamoxifen (35%). Tumor specimens were banked prospectively in this trial and were used to determine whether ErbB1 (epidermal growth factor receptor) and ErbB2 (HER2/Neu) expression affected the efficacy of tamoxifen treatment.[54] The frequency of tumors expressing ErbB1 or ErbB2 as well as ER was 15.2%, and letrozole was indeed much more effective than tamoxifen in this subset of tumors (88% vs 21%), $P = 0.0004$).[55] These data suggest that increased epidermal growth factor receptor expression may be one mechanism whereby ER-positive breast cancers become resistant to SERM activity.[56]

FUTURE DIRECTIONS IN SERM THERAPY

Although several novel SERMs have gone through preclinical and clinical testing in the past decade, most of these compounds have been found to be non–cross-resistant with tamoxifen and therefore have not been added to the treatment choices for ER-positive breast cancer. The predicted three-dimensional structure of the ligand-binding domain of the ER suggests that the non–cross-resistance of some SERMs (e.g., fulvestrant and possibly arzoxifene) is

probably due to functional differences in the ER conformation that results following SERM binding. These three-dimensional effects alter the ER's interaction with corepressors and coactivators, resulting in changes in gene expression that vary significantly between individual SERMs. The AIs also appear to have significant non–cross-resistance with tamoxifen and may be superior to tamoxifen for the first-line treatment of advanced disease in postmenopausal women. As the results of the ATAC trial mature, the AIs may also become the treatment of choice for adjuvant therapy for postmenopausal women.

In premenopausal women, the question of whether ovarian suppression with AI treatment or ovarian suppression with or without tamoxifen is the better treatment for metastatic breast cancer is still under study. In the near future, an international trial will address the question of adjuvant therapy with ovarian suppression with or without AI or tamoxifen in premenopausal women (G. Fleming, personal communication, 2002). The International Breast Cancer Study Group's Suppression of Ovarian Function Trial will randomly assign 3000 patients to treatment with tamoxifen alone for 5 years, tamoxifen with ovarian suppression (gonadotropin-releasing hormone analogue, radiotherapeutic ablation, or surgical oophorectomy), or exemestane with ovarian suppression. The answers to these important adjuvant therapy questions are likely to lead to improved endocrine therapy for premenopausal women in the neoadjuvant and metastatic settings as well. In the prevention setting, the benefits of current SERMs to particular subgroups of women who are at increased risk for breast cancer will continue to be studied carefully so that the appropriate high-risk patients can be identified for prevention strategies. In addition, the benefits of novel SERMs that have fewer detrimental side effects (e.g., less agonist activity in the endometrium) will continue to be evaluated in prevention trials, such as the STAR and MORE studies. Finally, the combined use of SERMs with other prevention strategies, such as cyclooxygenase inhibitors and retinoids, is likely to be implemented as new information that is relevant to the control of breast cancer is translated from the laboratory to the clinic.[57]

REFERENCES

1. Osborne CK, Zhao H, Fuqua SA. Selective estrogen receptor modulators: structure, function, and clinical use. J Clin Oncol 2000;18:3172–3186.
2. Shiau A, Barstad D, Radek J et al. Structural characterization of a subtype-selective ligand reveals a novel mode of estrogen receptor antagonism. Nat Struct Biol 2002;9:359–364.
3. Shiau A, Barstad D, Loria P et al. The structural basis of estrogen receptor/coactivator recognition and the antagonism of this interaction by tamoxifen. Cell 1998;95:927–937.
4. Brzozowski AM, Pike AC, Dauter Z et al. Molecular basis of agonism and antagonism in the oestrogen receptor. Nature 1997;389:753–758.
5. Tremblay GB, Kunath T, Bergeron D et al. Diethylstilbestrol regulates trophoblast stem cell differentiation as a ligand of orphan nuclear receptor ERR beta. Genes Dev 2001;15:833–838.

6. Peethambaram P, Ingle J, Suman V et al. Randomized trial of diethylstilbestrol vs. tamoxifen in postmenopausal women with metastatic breast cancer: an updated analysis. Breast Cancer Res Treat 1999;54:117–122.

7. Harper M, Walpole A. A new derivative of triphenylethylene: effect on implantation and mode of action in rats. J Reprod Fertil 1967;13:101–119.

8. Love RR, Mazess RB, Barden HS. Effects of tamoxifen on bone mineral density in postmenopausal women with breast cancer. N Engl J Med 1992;326:852–856.

9. Fisher B, Costantino JP, Wickerham DL et al. Tamoxifen for prevention of breast cancer: Report of the National Surgical Adjuvant Breast and Bowel Project P-1 study. J Natl Cancer Inst 1998;90:1371–1388.

10. Dhingra K. Selective estrogen receptor modulation: the search for an ideal hormonal therapy for breast cancer. Cancer Invest 2001;19:649–659.

11. Loprinzi C, Sloan J, Perez E et al. Phase III evaluation of fluoxetine for treatment of hot flashes. J Clin Oncol 2002;20:1578–1583.

12. Van Patten CL, Olivotto IA, Chambers GK et al. Effect of soy phytoestrogens on hot flashes in postmenopausal women with breast cancer: a randomized, controlled clinical trial. J Clin Oncol 2002;20:1449–1455.

13. Quella S, Loprinzi C, Barton D et al. Evaluation of soy phytoestrogens for the treatment of hot flashes in breast cancer survivors: a North Central Cancer Treatment Group trial. J Clin Oncol 2000;18:1068–1074.

14. Jacobson JS, Troxel AB, Evans J et al. Randomized trial of black cohosh for the treatment of hot flashes among women with a history of breast cancer. J Clin Oncol 2001;19:2739–2745.

15. Hard G, Latropoulos M, Jordan K et al. Major difference in the hepatocarcinogenicity and DNA adduct forming ability between toremifene and tamoxifen in female Crl:CD(BR) rats. Cancer Res 1993;53:4534–4541.

16. Pyrhonen S, Ellmen J, Vuorinen J et al. Meta-analysis of trials comparing toremifene with tamoxifen and factors predicting outcome of anti-estrogen therapy in postmenopausal women with breast cancer. Breast Cancer Res Treat 1999;56:133–143.

17. Holli K, Valavaara R, Blanco G et al. Safety and efficacy results of a randomized trial comparing adjuvant toremifene and tamoxifen in postmenopausal patients with node-positive breast cancer. J Clin Oncol 2000;18:3487–3494.

18. Roos W, Oeze L, Loser R et al. Antiestrogenic action of 3-hydroxytamoxifen in the human breast cancer cell line MCF-7. J Natl Cancer Inst 1983;71:55–59.

19. Haarstad H, Lonning PE, Gundersen S et al. Influence of droloxifene on metastatic breast cancer as first-line endocrine treatment. Acta Oncol 1998;37:365–368.

20. Dhingra K. Antiestrogens: tamoxifen, SERMs and beyond. Invest New Drugs 1999;17:285–311.

21. Johnston SR, Riddler S, Haynes B et al. The novel anti-oestrogen idoxifene inhibits the growth of human MCF-7 breast cancer xenografts and reduces the frequency of acquired anti-oestrogen resistance. Br J Cancer 1997;75:804–809.

22. Nuttall M, Bradbeer J, Stroup G et al. Idoxifene: a novel selective estrogen receptor modulator prevents bone loss and lowers cholesterol levels in ovariectomized rats and decreases uterine weight in intact rats. Endocrinology 1998;139:5224–5534.

23. Johnston S, Gorbunova V, Lichinister M et al. A multicentre double-blind randomized phase II trial of idoxifene versus tamoxifen as first-line endocrine therapy for metastatic breast cancer. Proc Am Soc Clin Oncol 2001;20:A113.

24. Johnston SRD, Howell A. Endocrine treatment of breast cancer: SERMs. In: Miller WR, Ingle James N, eds. Endocrine Therapy in Breast Cancer. New York: Marcel Dekker, 2002:47–77.

25. Buzdar A, Marcus C, Holmes F et al. Phase II evaluation of LY156758 in metastatic breast cancer. Oncology 1988;45:344–345.
26. Gradishar W, Glusman J, Lu Y et al. Effects of high dose raloxifene in selected patients with advanced breast carcinoma. Cancer 2000;88:2047–2053.
27. Sato M, Turner C, Wang T et al. A novel raloxifene analogue with improved SERM potency and efficacy in vivo. J Pharmacol Exp Ther 1998;287:1–7.
28. Baselga J, Llombart-Cussac A, Bellet M. Double-blind randomized phase II study of a selective estrogen receptor modulator in patients with locally advanced or metastatic breast cancer. Breast Cancer Res Treat 1999;57:A25.
29. Llombart-Cussac A, Bellet M, Guillem-Porta V et al. Efficacy and safety of two doses of the selective estrogen receptor modulator (SERM) LY353381 in locally advanced or metastatic breast cancer (LAMBC): a randomized double blind phase 2 study. Proc Am Soc Clin Oncol 2000;19:157a.
30. Labrie F, Labrie C, Belanger A et al. EM-652 (SCH57068), a pure SERM having complete antiestrogenic activity in the mammary gland and endometrium. J Steroid Biochem Mol Biol 2001;79:213–225.
31 Labrie F, Champagne P, Labrie C et al. Response to the orally active specific antiestrogen EM-800 (SCH-57070) in tamoxifen resistant breast cancer. Breast Cancer Res Treat 1997;42:A211.
32. Greenberger LM, Annable T, Collins KI et al. A new antiestrogen, 2-(4-hydroxy-phenyl)-3-methyl-1-[4-(2-piperidin-1-yl-ethoxy)-benzyl]-1-indol-5-ol hydrochloride (ERA-923), inhibits the growth of tamoxifen-sensitive and -resistant tumors and is devoid of uterotropic effects in mice and rats. Clin Cancer Res 2001;7:3166–3177.
33. Cotreau MM, Stonis L, Dykstra KH et al. Multiple-dose, safety, pharmacokinetics, and pharmacodynamics of a new selective estrogen receptor modulator, ERA-923, in healthy postmenopausal women. J Clin Pharmacol 2002;42:157–165.
34. Johnston SR. Endocrine manipulation in advanced breast cancer: recent advances with SERM therapies. Clin Cancer Res 2001;7:4376s–4387s; discussion 4411s–4412s.
35. Robertson JF. Estrogen receptor downregulators: new antihormonal therapy for advanced breast cancer. Clin Ther 2002;24[suppl A]:A17–30.
36. Robertson J, Howell A, De Friend D et al. Duration of remission to ICI 182,780 compared to megestrol acetate in tamoxifen-resistant breast cancer. Breast 1997;6:186–189.
37. Nabholtz J, Buzdar A, Pollak M et al. Anastrozole is superior to tamoxifen as first-line therapy for advanced breast cancer in postmenopausal women: results of a North American multicenter randomized trial. J Clin Oncol 2000;18:3758–3776.
38. Howell A, Robertson J, Quaresma Albano J et al. Fulvestrant, formerly ICI 182,780, is as effective as anastrozole in postmenopausal women with advanced breast cancer progressing after prior endocrine treatment. J Clin Oncol 2002;20:2296–2403.
39. Powles TJ, Tillyer CR, Jones AL et al. Prevention of breast cancer with tamoxifen: an update on the Royal Marsden Hospital Pilot Programme. Eur J Cancer 1990;26:680–684.
40. Veronesi U, Maisonneuve P, Sacchini V et al. Tamoxifen for breast cancer among hysterectomised women. Lancet 2002;359:1122–1124.
41. Veronesi U, Maisonneuve P, Costa A et al. Prevention of breast cancer with tamoxifen: preliminary findings from the Italian randomised trial among hysterectomised women. Italian tamoxifen prevention study. Lancet 1998;352:93–97.
42. Gail MH, Costantino JP, Bryant J et al. Weighing the risks and benefits of tamoxifen treatment for preventing breast cancer. J Natl Cancer Inst 1999;91:1829–1846.
43. Cuzick J. First results from the International Breast Cancer Intervention Study (IBIS-I): a randomised prevention trial. Lancet 2002;360:817.

44. Cummings SR, Eckert S, Krueger KA et al. The effect of raloxifene on risk of breast cancer in postmenopausal women: results from the more randomized trial. Multiple Outcomes of Raloxifene Evaluation. JAMA 1999;281:2189–2197.

45. Lippman ME, Krueger KA, Eckert S et al. Indicators of lifetime estrogen exposure: effect on breast cancer incidence and interaction with raloxifene therapy in the multiple outcomes of raloxifene evaluation study participants. J Clin Oncol 2001;19:3111–3116.

46. Fisher B, Land S, Mamounas E et al. Prevention of invasive breast cancer in women with ductal carcinoma in situ: an update of the National Surgical Adjuvant Breast Project experience. Semin Oncol 2001;28:400–418.

47. ATAC Trialists Group. Anastrozole alone or in combination with tamoxifen versus tamoxifen alone for adjuvant treatment of postmenopausal women with early breast cancer: first results of the ATAC randomised trial. Lancet 2002;359:2131–2139.

48. Winer E, Hudis C, Burstein HJ et al. American Society of Clinical Oncology technology assessment on the use of aromatase inhibitors as adjuvant therapy for women with hormone receptor-positive breast cancer: status report 2002. J Clin Oncol 2002;20:3317–3327.

49. Klijn JG, Blamey RW, Boccardo F et al. Combined tamoxifen and luteinizing hormone-releasing hormone (LHRH) agonist versus LHRH agonist alone in premenopausal advanced breast cancer: a meta-analysis of four randomized trials. J Clin Oncol 2001;19:343–353.

50. Coates AS, Simpson JF, Forbes JF. A randomized trial in postmenopausal patients with advanced breast cancer comparing endocrine and cytotoxic therapy given sequentially or in combination: the Australian and New Zealand Breast Cancer Trials Group, Clinical Oncological Society of Australia. J Clin Oncol 1986;4:186–193.

51. Mouridsen H, Gershanovish M, Sun Y. Superior efficacy of letrozole versus tamoxifen as first-line therapy for postmenopausal women with advanced breast cancer: results of a phase III study of the International Letrozole Breast Cancer Group. J Clin Oncol 2001;19:2596–2606.

52. Bonneterre J, Buzdar A, Nabholtz J et al. Anastrozole is superior to tamoxifen as first-line therapy in hormone receptor positive advanced breast carcinoma. Cancer 2001; 92:2247–2258.

53. Eiermann W, Paepke S, Appfelstaedt J et al. Preoperative treatment of postmenopausal breast cancer patients with letrozole: a randomized double-blind multicenter study. Ann Oncol 2001;12:1527–1532.

54. Yamauchi H, Stearns V, Hayes DF. The role of c-ERB-2 as a predictive factor in breast cancer. Breast Cancer 2001;8:171–183.

55. Ellis MJ, Coop A, Singh B et al. Letrozole is more effective neoadjuvant endocrine therapy than tamoxifen for erbB1- and/or erbB2-positive, estrogen receptor-positive primary breast cancer: evidence from a phase III randomized trial. J Clin Oncol 2001;19:3808–3816.

56. Newby J, Johnston S, Smith I et al. Expression of epidermal growth factor receptor and c-erbB2 during the development of tamoxifen resistance in human breast cancer. Clin Cancer Res 1997;3:1643–1651.

57. Sporn MB. Hobson's choice and the need for combinations of new agents for the prevention and treatment of breast cancer. J Natl Cancer Inst 2002;94:242–243.

5. Gottardis, M. M. & Jordan, V. C. (1988) Cancer Res. 48, 5183–5187
6. Wakeling, A. E. (1990) J. Steroid Biochem. Mol. Biol. 37, 771–775
7. Wakeling, A. E. & Bowler, J. (1987) J. Endocrinol. 112, R7–R10
8. Wakeling, A. E. & Bowler, J. (1988) J. Steroid Biochem. 31, 645–653
9. Wakeling, A. E. (1990) in Regulatory Mechanisms in Breast Cancer (Lippman, M. & Dickson, R. B., eds.), pp. 239–257, Kluwer Academic Publishers, Boston
10. Nicholson, R. I., Gotting, K. E., Gee, J. & Walker, K. J. (1988) J. Steroid Biochem. 30, 95–103
11. Wakeling, A. E., Newboult, E. & Peters, S. E. (1989) J. Mol. Endocrinol. 2, 225–234
12. Thompson, E. W., Katz, D., Shima, T. B., Wakeling, A. E., Lippman, M. E. & Dickson, R. B. (1989) Cancer Res. 49, 6929–6934
13. Wakeling, A. E., Dukes, M. & Bowler, J. (1991) Cancer Res. 51, 3867–3873

Received 22 July 1991

Design of ligands for the glucocorticoid and progestin receptors

G. Teutsch, M. Gaillard-Moguilewsky, G. Lemoine, F. Nique and D. Philibert
Centre de Recherche, Roussel-Uclaf, F-93230, Romainville, France.

Introduction

Steroid hormones act via their interaction with intracellular receptors that belong to a general class of regulatory proteins, the 'steroid-receptor superfamily'. This class includes the five 'classical' steroid receptors: oestrogen (ER), androgen (AR), progestin (PR), glucocorticoid (GR) and mineralocorticoid (MR) receptors as well as the receptors for thyroid hormone, vitamin D3, retinoic acid, and a number of 'orphan receptors' the ligands of which are not yet known.

Cloning and sequence determination of these receptors demonstrated that the common overall structure consists of essentially three domains: the variable *N*-terminal domain, the central DNA-binding domain and the *C*-terminal ligand-binding domain (LBD). Close examination of the compared sequences of the LBDs of the five 'classical' steroid-hormone receptors, confirmed what researchers in the steroid field have empirically known for many years: there is a high degree of sequence similarity between the LBDs of GR, MR, PR and AR, the receptors of the 3-oxo-Δ^4 steroids, which are quite different from the LBD of the ER whose natural ligand, oestradiol, has an aromatic A ring (see [1] for an overview).

These similarities are even more striking if, instead of considering the straightforward amino acid to amino acid identity, one compares the sequences by hydrophobic-cluster analysis [2], a technique which has recently permitted the elaboration of a tentative three dimensional structure of the steroid receptors [3]. However, for many years and up to the present time, we have had to rely solely on structural modification of the hormonal steroids to gain some indirect information on the topography of the receptor binding site: this crude technique is called 'mapping'. It was made possible only through the availability of receptor screening, which consists of measuring the binding affinities of various compounds for the steroid receptors. In the decade following the discovery of steroid-hormone receptors [4–6 for reviews] a simple screening procedure was set up in the Roussel-Uclaf company by J. P. Raynaud and coworkers, which allowed the comparison of the relative binding affinities (RBAs) of a large number of steroids with those of reference compounds [7]. It quickly became obvious that neither the natural hormones, nor the synthetic reference compounds were perfectly specific for their cognate receptor. While oestradiol bound to a small extent to the PR (2% of progesterone) and the AR (8% of testosterone) in addition to it own ER (100%), none of the 3-oxo Δ-4 steroids had any affinity for the ER.

Among the latter compounds progesterone appeared as having a significant affinity already for the GR, provided a receptor preparation of thymic origin was used. Indeed, liver preparations contain enzymes which metabolize the ligand very quickly, even at 4°C, giving a false impression of selectivity. Among synthetic hormones, R 1881 especially, an androgen of the oestra-4,9,11-triene series, displayed a remarkably unspecific binding profile [7]. These first results already indicate that most receptors, especially AR, PR, GR and MR share common features which allow them to bind some ligands quite unspecifically. This suggests that the steroid receptors may present a common gross shape of

Abbreviations used: ER, oestrogen receptor; AR, androgen receptor; PR, progestin receptor; GR, glucocorticoid receptor; MR, mineralocorticoid receptor; LBD, ligand-binding domain; RBA, relative binding affinity.

the binding site, with probably different three dimensional repetition of a few key amino acids which are responsible for the specificity observed with some compounds. Our goal, in the present paper, is to present a few of the less well known steroidal ligands for the PR and GR. The analyses of these structures, when attempted, are essentially speculative and intended as thought-provoking propositions, as well as an incentive for proper experimental verification.

General remarks about RBAs

Knowledge of the RBA of a compound for various receptors is undoubtedly useful information. However, a series of possible pitfalls associated with the RBA measurements should be kept in mind: (1) RBAs are not representative of the true equilibrium constants, but are expressed as relative affinity versus a reference compound whose true affinity can vary by one order of magnitude or more. Indeed, RBAs of reference compounds are taken arbitrarily as equal to 100%, independently of their K_A. (2) It has also been shown that RBAs can differ markedly depending on time of incubation, or on temperature [8]. In addition, determinations are generally not made at the physiological temperature. (3) One further problem is the heterogeneity of enzymic activity and of binding proteins in the tissues that are used for receptor preparations. This is quite striking for the GR, depending on whether it was isolated from liver or thymus, the former tissue being very rich in metabolizing enzymes. Thus, progesterone, which does not display any GR binding affinity when tested on the rat liver receptor, competes as well as cortisol on the rat thymus receptor (Table 1). (4) Species variability should not be overlooked either. This is especially important for synthetic compounds, as demonstrated very strikingly by the absence of binding of the antiprogestin RU 486 for the chicken [9, 10] and hamster [11, 12] progesterone receptors. (5) Finally, when comparing RBAs of a compound for the PR and the GR, we implicitly assume that the competition occurs at the true binding site and not at a secondary (allosteric?) binding site, which has repeatedly been suggested for the GR [13–16].

Table 1

RBAs for liver, versus thymus GR in the rat

Abbreviation: DOC, deoxycorticosterone

Compound	Incubation time (h)	Thymus	Liver
Progesterone	4	42 ± 3.5	0.24 ± 0.09
	24	17 ± 2	< 0.1
Cortisol	4	31.5 ± 5	34 ± 6
	24	13 ± 1.4	5 ± 2
Corticosterone	4	60 ± 5	17 ± 2
	24	31 ± 1	0.4 ± 0.17
DOC	4	50 ± 7	0.5 ± 0.1
	24	26 ± 3	0.08 ± 0.04
Desoximetasone	4	207 ± 30	148 ± 7
	24	217 ± 28	163 ± 9

Structure–affinity relationship

Table 2 lists a number of known as well as yet unpublished steroids, which have been chosen to illustrate some specific aspects of structure–affinity relationships on the PR and the GR.

11β and 17α hydroxyl groups

When looking at the structures of progesterone and the main natural glucocorticoids (cortisol in humans, corticosterone in rats), things appear quite straightforward: while all three of the compounds belong to the 4-pregnane-3,20-dione series, progesterone is not hydroxylated, cortisol can be considered as 11β,17α,21-trihydroxyprogesterone, and corticosterone as 11β,21-dihydroxyprogesterone. These additional hydroxyls were thought to provide the specificity for the GR until it was found that, when switching from the liver GR preparation to a thymus GR preparation, progesterone appeared to be as good a ligand as cortisol (Table 1). This behaviour still awaits a satisfactory explanation since progesterone does not display any glucocorticoid activity but rather acts as a weak antagonist [17].

Comparing cortisol and corticosterone, it has been known for a long time that while the 17α hydroxy group is not necessary for GR binding, it is nevertheless very efficient in suppressing PR binding.

The 11β hydroxy group, also reduces to some extent PR binding and, as stated above, is still generally considered as the prerequisite for GR binding. However, the synthesis of some 9α, 11β-dichloro analogues like dichlorisone [18] or RU 24476 (No. 6, Table 2) [19] showed that substitution of the hydroxyl by a chlorine leads to high affinity for both the GR and the PR. It should be stressed that this type of compound, unlike progesterone, displays a potent glucocorticoid-like activity *in vivo*. This result disturbs somewhat the well

liver receptor,
ıe rat thymus
ility should not
ally important
ınstrated very
g of the anti-
[9, 10] and
ırs. (5) Finally,
nd for the PR
t the competi-
and not at a
:, which has
[13–16].

ıp
ıs well as yet
:en chosen to
ıcture–affinity

gesterone and
(cortisol in
; appear quite
ɛ compounds
.eries, proges-
can be con-
;esterone, and
progesterone.
;ht to provide
.s found that,
:paration to a
: appeared to
ıble 1). This
explanation
ıy glucocorti-
ık antagonist

terone, it has
ıile the 17α
binding, it is
ng PR bind-

uces to some
ɔove, is still
site for GR
ne 9α, 11β-
[18] or RU
hat substitu-
:ads to high
It should be
ılike proges-
-like activity
ıat the well

Table 2

RBAs for GR* and PR**

Abbreviation used: n.a., not available

Structure	Entry	Designation	Substituents	GR*	PR**
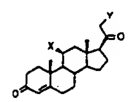	1	Progesterone	X = Y = H	17	100
	2	11-OH progest	x = OH, Y = H	7	28
	3	Corticosterone	X = Y = OH	31	3
	4	DOC	X = H, Y = OH	26	17
	5	RU 18723	X = OMe, Y = O	6	7.5
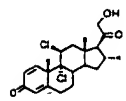	6	RU 24476		210	90
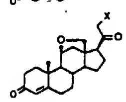	7	R 1132	X = H	0.7	1.1
	8	RU 28418	X = OH	1.8	0.3
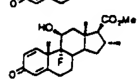	9	RU 25994		245	120
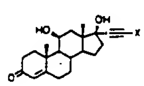	10	R 200	X = H	5	3
	11	RU 25458	X = Me	68	0.1
	12	RU 26275	X = Et	95	1.7
	13	RU 26356	X = Ph	120	6.5
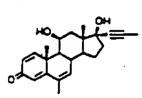	14	RU 28362		214	1.7
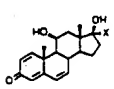	15	RU 26988	X = 1-propynyl	130	0.3
	16	RU 27728	X = 2-propynyl	3	0
	17	RU 27599	X = allyl	9	0
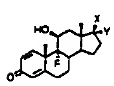	18	Tipredane	X = SMe, Y = SEt	≈ 75§	n.a.
	19	SQ 28223	X = SMe, Y = SCH_2CH_2F	> 100§	n.a.
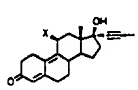	20	RU 38486	X = 4-Me_2N-C_6H_4	300	530
	21	RU 38502	X = tBu	50	0.7
	22	RU 38275	X = Me	60	240
	23	RU 40540	X = Et	60	22
	24	RU 42764	X = vinyl	340	350
	25	RU 39229	X = p-C_6H_5-C_6H_4	110	300
	26	RU 40900	X = 4Me-piperazino-C_6H_4	86	25
	27	RU 43780	X = 4-(phenylethynyl)C_6H_4	5	11
	28	R 2263	X = OH	0.1	0.1
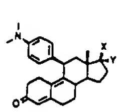	29	RU 38473	X = OH, Y = ethynyl	235	350
	30	RU 40016	X = ethynyl, Y = OH	120	4
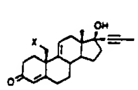	31	RU 39305	X = Ph	57	< 0.1
	32	RU 43044	X = 4-Me-C_6H_4	130	< 0.2
	33	RU 43195	X = ethynyl	240	17
	34	RU 43230	X = vinyl	90	11
	35	RU 43274	X = i-propenyl	110	0.1
	36	RU 45667	X = H	15	13
	37	RU 45526	X = Me	26	14

Table 2 – *continued*

Structure	Entry	Designation	Substituents	GR*	PR**
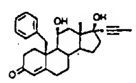	38	RU 44425		0.1	0
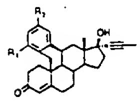	39	RU 56841	$R_1 = H, R_2 = Me$	100	260
	40	RU 56843	$R_1 = Me, R_2 = H$	105	10
	41	RU 56839	$R_1 = R_2 = H$	120	95
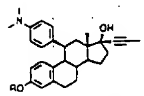	42	RU 41291	R = H	220	130
	43	RU 41685	R = Me	24	8
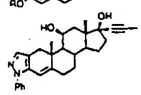	44	RU 27144		134	0
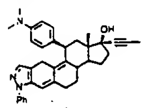	45	RU 40336		17	<0.1
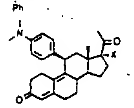	46	RU 40088	X = Me	27	230
	47	RU 44675	X = OAc	135	500
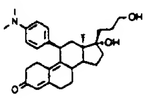	48	ZK 98299		40	35
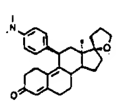	49	RU 50331		80	275
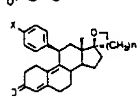	50	RU 45781	$X = NMe_2$, n = 2	50	310
	51	RU 50502	$X = NMe_2$, n = 1	40	410
	52	RU 49295	X = Ac, n = 2	25	520

*GR: Rat thymus. 24 h. 0°C. (Dexamethasone = 100).
**PR: Rabbit uterus. 24 h. 0°C. (Progesterone = 100).
§Estimated from reported IC values [24].

accepted idea of the necessity of a hydrogen-bond donor [20] at position 11β of the steroid. One possibility could be that both 11-OH and 11-Cl act as hydrogen-bond acceptors, but this hypothesis is not suitable for explaining the binding of progesterone. In any case, we checked the RBAs of the 11-oxo compounds 7 and 8 (Table 2), with the hope that the oxygen could act as an acceptor. The low affinities found are certainly not in favour of this hypothesis. We may now speculate that the binding site for the 11β-substituent is essentially hydrophobic, but that in the case of the hydrophilic 11β-hydroxy group it is a hydrogen bond which provides the necessary binding energy.

D-ring substitution

The fact that the 20-oxo-21-hydroxypregnane structure of classical corticoids is not an absolute necessity for a high affinity for the GR can be deduced from compounds such as the 17β carboxylic ester RU 25994 (No. 9, Table 2). However, this does maintain an equivalent to the 20-oxo group. A more radical structural change is represented by the 17α-alkynylandrosterone series (compounds 10 to 13, Table 2). Indeed, the 17α-propynyl-17β-hydroxy substitution pattern was found to mimic the classical corticoid side-chain [21]. Compounds like RU 28362 (compound 14, Table 2) display a high RBA for the GR along with

very low affinity for both the PR and the MR. So far, there have been no serious attempts to find an explanation for this surprising observation.

Most unexpectedly, displacement of the triple bond by one carbon (16, Table 2) totally abolished GR binding and replacement of propynyl by allyl (17, Table 2) had the same effect. On the contrary, long alkynyl groups were not deleterious for binding provided that the triple bond remained at the same place. This could either indicate a specific H-bond with the acetylenic orbitals [22] or a purely steric effect.

Androstene-17-thioketals (18 and 19, Table 2) have been reported by the Squibb group to display very high affinities for the GR (rat liver and mouse thymus), confirming that the classical dihydroxyacetone side-chain is not necessary for binding to the GR [23, 24]. These results taken as a whole suggest that the binding site around the D ring of glucocorticoids is hydrophobic in nature, and that there might exist two alternate binding interactions: (*a*) one of the 'classical glucocorticoids' involving specific hydrogen bonds, and (*b*) one rather nonspecific, involving hydrophobic interactions.

11β-substituted 19-norsteroids

Although it was known for a long time that some 19-norsteroids could display significant affinities for the GR especially in the trienone series [7, 25], the great novelty arose from the synthesis of 11β-alkyl and aryl oestradienones [26]. Some of these compounds not only bound tightly to the PR but also to the GR, leading ultimately to the design of RU 38486 (20, Table 2), both a potent anti-progestin and anti-glucocorticoid [27–30]. Beside the interest of this class of compounds as potent hormones and anti-hormones, they also proved to be quite useful in the comparative mapping of the PR and the GR [31, 32]. Indeed, the demonstration was made that these receptors must possess a large hydrophobic pocket within the hormone-binding site, able to harbour 11β-substituents as bulky as a biphenyl or t-butyl group. By comparing various alkyl- and aryl-substituted compounds we could deduce that there was a major difference in the section of the hydrophobic pockets of the PR and the GR in the vicinity (about 3 Å above) of C-11. Whereas this section was very narrow for the PR, being just able to accomodate 'flat' substituents such as vinyl or phenyl which are predicted to eclipse the C_9-C_{11} bond, it was much wider for the GR [31]. In this case, a substituent as bulky as t-butyl still could fit into the binding site, as demonstrated by the significant affinity for the GR or RU 38502 (21, Table 2). This compound however displayed a greatly reduced binding to the PR. These results tend to demonstrate that while it is possible to design 11β-substituted oestradienones with a selective affinity for the GR, the reverse is much less evident, as any 11β-substituent which fits in the hydrophobic site of the PR will also fit in the corresponding site of the GR. Compounds 22 and 24 (Table 2) are typical examples of such ubiquitous molecules. Lengthening of the substituents as in the biphenyl, piperazinophenyl or phenylethynylphenyl analogue 25, 26 and 27, showed that the pockets of GR and PR have similar depths and that no dissociation can be expected on this parameter.

One further observation which was made is that in this 11β-substituted 19-norsteroid series, 17α-substitution was much less critical than in the 11β-hydroxyandrostane series (compare 29 and 10 in Table 2), implying either an overwhelming weight of the lipophilic 11β-substituent or a different positioning of the 17α-alkynyl group in the two series. Curiously, inversing the 17 configuration (compare 29 and 30, Table 2) greatly reduced PR binding, a result which is reminiscent of the pregnane series. The very weak affinity of the 11β-hydroxy oestradiene derivative 28 for the GR may indicate that indeed the site in the GR associated with the β-face of the steroid is hydrophobic, an angular methyl group at 10β being necessary for 11β-hydroxysteroids to bind.

19-aryl androstanes

In fact, if we turn our attention to the superimposition of compounds 11 and 21 (Table 2), it appears that the 10β-methyl group of the former and the t-butyl group of the latter might protrude into the same hydrophobic pocket of the GR. For the PR such a large site does not seem available as deduced above, and also from the fact that 19-norprogestins display much higher RBAs than progesterone (compare progesterone, nor enones and nor dienones) [7].

With these elements in mind it seemed possible to design a compound endowed with a specific affinity for the GR, either by attaching a bulky substituent to the 11β-position or to the 10β-position. To this end, we imagined that introducing a benzyl group at 10β would bring the aromatic ring into the '11β-pocket' of the GR, while it would be too bulky to fit in the corresponding site of the PR. This was indeed what happened: 31 and 32 (see Table 2) bound specifically to the GR. It should be mentioned that this type of compound acted as a glucocorticoid antagonist *in vitro* [33]. Other 10β-

substituted compounds such as 33, 34 and 35 (Table 2) also displayed remarkable affinities for the GR. Interestingly, the smaller R groups, methyl and ethyl were associated with the lowest GR binding as well as with some affinity for the PR.

Surprisingly, compound 38 which has both a 10β-benzyl group and a 11β-hydroxyl substituent, did not display any affinity for the GR in spite of the fact that the calculated conformation of the benzyl group did not differ significantly from what it is in the parent compound 31. We have so far no convincing explanation for this result.

10β–11β cyclized compounds

Recently, the Schering AG group disclosed the cyclization of 10β-benzyl derivatives of the type discussed in the previous section, leading to compounds in which the aromatic ring was attached both to C-11 and C-19 [34, 35]. The claim that these compounds are potent anti-progestins was somewhat surprising with regard to our analysis of GR/PR specificity. Although molecular models showed that cyclization would bring the aromatic ring back to an orientation close to that found in the 11β-aryl oestradienone series, the bridging to C-19 was expected to reduce PR binding. In addition, another feature of this type of compound was of interest to us: by 'freezing' the conformation of the aromatic ring it would allow the mapping of the hydrophobic pockets of the GR and the PR with the *meta* substituent. Indeed, we had previously shown [31] that in the 11β-aryl series, displacement of the *para* substituent of the aromatic ring to the *meta* position would result in a significant dissociation in favour of the GR. However, there were two possible orientations of the *meta* substituent: over the plane of the steroid or away from it, in what one could call *endo* and *exo* arrangements. The compared results of 39 and 40 (Table 2) show that, while GR binding is unchanged, PR binding is highly affected by the orientation of the methyl group. This allows us to define with some more detail the outline of the PR binding pocket, confirming our previous observation [32] that it does not extend significantly over C-19 of the steroid but rather towards C-18.

Modification of the A-ring

As pointed out at the beginning of this paper, steroids with an aromatic A-ring barely interact with receptors other than the ER. Introduction of lipophilic 11β-substituents dramatically alters this situation: when RU 486 is aromatized, the resulting compound 42 (Table 2), still displays high affinity both for the GR and the PR. Replacement of the 3-OH group by a methoxy, as in compound 43 also greatly affects binding, suggesting that a hydrogen bond might be involved. Superimposing the C and D rings with the corresponding rings of the aro-

Fig. 1

Superimposition of compounds 20 and 42 (dashed line)

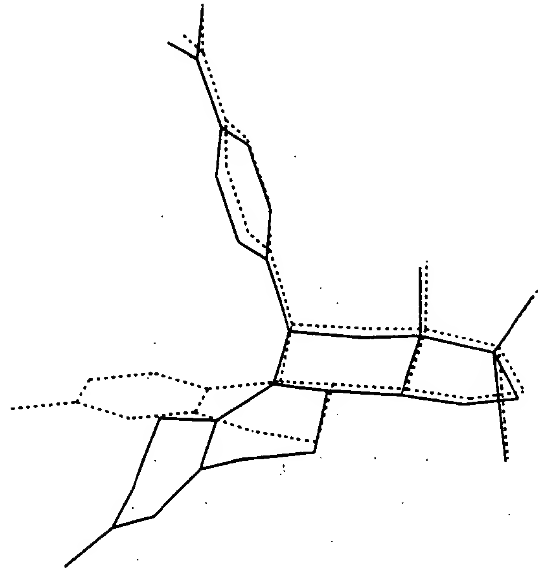

Fig. 2

Superimposition of compounds 44 and 45 (dashed line)

The distance between the 1′ carbons of the two phenyl groups on the pyrazoles is 3.2 Å.

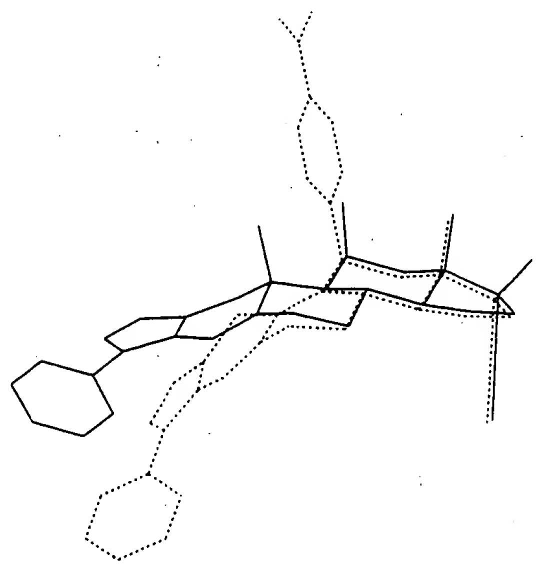

matic analogue, showed that the respective oxygens at position 3 were separated by about 4 Å (Fig. 1). This implies that the hydrogen bonds at 0-3 for the two steroids are engaged with different amino acids of the GR, unless one invokes an induced fit of hormone and receptor, a hypothesis which cannot be excluded at this time.

'Cortivazol'-type compounds

Whereas introduction of a fused phenyl–pyrazole ring at positions 2 and 3 of pregnane-type corticoids maintained or even improved affinities for the GR as in cortivazol, [36] the same modification on RU 38486 (20, Table 2) led to compound 45 which displayed a highly reduced affinity. Comparison of the three-dimensional structures of compounds 44 and 45 (see Table 2) showed that the phenyl rings of the respective pyrazoles occupy very different regions of space, implying the presence of a well-circumscribed hydrophobic pocket (Fig. 2).

Search for specific PR binding

This topic will be restricted to the 11β-substituted oestradienone series, mainly to compounds designed as anti-progestins. Indeed, there are some clinical indications for anti-progestins, involving long-term treatment, in which compounds without an anti-glucocorticoid component would be preferred. The most logical hypothesis to achieve this goal is to design RU 486 analogues which would bind selectively to the PR. As seen above, many modifications led to a reverse selectivity, that is, a higher affinity for the GR than for the PR. One of our first attempts in the desired direction was made in the norpregnane series to which belong the most selective progestins [7]. Although a significant dissociation of the RBAs was achieved (see 46, Table 2), the compound failed to be active as an anti-progestin at 3 mg/kg. However, the 17α-acetoxy analogue 47 proved to be quite active as an anti-progestin, but maintained a significant affinity for the GR as well as a non-negligible anti-glucocorticoid activity.

Reports by the Schering AG group that 13α-oestradienones such as onapristone, 48 (Table 2) [37] were dissociated anti-progestins prompted us to synthesize and test these compounds. In our hands, onapristone appeared as poorly dissociated at the receptor level whereas its cyclized analogue 49 (Table 2) showed improved dissociation. Similarly, in the natural series, the 17-spiroethers exemplified by compounds 50–52 displayed reasonable dissociations of the RBAs, a quality which was fully confirmed *in vivo* [33, 38].

Conclusions

From the above examples, one may like to draw a number of tentative conclusions, some of which appear quite straightforward, while others are more speculative in nature: (*a*) the necessity for more homogeneity in the RBA measurements, with reference to species, organs, time and temperature of incubations appears to be of prime importance. Caution should always be exercized when comparing RBAs from different origins. Expression of all the receptors, especially human receptors in a single cell type, could be considered as a progress, with special relevance to predictivity for human trials. (*b*) Experience has shown that affinity–activity correlation is not always reliable, a fact which should be kept in mind when screening for dissociated compounds. Testing *in vivo* cannot be circumvented yet. (*c*) Partial 'mapping' of the PR and the GR suggests that: (i) the binding site for the relevant steroids is hydrophobic and much larger than expected from a tight 'lock and key' model; (ii) there are instances where hydrogen bonds can be replaced by hydrophobic interactions. This finding would make sense insofar as specific hydrogen bonds are more likely to occur in a hydrophobic environment, and (iii) mapping is limited to those regions of the receptor site which are accessible by substituents of the probe which is used (generally a steroid). The possibility arises that some non-steroidal compounds could bind in a very different way, for instance in the large hydrophobic pockets which have been shown to harbour the bulky 11β and 17α substituents. If this were true, attempts to superimpose very dissimilar compounds would be totally disconnected from reality. (*d*) Additional methods of investigations are clearly needed to elaborate a less blurred picture of the steroid-binding site: affinity labelling, receptor mutations and three-dimensional modelling based on structures of homologous known proteins will hopefully come up with useful information. (*e*) The existence of a possible second binding site has to be considered seriously especially with reference to antagonist activity.

We thank Mrs S. Fritsch for typing the manuscript.

1. Evans, R. M. (1988) Science 240, 889–895
2. Mornon, J. P., Bissery, V., Gaboriaud, C., Thomas, A., Ojasoo, T. & Raynaud, J. P. (1989) J. Steroid Biochem. 34, 355–361
3. Lemesle-Varloot, L., Ojasoo, T., Mornon, J. P. & Raynaud, J. P. (1991) J. Steroid Biochem. Mol. Biol. in the press
4. Jensen, E. V., Mohla, S., Gorell, T. A. & DeSombre, E. R. (1974) Vitam. Horm. 32, 89–127

5. Baulieu, E. E., Atger, M., Best-Belpomme, M., Corvol, P., Courvalin, J. C., Mester, J., Milgrom, E., Robgel, P., Rochefort, H. & De Catalogne, D. (1975) Vitams. Horm. N.Y. **33**, 649–736
6. Gorski, J. & Gannon, F. (1976) Annu. Rev. Physiol. **38**, 425–450
7. Raynaud, J. P., Ojasoo, T., Bouton, M. M. & Philibert, D. (1979) in Drug Design (Ariëns, E. J., ed.), vol. 8, pp. 169–214, Academic Press, London & New York
8. Raynaud, J. P., Bouton, M. M. & Ojasoo, T. (1979) Biochem. Soc. Trans. **7**, 547–551
9. Groyer, A., Le Bouc, Y., Joab, I., Radanyi, C., Renoir, J. M., Robel, P. & Baulieu, E. E. (1985) Eur. J. Biochem. **149**, 445–451
10. Moudgil, V. K., Lombardo, G., Hurd, C., Eliezer, N. & Agarwal, M. K. (1986) Biochim. Biophys. Acta **889**, 192–199
11. Okulicz, W. C. (1987) J. Steroid Biochem. **28**, 117–122
12. Gray, G. O. & Leawitt, W. W. (1987) J. Steroid Biochem. **28**, 493–497
13. Suthers, M. B., Pressley, L. A. & Funder, J. W. (1976) Endocrinology (Baltimore) **99**, 260–269
14. Jones, T. R. & Bell, T. A. (1980) Biochem. J. **188**, 237–245
15. Svec, F., Teubner, V. & Tate, D. (1989) Endocrinology (Baltimore) **125**, 3103–3108
16. Srivastava, D. & Thompson, B. (1990) Endocrinology (Baltimore) **127**, 1770–1778
17. Rousseau, G. G., Baxter, J. D., Higgins, S. J. & Tomkins, G. M. (1973) J. Mol. Biol. **79**, 539–554
18. Robinson, C. H., Finckenor, L., Olivetto, E. & Gould, D. (1959) J. Am. Chem. Soc. **81**, 2191–2195
19. Teutsch, J. G., Costerousse, G. & Deraedt, R. (1977) Ger. Offen. DE 2709078
20. Wolff, M. E., Baxter, J. D., Kollman, P. A., Lee, D. L., Kuntz, I. D., Bloom, E., Matulich, D. T. & Morris, J. (1978) Biochemistry **17**, 3201–3208
21. Teutsch, G., Costerousse, G., Deraedt, R., Benzoni, J., Fortin, M. & Philibert, D. (1981) Steroids **38**, 651–665
22. Mornon, J. P., Delettré, J., Lepicard, G., Bally, R., Surcouf, E. & Bondot, P. 91977) J. Steroid Biochem. **8**, 51–62
23. Wojnar, R. J., Varma, R. K., Free, C. A., Millonig, R. C., Karanewsky, D. & Lutsky, B. N. (1986) Arzneim. Forsch. **36**, 1782–1787
24. Lutsky, B. N., Millonig, R. C., Wojnar, R. J., Free, C. A., Devlin, R. G., Varma, R. K. & Karanewsky, D. S. (1986) Arzneim. Forsch. **36**, 1787–1795
25. Delettré, J., Mornon, J. P., Lepicard, G., Ojasoo, T. & Raynaud, J. P. (1980) J. Steroid Biochem. **13**, 45–59
26. Bélanger, A., Philibert, D. & Teutsch, G. (1981) Steroids **37**, 361–382
27. Philibert, D, Deraedt, R. & Teutsch, G. (1981) 8th Int. Cong. Pharmacol. Tokyo, 1463A
28. Philibert, D., Deraedt, R., Teutsch, G., Tournemine, C. & Sakiz, E. (1982) 64th Annu. Meet. Endocrine Soc., San Francisco, 668A
29. Philibert, D. (1984) in Adrenal Steroid Antagonism (Agarwal, M. K., ed.), pp. 77–101, Walter de Gruyter & Co, Berlin & New York
30. Philibert, D., Moguilewsky, M., Mary, I., Lecaque, D., Tournemine, C., Secchi, J. & Deraedt, R. (1985) in The Antiprogestin Steroid RU 486 and Human Fertility Control (Baulieu, E. E. & Segal, J., eds.), pp. 49–68, Plenum Press, New York
31. Teutsch, G. (1984) in Adrenal Steroid Antagonism (Agarwal, M. K., ed.), pp. 43–75, Walter de Gruyter & Co, Berlin & New York
32. Teutsch, G. (1985) in The Antiprogestin Steroid RU 486 and Human Fertility Control (Baulieu, E. E. & Segal, J., eds.), pp. 27–47, Plenum Press, New York
33. Philibert, D., Costerousse, G., Gaillard-Moguilewsky, M., Nedelec, L., Nique, F., Tournemine, C. & Teutsch, G. (1991) in Antihormones in Health and Disease (Agarwal, M. K., ed.), pp. 1–17, Karger, Basel
34. Ottow, E., Wiechert, R., Neef, G., Beier, S., Elger, W. & Henderson, D. A. (1988) Eur. Pat. Appl. 0 283 428
35. Ottow, E., Neef, G. & Wiechert, R. (1989) Angew. Chem. Int. Ed. Engl. **28**, 773–776
36. Fried, J. H., Mrozik, H., Arth, G. E., Bry, T. S., Steinberg, N. G., Tishler, M. & Hirschmann, R. (1963) J. Am. Chem. Soc. **85**, 236–238
37. Henderson, D. (1987) in Pharmacology and Clinical Uses of Inhibitors of Hormone Secretion and Action (Furr, B. J. A. & Wakeling, A. E., eds.), pp. 184–211, Baillere-Tindall, Eastbourne
38. Philibert, D., Hardy, M., Gaillard-Moguilewsky, M., Nique, F., Tournemine, C. & Nédélec, L. (1989) J. Steroid Biochem. **34**, 413–417

Received 22 July 1991